QUANTIFYING THE PERFORMANCE OF SILVOPASTORALISM FOR LANDSLIDE EROSION AND SEDIMENT CONTROL IN NEW ZEALAND'S HILL COUNTRY

RAPHAEL ISAAC SPIEKERMANN

A dissertation presented in partial fulfilment of the
requirements for the degree of

Doctor of Philosophy
in
Physical Geography

at Massey University, Palmerston North, New Zealand.
September 2022

'He who exercises and cultivates his intelligence seems to be both in the best state and well loved by the gods.'

Aristotle, *Nichomachean Ethics*, X 9 1179a 23-24

ABSTRACT

Landslide erosion results in loss of productive soils and pasture. Moreover, sediment delivered to streams from landslides can contribute to the degradation of freshwater and marine receiving environments by smothering benthic habitats and increasing turbidity, light attenuation, and sediment-bound contaminants. Silvopastoralism is an important land management practice used to combat landslide erosion and improve the health of downstream aquatic ecosystems. Yet, the effectiveness of widely spaced trees in reducing shallow landslide erosion and sediment delivery at hillslope to catchment scales remains largely unknown. Previous studies have been limited by scale (e.g., hillslope) or method (e.g., univariate analyses). This research aims to develop spatially explicit modelling to assess the impact of differing tree species, planting densities, and individual tree location, on rainfall-triggered landslides and sediment delivery while accounting for varying environmental conditions, such as slope gradient, lithology, or soil type. As such, this thesis combines geospatial methods and statistical models to address key challenges related to erosion and sediment control in New Zealand's pastoral hill country.

First, using a study area in the Wairarapa, located in the southeast of the North Island, New Zealand (840 km^2), a method was developed using open-source remote sensing products to generate high-resolution individual tree influence models for the dominant tree species. The objective was to generate a spatial explicit representation of individual trees for landscape-scaled statistical slope stability modelling. The combined hydrological and mechanical influence of trees on slopes was inferred through the spatial relationship between trees and landslide erosion. These spatial distribution models for individual trees of different vegetation types represent the average contribution to slope stability as a function of distance from tree at 1-m spatial resolution. The normalised models (0-1) largely agree with the shape and distribution of force from existing physical root reinforcement models. Of exotic tree species that were planted for erosion and sediment control, poplars (*Populus* spp.) and willows (*Salix* spp.) make up 51% (109,000) of trees located on hillslopes at a mean density of 3 trees/ha. In

line with previous studies, poplars and willows have the greatest contribution to slope stability with an average maximum effective distance of 20 m. Yet, native kānuka (*Kunzea* spp.) is the most abundant woody vegetation species on hillslopes within the study area, with an average of 24 trees/ha, providing an important soil conservation function. A large proportion (56% or 212.5 km^2) of erosion-prone terrain in the study area remains untreated.

In a world-first, this allowed the influence of individual trees to be included in a statistical landslide susceptibility model using binary logistic regression to quantify the effectiveness of silvopastoral systems at reducing landslide erosion and to support targeted erosion mitigation. Models were trained and tested using a landslide inventory consisting of 43,000 landslide scars mapped across the study area. Model performance was very good, with a median Area Under the Receiver Operating Characteristic curve (AUROC) of 0.95 in the final model used for predictions, which equates to an accuracy of 88.7% using a cut-off of 0.5. The effect of highly skewed continuous tree influence models on the maximum likelihood estimator was tested using different sampling strategies aimed at reducing positive skewness. With an adequate sample size, highly skewed continuous predictor variables do not result in an inflation of effect size.

Application of the landslide susceptibility model was illustrated using two farms from within the study area (Site 1: 1,700-ha; Site 2: 462-ha) by quantifying the reduction in shallow landslide erosion due to trees. Compared to a pasture only baseline, landslide erosion was reduced by 17% at Site 1 and 43% at Site 2 due to all existing vegetation. The effectiveness of individual trees in reducing landslide erosion was shown to be less a function of species than that of targeting highly susceptible areas with adequate plant densities. The excellent model performance means spatial predictions are precise, which has implications for land management as the maps provide greater certainty and spatial refinement to inform landslide mitigation. The terrain occupied by the “high” susceptible class – defined as the terrain where 80% of mapped landslides were triggered in the past – occupies only 12% of Site 1 and 7% of Site 2. This

suggests there is great potential for improved targeting of erosion mitigation to these areas of the farms where landsliding may be expected in the future.

To enable biological mitigation to be targeted to critical source areas of sediment, determinants of sediment connectivity were investigated for a landslide-triggering storm event in 1977. In a first of its kind, a morphometric landslide connectivity model was developed using lasso logistic regression to predict the likelihood of sediment delivery to streams following landslide initiation. An experiment was undertaken to explore a range of connectivity scenarios by defining a set of sinks and simulating varying rates of sediment generation during runoff events of increasing magnitude. Sediment delivery ratios for the 1977 event ranged from 0.21 to 0.29, equating to an event sediment yield of 3548 t km^{-2} to 9033 t km^{-2}. The likelihood of sediment delivery was greatly enhanced where debris tails coalesce. Besides scar size variables, overland flow distance and vertical distance to sink were the most important morphometric predictors of connectivity. When scar size variables were removed from the connectivity model, median AUROC was reduced from 0.88 to 0.75.

By coupling landslide susceptibility and connectivity predictions in a modular form, we quantified the cost effectiveness of targeted versus non-targeted approaches to shallow landslide mitigation. Targeted mitigation of landslide-derived sediment was found to be approximately an order of magnitude more cost-effective than a non-targeted approach. Compared with a pasture-only baseline, a 34% reduction in sediment delivery can be achieved by increasing slope stability through spaced tree planting on 6.5% of the pastoral land. In contrast, the maximum reduction achievable through comprehensive coverage of widely spaced planting is 56%. The coupled landslide susceptibility and connectivity predictions (maps) provide an objective basis to not only target mitigation to areas where future shallow landslides are likely to occur, but – perhaps more importantly – target future tree planting to locations that are likely to be future sources of fine sediment. In this way, the research presented in this thesis is both methodologically novel and has immediate application to support land management decisions aimed at creating a more sustainable socio-ecological landscape.

ACKNOWLEDGEMENTS

There are many persons to whom I owe deep gratitude for the support they have shown me during the past three years of this PhD journey. First, I wish to thank my supervisors, Prof. Ian Fuller, Dr Hugh Smith, Dr Lucy Burkitt, and Dr Sam McColl for their continued guidance and encouragement. I am sincerely grateful that you urged me to challenge myself intellectually – to grow as a person and a scientist. It is thanks to you that I have gained an appreciation for new concepts and methods, and I have learned (yet again) to step outside of my comfort zone.

This research received financial support from the New Zealand Ministry of Business, Innovation and Employment research program "Smarter Targeting of Erosion Control (STEC)" (Contract C09X1804) and the Strategic Science Investment Fund (SSIF) allocated to Manaaki Whenua – Landcare Research. Thank you to the New Zealand taxpayer for your on-going support of science.

I am greatly indebted to Dr Chris Phillips and Dr Les Basher, who have been great mentors to me, and without whom I would never have had the opportunity to pursue doctorate studies. Special thanks also to Dr Jackie Aislabie and Dr Andrew Manderson for backing me and giving me time to undertake this study. I must also extend my thanks to Dr John Dymond for the many stimulating conversations early on and your continued mentorship.

There are many other individuals who have been an inspiration in terms of developing an interest in geomorphology. I should mention Prof. Dr Thomas Glade, whose lectures on landslides and geomorphology during my undergraduate studies first awoke my interest in human-landscape interactions. I wish to also thank my colleagues Harley Betts, Dr Simon Vale, Dr Andrew Neverman who stepped in for me to allow me to focus on my PhD research. Special thanks to Thomas Mackay-Smith for the many enjoyable conversations on silvopastoralism!

I will forever owe my wife Elizabeth deep gratitude for her endless support in this endeavour. Without you, this thesis would not have been possible. Thank you for persevering in this country so far from your home of Austria, for nurturing our young children so

wonderfully, and the care you showed me – especially with the many cups of coffee and tea in the early and late hours of the day! And it is my wife and children, Philippa, Felicity, Augustin, and Tommy, to whom I must express my gratitude for never failing to wake me from my thoughtful slumber – back to the real life of laughter, crying, and nappy-changing!

Lastly, I wish to acknowledge my parents, Karl and Karen. You instilled in me a keen desire to seek that which is good, true, and beautiful – as well as to not shy from accepting challenges. Thank you!

TABLE OF CONTENTS

LIST OF FIGURES

LIST OF TABLES

PART I

INTRODUCTION

1

1 INTRODUCTION

1.1 Background

Silvopastoralism is a form of agroforestry (Somarriba, 1992) that specifically refers to the inclusion of grazing by livestock as an important component of the agroecosystem and seeks to optimize benefits from biophysical interactions that are created when trees are combined with livestock (Plieninger and Huntsinger, 2018). As with agroforestry systems more generally, silvopastoralism seeks to optimise benefits from biophysical interactions that are created when trees are combined with livestock. Such benefits may include increased ecological, economic and/or cultural outcomes (Mackay-Smith et al., 2021). In areas with heightened risk of land degradation, silvopastoralism has been adopted in landscapes across the globe as a mitigative tool to improve land management (Benavides et al., 2009; Joffre et al., 1999; Peri et al., 2016). New Zealand is an example where silvopastoralism has played an important role in sustainable land management – with a primary focus on soil conservation (Kemp et al., 2018). The extent of New Zealand's broad reliance on silvopastoralism as a mechanism of erosion and sediment control is possibly unique in a global comparison.

Following arrival by European settlers in the 1800s, extensive deforestation for pastoral farming resulted in a geomorphic landscape response consisting of high erosion and sedimentation rates (Glade, 2003; Goff, 1997; Green, 2013; Phillips et al., 2018). Erosion processes in New Zealand remain very active – even in a global context (Jansson, 1988), due to a predisposed natural environment with steep slopes, weak sedimentary rocks, and a climate featuring high annual rainfall and relatively frequent high magnitude rainfall events (Basher, 2013; Hicks et al., 2011, 1996). While surface, fluvial and streambank erosion are important

processes and contributors to sediment loads, mass movement processes are geographically the most widespread type of erosion in New Zealand (Basher, 2013). The most common types of mass movement in New Zealand are shallow, rapid slides and flows involving soil and regolith (Crozier, 2005; Glade, 1998). Such landslides are generally triggered either by individual high-intensity-rainfall events or by small rainfall events after prolonged wet periods leading to high antecedent soil moisture conditions (Basher, 2013). There is evidence that in the long-term, shallow landslides make up the largest source of sediment from pastoral hill country in New Zealand (Dymond et al., 2016). In these steep and highly dissected pastoral landscapes, biological erosion control - either through widely spaced trees, blanket afforestation, or natural reversion to indigenous forest, has been the most common method to increase slope stability (Douglas et al., 2013; Phillips et al., 2021; Phillips and Marden, 2005). Besides soil and nutrient retention, the primary objective of integrating trees into a pastoral system is to improve outcomes in terms of water quality and aquatic habitat (Basher, 2013; Dymond et al., 2017a). However, trees also provide many other benefits, such as provision of shade and shelter for livestock, carbon sequestration, and regulation of catchment discharge (Benavides et al., 2009; Mackay-Smith et al., 2021).

In New Zealand, the enactment of the Soil Conservation and Rivers Control Act 1941 increased awareness for sustainable land management practices. In more recent times, erosion mitigation is a component of farm management plans (referred to as Whole Farm Plans (WFPs), Farm Environment Plans (FEPs), or Freshwater Farm Plans (FFPs)), which are comprehensive plans undertaken by regional councils and other industry groups in cooperation with landowners that integrate soil conservation and other contaminant mitigations into land management practices and farming operations. Moreover, high sediment yields and sediment connectivity can have detrimental outcomes on riverine and estuarine habitats by reducing the diversity, types, and abundance of fauna (Fuller and Death, 2018).

The introduction of sediment standards into New Zealand's National Policy Statement for Freshwater Management (NPS-FM) has required regional authorities to manage freshwater in

a way that considers the effects of land-use, including the effects on receiving estuarine environments (New Zealand Government, 2020a). Managing suspended fine sediment in view of ecosystem health is a component of the NPS-FM, whereby monitoring of visual clarity at measurement sites is a mechanism used to determine outcomes. Moreover, FFPs have been established as a legal instrument under the Resource Management Act (RMA sections 217A to 217M, New Zealand Government, 2020b) to identify environmental actions on farms in consideration of objectives for the catchment. The act specifies that an FFP must *"identify any adverse effects of activities carried out on the farm on freshwater and freshwater ecosystems"* and *"specify requirements that (i) are appropriate for the purpose of avoiding, remedying, or mitigating the adverse effects of those activities on freshwater and freshwater ecosystems; and (ii) are clear and measurable"* (section 217F, RMA). Therefore, understanding the impact of erosion and sediment control is important to achieve the desired environmental outcomes and – more specifically – sediment standards. The RMA suggests an FFP must provide clear (spatial) guidance on the risks with respect to freshwater. Furthermore, the impact of the actions must be measurable and quantifiable for auditing purposes.

In the case of sediment loss, the evidence base for the current assumptions on the effectiveness of silvopastoral systems as an intentional form of treatment on erodible terrain is poor. There are currently no methods to measure and quantify the effect of erosion and sediment mitigation at a range of scales – from hillslope through to catchment. Quantifying the effect of mitigation through in-stream measurement techniques such as suspended sediment samplers is challenging due to the temporal and spatial complexities involved in erosion, transport and deposition processes upstream of the point of measurement. There are several published and unpublished reviews that summarize knowledge of erosion processes and erosion mitigation (Basher et al., 2016; England et al., 2020; Marden, 2012; Quinn et al., 2009), including farm planning as an instrument for reducing adverse impacts of erosion (Manderson et al., 2007), and cost-benefit assessments of erosion control (Dominati et al., 2014; Jones et al., 2008). These reviews reveal a glaring paucity of quantitative data on the effect of trees on erosion and

sediment yields in silvopastoral systems at meaningful spatial and temporal scales. While issues surrounding freshwater contamination by excessive amounts of fine sediment is not unique to New Zealand, there is currently no method – and therefore science-based knowledge – to quantify individual tree effects in silvopastoral systems on hillslope erosion and sediment yields. Thus, implementation of environmental policy expressed in the NPS-FM and RMAA 2020 pertaining to fine sediment is largely relying on expert knowledge. While local knowledge and experience are invaluable, reliance on the subjective views of individual experts can lead to bias and siloed thinking, and a failure to recognise unknown areas of knowledge (Spiekermann et al., 2015b).

The research presented here is novel in that it seeks to quantitatively account for individual tree effects in silvopastoral landscapes both locally (hillslope) and in consideration of downstream impact. For the first time at farm to regional scale, quantitative methods are developed to investigate the role of silvopastoral systems in reducing the occurrence of shallow landslides and subsequent delivery of sediment to streams. The research aims to develop geospatial methods to test the performance of biological erosion and sediment control in silvopastoral systems – with a specific focus on rainfall-triggered shallow landslides. An examination of the literature shows that most previous studies have aimed to quantify the effect of biological erosion control by adopting one of the following methods:

1. An empirical approach by a paired comparison of the amount of soil eroded between treated (planted) and control sites (not planted) with similar terrain characteristics (G. Douglas et al., 2013a; Hawley and Dymond, 1988).

2. A physical, process-based approach using quantitative measures for root reinforcement to quantify the increase in soil cohesion and slope stability achieved (Giadrossich et al., 2017; Schwarz et al., 2010b; van Zadelhoff et al., 2021).

3. Statistical landslide susceptibility models that include vegetation or land cover as a preconditioning factor (Reichenbach et al., 2018).

Published reductions of shallow landsliding using paddock-scaled empirical data range from 70 to 95%. But measured or assessed reductions are often far less than this because plantings are inadequately spaced, poorly maintained, or not targeted to terrain prone to landsliding. There is an obvious gap between what is known in terms of the effectiveness of individual implemented works and the overall effectiveness of these measures at farm and catchment scales – particularly in consideration of downstream impact. For empirical and physical approaches, upscaling from tree stands or slope scales remains a challenge to inform on the effectiveness of erosion control across varying environmental terrains. This largely has to do with data availability and the difficulty associated with upscaling physical models beyond a tree stand or single slope. Furthermore, regional-scaled landslide susceptibility assessments do not account for the influence of individual trees. Thus, there is a clear knowledge and scale gap between physical models that quantify root reinforcement for tree stands, and landslide susceptibility modelling at regional scale using land cover data as a proxy for the effect of the hydrological and mechanical influences of woody vegetation.

Figure 1.1 illustrates the key components of this research and how they relate to one another. The research undertaken in this thesis is interdisciplinary in nature, broadly situated across domains that include remote sensing, geomorphology, and agroforestry science. Remote sensing techniques are applied at farm to catchment scales using very high-resolution imagery and digital elevation models (DEM) generated from light detection and ranging (LIDAR) data to generate large inventories of landslides and individual trees. These inventories are used to develop statistical models for slope stability that account for individual tree effects. This research thus integrates the process knowledge of slope stability with the statistical modelling techniques frequently applied at landscape to regional scales. Through consideration of slope-channel coupling, the methods developed in this study can inform land management decisions to increase the cost-effectiveness of erosion and sediment mitigation.

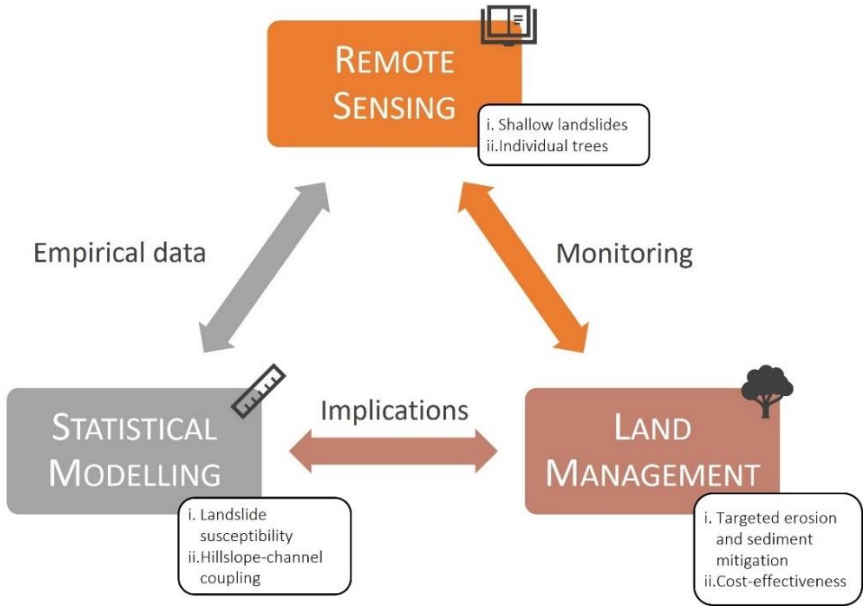

Figure 1.1 Conceptual framework underpinning the research.

1.2 Aim and Objectives

The overarching aim of this thesis is to develop spatially explicit modelling to assess the impact of differing tree species, planting densities, and individual tree location, on rainfall-triggered landslides and sediment delivery while accounting for varying environmental conditions, such as slope gradient, lithology, or soil type. To achieve this aim, the study addresses the following key objectives:

1. Use open-source high resolution remote sensing products (e.g., aerial photography) to develop methods for mapping shallow landslides and individual trees at landscape scale.
2. Test the hypothesis that the individual tree effect on slope stability can be ascertained by examining the spatial relationship between landslides and trees.
3. Determine the feasibility of modelling slope stability at the scale of individual tree using statistical landslide susceptibility models.
4. Develop quantitative methods that allow for both ex-ante and ex-post assessments of slope stability for silvopastoral systems at farm to regional scale, whereby individual tree effects are included through spatial explicit representation.

5. Develop a morphometric landslide connectivity model to quantify the effect of silvopastoral systems on sediment yields, providing an objective basis for targeted mitigation of shallow landsliding.
6. Determine the cost-effectiveness of targeting biological mitigation to critical source areas of sediment.
7. Propose a landslide erosion and sediment risk management framework for planning, implementing, and monitoring biological erosion and sediment mitigation in silvopastoral landscapes.

1.3 Thesis Organization

In Part I, this first chapter provides the research and policy context in which this thesis is situated and lists the key objectives of the thesis. Chapter 2 reviews the scientific literature on the key subjects relevant to this thesis, beginning with silvopastoralism as a land management practice that aims to improve environmental outcomes such as pasture, soil, and/or animal welfare. Next, the review introduces slope stability concepts. This includes the fundamentals of how trees promote slope stability, providing an overview of both the mechanical and hydrological processes involved. The review then briefly summarizes methods for quantifying root reinforcement, as well as how spatial predictions of root reinforcement can be included in physically based models. Statistical landslide susceptibility modelling is then introduced and contrasted to physical models by discussing key differences, including both challenges and benefits of these complementary approaches. The final section of Chapter 2 delves into the literature on the topic of sediment connectivity and hillslope channel coupling. Concepts and methods of connectivity are reviewed, limitations discussed, and knowledge gaps identified.

Since this is a thesis with publications, Part II comprises Chapters 3-5, which are standalone papers that have been published in international journals. Chapter 3 aims to respond to the first two stated objectives 1) and 2) of the thesis by developing an empirically based rationale for

the spatial-explicit representation of a tree's influence on slope stability. The aim is to improve on existing land cover data that can be used for statistical landslide susceptibility modelling at the scale of the individual tree for a variety of tree genera (e.g., coniferous species) and/or vegetation types (e.g., poplar/willow). Therefore, Chapter 3 begins by developing an individual tree classification using open-source LiDAR and multi-temporal imagery. Landslides are mapped for an 840 km^2 large area, resulting in an inventory of >43,000 shallow landslide scars. These two datasets of classified trees and landslide scars form the basis for this paper to test the hypothesis that the spatial relationship between i) the fraction of eroded soil due to landsliding and ii) distance from the nearest tree allows the average tree's influence on slope stability to be inferred. Does a pattern emerge from the data at landscape scale based on a function of distance from tree? And if so, how does it correspond to what we do know from root excavations and root reinforcement modelling? In many respects, Chapter 3 forms the basis of the entire thesis, since the resulting tree influence models on slope stability (TIMSS) are key inputs in the subsequent modelling undertaken in Chapters 4 and 5.

Chapter 4 tests the feasibility of statistical approaches to slope stability in silvopastoral landscapes – addressing the stated objectives 3) and 4) of the thesis (see 1.2 Aim and Objectives). In most existing landslide susceptibility models, land use or land cover data are used to capture the varying effect of vegetation composition. Yet, these data are rarely available at the scale required to quantify the effect of individual trees across a silvopastoral landscape. Therefore, in Chapter 4, the TIMSS are included as an explanatory variable in the development of a landslide susceptibility model to capture the effect of individual trees on slope stability for the four most abundant vegetation types in the study area (poplar/willow, eucalyptus, conifer, mānuka/kānuka). Due to the nature of silvopastoral landscapes, the TIMSS data are associated with a high positive skewness. The implication of skewness on the estimation of effect sizes using logistic regression modelling is investigated through use of different sampling strategies. Then, Chapter 4 concludes with an illustration of how the landslide susceptibility models can

be used at farm scale to quantify the effectiveness of silvopastoralism on reducing shallow landsliding.

The development of the techniques in Chapters 3 and 4 leads to their application in Chapter 5, which focuses on objectives 5) and 6). The primary aim here is the development of a statistical landslide connectivity model to quantify the effect of silvopastoral systems on sediment yields. Specifically, this piece of research links hillslopes to streams by determining the likelihood of sediment delivery to a stream in the event of a landslide being triggered at any given location. This is achieved by coupling the landslide susceptibility model developed in Chapter 4 with the landslide connectivity model in a modular fashion. Finally, land management scenarios are used to inform on the cost-effectiveness of different approaches to biological mitigation.

In Part III, Chapter 6 provides a synthesis of the research by examining how each of the stated research objectives has been addressed and further discusses the key findings and their implications for land management. Moreover, consideration is given to how this research contributes to the advance of science-based knowledge more broadly and with reference to the review of relevant scientific literature in Chapter 2. And lastly, a comprehensive conceptual framework for management of erosion and sediment in silvopastoral systems is proposed. The framework adopts a risk management approach, of which risk assessment is a key component. Drawing on the statistical models developed in this thesis, the application of the framework for erosion and sediment mitigation is demonstrated, and its implications for land management discussed in the context of silvopastoral systems. Finally, Chapter 7 provides a summary conclusion of the thesis followed by an outlook in Chapter 8 that explore future research needs and opportunities.

2

2 LITERATURE REVIEW: SILVOPASTORALISM AND SLOPE STABILITY

2.1 An Introduction to Silvopastoral Systems

Agroforestry is a planned approach to land use that incorporates trees into farming systems and allows for the production of trees and crops and/or livestock from the same piece of land (Gordon et al., 2018; Nair et al., 2021; Somarriba, 1992). It is generally considered a form of land management that recognizes the environmental, ecological, economic, and social benefits that can be gained from tree-crop or tree-livestock interactions. The concept of agroforestry has its roots in the context of sustainable land development – largely in the tropics and subtropics. An example of this are the Agroforestry Parklands in sub-Saharan Africa, which are a form of agrosilvopastoral system, with intercropping beneath discontinuous tree cover in the short wet season, and free-roaming grazing during the longer dry season (Nair et al., 2021). Indeed, the benefits of well-maintained agroforestry systems surrounding rural villages (green belts) in the semi-arid Sahel have been well documented (Brandt et al., 2014; Nair et al., 2021; Spiekermann et al., 2015a). The agrosilvopastoral intercropping amongst scattered trees results in healthier and more productive soils compared to less used secondary cropping fields that are mostly fallow and often degraded (Brandt et al., 2014; Spiekermann et al., 2015a).

Temperate agroforestry systems can be classified into silvoarable and silvopastoral systems. Silvoarable systems involve primarily timber trees intercropped with arable crops. Silvopastoralism (or wood-pastures) is a form of agroforestry that specifically refers to the inclusion of grazing by livestock as an important component of the agroecosystem (Plieninger and Huntsinger, 2018). Such tree and livestock interactions can be found where trees are used

for livestock shelter (shade, shelterbelts), where woodlands are grazed, or where grazed pasture or rangelands include a forest, tree or woody shrub component (Thevathasan et al., 2018). As with agroforestry systems more generally, silvopastoralism seeks to optimize benefits from biophysical interactions that are created when trees are combined with livestock. Trees are managed to maintain an herbaceous understorey as livestock forage, in recognition of the emergent properties of the ecosystem that can add both economic and environmental value to the land management system provided the overstocking does not degrade the land resource (Peri et al., 2016).

In terms of geographic extent, silvopastoralism is a common land use in many parts of the world. In Europe, wood-pastures make up close to 20% of all grasslands, featuring most prominently in terms of areal extent in the Mediterranean (Montado/Dehesa consisting mainly of oaks in Spain, France and Italy), but also in the Alpine region and the Black Sea region (Romania, Bulgaria) (Plieninger et al., 2015). The native ñire (Nothofagus antarctica), or southern beech, found in Chile and Patagonia, Argentina, forms the basis of extensive natural silvopastoral landscapes. Further examples include the rangelands of North America (Huntsinger et al., 2010; Huntsinger and Oviedo, 2014), Australia (Reid and Moore, 2018), China, and India (Nair et al., 2021).

Besides the diversified income streams through the sale of timber, the productivity of pasture under silvopastoral systems can increase in areas with severe water stress conditions (Peri et al., 2018, 2016). Trees in a pastoral system can have positive or negative effects on pasture productivity and biodiversity due to competition for light, water and nutrients (Callaway et al., 1991; Moreno and Pulido, 2008). The outcome can be manipulated through choice of tree species, planting density and spatial distribution (Mosquera-Losada et al., 2018; Nair et al., 2021; Plieninger and Huntsinger, 2018). An increase in pasture production beneath tree canopies have been found in many different landscapes globally (Callaway et al., 1991; Frost and McDougald, 1989; Moreno, 2008; Moreno Marcos et al., 2007; Peri et al., 2018),

while reductions in pasture productivity have been measured elsewhere (G. Douglas et al., 2013b; Moreno and Pulido, 2008; Wall et al., 2006).

In the Chilean ñire, understorey dry matter production was found to be dependent on soil water availability in interaction with light transmittance and provision of shade. While understorey production was significantly reduced for sites with moderate water stress, 40% - 60% transmissivity was the optimal for sites with severe water stress conditions (Figure 2.1), which is explained by a combination of soil moisture conserving mechanisms that reduce evapotranspiration, including reduced canopy temperature, reduced windspeed (up to 80%), and stomatal closure (Peri et al., 2016).

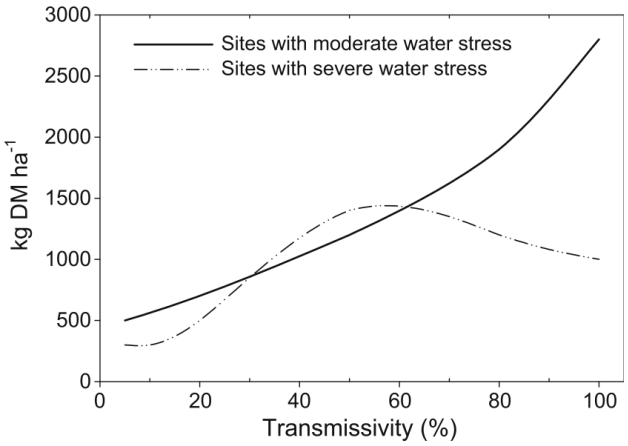

Figure 2.1. Mean dry matter (DM) grass understorey production in ñire silvopastoral systems under different light intensities (determined by a gradient of crown cover) and adjacent open areas (100 % transmissivity) in Southern Patagonia. Source: (Peri et al., 2016).

Benefits of trees integrated into a pastoral system are multifaceted and include economic activity produced by firewood, fruit, fodder, mushrooms, medicinal uses, pinyon nuts, and juniper berries used for gin (Plieninger et al., 2015; Plieninger and Huntsinger, 2018). Ecological benefits are many and include the increase in biodiversity (both flora and fauna) (Huntsinger and Oviedo, 2014; Tölgyesi et al., 2018), carbon sequestration (Hoogmoed et al., 2012; Montagnini and Nair, 2004), increased slope stability (G. Douglas et al., 2013a), and soil nutrient accumulation (Moreno Marcos et al., 2007; Obrador et al., 2004). Indeed, it has been stated that the ecological function of scattered trees is disproportionately large relative to their spatial extent, as they provide a microhabitat within an otherwise uniform pastoral structure

(Manning et al., 2009). Thus, silvopastoral systems have been found to accommodate greater biodiversity compared to bare pasture or closed forests (Fischer et al., 2010; Plieninger et al., 2015). Extensive year-round grazing in Chilean woodlands was associated with greater tree regeneration than spring-time grazing only (Root-Bernstein et al., 2022). This was explained by the selective foraging of grasses and herbs by experienced cattle – a social learning effect not acquired by cattle temporarily exposed to these systems (Provenza and Balph, 1988). Thinning and pruning of forests also reduces risk of fire propagation, which is a common practice in the Mediterranean region (Ruiz-Mirazo and Gonzalez-Rebollar, 2013).

Having provided the international context of silvopastoral systems research and summarized its concept and practice, the following section explores silvopastoral systems and reviews relevant scientific literature specifically for the New Zealand context.

2.2 Silvopastoralism in New Zealand

2.2.1 Introduction to Silvopastoral Systems in New Zealand

In contrast to traditional forms of silvopastoralism that use natural forage (e.g., range management in Canada) and/or native trees (e.g., southern beech of Patagonia), silvopastoralism in New Zealand is an ecosystem that has been shaped by active land management practices – in a similar way to the Californian Oak woodlands (Huntsinger and Oviedo, 2014). For this reason, it can be viewed as a social-ecological system, which is the product of human industry and ecosystem services, acknowledging the human role as a cogenerating factor (Huntsinger and Oviedo, 2014).

Previous research on silvopastoralism in New Zealand has predominantly been focused on poplar (*Populus* spp.) and radiata pine systems (Benavides et al., 2009; Hawke, 1991; Kemp et al., 2018; Wilkinson, 1999). Fewer studies have assessed pasture interactions with less abundant tree species such as *Acacia*, *Alnus*, *Eucalyptus* and *Salix* spp. (Devkota et al., 2009;

Power et al., 2001). Little attention has been given to native alternatives – with the exception of a recent study that contrasted silvopastoral outcomes of poplar and kānuka (*Kunzea* spp.) (Mackay-Smith et al., 2021). The main perceived benefit of silvopastoralism has been related to soil conservation in pastoral hill country, with most research focused on quantifying the soil-conserving effect (G. Douglas et al., 2013a; Thompson and Luckman, 1993), as well as tree-effects on soils and pasture (Benavides et al., 2009; Cooper, 2015; Devkota et al., 2009; Douglas et al., 2006a, 2006b; Guevara-Escobar et al., 2002, 1997; Power et al., 2001; Wall et al., 2006, 1997).

However, added benefits, such as supplementary fodder, shade and shelter for livestock, and cultural values, have also been well documented for poplar and willow silvopastoral systems (Benavides et al., 2009; Mackay-Smith et al., 2021; McGregor et al., 1999). In a rare quantitative approach, the value associated with poplar silvopastoral systems was estimated using benefit cost analysis (Dominati et al., 2014). The results indicate that widely-spaced tree planting of poplars for soil conservation is only profitable when considering the economic value associated with the provision of other ecosystem services such as the provision of wood, feed, shelter/shade to livestock. Due to the lack of economic incentive for land owners to plant trees in steep pastoral terrain, soil conservation continues to be promoted through subsidy schemes (Parminter et al., 2001).

With the focus on soil conservation and pasture production, research on the biophysical mechanisms that drive additional outcomes from silvopastoral systems, such as animal welfare, biodiversity, carbon sequestration, hydrological impacts, and soil nutrient effects, have received comparatively little attention. This reflects the environmental challenges faced in much of New Zealand's pastoral hill country related to soil erosion and its negative effects on freshwater quality and aquatic ecology. Yet, other benefits from silvopastoral systems are not necessarily less meaningful; they are, however, less well understood. The following sections provide a summary of research findings in different types of silvopastoral systems found in New Zealand.

2.2.2 Tree Interactions and Effects

Pine silvopastoralism

The most rigorous long-term silvopastoral trial undertaken in New Zealand to date was the Tikitere trial at Rotorua (Hawke, 1991). Planted in 1973, the trial contained plantings of *Pinus radiata* at 50, 100, 200 and 400 stems/ha, as well as open pasture for comparison purposes. Data obtained through biannual measurements of pasture regrowth and botanical composition shows decreasing pasture yields with increasing tree density and age. At 200 stems/ha, the pasture yield was 18% of open pasture compared to 50% at 100 stems/ha. The initial decline was attributed to competition for light, soil nutrients and water, and smothering of pasture from pine needles at a later stage. The Tikitere project provides evidence for the adverse effects of pine silvopastoralism on wood quality and volume, pasture production and animal performance (G. Douglas et al., 2013b; Hawke, 1991; Kemp et al., 2018).

Poplar and willow silvopastoralism

Impacts of widely spaced trees on understorey pasture yield and quality has been quantified for poplars (Benavides et al., 2009; Douglas et al., 2006a, 2006b, 2001; Guevara-Escobar et al., 1997; Wall et al., 1997), showing an overall negative influence, which is attributed mainly to reduced light transmission due to canopy shading (Dodd et al., 2005). Based on measurements of pasture dry matter production for 12-24 months across a range of poplar canopy closures, including open pasture, annual pasture DM production was predicted to be 77%, 60%, and 48% of open pasture beneath 25%, 50%, and 75% of canopy closure respectively (Wall et al., 2006). While the degree of reductions in understorey pasture production compared to open pasture differed with species, canopy closure, tree maturity, slope aspect, climate, and soil, the consistent finding is that widely spaced poplar trees result in a reduction of pasture dry matter accumulation.

Beneath widely spaced, mature *Populus deltoides* with almost complete canopy closure, a 40% reduction in total pasture dry matter accumulation was found for the 12 month study in the Pohangina Valley (North Island, New Zealand), with differences being most pronounced during the productive period of the year (January-March) (Guevara-Escobar et al., 1997). The difference between understorey and open pasture production can be partly explained by lower soil moisture at 0-150 mm in the tree understorey compared to open pasture despite lower soil temperature year-round, which – besides the reduced effective rainfall due to interception – may indicate competition for soil moisture between pasture and the shallow roots of the poplars. The authors also found the botanical composition of the pasture to be of lower feed quality than that of open pasture. Seasonal soil understorey moisture trends were identified elsewhere (Douglas et al., 2006a), with lower soil water content during summer and wetter soil in winter compared to open pasture. However, a further study investigating pasture growth at a site also in the Pohangina Valley measured only 23% reduction compared to accumulation in the open (Douglas et al., 2006a). The difference was attributed to the degree of canopy closure. Tree management, including regular pruning and pollarding can increase light transmissivity to maintain increased pasture production (Benavides et al., 2009; Devkota et al., 2009).

These findings are largely corroborated by a similar study, which also considered the influence of the aspect of slopes (Douglas et al., 2001). Overall, annual pasture growth was reduced by 10.5% at the Pohangina site (Manawatu catchment, North Island; average rainfall: 1250 mm/a) and by 27% at the drier Otago site (average rainfall: 700 mm/a), southwest of Dunedin (South Island). A significant slope aspect effect interacted with the tree effect by reducing understorey pasture growth by 20% and 34% on north and south aspects at the Otago site and 7% and 14% at the Pohangina sites, respectively.

However, tree-pasture interactions can vary considerably with respect to local environmental conditions. No significant difference was found when comparing pasture production near the trunk of mature poplars with open pasture just beyond the tree canopy for a study in the dry east coast region of the North Island (Gilchrist et al., 1993). This is an example

where limiting factors other than shade, such as moisture and nutrient competition, can be more important in terms of modifying tree effects on pasture outcomes (Power et al., 2001).

Poplar and willow silvopastoral systems also add value to the farm operation through animal welfare functions (shade, shelter, and quality supplementary fodder) and carbon sequestration (McIvor et al., 2011). Dominati et al. (2014) quantified the long-term costs and benefits of space-planted trees in a pastoral farming context using an ecosystem services approach. Amongst the factors, the authors accounted for 1) reduction in pasture production under trees; 2) reduction in runoff due to interception of rainfall (McIvor et al., 2009); 3) improvement in soil physical characteristics and filtering capacity as a result of increased water uptake; 4) an increase in carbon and nitrogen mineralization; and 5) increased soil pH and exchangeable cations (Ca, K and Mg) compared to open pasture. Despite the decrease in pastoral production below tree canopy, results indicate that planting wide-spaced trees in pastural hill-country is economically beneficial in the long-term due to the increase in provision of ecosystem services including forage from trees, wood, provision of shade and shelter for animals and net carbon accumulation in wood.

Indigenous alternatives

Despite indigenous tree species being the predominant make up of silvopastoral systems elsewhere, there has been very little research undertaken in New Zealand to explore native alternatives for silvopastoralism. A recent two-year study found a 108% increase in green dry matter production under fully mature kānuka trees compared to paired areas of open pasture in the same paddock at two sites (Mackay-Smith et al., 2022a). This increase was associated with 116% and 49% higher plant available P and soil organic matter under the trees, respectively, as well as a significant increase in soil porosity. This is the first time in New Zealand that the presence of ≥ 15-year-old trees in a pastoral system has resulted in a measured increase in pasture production. Thus, a tree-pasture system is a potentially transformational management

practice to overcome key trade-offs between production, environmental, and cultural outcomes. Yet, further research is required to substantiate these findings.

2.2.3 Soil Conservation

Previous research undertaken to investigate tree effects on pasture outcomes suggests that reductions in pasture productivity as a result of the presence of trees must be balanced against the benefit of reduced soil loss from hillslope erosion processes, which can likewise have long-term consequences on productivity (B. J. Rosser and Ross, 2011; Trustrum et al., 1984). Poplars (*Populus* spp.) and willows (*Salix* spp.) are the most common trees used for erosion control in New Zealand's steep pastoral land (Hathaway et al., 1987; Mackay-Smith et al., 2021; Van Kraayenoord and Hathaway, 1986; Watson et al., 1999; Wilkinson, 1999). Other less common species include *Acacia* or *Eucalyptus*, which are better suited to drought prone areas (Millner and Kemp, 2012). Widely spaced poplars and willows to mitigate mass movement erosion is a management technique that has been well documented (Les Basher et al., 2008; Basher, 2013; Phillips et al., 2008; Phillips and Marden, 2000; Wilkinson, 1999). There are many reasons why these species have been the preferred option for erosion control. Both species can be established from large poles produced at nurseries and can tolerate the presence of stock with a minimum of protection with plastic sleeves (Wilkinson, 1999). Furthermore, they are easily transported and planted on steep slopes and are very tolerant of wet soil conditions, which is likewise where mass movement is more likely to occur.

Individual, mature poplar and willow trees can rapidly develop large root systems (Table 2.1 Dimensions of six excavated Populus × euramericana 'Veronese' trees excavated on a pastoral hillslope. Source: McIvor et al. (2009, 2008)), and the influence of neighbouring trees through intermeshing of roots has also shown to be important (Hawley and Dymond, 1988). Once established, individual trees increase the stability of slopes, whereby the added strength imparted to the soil is dependent on many factors that include tree maturity, root system

architecture, root tensile strength, soil type, etc. (Phillips et al., 2014). Table 2.1 Dimensions of six excavated Populus × euramericana 'Veronese' trees excavated on a pastoral hillslope. Source: McIvor et al. (2009, 2008) provides an overview of data derived from full excavations of six poplar clones (*Populus × euramericana 'Veronese'*) (McIvor et al., 2009, 2008). Based on these observations, lateral roots from poplar varieties can establish large root systems in the space of a short period (up to 14 m in lateral extension in 10 years). The authors suggest soil depth and water storage capacity were important limiting factors for growth and root development. Moreover, there were indications that terrain morphology influences the root system architecture, with roots extending further uphill on steeper slopes.

Table 2.1 Dimensions of six excavated Populus × euramericana 'Veronese' trees excavated on a pastoral hillslope. Source: McIvor et al. (2009, 2008).

Tree age (yr)	Height (m)	DBH (cm)	Max lateral root distance (m)	Total coarse root length (m)	Slope (°)
5	7.3	8.4	8	79	22
7	9.3	14.4	11	349	21
9.5	13.3	21.3	14	664	22
11	13.4	29.0	12	1611	32
11	12.95	27.2	8	1131	29
11	11.15	18.9	10	293	22

Both initial establishment of plantings and subsequent maintenance are important to ensure survival and effectiveness in terms of slope stability. There are many factors that influence successful establishment of space planted poplars and willows. A study that examined survival of poplar and willow poles planted in the Gisborne–East Coast area found 24% of poles had died within 24 months, and 40% had died within 45 months (Marden and Phillips, 2013). They attributed this to a combination of poor pre-treatment of poles, poor planting technique, site factors, and stock damage. Yet, quantitative trials aimed at increasing understanding of determinants of mortality are largely lacking. Observations from land managers in the field suggest successful establishment of poles on steeper slopes can be challenging and survival rates in these areas are poor due to shallow soils, exposure to wind gusts, and reduced soil moisture. Depth of soil to bedrock reduces the rootable soil volume (Leenaars et al., 2018), which can inhibit the establishment of plants in shallow soils. Furthermore, there is evidence

that certain species may not penetrate the underlying bedrock, such as massive mudstone (Marden et al., 1991). With only shallow lateral root systems and no basal root reinforcement, trees are prone to windthrow.

Most empirical studies aimed at quantifying the effectiveness of biological erosion control under silvopastoral systems have been carried out in New Zealand (e.g., Douglas et al., 2011). Despite the widespread use of discontinuous tree cover, there has been relatively little experimental or quantitative work to establish their effectiveness in reducing erosion in relation to factors such as tree size, planting density, slope gradients (Basher, 2013). Furthermore, to date no study has quantified the effect of spaced trees on sediment yields.

Semi-quantitative and qualitative approaches tend to be site, transect or catchment-based and have a broader perspective but limited measurement and require an assessment of trends in erosion status which are generally subjective (Thompson and Luckman, 1993). Past evaluations of effectiveness of soil conservation planting have undertaken paired comparisons between treated and untreated areas (G. Douglas et al., 2013a), or how erosion status has changed as a result of the treatment. These quantitative approaches measure the effectiveness of individual trees or tree stands in terms of relative reduction in bare ground or amount of landsliding (G. Douglas et al., 2013a; Douglas et al., 2009; Hawley and Dymond, 1988; McIvor et al., 2011, 2015).

A novel method was developed by Hawley and Dymond (1988) to quantify the fraction of eroded soil following landslide-triggering storm events at increasing radial extents from trees. For their study area in Ngatapa, Gisborne, where a rainfall event in March 1985 triggered extensive shallow landsliding, spacing of 14-year-old trees was 20 m and 66% of the planted trees had survived. The measured reduction in landsliding due to trees for the storm event was 13.8%. However, because the fraction of eroded soil increased with distance from trees, Hawley and Dymond (1988) calculated that if trees had been planted at 10-m spacing, the reduction in landslide damage achieved would likely have been 70% if trees were fully

established and all had survived. This is because the fraction of eroded soil between 0-5 m was considerably less than between 5-15 m from the tree. The potential reduction of 70% was calculated based on a single storm event and on a single steep slope underlain by ash over unconsolidated mudstone. The site was assumed to be uniform, that is to say, the influence of other factors, such as variation in slope gradient, was not considered. However, this study was the first to suggest that the influence of trees could be inferred through the spatial relationship to bare ground from landslide erosion.

A paired comparison study following a storm event in April 2011 in the Hawke's Bay, selected 86 sites with trees (defined as stands of 1-14 trees) and 25 control sites with pasture only (McIvor et al., 2015). Groups of trees were chosen by i) location on upper and mid slope, ii) the presence of slips nearby and iii) trees with small canopy indicating a young age. The control sites were in close proximity to a treed site and likely had slips located within them. Landslide erosion was 78% less on sites with trees compared to the pasture control sites.

A similar method was used across 65 sites in the Manawatu and Wairarapa following storms in 2004 and 2006, respectively (G. Douglas et al., 2013a). Besides quantifying the extent to which spaced trees reduced the occurrence of shallow landslides on pasture-covered slopes, the objective was to determine the influence of selected site and above-ground tree attributes on the extent of landsliding. Trees reduced landslide occurrence by 95 % compared to paired pasture control sites (0.4% vs. 7.9% scar area, respectively), and scars occurred on fewer sites with trees than pasture (10 vs. 45). Logistic regression and discriminant analyses were performed by comparing sites with and without landsliding. An interesting result was that smaller values of slope roughness (standard deviation of slope) tended to increase the probability of landslide occurrence. The paired comparison studies assume a uniform influence of all trees up to a radius of 10-m (G. Douglas et al., 2013a; McIvor et al., 2015). However, Hawley and Dymond (1988) demonstrated that the tree effect on slope stability decreases rapidly following a sigmoidal curve.

Having introduced silvopastoral systems, summarizing previous research related to tree effects on pasture and soil conservation, the following section will delve more deeply into the concept of slope stability, with a focus on the biophysical mechanisms of trees that can modify hillslope processes.

2.3 Slope Stability

2.3.1 Introduction to Slope Stability

Slope (in)stability can be defined as the propensity for a slope to undergo morphologically and structurally disruptive landslide processes (Glade and Crozier, 2005). Slopes that fail by shear are unstable when the forces of gravity acting on the soil mass (shear stress) exceed the strength of the soil at its base and within it (shear strength) (Barnes, 2016). The degree of stability can be approximated by quantifying balance between the shear strength and shear stress of the soil. On a slope, the force of gravity can be resolved into two components: a component acting normal to the slip surfaces and a component acting tangential to the slip surfaces. The normal force, *N*, acting on the soil helps to hold the object in place on the slope (Figure 2.2). The tangential component of gravity, *T*, causes a shear stress parallel to the slope that pulls the object in the down-slope direction parallel to the slope. As a slope steepens, the shear stress or tangential component of gravity, *T*, increases and the normal component of gravity, *N*, decreases. Shear strength is defined as the maximum value of shear stress the soil can withstand (Duncan et al., 2014). In its basic form, shear strength is a function of normal stress on the slip surface (σ), cohesion (c), and internal friction angle ($\emptyset$) (Figure 2.2). Cohesion is the bonding of soil particles (clays and silts), whereas the internal friction angle is the interlocking of individual grains or aggregates (Sidle and Ochiai, 2006). Controlling factors of shear strength include soil composition (e.g., grain size, shape of particles, etc.), soil structure (arrangement of particles, e.g., compacted, cemented, isotropic), and loading conditions. Clay-

rich soils are generally highly cohesive due to the increased surface contact area of clay particles; whereas granular materials (e.g., sands) are cohesionless since the particles do not bond or adhere to another (Duncan et al., 2014; Sidle and Ochiai, 2006).

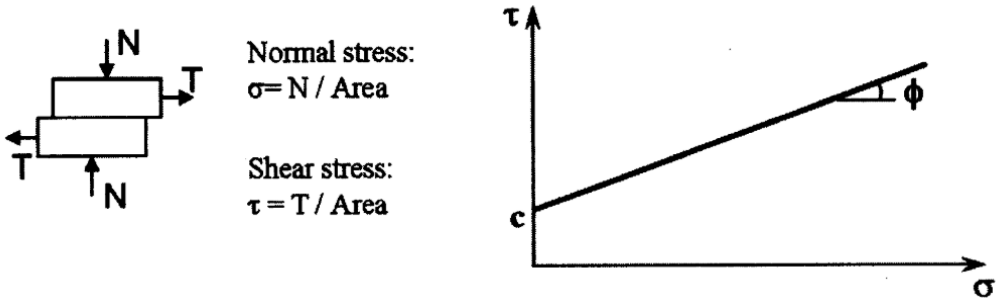

Figure 2.2. Mohr-Coulomb failure envelope describing the shear strength of soils, with the cohesion value (c) shown as the r-axis intercept. N and T are the normal and tangential forces on the slip surface within a slice, respectively. Source: Sidle and Ochiai (2006).

Shear strength of soil can be expressed using the general Mohr-Coulomb failure criterion:

$$s_s = c + \sigma(\tan \emptyset)$$

where cohesion (c) is the inter-particular attraction of like materials; the internal friction angle ($\emptyset$) is the stress-dependent component which is similar to sliding friction of two or more soil particles; and normal stress (σ_n) is due to the weight of the soil and water. Increased pore pressure resulting from heavy rainfall and/or rising groundwater levels reduce the effective stresses in slopes. This reduction in shear strength can be included as:

$$s_s = c' + (\sigma - \mu)\ (\tan \emptyset)'$$

where μ is the positive pore water pressure. The prime refers to effective normal stress in saturated soil, which is the difference between total normal stress σ and positive pore water pressure μ (Sidle and Ochiai, 2006). Cohesion is also reduced in saturated soils since water films surrounding individual particles leads to a reduction in shear resistance.

The shear strength of a soil is the maximum stress the soil material can sustain against the force of a failure. The ratio of the available shear strength to shear stress is the factor-of-safety:

$F_S = R/L$

where F_S is the factor of safety, R is the resistance of stabilizing forces (i.e., soil shear strength) and L is the load from destabilising forces, composed of the gravitational driving forces of the soil mass (i.e., the shear stress) (Wu, 1995).

Where $F_S > 1$, the slope is considered stable or in a static state. For unstable slopes, at the point of movement, the shear stress along the failure surface reaches the shear strength, so that the factor-of-safety is assumed to equal 1. There are multiple reasons for temporal changes to F_S, and include short-term (e.g., rainfall event) or seasonal changes in water content, increasing the soil weight and leading to changes in soil suction and pore water pressure; or the influence of changes in vegetation cover (e.g., following forest harvest) that can reduce the additional soil strength and alter the physiochemical characteristics due to root growth and decay processes (Lucas et al., 2019; Murgia et al., 2022; Ziemer, 1981). It has been argued that the excess of strength is a more appropriate measurement of slope stability than the ratio expressed by F_S, as two slopes may have the same ratio of shear strength to shear stress, but entirely different absolute values of excess strength (Glade and Crozier, 2005). The excess strength is the more consequential measure for slope stability, as it represents the quantity which must be reduced before slope failure can occur. This measure is referred to as the margin of stability, and together with the factor of safety can inform on the degree of slope stability.

In a very broad sense, slope instability can also be determined by the magnitude and frequency of external destabilising forces acting on the slope. Slopes can be represented along a line of stability ranging from a high margin of stability to a low margin of stability (Figure 2.3). Three differing states of stability can be defined along this spectrum. Slopes classified within the “stable state” have a margin of stability great enough to withstand natural destabilizing forces typical of the given environmental system. Marginally stable slopes are slopes which are currently stable, but susceptible to failure as soon as dynamic external forces exceed a certain threshold. The third conceptual stability state is the actively unstable state, corresponding to slopes with a margin of stability near zero, which experience continuous or

intermittent movement (Glade and Crozier, 2005). This conceptual model which includes the three states of stability recognizes the causes and development of slope instability through time.

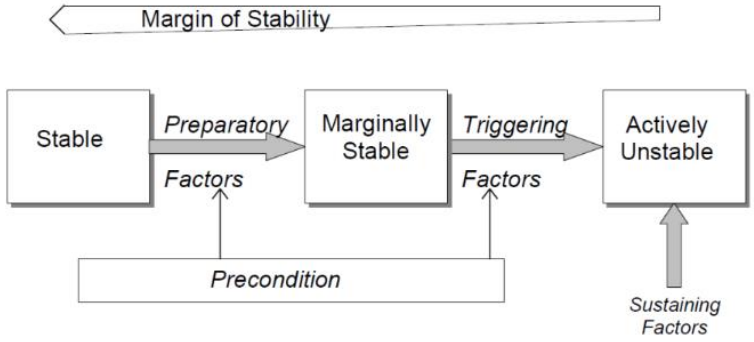

Figure 2.3 Stability states and destabilizing factors. Source: Glade and Crozier (2005).

Moreover, it is important to distinguish between preparatory, triggering and sustaining factors that influence slope stability in different ways (Figure 2.3). Preconditioning or pre-disposing factors include all intrinsic factors of an area which provide the circumstances for destabilizing factors to work more effectively. An example would be a steep slope with an underlying failure plane rich in clay, which under the influence of a prolonged rainfall event could provide the ideal setting for slope failure. Preconditioning factors can be defined as preparatory or triggering factors. Preparatory factors decrease the margin of stability over time without triggering slope failure, thus causing a shift from a stable state to a marginally stable state. Preparatory factors may act over all time scales. Factors operating over long periods include tectonic uplift and/or climate change, whereas processes such as deforestation or slope oversteepening due to erosion activity or slope excavations are examples of shorter time scales. Triggering factors are processes that initiate the movement, causing a shift from a marginally stable state to an actively unstable state. Typical triggering factors include high intensity rainfall, prolonged rainfall, rapid snowmelt, earthquakes, and slope undercutting. Finally, sustaining factors determine the behaviour of actively unstable slopes, e.g., duration, rate, and the form of movement. These may either be dynamic external factors like rainfall or may e.g., relate to the path of the landslide and potential obstacles it may encounter. Land cover change can be an important preparatory factor when it reduces the slope stability (e.g., deforestation).

Indeed, woody vegetation provides an important role in terms of slope stability in many parts of world – frequently acting as an actively managed protection to infrastructure (Dorren and Schwarz, 2016). Based on this brief introduction on slope stability, the following section considers how trees modify slopes to increase the margin of stability.

2.3.2 The Role of Trees in Modifying Slope Stability

There are two mechanisms by which vegetation influences slope stability: hydrological and mechanical (Table 2.2). First, vegetation modifies water infiltration and soil moisture content – most importantly through interception (water storage) and evapotranspiration (Phillips and Marden, 2005; Sidle and Ochiai, 2006). Hydrological mechanisms that reduce pore-water pressures in the soil are beneficial, whereas processes that increase pore pressure are adverse. Second, the mechanical influence through lateral and basal root reinforcement increases soil shear strength and thus promotes slope stability in shallow soils (Schmidt et al., 2001).

Table 2.2. Relative influences of woody vegetation on slope stability from Sidle and Ochiai (2006). 'A' denotes mechanisms adverse to stability, 'MA' denotes marginally adverse, and 'B' denotes beneficial mechanisms.

Mechanisms	**Influence on shallow, rapid landslides**
Hydrological mechanisms	
1. Interception of rainfall and snow by canopies of vegetation, thus promoting evaporation and reducing water available for infiltration	B
2. Root systems extract water from the soil for physiological purposes (via transpiration), leading to lower soil moisture levels	B
3. Roots, stems, and organic litter increase ground surface roughness and soil's infiltration capacity	MA
4. Depletion of soil moisture may cause desiccation cracks, resulting in higher infiltration capacity and short-circuiting of infiltrating water to a deeper failure plane	MA
Mechanical mechanisms	
5. Individual strong woody roots anchor the lower soil mantle into the more stable substrate	B
6. Strong roots tie across planes of weakness along the flanks of potential landslides	B
7. Roots provide a membrane of reinforcement to the soil mantle, increasing soil shear strength	B
8. Roots of woody vegetation anchor into firm strata, providing support to the upslope soil mantle through buttressing and arching	B
9. Weight of trees (surcharge) increases the normal and downhill force components	MA
10. Wind transmits dynamic forces to the soil mantle via the tree bole	A

This is achieved through an apparent cohesion produced by root fibre reinforcement in the soil mantle, which is a function of the topology and morphology of root systems, the spatial arrangement and soil-root mechanical (frictional) interactions. The following two sections summarize these two mechanisms that influence soil reinforcement.

Hydrological mechanisms

Hydrological effects of plants have direct influence by means of interception of precipitation, evapotranspiration, and preferential runoff along stems and roots (Phillips and Marden, 2005). Interacting processes between soil, plant and atmosphere generate a hydrological effect that can be divided into wetting (i.e., the rainfall event) and drying components (Gonzalez-Ollauri and Mickovski, 2017). Drying mechanisms include all processes that reduce the soil moisture content during and following the wetting event. During a wetting event, precipitation is intercepted by the canopy, which reduces the amount of rainfall reaching the soil in the short-term. The effectiveness of interception as a water storage function is governed by the size of a canopy and foliage. Canopy cover can be defined as the "*proportion of the forest floor covered by the vertical projection of the tree crowns"* and is not to be confused with canopy closure, which refers to *"the proportion of sky hemisphere obscured by vegetation when viewed from a single point"* (Jennings et al., 1999). There are three broad approaches to estimating canopy cover: 1) field measurements, 2) statistical models, and 3) terrestrial or airborne laser scanning. Ground-based techniques for estimating canopy cover based on the vertical projection include the Cajanus tube (Korhonen et al., 2006). Many other ground-based measurements of above-ground biomass have been proposed (Seidel et al., 2011). More recently, terrestrial laser scanning has been used to develop allometric models for upscaling for estimates of forest biomass (Lau et al., 2019).

While intercepted rainfall can evaporate directly back into the atmosphere, its effect will be reduced for landslide-triggering rainfall events of short duration and high intensity. In such instances, canopy saturation can be reached which leads to a decrease in the interception

capacity (Gonzalez-Ollauri and Mickovski, 2017; Van Dijk and Bruijnzeel, 2001). Rainfall storage and evaporation from the tree canopy are more important for regulating soil moisture during long-duration and moderate-intensity rainfall. Preferential flow-paths along the stem can counteract the positive influence of interception on slope stability (e.g., 11% of total rainfall was concentrated around the stem in a study by Gonzalez-Ollauri and Mickovski (2017)). Bypass flow channels water to the tree base, which can enter the soil more easily following existing root channels (Levia and Germer, 2015). However, preferential flow along root systems also provides better drainage – particularly in soils with high macroporosity (Liang et al., 2011; Lucas et al., 2019).

Plant transpiration is the most important drying mechanism of plants and involves the uptake of water from the soil to meet the physiological needs of the plant and transpiration into the atmosphere through stomatal openings in the foliage (Laio, 2006; Sidle and Ochiai, 2006). Transpiration is influenced largely by the potential evapotranspiration of the atmosphere, water supply from the root zone, and the capacity of water conveyance of the vegetation (Wang et al., 2019). The canopy leaf area index (LAI) is an important functional parameter for both evaporation and transpiration, following interception by the canopy. It is commonly defined as one half of the total leaf area per unit ground area (Jennings et al., 1999; Jonckheere et al., 2004). Generally, the higher the leaf-area index, the greater the transpiration rates, although the relationship follows a sigmoidal shape, with transpiration increasing with LAI then gradually reaching an asymptotic threshold at which point transpiration is stable (Van Dijk and Bruijnzeel, 2001; Wang et al., 2019).

Whitehead and Kelliher (1991) modelled the annual water balance components for a Pinus radiata stand in New Zealand and found the combined effects of transpiration and evaporation (both by tree canopy and understorey) to account for 62% of annual rainfall. This demonstrates that hydrological mechanisms can significantly modify soil moisture over long time scales and thus reduce pore water pressure preceding a rainfall storm event (Wahren et al., 2009). Indeed, the temporal component of hydrological plant processes is an important consideration. In

temperate climates, plant transpiration is a seasonal process and rates of evapotranspiration can vary with changes in interannual precipitation and associated soil moisture, and atmospheric water demand (Wever et al., 2002). Moreover, shading produced by the plant canopy can reduce direct soil evaporation, which can be seasonal depending on species and foliage (Raz-Yaseef et al., 2010). This drying mechanism is likely to be more significant in silvopastoral and other agroforestry systems with limited canopy cover compared to forest stands. And outside of the growing season, direct soil evaporation is the primary hydrological mechanism that modifies soil moisture, reducing pore-water pressures and potentially increasing soil strength prior to a rainfall storm event.

The hydrological plant mechanisms are difficult to quantify (Stokes et al., 2014; Zillgens et al., 2007). Gonzalez-Ollauri and Mickovski (2017) proposed a framework for quantifying the hydrological mechanisms of vegetation against rainfall-induced landslides. The authors found that during heavy rainfall events most of the rainfall reaches the ground following canopy saturation. Therefore, the interception is likely to be more effective at regulating soil moisture levels during prolonged periods of moderate rainfall – particularly compared to non-vegetated, fallow soil. As previous studies have hypothesised (e.g., Stokes et al., 2014), plant-water uptake was shown to be the most important hydrological mechanism by which plants increase slope stability. Bypass flow triggered by stemflow had a negligible effect on slope stability. And most importantly, under critical hydrological wetting conditions, the effect on slope stability was only minimal, a result which points to the mechanical mechanism of root reinforcement being of greater importance for slope stability. During the winter rainy season of temperate climates, and relative to mechanical mechanisms, the hydrological effect of vegetation on slope stability is relatively minor since soils are always relatively close to saturation (Sidle and Ochiai, 2006). However, when large rainfall events occur during drier conditions, evapotranspiration of trees modify antecedent soil moisture conditions, which affects landslide initiation. The influence of seasonally dormant deciduous trees on soil moisture is more pronounced during the drier summer months in temperate climates, with interception of rainfall by foliage and greater

evapotranspiration relative to winter months. This is an important consideration in the New Zealand context, where high magnitude rainfall events – often in the form of ex-tropical cyclones – are a frequent occurrence during warmer, drier months of the year (Bergin et al., 1995; Dymond et al., 2006; Marden and Rowan, 1993; Smith et al., 2021). However, the contribution of tree roots to slope stability is generally considered to be more important than the combined hydrological processes that modify soil moisture (Sidle and Ochiai, 2006)

Mechanical mechanisms

Vegetation roots stabilize slopes by increasing the shear strength of the soil. This is achieved through an apparent cohesion produced by root fibre reinforcement in soils, which is a function of the tensile strength of the roots in combination with the binding action in the root fibre/soil composite and adhesion of soil particles to roots (Reubens et al., 2007; Roering et al., 2003; Schmidt et al., 2001; Sidle and Ochiai, 2006; Styczen and Morgan, 1995). The primary mechanical function relevant to shallow landsliding is through basal root reinforcement, which is achieved when roots penetrate the shear plane, thus increasing the basal shear strength (Schwarz et al., 2010b). Lateral root reinforcement governs the onset and size of shallow landslides (Roering et al., 2003; Schmidt et al., 2001; Schwarz et al., 2010b). The influence of root reinforcement is expressed as a cohesion term (root cohesion c_r) in the Coulomb failure criteria where the soil increases the soil-root composite shear strength:

$$S_{sr} = c'_s + c_r + (\sigma - \mu) \tan \emptyset'$$

where c'_s is the effective cohesion of the soil, σ is the normal stress due to the weight of the soil and water of the sliding mass, u is the soil pore-water pressure, and $\emptyset'$ is the effective internal friction angle of the soil that is assumed unaltered by the presence of roots. However, various studies have shown that roots can change the aggregate formation of soils resulting in an increase in the friction angle and aggregate stability (Bast et al., 2014; Graf et al., 2009).

Vegetation roots can be defined and classified in different ways (Gregory, 2006; Reubens et al., 2007; Styczen and Morgan, 1995). Taproots are the main vertical roots below the bole of the tree; lateral roots extend from the central bole in the horizontal plane; sinker roots are vertical roots that branch out from lateral roots (Phillips and Marden, 2005). Root system architecture impacts on slope stability. Therefore, tree selection is important with respect to soil type, lithology, and mass movement process (Figure 2.4).

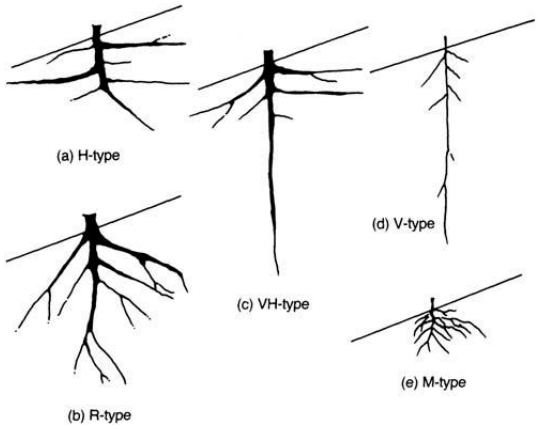

Figure 2.4. Representation of root classes illustrated by Styczen and Morgan (1995): a) H-type maximum root development occurs at moderate depth (>80% of biomass found in top 60 cm), with most roots extending horizontally and having a wide lateral extent; b) R-type: maximum root development is deep with only 20% of the root matrix found in the top 60 cm; most of the main roots extend obliquely or at right angles to the slope and their lateral extent is wide; c) VH-type: maximum root development is moderate to deep but 80% of the root matrix occurs within the top 60 cm; there is a strong tap root but the lateral roots grow horizontally and profusely, and their lateral extent is wide; d) V-type: maximum root development is moderate to deep; there is a strong tap root but the lateral roots are sparse and narrow in extent; e) M-type: maximum root development is deep but 80% of the root matrix occurs within the top 30 cm; the main roots grow profusely and massively under the stump and have a narrow lateral extent. H- and VH-types are considered beneficial for slope stabilization and wind resistance. H- and M-types are beneficial for soil reinforcement. The V-type is wind resistant.

Root reinforcement is generally a function of the root tensile strength (differing with tree species), topology and morphology of root systems (e.g. length, diameter, branching), the spatial arrangement (distribution and density of fine and course roots; maximum root length), and soil-root mechanical (frictional) interactions (Cohen and Schwarz, 2017; Schwarz et al., 2010b). Fine and coarse roots have different functions: A dense network of fine roots are more effective at soil fixation than coarse roots (Reubens et al., 2007). Fine roots stay in position relative to the soil particles, thus having a stiffening effect on the soil mass (Cohen and Schwarz, 2017). While fine roots tend to break during slope failure, coarse roots can slip out of soil. However, the reverse has also been observed, i.e., situations in which fine roots slip and

coarse roots snap (Giadrossich et al., 2019). It was therefore suggested that the root behaviour varies as a function of landslide head scarp orientation relative to root orientation from nearby trees. However, only the coarse roots are able to reinforce shallow soils by anchoring deeply into firm strata, which is particularly effective when sinker or tap roots extend deeper than the position of failure surface of a potential shallow landslides (Cohen and Schwarz, 2017; Reubens et al., 2007).

The development of root systems is influenced by environmental factors, which include the soil type (compression properties), as well as available soil water and nutrients. Generally, root morphologies are modified by edaphic factors that include physical soil conditions, particularly stoniness, drainage conditions, depth of the water table, bedrock conditions or the strength and permeability of strata (Figure 2.5; Phillips and Marden, 2005). For example, shallow plate-like root structures can be found on steep slopes where shallow soils directly overlie massive bedrock (Marden et al., 1991).

The contribution of roots to soil cohesion is dependent on the material properties of the roots as well as the morphology of root systems (Stokes et al., 2009). Besides the influence of soil properties, the rate at which soil is colonised by roots is dependent on the lateral and vertical growth rate of a given species and planting density (Phillips et al., 2011a). When root system architecture is known, planting densities can account for the root lengths to permit root site-occupancy, i.e., the state where roots contribute to soil reinforcement through interlocking root systems (Phillips et al., 2011a; Watson et al., 1999).

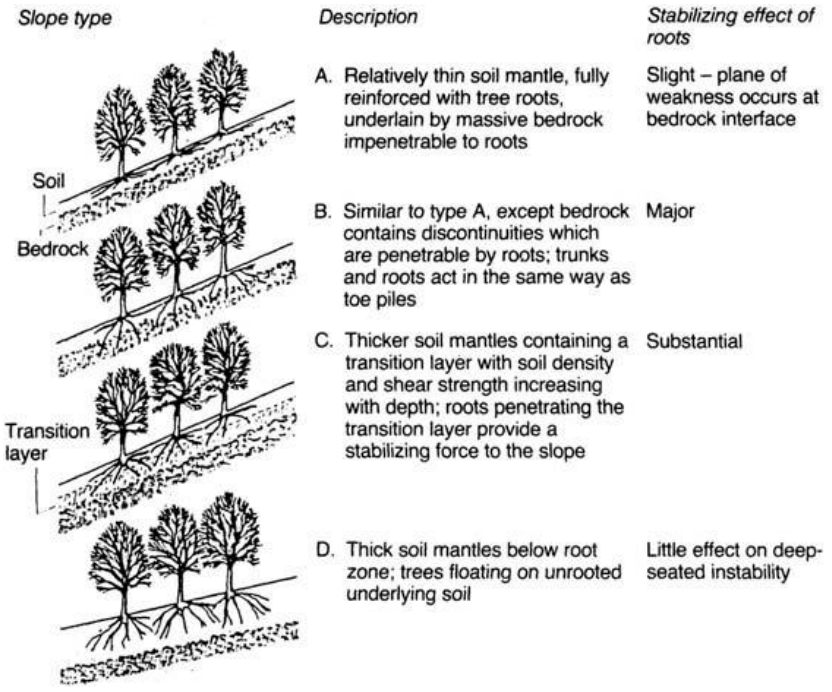

Figure 2.5 Classes of plant-root reinforced and anchored slopes (Source: Styczen and Morgan, 1995).

This variation of root morphology and distribution is difficult to predict due to the interplay of biological mechanisms and environmental factors (Reubens et al., 2007). Indeed, root system architecture can be highly variable - even within a single species growing in different environments (Schmidt et al., 2001; Schwarz et al., 2016). This complexity of parameters that influence the growth of root systems poses challenges to the quantification and spatial-explicit modelling of root reinforcement. The following section introduces some common methods for measuring root strength and developing root reinforcement models.

Root reinforcement modelling

Resistance to soil failure is maximised when the tensile strength of roots is fully mobilised under strain, which can occur when roots are stiffly bound to the soil to cause a compatible behaviour between soil and roots (Styczen and Morgan, 1995). When the tensile strength is exceeded by the shear force acting on a slip plane, roots fail by rupture. Root failure by pull-out (slipping) occurs prior to reaching peak tensile strength when the bond of the soil-root composite is not as strong. Thus, the increase in soil cohesion due to root reinforcement

(apparent root cohesion) is primarily a function of the tensile strength of individual roots and root systems (Schwarz et al., 2010b).

There are several techniques that can be used to quantify the tensile strength of roots. These experimental methods for root reinforcement can be broadly classified into tests on individual roots and tests on the soil-root matrix (Giadrossich et al., 2017). The key difference is that data obtained from tests on individual roots represent a measure of the specific behaviour of that root, whereas roots in a soil-root matrix are part of the soil system so that the resulting measure captures the variation of friction at the root-soil interface, the influence of branching points, and the stress-strain relationships of a population of root fibres (Cohen et al., 2011; Giadrossich et al., 2017; Schwarz et al., 2010b, 2010c). The strength of individual roots is measured in the laboratory using tensile tests (e.g., Nilaweera and Nutalaya (1999)). Direct shear tests are the most common method for testing the root-soil matrix using a shear-box in the laboratory or in the field (Wu and Watson, 1998). These two experimental methods mirror the evolution of modelling frameworks for root reinforcement and have implications for model assumptions and predictions of root cohesion.

Root reinforcement models can be classified according to assumptions about root failure dynamics (Giadrossich et al., 2017). The 'all-at-once' breakage method or 'Wu/Waldron model' (Waldron, 1977; Wu et al., 1979) assumes simultaneous breakage of the roots. These models consider the root force independent of displacement and fully available at all displacement, that is, the maximum tensile strength is fully mobilised. Moreover, it is assumed that breakage of the root occurs at the shear plane. However, this has been demonstrated to be invalid since breakage often occurs below the shear surface where the root diameter is smaller than at the shear plane (Giadrossich et al., 2017, 2013; Hubble et al., 2010; Vergani et al., 2016). These limitations led to the development of root bundle models, which consider the dynamic stress-step or strain-step loading of a root system (Cohen et al., 2011; Pollen and Simon, 2005; Schwarz et al., 2013, 2010b). The advantage of these models is that they consider root strength as a function of displacement.

The study by Schmidt et al. (2001) is an example where root reinforcement is quantified based on the Wu and Waldron model, that is, on the assumption that the interaction between root threads and the soil matrix is such that root cohesion is limited by the thread strength of the roots themselves, not the bond between the roots and soil. The objective of the study was to back calculate root cohesion based on measurements on landslide scarps, combined with pits on stable ground to help explain the spatial pattern of landsliding. The model assumed all roots break simultaneously, and that roots cross a shear zone perpendicularly and the ultimate thread strength is mobilized, so that the total tensile root-thread strength of a given species per unit area of soil t_r, is expressed as:

$$t_r = \sum_{i=1}^{n} T_{ri} \left(\frac{A_{ri}}{A_s} \right)$$

where A_{ri} / A_s is the root area ratio or proportion of root cross-sectional area to soil cross-sectional area (A_s), T_{ri} the tensile strength of an individual root thread, and *n* is the number of roots in area A_s. Regression curves of thread strength versus root diameter data were then used to extrapolate root tensile strength. Based on the attributes from the root inventory, a spatially weighted mean was calculated to represent a single value of root cohesion for each site. This method helped increase understanding of variation in root cohesion within and between forested landscapes as a function of species and age of vegetation as well as clear-cuts. However, the model does not quantify root cohesion as a function of distance from tree stems.

Two examples of spatially distributed modelling of root reinforcement at tree stand scale are Sakals and Sidle (2004) and the framework introduced by Schwarz et al. (2010a). The former of these was developed to assess the spatial variability of root cohesion based on a calibration of measured root cohesion from a Douglas-fir stand of 20 root systems using an intermediate value of 12.0 kPA. Root cohesion was expressed as a function of volume of root biomass (Ziemer, 1981), approximated using a disc of regular radii regardless of slope. Furthermore, root cohesion was expressed as the summation of components from neighbouring

trees where roots were assumed to interlock. The root influence radius was defined as the radius at which the root density dropped by 99%. Based on data from the 20 inventoried root systems, this relationship was expressed as a linear function of age of tree. The relationship between normalized root densities and root influence radii was found to be sigmoidal in shape, differing slightly between two age groups of trees. The resulting horizontal distribution of root cohesion is a function of distance from the bole of a tree of a given age, assuming an increase in soil strength results from an increase in root biomass.

Cohen et al. (2011), Schwarz et al. (2010a, 2010b) developed a spatially explicit root reinforcement model called the Fiber/Root Bundle Model (RBM). The primary improvement to pre-existing models (e.g., (Schmidt et al., 2001) is the estimation of progressive root reinforcement of root bundles based on the observation that activation of root strength within bundles is not synchronous due to progressive root failure (Schwarz et al., 2012). The RBM was applied at stand scale to obtain a quantitative estimate of root reinforcement (Schwarz et al., 2012). The RBM introduces a strain-step loading approach to calculate the force-displacement behaviour of individual roots of a bundle while considering the progressive failure of roots as a function of displacement (Schwarz et al., 2016). The framework consists of two main components: 1) a root distribution model, and 2) mechanical properties of individual roots (Schwarz et al., 2010b).

The root distribution model is based on information on the fine-root distribution (< 1.5 mm diameter), which can be estimated based on an allometric parameter (P) of a tree such as crown volume or stem diameter:

$$N_{fr} = \mu \cdot P$$

where N_{fr} is the total number of fine roots, μ is a 'pipe theory' coefficient (N^o/m^2). Similarly, the maximum radial extent of a root system can be estimated using empirical relationships to above-ground biomass (Ammer and Wagner, 2005; Roering et al., 2003). For example, an empirical relationship with the diameter at breast height (DBH) has been used

(Schwarz et al., 2016, 2010b). The distribution of course roots of primary and secondary root systems is assumed to correlate with the mean fine-root distribution, and is estimated as a function of distance from the tree stem assuming a constant value of branching distance (Ozier-Lafontaine et al., 1999). At each branching point, a coarse root splits into smaller diameter roots, maintaining a constant proportionality factor between pre-branching cross-sectional area and the sum of cross-sectional areas of finer roots after branching. Thus, the maximum root diameter is calculated for each distance from tree stem. In so doing, the root distribution is established as a function of distance from tree stem and calibrated based on empirical data related to the number of roots in each root diameter class (Schwarz et al., 2010b).

The mechanical behaviour of individual roots with different diameters are estimated considering various mechanical and geometrical interactions. Two factors are of primary importance. The first is the observation that Young's modulus increases with initial strain applied – owing to the geometrical adjustment of roots from their initially tortuous arrangement as the stretch – then as the strain increases, Young's modulus decreases once the entire root is activated and contributes to root-soil friction (Commandeur and Pyles, 1991; Hamza et al., 2007; Schwarz et al., 2010b). The second factor is the presence of branching points, which increase resistance depending on soil moisture and branching order. The geometrical and mechanical characteristics of roots are given by power-law equations that relate root diameter to tortuous root length, apparent Young's modulus, and maximum tensile force (Schwarz et al., 2012).

The models for root density distribution and mechanical behaviour of individual roots allows the stress-strain relationship for root bundles to be quantified. Geometrical parameters for each root (e.g., root length, number of branching points) are combined with mechanical parameters (e.g., maximum strength of individual root) to obtain the dominant failure mechanism, that is, stretching, slipping out, or breaking(Schwarz et al., 2010b). A Weibull survival function is used that considers the mechanical variability of root strength due to root material properties, root geometry, and soil mechanical conditions (Schwarz et al., 2016, 2013).

The RBM was calibrated using data obtained from poplars in Gisborne and Palmerston North, New Zealand. The results were used in slope stability calculations to quantitatively evaluate the mechanical stabilization effects of spaced trees on pastoral hill country (Schwarz et al., 2016).

Physical slope stability modelling that incorporates root reinforcement models – as introduced here, have the advantage that a landslide inventory is not necessarily a requirement to quantify the effect of biological erosion mitigation, since the increase in shear strength due to the presence of trees can be quantified independently to inform on the effectiveness under a range of scenarios (e.g., fully saturated soils, failure at different depths). A rainfall-induced landslide event is commonly used for validation purposes. A disadvantage of this method is that soil strength parameters (cohesion, internal friction angle) are generally not available at the scale required and many assumptions related to the variation in root systems and environmental conditions must be made. Furthermore, the method is generally used for landscapes with homogenous vegetation (e.g., forestry) since root data collection for multiple species and age classes is too time-consuming and costly. Moreover, there is currently a paucity of root data from silvopastoral systems since most research on root reinforcement has been focused on protection forests in Europe and North America. As a consequence, the root reinforcement models may underestimate the extent of below-ground biomass of trees in silvopastoral systems given the reduced competition for nutrients, water and light compared with high density plantation forests. A recent review of physically-based models provides further details on the strengths and weaknesses of the different approaches, including data requirements, parameters, and assumptions (Murgia et al., 2022).

Having summarised how trees modify slope stability and how these processes can be quantified and incorporated into (physical) slope stability models, the following section introduces statistical approaches to slope stability.

2.3.3 Statistical Landslide Susceptibility Modelling

A vast quantity of literature deals with the subject of slope stability modelling from slope to national scales (e.g., (Guzzetti et al., 2006; Reichenbach et al., 2018; Van Den Eeckhaut et al., 2006; van Westen et al., 2008). There are generally two data-driven approaches to modelling slope stability: i) physically-based or ii) statistical modelling. The first of these approaches are physically-based models that aim to quantify the soil shear strength and stresses, commonly using the safety factor to determine (in-)stability – frequently simulating a range of rainfall scenarios that alter the hydrological soil conditions (e.g., Wu and Sidle, 1995). However, due to the data requirements relating to the physical parameters of the soil (cohesion, internal angle of friction, hydrological parameters) and knowledge of failure mechanism (e.g., depth of failure plane) – which can be highly variable in hilly or steep landscapes, such approaches are best suited to hillslope scale and less practical at regional scales (Holcombe et al., 2012; Masi et al., 2021). For larger areas, simplified assumptions must be made (Salvatici et al., 2018), which can result in poorer performance of physical models compared with statistical methods (e.g., Cervi et al., 2010).

The alternative approach to slope stability modelling is statistical landslide susceptibility modelling. Statistical models differ to physically-based models in that they do not attempt to model the physical processes that control slope stability. Rather, and in the absence of geotechnical soil data, statistical models use readily available surrogate data and therefore have less stringent data requirements compared with physical models. Thus, statistically conceived, landslide susceptibility is the probability of future landslide occurrence for a given areal unit given local environmental conditions (Brabb, 1984). Statistical landslide susceptibility models provide an estimation of where future landslides are likely to occur based on the identification of areas of past landslide occurrences. Thereby, an assumption is made that locations with similar physical characteristics to where past failures have occurred are also likely to fail in

future. Indeed, past observations provide "the key to the future" (van Westen et al., 2008). Indeed, this is the major assumption underlying statistical approaches to slope stability.

To elaborate further on landslide susceptibility, definition by negation can be useful to avoid confusing the related concepts of landslide susceptibility, hazard, and risk. Landslide hazard has been defined as "the probability of occurrence of a potentially damaging phenomenon within a given area and in a given period of time" (Guzzetti et al., 1999). Thus, while susceptibility provides spatial information as to the likelihood of future occurrence, and therefore answers the question of *"Where?"*, hazard assessments attempt to determine the location (where), frequency (when) and magnitude (what extent) of the process assessed. Landslide susceptibility modelling is therefore a prerequisite for hazard assessment. Risk assessments look to quantify the adverse consequences (damage) of the hazard, which results through the interaction of a hazard with vulnerable and exposed elements at risk (e.g., a population or infrastructure) (Aleotti and Chowdhury, 1999).

A range of methods can be used to model landslide susceptibility. These are generally grouped into qualitative and quantitative methods (Aleotti and Chowdhury, 1999). Qualitative methods rely heavily on expert knowledge to weight conditioning factors and include heuristic zoning (using expert knowledge). Quantitative methods include a multitude of statistical methods (e.g., bivariate analysis, discriminant analysis, logistic regression, weight-of-evidence, fuzzy logic). Heuristic methods are qualitative and portray susceptibility using descriptive terms, while statistical methods are quantitative based on probability distributions that result in numerical estimates of slope stability. Yet quantitative approaches also rely on heuristic knowledge to identify factors controlling susceptibility to include in the model. Selection of explanatory variables to include in model development ought to be based on an understanding of the geomorphic process being assessed, i.e., all selected factors must have direct physical process relevance for slope stability. For this reason, the vast majority of statistical landslide susceptibility models include lithologic, topographic (e.g., slope gradient, aspect), and

vegetation cover as factors. Regardless of the statistical method applied, statistical approaches to landslide susceptibility rely on past observations of landslides to train and test the models.

Geo-environmental variables commonly used in statistical landslide susceptibility models can be broadly categorized into four groups: 1) morphology, 2) geology and soil, including geotechnical properties, 3) land cover, and 4) hydrological (Reichenbach et al., 2018; van Westen et al., 2008). The following section summarizes these thematic classes and briefly explains their importance for slope stability based on theoretical and empirical observations.

Terrain morphology

Morphological variables are commonly derived from a digital elevation model (DEM) to produce spatial layers representing slope gradient, aspect, curvature, relative relief, or terrain roughness. The utility and effectiveness of morphometric variables is dependent on the scale and accuracy of the elevation data used. Furthermore, if very high-resolution elevation data (e.g., obtained from airborne LiDAR sensors) is available, care must be taken to consider implications related to the acquisition date of the data. Where possible, morphological parameters should be derived from a DEM acquired prior to slope failures. However, processing techniques can also be used to modify the terrain to approximate pre-event morphology (Wechsler and Kroll, 2013).

Terrain slope, (or slope gradient), is the most important environmental variable used in landslide susceptibility modelling (Budimir et al., 2015; Chung and Fabbri, 2003; Reichenbach et al., 2018). The reason for its effective explanatory power is directly related to the physics of gravitational failure: the slope gradient controls the stresses and resistance acting on a slope to maintain stability (Wu and Sidle, 1995). The greater the slope gradient, the greater the resistance force mobilized in response to increasing driving force. Particularly in combination with thematic variables pertaining to the mechanical properties of soil and lithology, terrain slope can be a very good predictor of slope failure (Betts et al., 2017).

Slope aspect is frequently used as a predisposing factor in landslide susceptibility assessments (e.g., Galli et al., 2008; Ruff and Czurda, 2008; Salter et al., 1983; van Westen et al., 2008). It has been suggested that contrasting microclimate between slopes of different aspect can produce asymmetric valley morphology through control of slope weathering and erosional and depositional processes (Burnett et al., 2008). The direction of incoming weather events may also create a 'shadow effect', impacting some slopes more than others (Liu and Shih, 2013). Statistical analyses of the distribution of landslides triggered in the winter of 1977 in the Wairarapa of New Zealand found a strong preference for northerly aspects (61.6% of slips on N, NW, and NE octants; Crozier et al., 1980). Similarly, another Wairarapa-based study reports a preference for northerly aspects, which they suggest is a product of deeper weathering from increased solar radiation and wetting and drying cycles experienced by north-facing (southern hemisphere) slopes (Gao and Maro, 2010). Wetting and drying cycles also initiate cracking, resulting in reduced soil cohesion (He et al., 2020) and allowing water to penetrate down to the less permeable bedrock which acts as the surface of rupture (Brooks et al., 2002). The effect of aspect can also be related to structural geology (e.g., dip direction and dip angle of bedding planes; (Ruff and Czurda, 2008). There are indications that landslide preference to a particular slope aspect can be temporally dynamic: Crozier et al. (1980) found weakest conditions at the bedrock/regolith interface on southerly slopes, and north to west-facing slopes were less disturbed. They therefore postulate that following removal of the original forest cover for pastoral farming, mass movement processes may have initially favoured southern slopes, providing a more extensive, weaker, and undisturbed regolith on north-facing slopes – which was more severely affected in recent times (e.g., the 1977 landslide-triggering rainfall event (Crozier et al., 1980; Gao and Maro, 2010)). Indeed, this is in concert with the conception of landslide susceptibility as temporally dynamic (Gorsevski et al., 2006).

Other common terrain variables included in a landslide susceptibility model are related to hydrological influences on slope stability. Slope curvature (e.g., profile, planar) is the third most used morphological variable in statistical models (Reichenbach et al. 2018). Concave

slopes concentrate surface runoff and subsurface groundwater flow, increasing pore water pressure. The topographic wetness index (TWI) is another hydrologically relevant variable as a measure for accumulated water or soil saturation (Moore et al., 1991, 1988).

Lithology

Geological data are important in landslide susceptibility modelling, because the material type directly influences soil properties such as hydraulic conductivity and texture (Smith et al., 2021). For example, Crozier et al. (1980) found fewer shallow landslides in areas of alluvium, limestone, and sandstone compared with less permeable formations of mudstone and alternating sedimentary rocks. The value of the spatial dataset is dependent on the scale and type of information represented. Most often, the type of rock is related to the chronostratigraphic units and formations that may not necessarily have a relationship with the mechanical properties of the materials that are relevant for the geomorphological process being assessed (Reichenbach et al., 2018). QMAP, the 1:250,000 scale geological map of New Zealand, is accompanied by detailed texts that describe mapping units with regard to regional geomorphology, tectonic history, engineering geology, geological hazards and resources (Rattenbury and Isaac, 2012). Supplementary information can potentially be carefully prepared to extract relevant thematic variables to include in a model. However, the small scale of geological mapping units is likely to be a significant limitation. Lithological maps may be of more value, since they include data on the near-surface rock type, which – depending on the mass movement process, may be more relevant than larger stratigraphic units.

Land use and land cover

Vegetation, land use and land cover data (LULC) are frequently used in landslide susceptibility analyses (Knevels et al., 2021, 2020; Reichenbach et al., 2014; Schlögel et al., 2018). Land cover or land use maps are commonly obtained through visual interpretation of aerial photography, by processing of multispectral (incl. LiDAR) or hyperspectral data (Pan et

al., 2020; Weinmann and Weidner, 2018; Yang et al., 2022). In the absence of detailed vegetation classifications that would provide greater resolution in terms of the mechanical and hydrological mechanisms (e.g., root distribution models, canopy cover), land cover maps are often a useful surrogate dataset at landscape and regional scales. However, LULC can be temporally dynamic due to deforestation, construction, etc., and are certainly less static than other geo-environmental variables. Therefore, care must be taken to include LULC data that corresponds to the timing of the event (van Westen et al., 2008). Since the resulting landslide susceptibility prediction depicts a snapshot in time, scenarios that incorporate potential LULC changes can inform on impacts on slope stability.

2.4 Sediment Connectivity

2.4.1 Introduction to Sediment Connectivity

'Connectivity' refers to the efficiency of transfer of water and sediment between components of the catchment system (Wohl et al., 2019). Connectivity has been described as an emergent property of the geomorphic system, since it is an intrinsic characteristic of the system itself that describes the material fluxes moving across and through it (Heckmann et al., 2018; Wohl et al., 2019). In this sense, flux refers to the solid volume of sediment particles and water that are transferred across a surface with a particular spatial and temporal dimension (Bracken et al., 2015). Given the different types of solids within these fluxes, connectivity can be further classified as *hydrological connectivity*, which refers to the transport of water between different system components, and *sediment connectivity*, which relates to the physical transfer of sediments (Bracken and Croke, 2007). Hydro-geomorphic connectivity is used here to refer to the transfer of suspended sediment via saturation overland flow.

Sediment connectivity consists of the processes of sediment detachment and transfer through the catchment system – from source to sink (Bracken et al., 2015). It encompasses both

the potential and efficiency of a catchment to facilitate the conveyance of sediment between its components (Heckmann and Vericat, 2018). There are a variety of landforms and temporal and spatial scales where connected sediment transfer takes place, and the degree of coupling between these landforms has implications for sediment connectivity as well (Harvey, 2002, 2001). In fact, the degree of coupling of hillslope and channels within a catchment has been described as landscape connectivity, whereby vertical (surface – subsurface), lateral (slope – valley floor), and longitudinal (upstream – downstream) are distinguished (Brierley et al., 2006).

Continuity of sediment transfer from source to sink is stressed as an important distinction to coupling, which describes linkages between morphologic components at a certain point (Bracken et al., 2015; Hooke and Souza, 2021). Landforms where sediment transfer takes place broadly include on hillslopes, between hillslopes and channels, and within channels (Brierley et al., 2006; Fuller and Death, 2018; Hooke, 2003). An important aspect of sediment transfer and connectivity is that while processes of erosion, transport, and deposition can act at the grain scale, the resulting landforms (e.g., debris fans) can be orders of magnitude greater in size (Bracken et al., 2015).

Sediment connectivity is an important concept for i) understanding spatial and temporal variability of sediment fluxes, ii) identifying sources and sinks, iii) the geomorphic sensitivity to disturbance, as well as iv) managing sediment (Poeppl et al., 2020; Turley et al., 2021). For example, when considered as a functional, process-based framework (e.g., Bracken et al., 2015), it can help anticipate downstream impacts of erosion processes and sediment delivery on water quality, ecosystem health, and flood risk (Dymond et al., 2017a; Fuller and Death, 2018; Poeppl et al., 2020). When sediment delivery exceeds the transport capacity of a stream, stream health can be adversely affected (Fuller and Death, 2018). Moreover, consideration of connectivity is essential from a sediment management perspective, as it allows for the prioritizing of erosion mitigation on hillslopes to reduce sediment delivery to streams or to improve sediment continuity in catchments (Hooke and Souza, 2021; Simoni et al., 2017).

Having introduced the general concept of sediment connectivity, the following section provides a brief synthesis of important conceptualizations that have been proposed for connectivity. The objective here is to provide an overview of the theoretical development in connectivity concepts, and their implications for understanding the hydro-geomorphic system. Section 2.4.3 will then review the quantitative literature, with a special focus on landslide connectivity.

2.4.2 Conceptualizations of Sediment Connectivity

Hydrological connectivity for runoff dominated geomorphic systems

Five major components of catchment connectivity were identified by Bracken and Croke (2007) that influence hydrological connectivity, and are equally important for considering sediment connectivity in the context of surface erosion (Figure 2.6a). Components of the framework include 1) climate, 2) hillslope runoff potential, 3) landscape position, 4) delivery pathway and 5) lateral buffering. Climate impacts on the runoff regime, primarily through the temporal and spatial rainfall distribution within a catchment. In temperate and humid climates, runoff is largely composed of saturation overland flow, which means connectivity requires continuity of saturated areas. In this context, antecedent soil moisture conditions are important for (re-)establishing connectivity in runoff. A further important climatic variable is storm duration and intensity, as well as temporal and spatial variation of storm rainfall within the catchment. In combination with the catchment morphology, rainfall patterns ranging from high intensity, short duration events to low intensity – long duration events, can result in very different hydrographs, which expresses connectivity and its dependence on rainfall patterns. An important aspect here is in relation to scale: hillslope hydro-geomorphic connectivity can be initiated by shorter, low-intensity rainfall, whereas long-duration high magnitude events are needed for catchment-wide connectivity. There are also many factors that influence surface

runoff generation – and hence connectivity - besides rainfall patterns. These include the infiltration rate, antecedent conditions, surface roughness, vegetation, and land management.

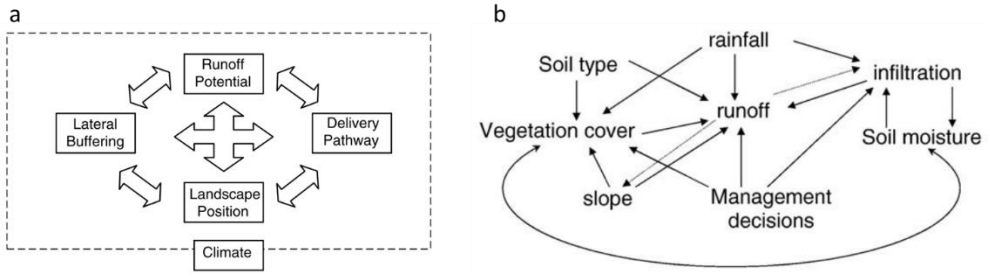

Figure 2.6 Components of catchment connectivity frameworks proposed by a) Bracken and Croke (2007) b) Lexartza-Artza and Wainwright (2009).

Runoff potential on hillslopes is recognised as an important component of the framework, which is controlled by the geological, pedological and land management properties. Spatial variation across hillslopes within the catchment can lead to both non-uniform and non-linear responses to rainfall events and flooding. Infiltration is a key control on surface runoff and dictates whether runoff can be generated and sustained downslope, whereby transmission losses can decrease the volume of surface runoff and may disconnect flow. *Landscape position* refers to the likelihood of connectivity based on distance from source to sink – which can be a stream or outlet. In this context, slope length is an important factor, with longer slopes increasing opportunity for infiltration (Bracken and Croke, 2007). Equally, there is evidence that low infiltration capacity on slopes can have the reverse effect of increasing runoff with distance due to convergence of flow (Scheip and Wegmann, 2022). The *delivery pathway* from runoff or sediment source to sink is dependent on landscape position, land management practices, topography (e.g., steepest slopes, hollows), and human-made structures. Pathways can be incisional/channelised or dispersive, the former being a feature of rills and gullies, which are fully connected to the drainage network, resulting in high hydrological connectivity. *Lateral buffering* refers to the degree of slope-channel coupling, which influences the transport of sediment to channels. Where hillslopes are directly connected to channels, for example, in narrow headwaters, the hydro-geomorphic connectivity will be greater than where the presence

of extensive riparian vegetation or adjacent floodplain or terrace can result in decoupling between slope and channel.

While this framework by (Bracken and Croke, 2007) was designed for hydrologically dominated systems, the elements considered are all relevant for sediment connectivity. A similar framework by Lexartza-Artza and Wainwright (2009) extends that of Bracken and Croke (2007) by specifically referring to many of the processes described above. However, conceptual frameworks will struggle to capture the full complexity of the many hydro-geomorphic processes acting at a range of spatial and temporal scales while maintaining simplicity required to maintain relevance and meaning (Hooke and Souza, 2021). While these frameworks provide a basis for exploring further conceptual developments, there are limitations associated with a hydrological perspective for sediment connectivity. For example, sediment transport can be disconnected from the flows transporting them, given the inverse relationship between particle size and transport distance. The following framework by Bracken et al. (2015) builds on the concepts discussed here to capture the nuances and particularities specific to sediment connectivity.

A multi-scale sediment connectivity framework

The sediment connectivity framework by Bracken et al. (2015), and introduced here, has at its foundation a holistic view of sediment connectivity that comprises the entirety of the geomorphic system. Sediment connectivity is both a function of the more static structure of morphology of system components and the geomorphic processes that act within it, which interact in the long-term sediment flux to induce changes in landform. Once sediment is detached at a source, further entrainment and transport is dependent on the configuration of connections between sediment sources, the flow of energy vectors in relation to the morphology of pathways.

The framework proposed by Bracken et al. (2015) integrates the elements of i) the frequency–magnitude distributions of sediment detachment, transport and deposition

processes; ii) spatial and temporal feedbacks between sediment detachment and transport processes; and (iii) mechanisms of sediment detachment and transport (Figure 2.7). The novelty of this framework is the recognition that different detachment/erosion processes act according to different frequency/magnitude scales. For example, the diversity in recurrence interval associated with mass movement, glacial, or aeolian processes has repercussions for transport processes as well.

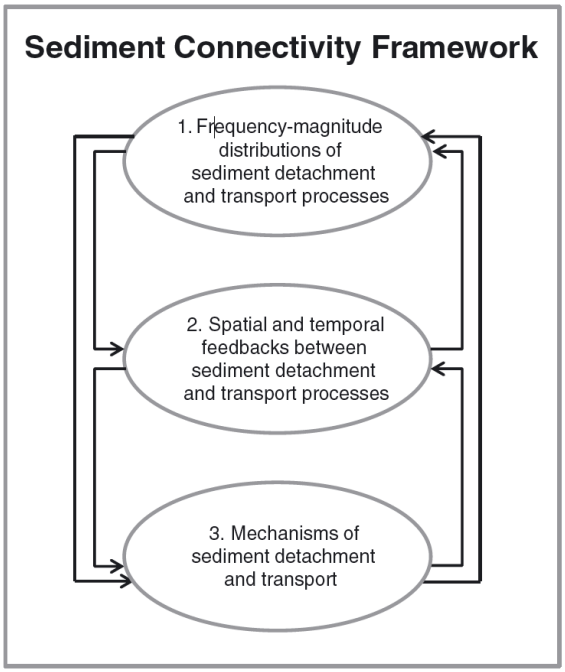

Figure 2.7 Sediment connectivity framework proposed by Bracken et al. (2015).

The first major component of the framework considers the dependency of sediment detachment and transport on the frequency-magnitude distributions of rainfall events that influence sediment supply available for transport (Figure 2.8). This relationship has important implications for connectivity since the chosen timescale can largely determine the degree of connectivity and also time since previous rainfall event (Wolman and Miller, 1960). While the geomorphic processes of detachment, transport and deposition of sediment result in changes to landforms across space and time expressed as frequency/magnitude relationships, landforms also function as controls of these processes. This relationship, which represent the second component of the framework expressed as the spatial and temporal feedbacks between sediment detachment and transport processes, has implications for connectivity and sediment delivery.

Both positive and negative feedbacks can take effect over different time scales. For example, topographic controls on surface and sub-surface flow and water content not only impact landslide occurrence, but also have implications for the behaviour of debris runout. As the landslide mass proceeds downslope, its mobility can increase in the presence of greater surface water flows resulting from convergence in flow paths and larger drainage area. This has the effect of increasing the liquid fraction of the landslide deposit, which reduces internal friction, resulting in greater run-out down-slope (Scheip and Wegmann, 2022). Thus, there are two distinct components of positive feedback observed in a short time scale: i) the initial failure, where the morphology interacts with the process/mechanism, and ii) the propagation of soil mass downslope. An example of negative feedback would be a landslide dam impeding sediment connectivity over a range of temporal scales (Abad et al., 2022), or landslide deposits on lower slopes can result in sediment storage and aggradation, thereby reducing sediment connectivity within the upper slope – valley bottom system in subsequent events.

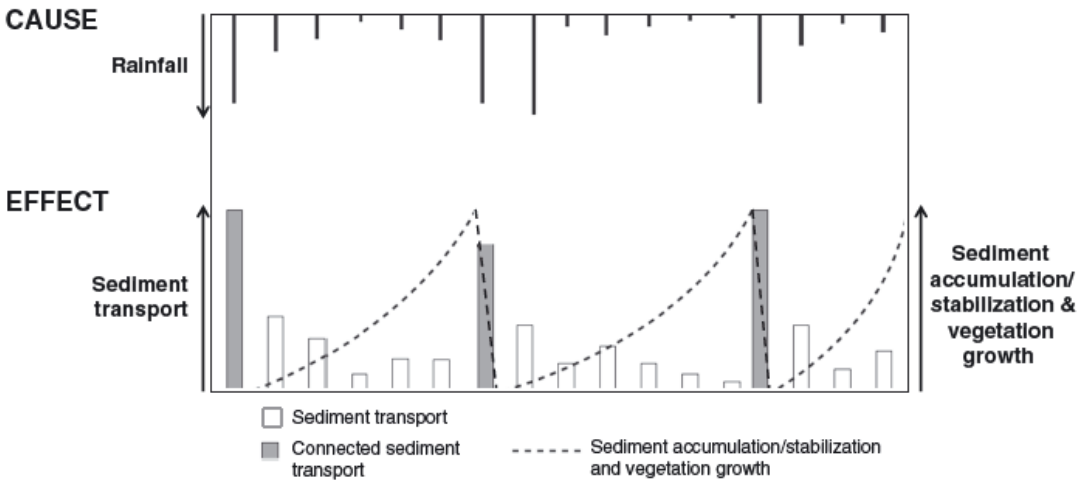

Figure 2.8 Conceptual diagram showing the relationship between frequency/magnitude of rainfall events and sediment accumulation and transport. Source: Bracken et al. (2015).

The third major component of the framework (Figure 2.7) refers to the mechanisms of sediment detachment and transport in relation to their effects on sediment fluxes. Sediment detachment and transport can be to a greater or lesser extent hydrologically controlled. The detachment mechanism of landslides can be both hydrologically controlled (rainfall-triggered

through rising in pore water pressure reducing the internal friction of soil particles) or less hydrologically controlled by seismic events (e.g., Kasai and Yamada, 2019).

The framework proposed by Bracken et al. (2015) provides an important reflection on the spatial and temporal dynamics of geomorphic processes acting within a catchment system. In contrast to the previous framework introduced (Bracken and Croke, 2007), the novelty of the framework is in its emphasis on frequency/magnitude distributions in relation to sediment detachment, transport, and deposition processes and the degree to which these are synchronised in space and time. Moreover, the feedbacks between detachment and transport are important considerations for connectivity. All components of the framework have direct relevance for connectivity of sediment derived from shallow landsliding, and can help explain the dynamics of landslide failure, transport and deposition – particularly with regard to sequencing of processes in relation to the recurrence of landslide-triggering events in time and space.

Interpretations of structural and functional connectivity

The third framework by (Wainwright et al., 2011), which adds to the previous connectivity frameworks discussed, introduces the concepts of *structural* and *functional* connectivity. Structural connectivity refers to the physical linkages between landscape units and generally refers to the role of morphology in promoting or preventing continuity in sediment transfer. In this sense, contiguity in pathways for sediment transport from source to sink are important for promoting structural connectivity. Functional connectivity describes the process-specific linkages between landscape elements, describing the mechanisms of material and energy fluxes through the geomorphic system. Structural and functional connectivity do not exist in isolation but rather interact and modify each other. They are thus both spatially and temporally dynamic across multiple time scales. These interactions are similar in nature to the examples discussed above in the context of feedbacks between geomorphic processes of detachment and transport that result in changes to landforms, which in turn can affect responses to future sediment input (Bracken et al., 2015).

Having reviewed the key concepts of connectivity frameworks, the following section provides an overview of previous research that has developed and demonstrated quantitative methods for landslide connectivity. A comprehensive review of concepts and approaches to sediment connectivity was published recently by Najafi et al. (2021), and covers approaches based on conceptual frameworks, morphological approaches, use of connectivity indices. While the authors further classify the approaches by scale, method, and metric, they do not categorize by erosion process as the majority of studies are focussed on surficial erosion processes. Given the objectives stated in this thesis (see Chapter 1.2), connectivity approaches specific to landsliding are reviewed below.

2.4.3 Quantifying Landslide Connectivity

The importance of shallow landslides as a contributor to catchment sediment budgets is spatially and temporally variable as a function of i) the predisposition of the terrain to landsliding, ii) the frequency and magnitude of both the triggering mechanism (rainfall or earthquake) and the response (i.e., the size and density of landslides), and iii) sediment connectivity that determines off-slope sediment delivery rates. Landslide connectivity is an important consideration for land management decisions concerned with the health of aquatic systems (Fuller and Death, 2018). In this context, knowledge of landslide source areas and the transport capacity of sediment from source to sink is a prerequisite for managing erosion and sediment.

The most common methods used to determine landslide connectivity are i) a limiting criterion (Dymond et al., 2006), ii) empirically fitted run-out models (Rickenmann, 2005), iii) a combination of slope-thresholds and run-out models (Bathurst et al., 1997), and iv) repeat digital elevation models (DEM of difference – DoD; Heckmann and Vericat, 2018)). The first of these methods involves setting a threshold for critical slope and deposition zones. An example of such a limiting criterion is the use of a slope threshold of 4° to determine the zone

of deposition along a flow path of landslide deposits (Dymond et al., 2006). Use of thresholds has also been combined with simple run-out models to determine the fraction of eroded material delivered to the stream channel (Bathurst et al., 1997). In this study, a simple empirical relationship for runout distance – fitted using the elevation difference between the head of the landslide scar and the point at which deposition begins, is used in combination with runout criterion based on slope thresholds to determine the percentage of eroded material deposited to stream.

Runout models

Most run-out models include some variation of an empirically fitted relationship between landslide volume V and runout length L:

$$L = aV^b$$

where a and b are empirical coefficients (Cislaghi and Bischetti, 2019; Hürlimann et al., 2015; Legros, 2002).

This relationship is frequently extended to include additional factors influencing run-out distance such as travel angle or total fall height, H, defined as the elevation difference between the maximum point of initiation and the furthest point of deposition (Bessette-Kirton et al., 2020; Corominas, 1996; Qarinur, 2015):

$$L = aV^bH$$

Numerical modelling approaches have also been used to simulate landslide-runout behaviour (Qiao et al., 2018; Yang et al., 2019). Using a set of 12 loess landslides, the apparent friction angle (ratio H/L) was found to be approximately 25°. Thus, a simple empirical relationship was used to approximate the runout distance based as $L = 2.15H$, which can then be used to estimate landslide risk under a range of scenarios (Yang et al., 2019). Other approaches to determine relationships between erosion source and deposition areas include the

use of repeat digital elevation models (Croke et al., 2013; Heckmann and Vericat, 2018; Scheipp and Wegmann, 2022). Less common methods to compute landslide connectivity include mathematical graph theory (Heckmann and Schwanghart, 2013), and a two-parameter friction model (Wichmann et al., 2009).

While runout models are useful for ex-post estimation of sediment delivery to streams and evaluating risk associated with landslide deposition, they do not inform the likelihood of landslide initiation, which varies in space and time. Therefore, various authors have proposed a coupled or modular approach to landslide connectivity that both predicts the occurrence of landslides and provides estimates of sediment delivery (Cislaghi and Bischetti, 2019). Similar approaches have been used for modelling sediment delivery from debris flows (Burton and Bathurst, 1998), and large wood recruitment to streams (Rigon et al., 2012). These approaches adopt either physical or statistical models to predict slope stability, followed by either i) a prediction of run-out length (Burton and Bathurst, 1998; Cislaghi and Bischetti, 2019) or ii) a slope decay function involving distance and steepness of slope (Rigon et al., 2012) to determine the degree of connectivity. They are thus concerned with sediment connectivity in terms of lateral linkages that drive the supply of materials from slopes to the channel network (Brierley et al., 2006).

Index of connectivity

A number of studies have used similar modular approaches, combining estimates of sediment sources with the index of connectivity (Broeckx et al., 2016; Najafi et al., 2021b, 2021a; Persichillo et al., 2017; Poeppl et al., 2019; Scorpio et al., 2022; Zanandrea et al., 2019; Zhao et al., 2020). The index of connectivity (IC) was first proposed by Borselli et al. (2008) and further developed by Cavalli et al. (2013). In its simplest form, IC consists of an upstream component D_{up} and a downstream component D_{dn}:

$$IC = log_{10}\left(\frac{D_{up}}{D_{dn}}\right)$$

The upstream component is a function of the upslope contributing area and its mean slope gradient. The downstream component is a function of the length of the flow path to the nearest pre-defined sink and considers the slope gradient along the flow path.

While the IC has clear limitations related to the interpretation of the index as well as the lack of quantitative validation (Najafi et al., 2021b). However, recent efforts have been made to demonstrate its utility and interpretational value by including it as input to a logistic regression analysis (Martini et al., 2022; Scorpio et al., 2022). Moreover, the IC has been successfully used as a predictor of muddy flood-affected sites (de Walque et al., 2017) and sediment transfer between sediment sources (e.g., landslides, debris flows) and water channels (Martini et al., 2022). Najafi et al. (2021) also made an important distinction in terms of structural and functional connectivity concepts. The IC aims to represent structural sediment connectivity based on (high-resolution) topographic influences on sediment flux. Since the IC fails to represent process-specific characteristics of sediment source and transport, inconsistencies can arise when comparing IC values to process-specific modelling (Cislaghi and Bischetti, 2019; Poeppl et al., 2019; Zhao et al., 2020). Thus, the IC is a useful tool for representing structural connectivity but has limited value for modelling functional connectivity (Cislaghi and Bischetti, 2019; Hooke and Souza, 2021; Martini et al., 2022; Poeppl et al., 2019).

2.5 Summary

This review provides an overview of relevant literature related to key components for the research that follows. Silvopastoral systems best describe the thematic context for where this thesis is situated. The same is true regarding the methodological challenges that characterise the research undertaken. As will be shown, the inherent nature of silvopastoral systems, characterised by scattered trees integrated into a pastoral landscape, present some unique challenges resulting from the heterogeneity of the system compared with landscapes of more uniform land uses (e.g., treeless pasture). Given this context, an understanding of silvopastoral

systems is important. Having introduced silvopastoralism, including those forms particular to New Zealand, the review in section 2.2 summarised the evidence related to soil conservation in silvopastoral systems, which was sourced largely from empirical studies.

Slope stability concepts were introduced as well as the mechanisms by which trees modify slope stability. Much of the understanding documented here is sourced from experimental research, but also fundamental physical understanding of the gravity-driven downslope forces that are resisted by the strength of forces inherent in soil material. Knowledge of these physical processes and how trees interact on a slope is important for identifying the strengths and weaknesses of the different approaches to slope stability modelling (e.g., data requirements). Indeed, this review provides the initial justification for the direction of methodological approach selected for this research, given the context and scale requirements that characterise the objectives of the specified research agenda presented in Chapter 1.2.

It is clear root reinforcement models rely heavily on large numbers of measurements of root tensile strengths and morphological data of root systems. Yet, due to constraints involved in such destructive sampling methods, the data are generally limited to a small number of trees. For this reason, many assumptions must be made concerning the root systems and how they vary according to species, maturity, and different environmental settings (e.g., competition through planting density; soil type, soil moisture at the time of in-situ pull-out tests). This presents a key barrier to silvopastoral systems, where a multitude of tree species are found across a range of environmental gradients.

Statistical approaches to slope stability present an alternative approach to physically based models – particularly related to data requirements. Key concepts for statistical landslide susceptibility were introduced in Chapter 2.3.3. While statistical approaches offer advantages over physical modelling - particularly in environments with sparse geotechnical data, the review of scientific literature found a gap in scale pertaining to the use of land cover data. This may be due to the lack of silvopastoral systems in steep terrain elsewhere in the world where

landslide erosion poses a challenge to sustainable land management. The pastoral hill country of New Zealand is a landscape that is somewhat unique– particularly given its geological setting with soft rocks, a climate featuring frequent high magnitude rainfall events, as well as the rapid land use change in recent history, - all factors that precondition this landscape to be highly active in geomorphological terms. Regardless of the cause for the identified gap in i) knowledge, ii) scale, and iii) methodology related to statistical modelling, the research undertaken in this thesis aims to respond by developing landslide susceptibility models that incorporate the effect of individual trees in silvopastoral landscapes.

The review also demonstrated the multifunctionality of silvopastoral systems: Slope stability is an important outcome alongside co-benefits that include animal welfare through shade and shelter, a potential source of additional fodder, and can even add value to pasture production (Mackay-Smith et al., 2022a). An important additional benefit that has gained prominence in the New Zealand context pertains to its impact on sediment yields. Yet, the impact of silvopastoral systems on landslide-derived sediment yields remains largely unquantified at farm- through to catchment-scales. These impacts can be informed by adopting an approach considering sediment connectivity. Several conceptualizations of sediment connectivity have been discussed and the most common approaches to quantifying landslide connectivity reviewed, providing a theoretical and conceptual underpinning for this research. Thus, the literature review provides both the backdrop and initial justification for the research presented in the following three chapters of the thesis.

PART II

PUBLICATIONS

3

3 QUANTIFYING THE INFLUENCE OF INDIVIDUAL TREES ON SLOPE STABILITY AT LANDSCAPE SCALE

Raphael I. Spiekermann[1,2], Sam McColl[1], Ian Fuller[1], John Dymond[2], Lucy Burkitt[1], Hugh G. Smith[2]

Journal of Environmental Management (Elsevier), Vol. 286:112194, May 2021, p. 1-18
Submitted 18 November 2020
Accepted 13 February 2021
Available online since February 2021, reprinted with permission from Elsevier.
https://doi.org/10.1016/j.jenvman.2021.112194

This publication develops a method to provide high-resolution spatially explicit individual tree influence models at landscape scale for the dominant tree species in New Zealand's pastoral hill country. The combined hydrological and mechanical influence of trees on slopes is inferred through the spatial relationship between trees and landslide erosion. First, individual tree crowns are delineated and classified into the four most abundant tree types. This is the first classification of individual trees at landscape scale in New Zealand using freely accessible data. Second, tree influence models for each tree type are developed. The inferred empirically based tree influence models largely agree with the shape and distribution of existing physical root reinforcement models. The tree influence models presented in this study can be integrated into landslide susceptibility modelling in silvopastoral landscapes to both quantify the reduction in landslide susceptibility achieved and support targeted landslide erosion (see Chapter 4).

[1] School of Agriculture and Environment, Massey University, Palmerston North, New Zealand

[2] Manaaki Whenua – Landcare Research, Palmerston North, New Zealand

3.1 Introduction

Woody vegetation significantly modifies hillslope hydrological and mechanical properties that control shallow landslide triggering processes and is an effective nature-based erosion mitigation instrument (Cohen and Schwarz, 2017; de Jesús Arce-Mojica et al., 2019; Istanbulluoglu and Bras, 2005; Phillips and Marden, 2005; Schmidt et al., 2001; Schwarz et al., 2010b). Several previous studies have aimed to quantify the influence of woody vegetation on slope stability, albeit mostly limited to protection forests (e.g., Cislaghi et al., 2017; Phillips et al., 2011b). Irrespective of the type of woody vegetation, methods to quantify the effectiveness of biological landslide erosion control generally use i) empirical, ii) physical-, process-, or iii) statistical-based approaches for landslide susceptibility assessments.

Quantitative empirical studies aim to measure the degree to which soil conservation treatment has reduced landslide erosion compared with untreated areas (G. Douglas et al., 2013b; Douglas et al., 2009; Hawley and Dymond, 1988; Hicks, 1989a, 1989b, 1992; McIvor et al., 2011, 2015; Phillips et al., 2008; Thompson and Luckman, 1993). These studies show space-planted trees reduce landslide erosion by 70–95% within their assumed sphere of influence (e.g., a 10-m radius) compared with paired control sites.

Physical models of tree influence use quantitative measures for the mechanical and hydrological mechanisms of vegetation to estimate the increase in soil cohesion and slope stability achieved (e.g., Cislaghi et al., 2017; Cohen et al., 2011; Gonzalez-Ollauri and Mickovski, 2017; Moos et al., 2016; Schmidt et al., 2001; Schwarz et al., 2016a, 2012). Physical slope stability models that incorporate such measures of root reinforcement are sophisticated in replicating the processes governing slope stability, but their data requirements are significant, and extrapolation of measurements beyond individual sites remains a challenge. Furthermore, root morphologies are modified by climatic and edaphic factors, which include physical soil conditions, resulting in highly variable root morphologies – even within a single species

growing in different environments (Coppin and Richards, 1990; Phillips and Marden, 2005; Phillips and Watson, 1994; Schmidt et al., 2001; Stone and Kalisz, 1991; Watson and O'Loughlin, 1990). Therefore, physical slope stability models are generally used for landscapes with homogenous vegetation such as protection forests (e.g., Genet et al., 2010; Moos et al., 2016; Temgoua et al., 2016). The advantages of physical root distribution models, and their integration into slope stability models, was demonstrated by Schwarz et al. (2016), who determined optimal planting strategies using poplar trees for erosion control at hillslope scale for a New Zealand case study.

Statistical landslide susceptibility modelling is a common method used to disentangle the influence of a range of drivers that determine spatial variation in the probability of landsliding (Guzzetti et al., 2006; Kanungo et al., 2009; Reichenbach et al., 2018; Smith et al., 2021; Van Den Eeckhaut et al., 2012, 2009; van Westen et al., 2008). In the absence of detailed vegetation classifications that would provide greater resolution in terms of the mechanical and hydrological mechanisms (e.g., root distribution models, canopy cover), land cover data are often used as surrogate datasets (Reichenbach et al., 2018). However, current land cover data are not at the resolution to account for the influence of space-planted trees in silvopastoral landscapes. Furthermore, simply representing individual trees as a point, mapping tree canopies, or using an arbitrary radius to define an area of influence of a tree, fails to acknowledge the spatial variation in the distribution and strength of roots in the soil as well as the influence on soil moisture.

In New Zealand, erosion processes are very active due to steep slopes, weak sedimentary rocks, high annual rainfall, and relatively frequent high magnitude rainfall events (Basher, 2013; Basher et al., 2011). New Zealand's history of land management includes extensive deforestation for pastoral farming which has exacerbated erosion rates (Glade, 2003; Phillips et al., 2018). Given this setting, it is not surprising that most research on the impact of trees on landsliding in silvopastoral and agroforestry landscapes has been undertaken in New Zealand (England et al., 2020). Since the enactment of the Soil Conservation and Rivers Control Act

1941, which helped increase awareness for sustainable land management and soil conservation, spaced planting of trees has been an important erosion and sediment control measure (L Basher et al., 2008; Basher, 2013; Phillips et al., 2008; Phillips and Marden, 2000; Van Kraayenoord and Hathaway, 1986) , whereby poplars (*Populus* spp.) and willows (*Salix* spp.) are planted as young, unrooted stems (poles) at densities ranging from 20 to 200 trees ha^{-1} (Benavides et al., 2009; Kemp et al., 2018; Wilkinson, 1999). The objective of this form of silvopastoralism is generally to protect infrastructure and conserve soils to reduce sediment yields and improve freshwater health (Basher et al., 2020). Space-planted trees also offer shade, shelter, quality fodder (especially during drought periods), and carbon sequestration (Benavides et al., 2009; McIvor et al., 2011). Dominati et al. (2014) quantified the long-term costs and benefits of space-planted trees in a pastoral farming context using an ecosystem services approach and found that despite the decrease in pastoral production below tree canopy, planting is economically beneficial in the long term due to the reduction in erosion risk and the increase in provision of ecosystem services including forage from trees, wood, provision of shade and shelter for animals, and net carbon accumulation in wood.

Despite the widespread use of space-planted trees in New Zealand's pastoral hill country, there has been relatively little experimental or quantitative work to establish their effectiveness in reducing erosion in relation to factors such as tree species, planting density, slope gradients, and there are no published studies on their measured effect on sediment yield (Basher, 2013; Douglas et al., 2009). Nor is there any information on their effectiveness over a range of different storm magnitudes. This is largely due to the lack of spatially explicit data on individual trees and their influence on slope stability. Therefore, it is difficult to determine the extent to which erosion and sediment control measures have targeted slopes susceptible to landslide erosion and prioritized treatment of susceptible hillslopes.

Root data collection for multiple species and age classes is time-consuming and costly, partly explaining the paucity of quantitative data on the effectiveness of space-planted trees on slope stability in silvopastoral landscapes (Hairiah et al., 2020). This study introduces an

empirical method to fill the gap in scale between i) physical models that quantify root reinforcement for individual trees and slope stability at hillslope scale, and ii) landslide susceptibility modelling at regional scale using land cover data. The objectives are: 1) to delineate individual tree crowns (ITCs) at landscape scale and classify into dominant species classes found in New Zealand's pastoral hill country; and 2) develop a spatially explicit tree influence model for each species class by means of inductive inference. The tree influence models represent the combined hydrological and mechanical influence of trees on slopes, which is inferred through the spatial relationship between individual trees and landslide erosion.

3.2 Methods

3.2.1 Study Area

The study area was chosen based on five criteria: i) availability of airborne LiDAR (Light Detection and Ranging); ii) recent occurrence of storm events that resulted in a high density of shallow landslides; iii) pastoral farming as the dominant land use; iv) spanning a range of rock types; and v) a significant history of soil conservation practices that has resulted in a silvopastoral landscape. Following an inspection of historic Google Earth imagery to examine evidence of widespread landsliding, an 843 km^2 area was selected in the Wairarapa, located in the south-east of the North Island of New Zealand (Figure 3.1). Approximately 92% of this area, or 776 km^2, is used for pastoral farming.

The study area is primarily underlain by unconsolidated, tectonically deformed Pliocene-age mudstone and fine siltstone (Figure 3.1). Much of the area is covered in a mantle of loess. These soils have a dense subsoil zone of low permeability that is the failure plane for many landslides (De Rose, 2013). A band of limestone forms the central and south-western part of the study area. The terrain has low to moderate relief (<150 m) that is intensely dissected, with narrow ridge and spur crests, hillslopes mostly between 15° and 35°, and narrow valley floors.

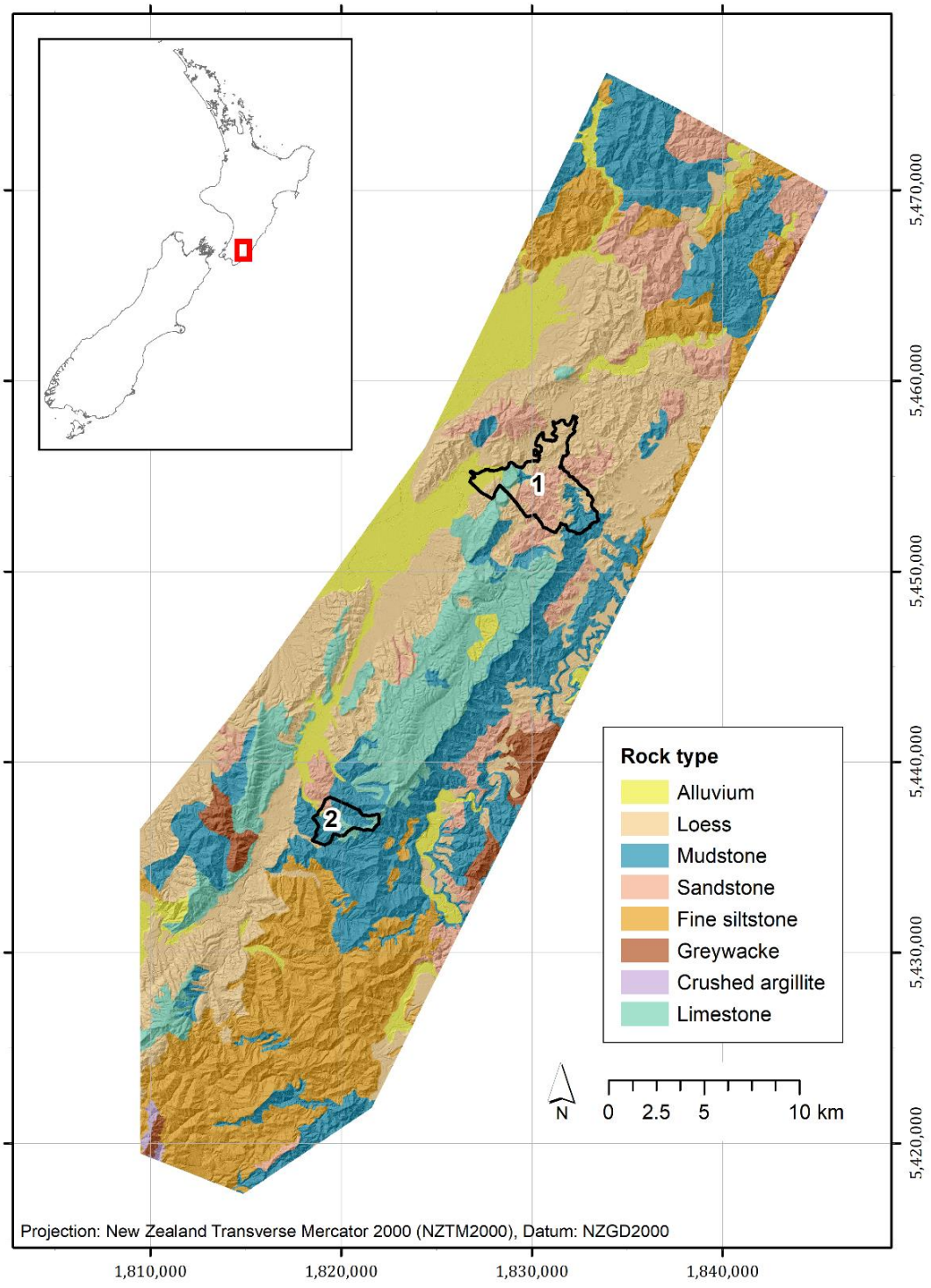

Figure 3.1. Location of study area in Wairarapa, New Zealand, showing a range of rock types (New Zealand Land Resource Inventory) and location of study sites 1 and 2. Map projection is New Zealand Transverse Mercator (NZTM).

Significant areas of colluvium (landslide debris) have accumulated along the base of many hillslopes, and in mid- and upper-slope hollows. Mean annual rainfall is 1100 mm, characterised by winter maxima and summer droughts. Long duration, low intensity rainfall is

typical with low daily rainfall totals. However, landslide-generating storms have occurred frequently since climatic records began in the 1880s. Most of these storms do not have particularly high storm or daily rainfall totals (100–200 mm) but often occur when antecedent moisture conditions are high (Basher et al., 2018; De Rose, 2013).

The study area was affected by two storm events in March 2005 and July 2006, with a median recorded rainfall of 175 mm and 204 mm over 48 and 72 hrs, respectively. These events triggered thousands of landslides across the entire study area. Three further storms, in late July 2006, October 2006, and June 2009, were more localised events recorded at Hikawera station in the south of the study area – the highest magnitude in 2009 with 197 mm in 24 hrs, with a resulting landslide distribution that was also localised to just part of the study area (Figure 3.7). Shallow, rapid slides and flows involving soil and regolith are the most common types of landslides in New Zealand and consist of small scars (50–100 m^2) and long narrow debris tails (Basher, 2013; Crozier, 2005; Glade, 1998). Such landslides are generally triggered either by single, high-intensity and -magnitude rainfall events or by low-magnitude rainfall events following prolonged wet periods that led to high antecedent soil moisture conditions (Basher, 2013).

3.2.2 Landslide Mapping

To evaluate the influence of trees on slope stability at the study site, the distribution of rainfall-triggered landslides needed to be mapped. To do this for the storm events captured in this study, a semi-automated mapping procedure, using an object-based image analysis (OBIA) method was applied to identify and classify landslide scar features assumed to have been triggered in the 2005 and later storm events in the study area (Figure 3.2). The OBIA method combines image processing and GIS functions to delineate and classify homogenous objects (Blaschke, 2010; Blaschke et al., 2014). The primary advantage of this approach over manual delineation of scars is that it enables rapid mapping using a set of defined rules that ensures

consistency across complete study areas and between landslide generations. We used Trimble's eCognition software and employed a knowledge-based ruleset (Hölbling et al., 2016; Smith et al., 2021) (Figure 3.2).

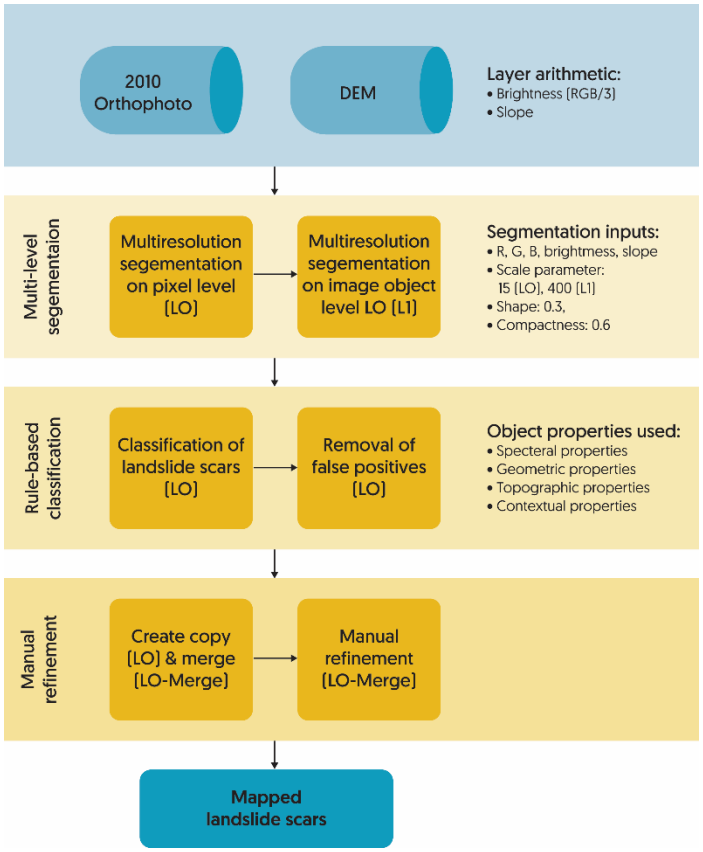

Figure 3.2. Workflow for OBIA mapping of shallow landslide scars across study area.

Landslide scars were classified in the 2010 imagery provided by Greater Wellington Regional Council, which is 3-band (RGB) optical imagery at 0.4 m ground space distance (GSD). Following a comparison with QuickBird II imagery from 30/01/2008, it was evident that the landslide scars triggered by the 2005 and 2006 rainfall events had not revegetated and could successfully be classified in the 2010 imagery. This visual inspection is supported by data on pasture dry matter production on slip scars by Lambert et al. (1984) and Rosser and Ross (2011), who found pasture production at ~20% of the yields produced on uneroded ground, which was estimated to increase to ~30% after 5 years. There was a marked difference in the southern part of the study area, where scars triggered by the local event in 2009 were more clearly visible since revegetation of exposed regolith was not as advanced.

The 2010 RGB imagery was resampled to 1 m – the resolution of the LiDAR DEM. Image objects were created using the multiresolution segmentation algorithm based on spectral information of the imagery (i.e., identifying bright scars stripped of vegetation) and slope derived from the LiDAR DEM (i.e., to set topographic rules for realistic landslide geometries and slope locations). The landslide classification used two object levels in a multi-scaled segmentation approach, which organizes the objects into a hierarchy (Blaschke et al., 2014). The level 0 objects (L0) were created at the pixel level (1-m spatial resolution), whereby scale, shape and compactness parameters were optimized until image objects represented small landslide scars or components of larger landslides. The level 1 objects (L1) were generated through a second multi-resolution segmentation based on the L0 objects. This generally resulted in the delineation of individual paddocks/land parcels, which are related to the topology of the underlying L0 objects (Blaschke et al., 2014). The advantage of this approach is that the characterisation of low-level objects is enhanced through consideration of their local environmental setting (contextual properties). This was achieved by calculating the ratio and the mean difference in brightness between L0 and L1, which increases local contrast and removes significant errors (false positives/negatives) that occur when thresholds are set for complete study areas. Thus, for the classification of landslide scars at L0, scars were defined using i) mean brightness >140, ii) a ratio to L1 mean brightness >1, and iii) mean slope >20°. An automated procedure aimed at removing false positives by considering geometric (e.g., length, length/width ratio) and topographic (e.g., standard deviation of slope, elevation range) properties of image objects as well as objects less than 20 square metres in size, since it was difficult to verify on-screen whether or not these small objects were landslide scars. Further object-based manual refinement of the classification was performed across the entire study area by selecting and removing falsely classified objects. The age of most of the landslide scars (4–5 years since failure) meant there was less local contrast to surrounding non-landslide pixels than would otherwise be expected, and consequently, an unusually high number of false positives were classified as landslides. Most of the false positives were associated with bright

objects such as farm tracks, areas of dry pasture, or exposed stream beds. 27 objects identified as landslide scars with areas > 1500 m^2 were removed, as these were mostly components of actively eroding gully systems. This resulted in a preliminary dataset of 43,069 landslide scars.

3.2.3 Rural Tree Species Classification

Two farms were selected for mapping tree species to generate the ground data required for training the support vector machine (SVM) classifier (Figure 3.1). Both farms have a history of landslide and soil erosion research activity (e.g., Lambert et al. 1984, 1993; De Rose, 2013; Douglas et al., 2013; Basher et al., 2018) and significant space-planting since 1990 (Site 1) and 1954 (Site 2) (Figure 3.3). Site 1 is a 1,700-ha sheep and beef farm, located approximately 15 km east of Masterton, in a region of steep pastoral hill country underlain by erodible Tertiary siltstones, mudstones, as well as some limestone. Here, the original landcover was predominantly podocarp-hardwood native vegetation that was cleared between 1860 and 1890 (Lambert et al., 1984). Soil conservation works in the form of space-planted poplar, willow, and eucalyptus trees began in the late 1990s. While planting has been sustained since commencement, the density of trees on hillslopes differs across the farm and is less than Site 2 (Figure 3.3).

Site 2 is an 815-ha sheep and beef farm located at the upper catchment of the Waikoukou Stream, a tributary of the Wangaehu and has been continuously active in soil and water conservation since 1956. The main objectives of these conservation works were to intensively plant slopes and gullies prone to severe erosion using poplars, willows, and protected seedlings, install regulating dams to restrict peak flows and sediment loads entering waterways, and establish conservation woodlots in areas of severe gully and earthflow erosion. The original land cover consisted of light bush, kānuka, and fern with heavier podocarp species in the wider valleys. Several bush remnants of kānuka remain distributed across the farm. Soils are silt loam derived from mudstone and are generally typical of the soils found in the wider study area.

Figure 3.3. Space-planted trees (kānuka, poplars and willows on slopes, cabbage trees lower right) at Sites 1 (above) and 2 (below), showing a range of species: Pinus radiata, poplars/willows, kānuka, eucalyptus. Sustained efforts over prolonged periods have resulted in higher density of planting at Site 2.

Tree mapping was carried out in the field at Sites 1 and 2 following two primary objectives: 1) to identify tree species to be used as samples in the tree species classification, and 2) to count the number of stems in selected densely planted stands across different species classes (Table 3.1). Trees were mapped on printed sheets of aerial photography (2013/14) at a scale of 1:2,500. Site visits found four dominant classes of tree species in paddocks used for pasture: poplar (*Populus spp.*) and willow (*Salix spp.*) varieties, eucalyptus (*Eucalyptus* spp., e.g. *Eucalyptus globulus*), kānuka (*Kunzea* spp.), and *Pinus radiata* (hereafter referred to as conifers) (Table 3.1). These species made up 90% of all species mapped at the two sites. These four classes therefore formed the basis of the rural tree species classification. Other less common species

mapped include acacias, other coniferous species such as cedar, Douglas fir, and spruce, and species native to New Zealand such as tōtara, (*Podocarpus totara*) and cabbage trees (*Cordyline australis*). Kānuka are often found with other species such as mānuka. Due to their greater height (10–20 m), kānuka eventually forms the dominant canopy (Allen et al., 1992; Bergin et al., 1995; Mackay-Smith et al., 2021; Smale et al., 1997), resulting in homogenous mature kānuka stands as observed at sites 1 and 2.

Table 3.1. Tree samples (count, %) used for rural tree species classification.

	Eucalyptus	**Kānuka**	**Poplar/willow**	**Conifer**	**Other**	**Total**
Site 1	316	1387	2225	132	909	4969
Percentage of total	6%	28%	45%	3%	18%	100%
Site 2	632	1801	1598	1169	169	5369
Percentage of total	12%	34%	30%	22%	3%	100%
Total	948	3188	3823	1301	1078	10338
Percentage of total	9%	31%	37%	13%	10%	100%

In 2013 and 2014, the Wellington Regional Council commissioned a LiDAR survey with a minimum point density of 1.3 pts/m^2, a mean of 5.8 pts/m^2, and a vertical accuracy of ±0.15 m over the Wellington region (812,000 ha). These high-frequency LiDAR pulses are reflected by tree canopies (first return) and other surfaces, including leaves, branches and ultimately the ground (generally the last return). The travel distance of the different returns is then calculated as a function of return time, which provides very accurate point measurements of elevation. These point clouds can be classified and interpolated to generate digital terrain models (DTM) and digital surface models (DSM). The difference between these elevation models is a canopy height model (CHM) (Lefsky et al., 1999). Since the advent of LiDAR point clouds and digital elevation models (DEMs), many algorithms have been developed for automated delineation of ITCs (Bunting and Lucas, 2006; Dalponte and Coomes, 2016; Pirotti et al., 2017; Zhen et al., 2016). Here, we used the pycrown algorithm developed by Zörner et al. (2018) to delineate ITCs in the study area using the LiDAR-derived DTM and CHM at 1 m GSD (Figure 3.4). Pycrown first identifies local maxima in a circular moving window, which represent treetops in the CHM. These local maxima are used as the seeds from which ITCs are grown, whereby

growth is restricted by four defined thresholds: i) a threshold below which a pixel cannot be a tree (*th_tree*); ii) a growing threshold to determine whether a pixel is added to the tree crown, which must be greater than the mean height of the current crown multiplied by this value (*th_seed*); iii) a second growing threshold, whereby a pixel is added to the crown if its height is greater than the current mean height of the region multiplied by this value (0-1) (*th_crown*); and iv) a maximum value of the crown diameter of a detected tree (*max_crown*). We used stem counts of different species from the field to optimize parameterization of pycrown for the trees in our study area. We refer to Zörner et al. (2018) for a more detailed explanation of parameterisation.

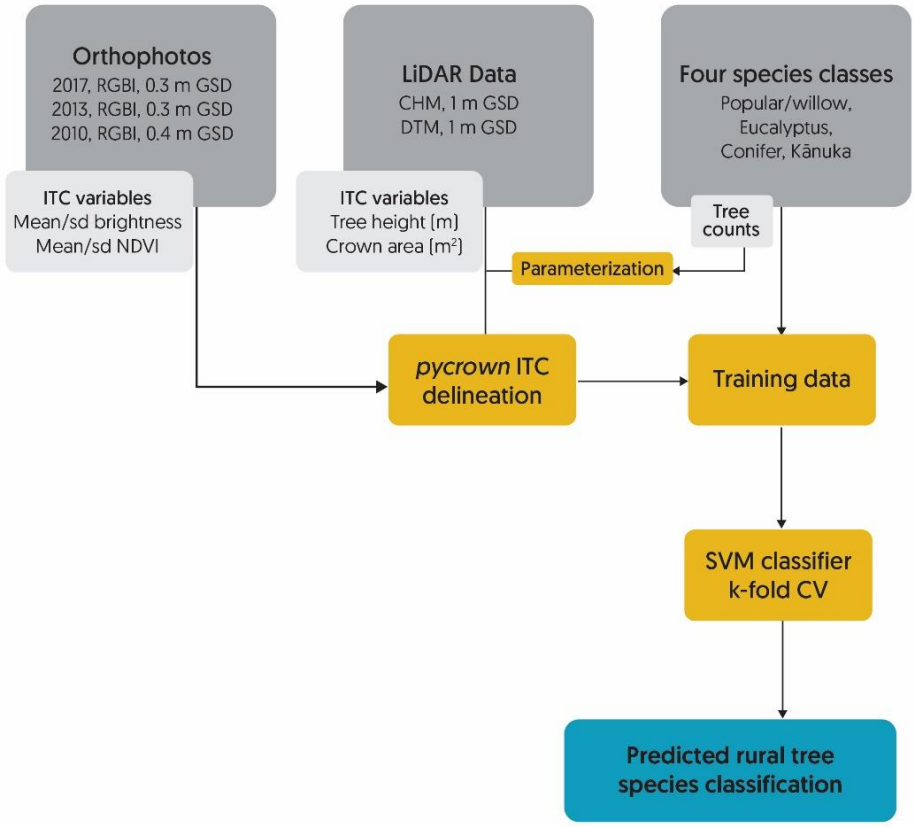

Figure 3.4. Workflow and data inputs for rural tree species classification using an SVM model.

The most important parameter of pycrown is the window size used for identifying treetops with local maxima, since it has significant implications on the number of seeds identified and, thus, crowns delineated. Besides *th_tree*, the remaining thresholds determine the final crown geometry. Experimentation with three window sizes (3, 4, 5) found that 5 m yielded optimal

results for space-planted trees. Therefore, a radius of 5 m was chosen, as well as default thresholds for crown growth of 0.45 (*th_seed*) and 0.55 (*th_crown*). The radius *max_crown* was set to 8 m due to a slight spatial incongruence between the LiDAR dataset and the orthophotos, which is minimal at nadir and reaches a maximum offset with increasing off-nadir viewing angles. By limiting the crown radius, the calculation of crown statistics (brightness, NDVI) using the orthophotos (Figure 3.4) is less likely to include adjacent pixels not associated with the crowns (e.g., pasture).

Through overlay of field-based species mapping with ITCs in a GIS environment, ITCs within Sites 1 and 2 were labelled according to the mapped species. Besides tree height and crown area derived from LiDAR data, zonal statistics on spectral data (mean, standard deviation of the mean (SD)) were calculated for each tree crown in the study area using freely available high resolution multi-spectral aerial photography from three surveys flown in 2010, 2013/14 and 2016/17 (Table 3.2) and used as predictors in the SVM model (Figure 3.4). By including a multi-temporal dataset, seasonal variations in canopy characteristics improve the capability of the model to differentiate species.

Table 3.2. Inputs derived from LiDAR data and optical imagery used in rural tree species classification

Data	**Model inputs**	**Variable abbreviation**
Regional LiDAR 2013	Tree height (m) Tree area (m^2)	TH Area
RGB 2010 imagery, 0.4 m GSD	Mean brightness Standard deviation brightness	br_10_m br_10_sd
RGBI 2013/14 imagery, 0.3 m GSD	Mean brightness Standard deviation brightness Mean NDVI Standard deviation NDVI	br_13_m br_13_sd ndvi_13_m ndvi_13_sd
RGBI 2016/17 imagery, 0.3 m GSD	Mean brightness Standard deviation brightness Mean NDVI Standard deviation NDVI	br_17_m br_17_sd ndvi_17_m ndvi_17_sd

Furthermore, we hypothesised that including SDs as predictors would improve the model, since conifers and poplars/willows exhibit less spectral variance in the canopy than kānuka and eucalyptus. This compiled dataset was used as training and test data for an SVM model using the caret package (Kuhn, 2008) in R to develop a rural tree species classification of ITCs across the entire study area. SVM was originally developed as a binary classifier and later extended

for multi-class classifications, and routinely outperforms more conventional approaches (Dalponte et al., 2012; Dymond et al., 2019; Fassnacht et al., 2016, 2014; Torabzadeh et al., 2019).

Using all 9,260 tree crowns, we explored the best combinations of model inputs by performing 10-fold cross-validation, in which the data are randomly partitioned into ten equal sized subsamples and each subsample is used to test the remaining nine subsamples assigned to training. The 10-fold cross-validation was repeated 5 times with different random selections of subsamples to get an average overall classification accuracy, which we aimed to maximise. For the identification of the best performing variables, parameters for cost penalty (=10) and σ (=0.05) were kept constant with a radial kernel function (RKF). Variable importance was evaluated using all training samples and receiver operating characteristic (ROC) curves and calculation of the area under curve (AUC). For multi-class outcomes, the problem is decomposed into all pair-wise problems and the AUC is calculated for each class pair. For a specific class, the maximum area under the curve across the relevant pair-wise AUCs is used as the variable importance measure. An AUC value of 0.5 corresponds to performance no better than a random guess, while an AUC of 1 would indicate perfect classification. Following variable selection, the final model tuned the hyperparameters of cost penalty and σ to achieve best performance, whereby a range of values for cost penalty (1:15) and σ (= 0.01,0.05,0.1) were tested. Model performance was characterised by overall accuracy (%) following 5 repeats of 10-fold cross-validation, and Cohen's Kappa, which accounts for expected accuracy resulting from uneven sample sizes across the classes (Cohen, 1960).

3.2.4 Empirical Tree Influence Models on Slope Stability

The landslide database and tree classification were used in an empirical approach to quantify the influence of an individual tree on landslide activity. The method determined whether landslide scars occur preferentially close to or remote from trees. The overarching hypothesis

is that by using spatial relationships and accounting for variability in the influencing factors, the influence of trees on landslide erosion may be inferred (Hawley and Dymond, 1988; Romeijn, 2009). Moreover, we assert that observations and patterns in the spatial distribution of tree location and landslide erosion allow the physical properties of trees that govern slope stability to be inferred. This supposition may be verified through existing knowledge of physical properties of trees and root systems and the mechanisms by which trees increase slope stability (see section 4.2). The method builds on that proposed by Hawley and Dymond (1988), whereby the spatial relationship between landslide scars and trees is quantified as a function of distance. Their study was limited to a single hillslope, single species, and treated as uniform in terms of slope stability in the absence of trees. Given that the properties of trees will vary in response to their environmental setting, observations over large areas are essential to infer the average tree influence. The high magnitude rainfall events between 2005 and 2010 triggered thousands of shallow landslides which span a variety of environmental gradients and will increase the likelihood for patterns to emerge from observations at landscape scale.

For each class (j) of the four dominant tree species classes, the tree influence model M_j is developed as a function of soil surface eroded by landsliding $f(r)$, as follows: we denote the distance from the nearest tree as r and $b = f(r)$ is the fraction of soil eroded (Figure 3.5). We will examine the relationship between b and r, whereby the effect of the trees is expected to decrease with increasing r until $f(r)$ approaches an asymptote $b = constant$ at a larger r. This asymptotic value of b is denoted by b_c and the value of r where $b = constant$ denotes the radius of the maximum distance of influence of the "average" tree, r_{max}. Note, all reference to eroded soil surface in this analysis is planar in nature, not volumetric.

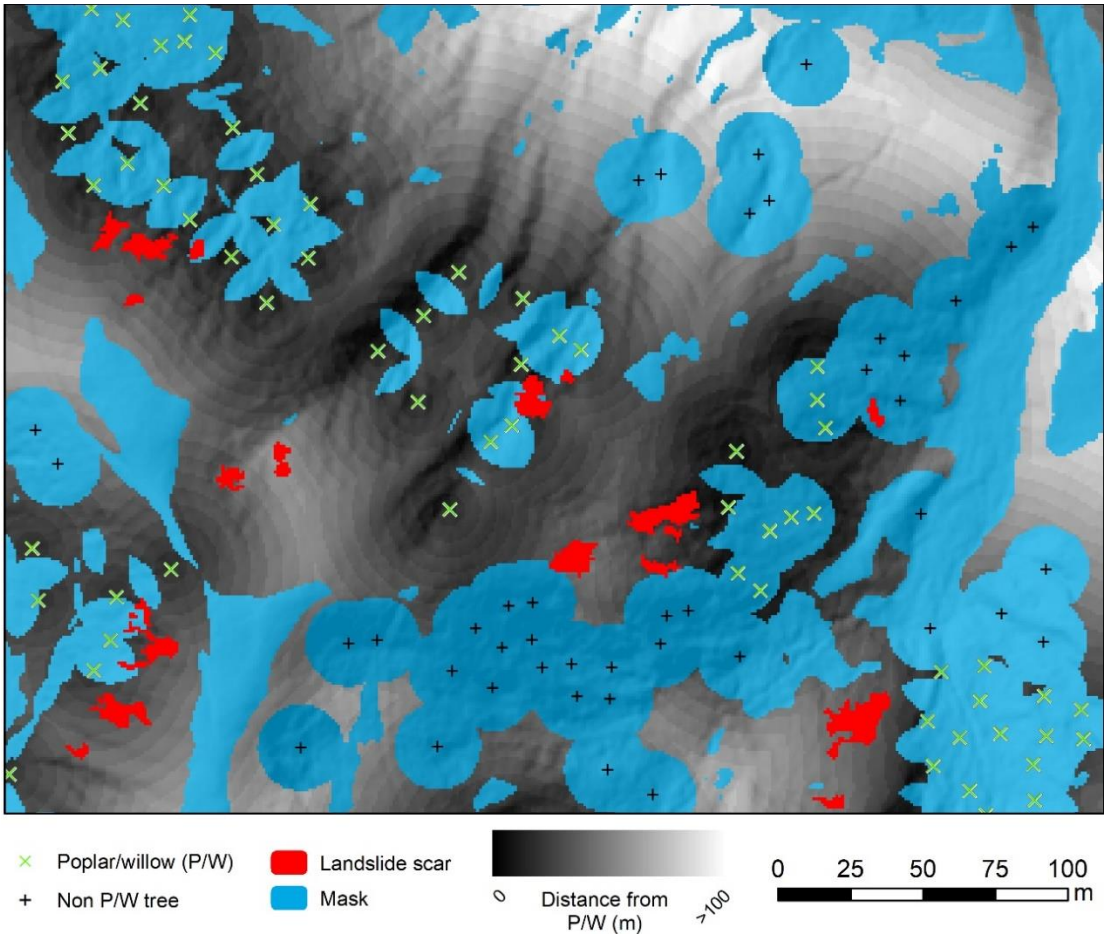

Figure 3.5. Illustration of method used to determine the influence of individual trees on slope stability as a function of distance (r) – here for the poplar/willow (P/W) class: The fraction of soil eroded is calculated at 1-m intervals from P/W trees. To isolate the effect of individual P/W trees, a mask is used to remove 1) 15-m buffers around all non-PW trees, 2) intersecting 15 m buffers of P/W trees, and 3) slopes less than 17.5 degrees.

Here, we specifically wish to isolate the influence of individual trees on slope stability in pastoral hill country, which we define using land cover classes from the NZ Land Cover Database of New Zealand (LCDB v4.1[1]) and a slope threshold. LCDB is a manually-mapped land cover classification with a minimum area unit of 1 ha, which means most silvopastoral landscapes are classified as ‘Grasslands’ (85.4% of study area) or depending on the density of trees, as one of the following classes: 'Broadleaved Indigenous Hardwoods' (1.1%), ‘Deciduous Hardwoods’ (1.3%), 'Gorse and/or Broom' (0.3%), 'Mānuka and/or Kānuka' (3.9%). Exotic forests (3.8%), indigenous forests (0.9%), and ‘Short-rotation cropland’ (2.6%) were removed. In addition, trees were excluded if located on slopes where landsliding was unlikely to occur,

[1] https://doi.org/10.7931/L17H3

defined as slopes below the 1st percentile in the slope density distribution of the landslide inventory, which is 17.5° (Figure 3.6). Thus, 92.3% of the study area is classified as a land cover typical of pastoral hill country, and 52.0% of the study area exceeds the threshold of 17.5°, resulting in a slope-pasture mask of 377.8 km^2. Therefore, according to this simplified definition, 44.8 % of the study area is pastoral hill country. To isolate the influence of a single tree at a given pixel, areas of potential co-influence are removed by creating 15-m buffers around tree points and removing intersecting areas (Figure 3.5).

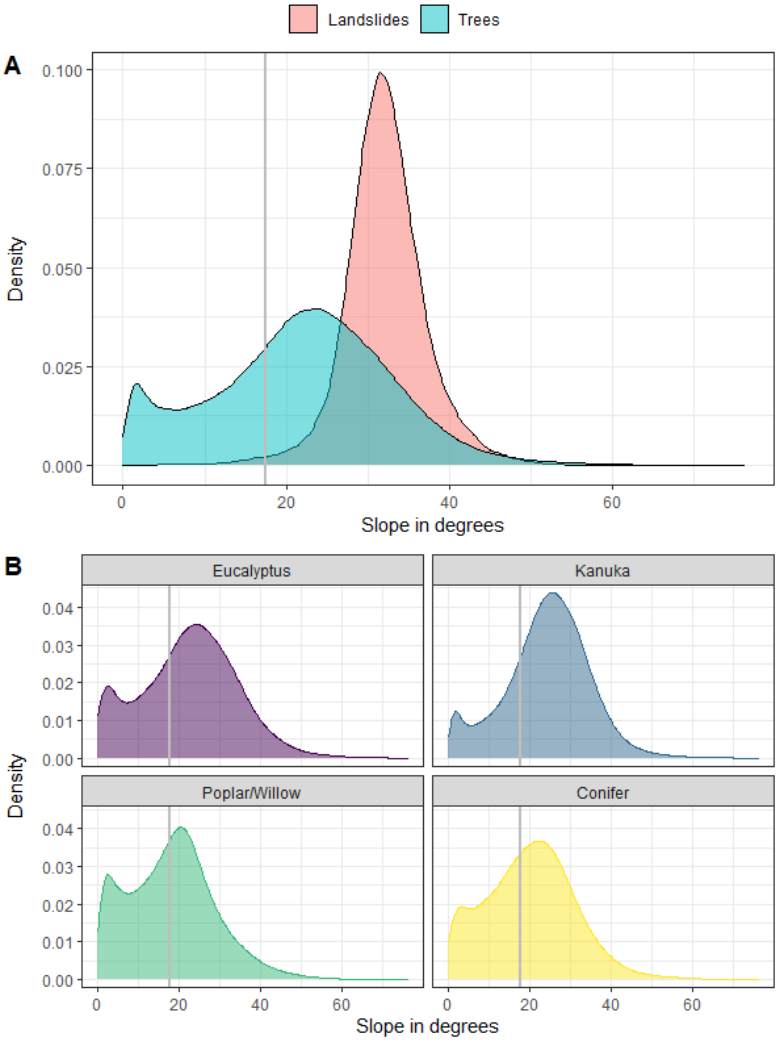

Figure 3.6 A: Density plots of shallow landslide scar slopes and slopes where trees are located on pasture. B: Density plots of slopes according to species class within pasture mask. The vertical line represents the 1st percentile (17.5°) of landslide slopes, which is the cut-off used for tree selection.

A 15-m radius centred on a tree point, and its vertical below-ground extension, is a conservative estimate of the ground area likely to contain most roots and affect slope stability (e.g., Douglas et al. (2013)) used a 10-m radius). Tree points represent the centroid of delineated tree crowns generated by pycrown, hereafter referred to as treetops. Further, a 15-m buffer is drawn around all trees not belonging to species class *j* in an iterative process to create a species-specific mask to treat each class independently (Figure 3.5).

Two final steps were involved in the calculation of the empirical tree influence models on slope stability (TIMSS) for each of the four species classes. A raster was generated using a Euclidean distance algorithm, representing the distance to the rasterized treetops at 1 m GSD. Landslide scars were merged using unique distance codes, resulting in a raster with values indicating distance from treetop and presence/absence of landslide scars. The fraction of soil surface eroded as a function of distance from tree could then be calculated for each tree species using the number of spaced trees within the slope-pasture mask and landslide scars (Table 3.5).

A nonlinear least-squares logistic regression model was used to fit $f(r)$ for each of the four species classes (Bates and Watts, 1988). The $f(r)$ curves are sigmoidal in shape, which has been found in other root distribution models, for example, in relation to root density (Sakals and Sidle, 2004) and root reinforcement (Schwarz et al., 2012). The logistic growth function is defined as:

$$f(r) = \frac{b_c}{1+e^{\frac{xmid-r}{scal}}} \quad (1)$$

where b_c is a parameter representing the asymptote; $xmid$ is a parameter representing the r value at the inflection point of the curve; and $scal$ a scale parameter on the input axis.

The Selfstart function SSlogis in R first evaluates the logistic function and its gradient, then creates initial estimates of the parameters b_c, $xmid$, and $scal$, which are fed to the nonlinear function to find the best-fit logistic equation. Goodness of fit was calculated using R-squared,

and 95% confidence and prediction intervals were calculated for each model. The maximum effective distance r_{max} is defined as the point where $r = .95b_c$.

Thus, for each species class j, the TIMMS (M_j) are defined as the reduction in soil surface eroded, expressed as:

$$M_j = b_c - f(r) \qquad (2)$$

Inserting $f(r)$ from equation 1, and following normalization to 0-1, M_j is quantified as:

$$M_j = 1 - \frac{1}{1+e^{\frac{xmid-r}{scal}}} \quad (3)$$

where M_j is the species-specific mitigation at a given pixel for an individual tree. When applied spatially, the influence of more than one tree is assumed to be additive, whereby the upper bound of trees contributing to slope stability at a given pixel is assumed to be 4. The TIMSS are thus a 2-dimensional representation of biophysical erosion and sediment control at 1 m GSD.

3.3 Results

3.3.1 Landslide Inventory

The final landslide dataset consists of 43,069 landslide scars that were triggered by the 2005 and later storm events (Figure 3.7). Median scar area is 49 m^2, mean 82.1 m^2, which is consistent with findings of previous studies (De Rose, 2013; Betts et al., 2017; Smith et al., submitted). The bands of limestone within the study area are notably absent of landslide scars (Figure 3.1 and Figure 3.7). The highest density of scars is found in the southern part of the study area, where high-magnitude rainfall events in 2005, 2006 and 2009 (72 hr totals of 197–283 mm) coincided with the steep and highly susceptible terrain, underlain by mudstone and fine siltstone. Mean slope of landslide scars is 32.2°, with a standard deviation of 5.1° (Figure 3.6).

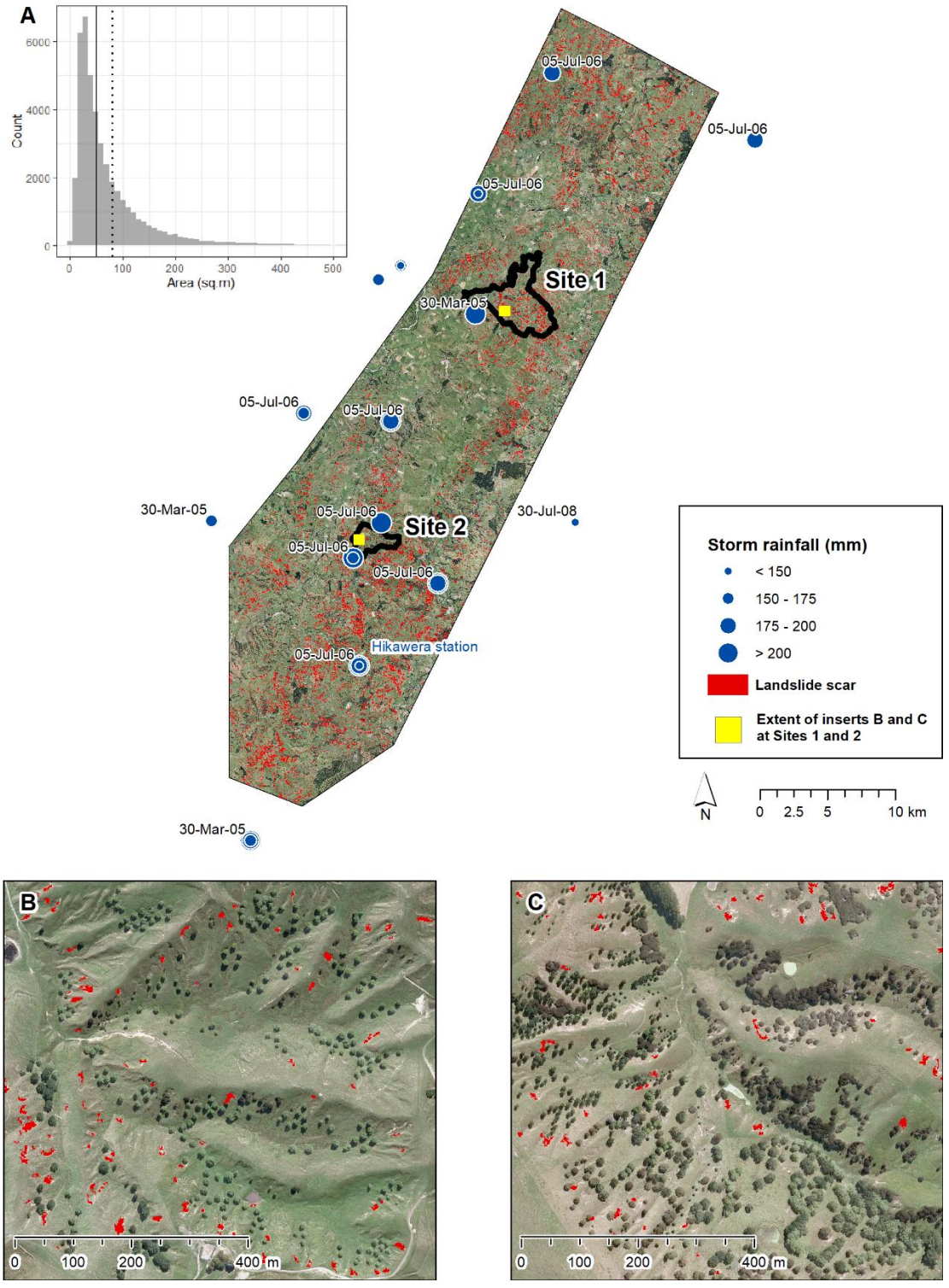

Figure 3.7. Distribution of storm-triggered landslides (red polygons) mapped in this study, and the rainfall magnitude of storms > 120 mm for the period March 2005 to January 2010. The beginning date of the events which recorded the highest rainfall during this period are labelled at each rain gauge. The extent of farms (sites 1 and 2) used for tree species field mapping is also shown. Insert A: Distribution of landslide scar size (m^2), including vertical lines of median (49 m^2) and mean (81.1 m^2); Insert B is the extent of yellow frame at Site 1; Insert C is the extent of yellow frame at Site 2.

3.3.2 Rural Tree Species Classification

The results of the SVM rural tree species classification are dependent on the performance of both ITC delineation using pycrown and the species classification using SVM and selected set of predictors (Table 3.2). In dense stands of kānuka and coniferous species, the number of trees was consistently underestimated (Table 3.3). This is partially explained by reasonably smooth canopies in areas of dense kānuka. Reducing the window size to a 3-m radius resulted in a slight improvement in the kānuka (0.39 of field counts; compare Table 3.3) and conifer (0.47) classes but led to an overestimation in the eucalyptus (1.07) and poplar/willow (1.15) classes.

Table 3.3. pycrown calibration results, and parameters used: Window size (ws); Hmin – threshold below which a pixel cannot be a tree; th_seed – Growing threshold 1; th_crown – Growing threshold 2; Maximum crown value of the crown diameter.

Species class	Field count	pycrown count	Proportion of field count
Conifer	693	238	0.34
Kānuka	278	97	0.35
Eucalyptus	341	329	0.96
Poplar/willow	1179	1,174	1.00
Other	239	97	0.41
Total	2491	1,838	0.74
pycrown parameters:	ws 5, Hmin 1.5, th_seed 0.45, th_crown 0.55, max_crown 8		

In terms of performance of predictors, variable selection for the tree classification was informed by the pair-wise ROC curves and calculation of the AUC scores. Tree height (TH) was the sole variable to score consistently less than 0.6 across all species classes (Figure 3.8). Removal of *TH* resulted in a marginal improvement of the model (0.1%) and confirms TH as a poor predictor (Table 3.4). The Kappa score also increased from 0.8879 to 0.8895. The next lowest AUROC score was the SD of NDVI from 2013 imagery (ndvi_13_sd). However, removal of *ndvi_13_sd* led to a reduction in mean accuracy. The ranking of variables using AUROC across classes shows there is no further variable that is clearly under-performing and potentially reducing the predictive power of the model. However, a correlation matrix of all variables found a strong correlation (–0.91) between mean brightness (2013) and mean NDVI

(2013). Yet, removal of mean brightness (2013) resulted in a significant reduction of accuracy, and therefore contributes to the performance of the classifier in interaction with mean NDVI (2013). Therefore, the final SVM model includes 11 predictors following removal of *TH* (Table 3.4) and trained on 9260 tree crowns from sites 1 and 2. A final accuracy of 92.6% and a Kappa value of 0.89 proves the SVM model to be an excellent classifier for these tree species classes.

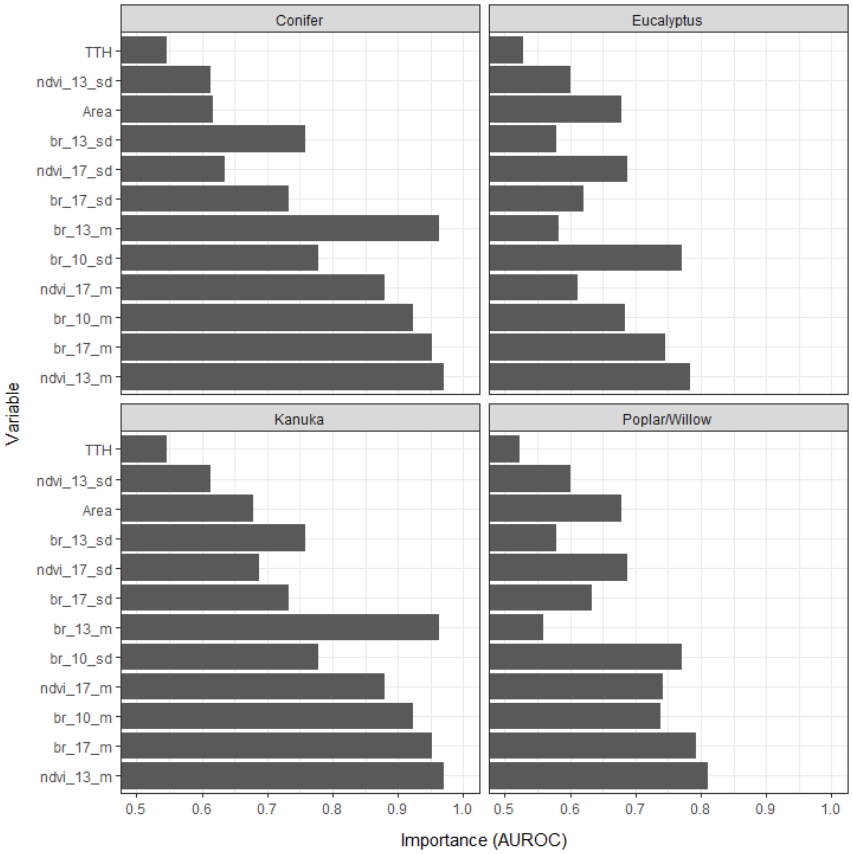

Figure 3.8. Variable importance using AUROC for selection of best predictors. An AUC of 1 would indicate perfect classification, while an AUC score of 0.5 equates to performance no better than a random guess. See Table 3.2 for interpretation of abbreviated variable names.

Table 3.4. Classification accuracy following 5x 10-fold cross-validation (σ = 0.05, cost penalty = 10) with different input variables. Accuracy of the final model was improved following extensively tuned (best model: σ = 0.05, cost penalty =15)

Tree Height (m)					
Tree crown area (m2)					Final model
Mean brightness 2010					
Standard deviation brightness 2010					
Mean brightness 2013					
Standard deviation brightness 2013					
Mean NDVI 2013					
Standard deviation NDVI 2013					
Mean brightness 2017					
Standard deviation brightness 2017					
Mean NDVI 2017					
Standard deviation NDVI 2017					
Accuracy (%)	92.40	92.51	92.05	89.83	92.58
Cohen's Kappa	0.8879	0.8895	0.8828	0.8496	0.8905

Table 3.5 presents the results of the classification. Trees that fall outside the pasture mask are either forestry blocks, areas of scrub, or indigenous vegetation. Thus, the dominant species in areas of pasture (776 km^2) is kānuka (373,000 trees), followed by poplar and willow species (207,000). When considering the underestimation of pycrown for the kānuka and conifer species, the corrected number is likely to be approximately 1.07 million kānuka, and 111,000 conifer stems. Interestingly, a large proportion of kānuka (76.4%) are located on steep slopes (>17.5°), where landslide erosion is more likely (Figure 3.6). Since kānuka is often found alongside mānuka, and difficult to distinguish spectrally, the classified kānuka in the study area includes mānuka. A lesser proportion of poplar and willows (52.9%) and eucalyptus trees (66.9% of the 60,500) are found in the same slope category.

Table 3.5. Tree selection for tree influence models.

	Eucalyptus	Kānuka	Poplar/willow	Conifer	Total
Total number of trees in study area	77,920	405,649	261,656	118,631	863,856
Number of trees in pastoral land	60,524	372,579	206,773	37,614	677,490
Number of trees in pastoral hill country	40,508	285,251	109,015	22,307	457,081
Number of trees spaced > 15 m	5,476	53,974	25,006	1,429	85,885
Trees selected of total (%)	7%	13%	10%	1%	10%
Area of species-specific mask (km^2)	243.7	279.5	266.1	252.1	-

3.3.3 Empirical Tree Influence Models on Slope Stability

Table 3.5 lists the number of trees used to develop the TIMSS for each of the four species groups. According to the results of the classification, kānuka is the most dominant species in pastoral hill country (slopes >17.5°) in the study area, making up 62% of all trees, or 79% using the correction factor. Of the 262,000 poplars and willows, 109,000 are within the pasture-slope mask, of which 25,000 are spaced at a minimum of 15 m and were used to isolate the influence of an individual poplar/willow on slope stability. Since most conifers (*Pinus radiata*) are found in forestry blocks or shelter belts located on farms within the study area, merely 1% of all pines and 7% of eucalyptus are located as space-planted trees on slopes in areas of pasture. This underscores the need for a large study area to successfully use the inferential method, since different species are planted at different densities and locations depending on their purpose.

The results of $f(r)$ and M_j for the four species classes are shown in Figure 3.9 and Figure 3.10, respectively. The points in Figure 9 are the measured mean values of fractions of eroded soil at each 1 m increment away from the trees. The four non-linear models were then used to predict the maximum distance of influence and are plotted in Figure 3.9, as follows: A) poplar/willow 20 m; B) kānuka 17 m; C) conifer 17 m; and D) eucalyptus 13 m. The asymptotic value b_c is different for each of the four species groups, which reflects the local environment in which the trees selected for the analysis are predominantly located. Based on Figure 9, eucalyptus, poplars, and willows are situated on slopes with higher rates of erosion than kānuka and coniferous species, and consequently have larger asymptotic values.

Figure 10 shows the results of the normalized reduction in eroded soil $b_c - f(r)$, that is, M_j. Where the layout of trees is such that more than one tree contributes to slope stability at a given location, the influence on slope stability is assumed to be additive. Therefore, TIMSS values can exceed 1 when applied spatially (Figure 3.12). Eucalyptus trees have the greatest mean influence between 0 and 5 m from trees, but the least reach, with a maximum effective

distance of 13 m. Poplars and willows have the greatest maximum effective distance of 20 m, and the tree influence decreases more slowly with increasing r compared to the other three curves. The influence on slope stability of the conifer class decreases rapidly with increasing r, reaching a value of 0.3 at 9 m, and a maximum effective distance of 17 m. Kānuka has the same maximum effective distance as conifers, yet reaches an TIMSS value of 0.3 at 10 m. In total, 43.8% of the area (165.3 km^2) comprising pastoral hill country in the study area has increased slope stability due to the presence of trees, that is, a TIMSS value greater than 0. The remaining 56.2% of pastoral hill country (212.5 km^2) are untreated slopes that are highly susceptible to landslide erosion.

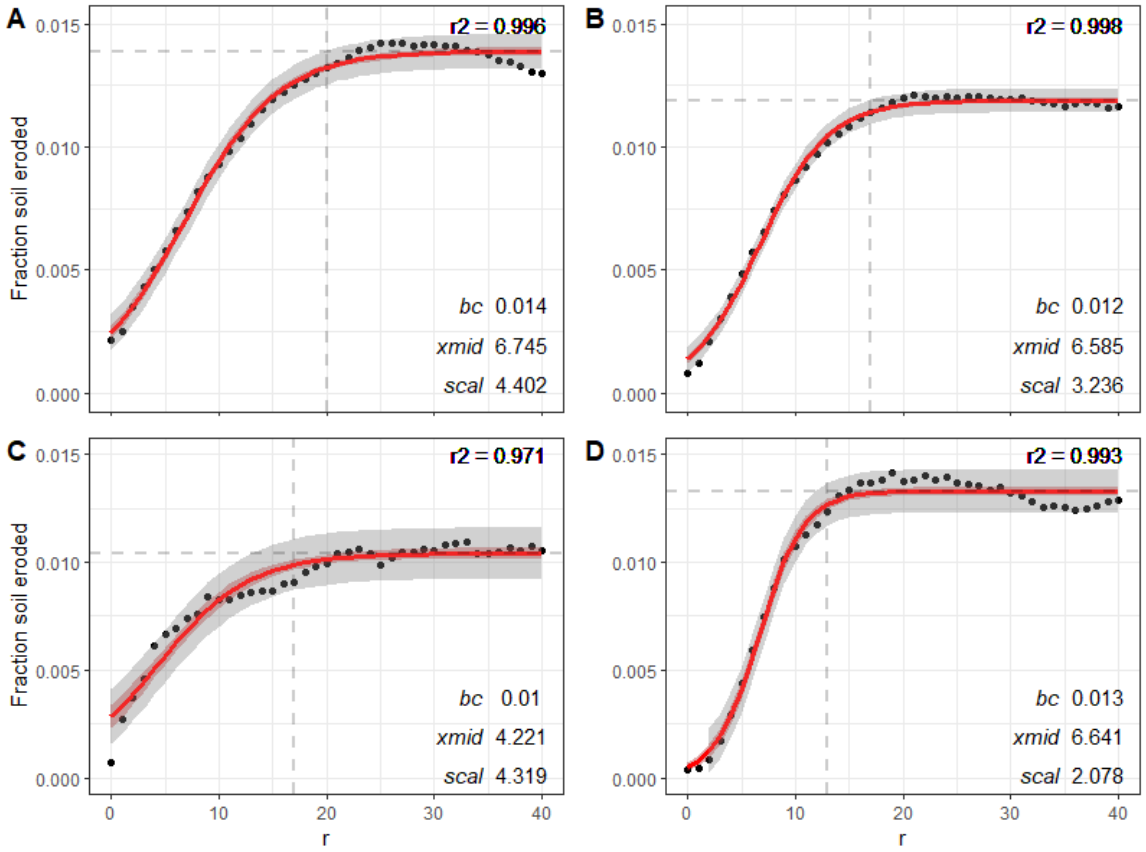

Figure 3.9. For the four species classes A) poplar/willow, B) kānuka, C) conifer, and D) eucalyptus: Mean fraction of eroded soil $f(r)$ at distance (m) from tree, fitted using non-linear logistic model SSlogis with 95% confidence (red) and prediction (grey) bands.

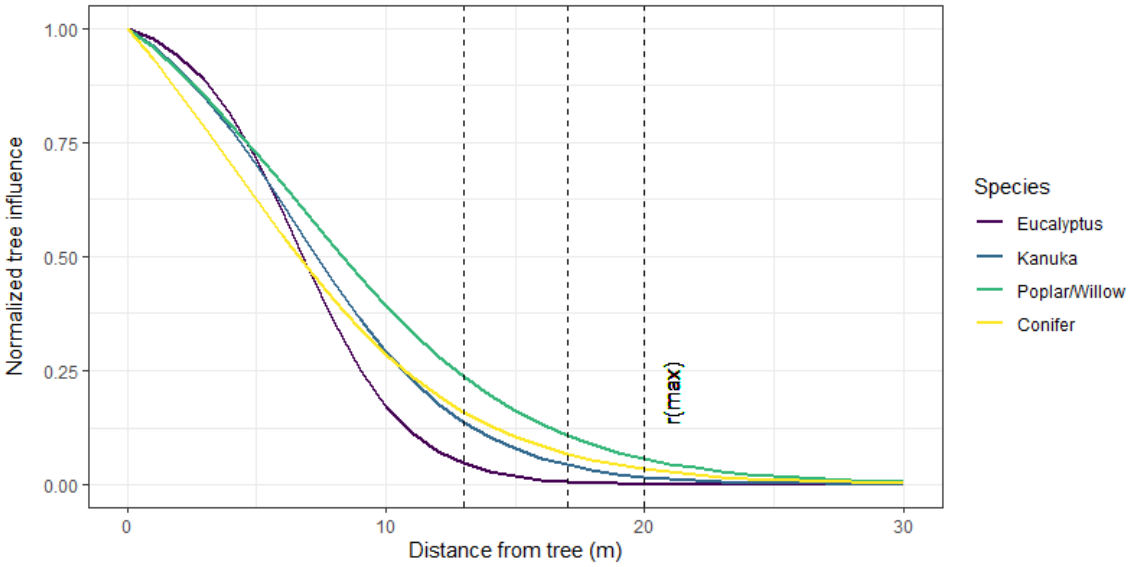

Figure 3.10. For the four species classes conifer, eucalyptus, kānuka and poplar/willow: Normalized mean tree influence M_j (0 – 1) for an individual tree, as reduction in eroded soil $b_c - f(r)$. Vertical lines show the maximum effective distance of 13 (Eucalyptus), 17 (conifer, kānuka) and 20 (poplar/willows) meters.

3.4 Discussion

3.4.1 Rural Tree Species Classification

Inclusion of both mean and SD brightness/NDVI were shown to be good predictors and enhanced the discrimination between species classes. Yet, tree height was found to be a poor predictor of species. This can be explained by the significant variation within species classes and similar mean tree heights across classes, which is likely due to a range of tree ages (Figure 3.11). The overall accuracy using k-fold cross-validation with the entire dataset of >10,000 tree crowns is a good measure of expected accuracy achievable in the wider study area. Yet, according to the data obtained in the field, approximately 10% of tree species in the study area do not fit into the four dominant species classes used here. Accounting for this source of error, the overall classification accuracy is likely to be 83.3% since predictions can only be made with the classes available to the SVM classifier. To further improve the model, further training samples from additional classes are needed.

This is the first attempt at tree species classification of ITCs at landscape scale in New Zealand. In their review on tree species classification, Fassnacht et al. (2016) acknowledge the significant challenge of developing classifications over large geographic extents. Field counts of stems showed that LiDAR based delineation of individual tree crowns with pycrown (Zörner et al., 2018) produced very accurate results for space-planted poplar, willow, and eucalyptus trees. However, since kānuka is most often found in relatively dense stands with little variability in tree heights, we counted an average of 2.86 stems in the field for every pycrown-delineated tree crown. Coniferous species are often planted as shelterbelts, or as relatively small, densely planted blocks (e.g., 2 ha). Their close spacings present a similar difficulty for accurate tree crown delineation, with an average of 2.94 stems per delineated tree crown.

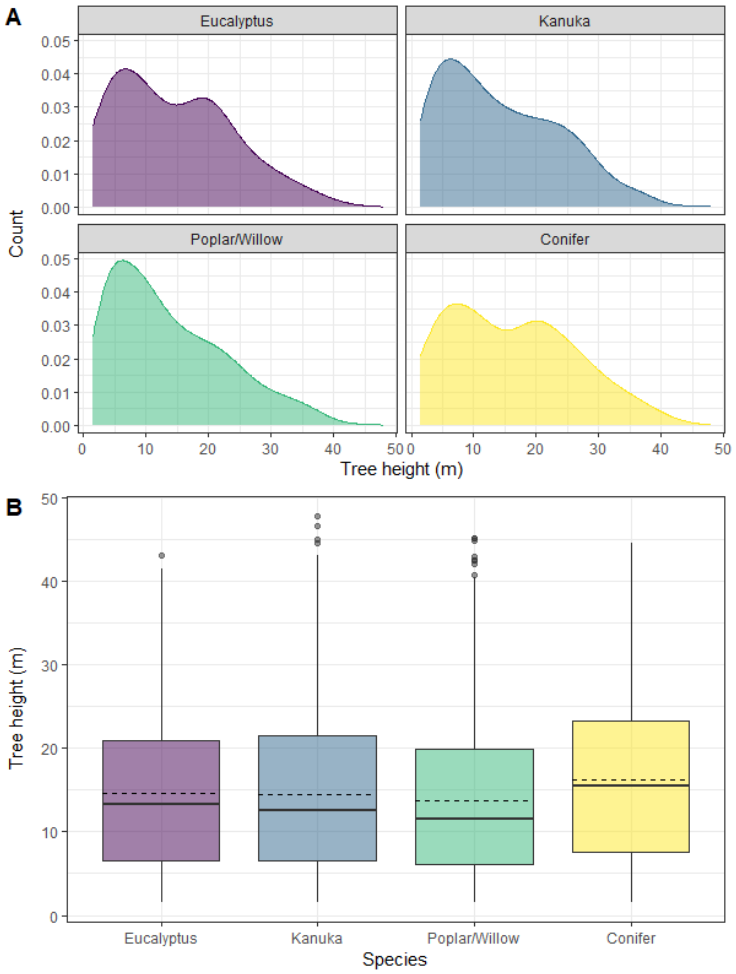

Figure 3.11. For the four species classes at Sites 1 and 2 combined: A) Density plots and B) boxplots of tree heights with median (solid line) and mean (dashed line) shown.

To improve discrimination of individual kānuka crowns, increasing the resolution of the LiDAR DEMs (e.g., 0.5 GSD) may help. While this would improve the gradient between trees, it can also result in an overestimation of tree crowns, as subcomponents of crowns such as individual branches, can be delineated as separate objects. Recent advances have been made using machine learning to integrated crown delineation from LiDAR with optical imagery and provide a highly adaptable means for accurate delineation across multiple forest types (Weinstein et al., 2020a, 2020b, 2019). However, on pastoral land, conifers only make up a small proportion of all trees (111,000 ± 16.7%), or 1.4/ha. As to be expected, eucalyptus is the least common species class, accounting for only 4% of trees in pastoral land in the study area. Poplar and willow species amount to 14%, and 11% on hillslopes, making up 109,000 trees in pastoral hill country, which amounts to an average of 3.2 sph. Poplars and willows are therefore the most abundant exotic species (51% of exotics) that have been intentionally planted for erosion and sediment control.

A somewhat unexpected finding is the dominance of kānuka in the study area, which consists of original bush remnants and natural regenerated trees. Kānuka makes up 79% of trees in pastoral hill country in the study area, averaging 24.1 sph following correction (Table 3.6). However, only 19% of these kānuka are spaced more than 15 m apart (Table 3.5), so the majority are growing in dense patches, which promotes slope stability, but likely reduces pasture productivity. Kānuka are successional species and are among the first to colonise marginal land, including eroded hillslopes (Smale et al., 1997). Indeed, 76.6% of the kānuka on pastoral land are on susceptible hillslopes (>17.5°) – which is a large proportion compared to 52.7% of poplars and willows on pastoral land (Table 3.6; Figure 3.6). Despite being abundant in pastoral hill country, research on the impacts of kānuka on landslide erosion are limited (Ekanayake et al., 1997; Watson et al., 1999, 1995) and mostly have high density stands of naturally reverting kānuka and mānuka as the object of their investigation – as opposed to widely spaced, low-density kānuka.

Investigating landslide densities in reverting kānuka and mānuka, Bergin et al. (1995) found landslide damage to 10-year-old stands was estimated to be 65% less than that sustained by pasture and 90% less in 20-year-old stands, and almost 100% in still older stands. They also found a relationship between stem density and age, with young stands of < 10 years age typically containing 20,000 sph and older stands (30–40-year age class) 3000 sph. Bergin et al. (1995) further note that under-stocked stands gave a reduction in landsliding comparable with fully stocked stands of similar age. This indicates that thinning kānuka stands on hillslopes may be a reasonable erosion mitigation strategy to both increase pasture productivity while maintaining increased levels of slope stability. Furthermore, these findings challenge the common perception of kānuka as a weed and the related scrub-clearing method aimed at increasing pasture productivity (Allen et al., 1992). In commenting on the practice of kānuka clearance, Norton et al., (2020) suggest landowners need to be better incentivised to promote land management practises that retain and enhance biodiversity outcomes. Results of this study can inform the densities required to achieve added slope stability, which is discussed in the following section.

Table 3.6. Corrected tree counts and mean densities in pastoral land and in pastoral hill country in study area. The combined error tree species classification and absent species classes is ± 16.7%. Pastoral hill country is defined using a slope threshold of 17.5˚.

Corrected tree counts	Eucalyptus	Kānuka	Poplar/willow	Conifer	Total
Number of trees in pastoral land (sph)	60,524 (0.8)	1,064,511 (13.7)	206,773 (2.7)	110,629 (1.4)	1,442,438 (18.6)
Number trees in pastoral hill country (sph)	40,508 (1.2)	815,003 (24.1)	109,015 (3.2)	65,609 (1.9)	1,030,135 (30.8)
Trees in pastoral land (%)	4%	74%	14%	8%	100%
Trees in pastoral hill country (%)	4%	79%	11%	6%	100%

3.4.2 Interpretation of Empirical Tree Influence Models

Further developing a method first introduced by Hawley and Dymond (1988), we have demonstrated an alternate approach to existing physical root distribution models aimed at generating a tree influence layer for the dominant species found in New Zealand's pastoral hill

country (Figure 3.12). Such layers can subsequently be incorporated into landslide susceptibility analyses to quantify the species-specific reduction in probability of landsliding achieved due to the presence of space-planted trees and pre-existing woody vegetation such as kānuka. Thus, we aim to fill the gap in scale between physical models that quantify root reinforcement for homogenous tree stands, and landslide susceptibility modelling at regional scale that commonly uses land cover data as a proxy for the effect of the hydrological and mechanical influences of woody vegetation. It is important to note that the normalized TIMSS are a relative measure of individual tree influence on slope stability and, besides the distribution of the curves, are not directly comparable. For a given location, a value of 1.0 for the poplar and willow TIMSS will equate to a greater increase in soil shear strength than a value of 1.0 in the conifer TIMSS since the magnitude of increase in root reinforcement differs due to variations in the tensile strengths of root fibres and resulting soil-root frictional interactions (Schmidt et al., 2001; Schwarz et al., 2010c, 2010b).

Future research is needed to quantify differences in the magnitude of TIMSS by: i) calibration using published datasets of tensile strength measurements, such as the mean live-root wood tensile strengths of common indigenous, plantation and scrub species by Watson and Marden (2004); or ii) landslide susceptibility assessments, which can quantify the relative contribution of the four different TIMSS as a reduction in the probability of landslide occurrence. Additionally, the TIMSS have potential to be further split by tree height as a proxy for age (Figure 3.11), since the influence of trees on slope stability increases with above- and below-ground biomass growth. If successful, this would allow the tree influence on slope stability to be predicted based on allometric variables for each species class, which would provide a more nuanced representation of added soil shear strength due to trees.

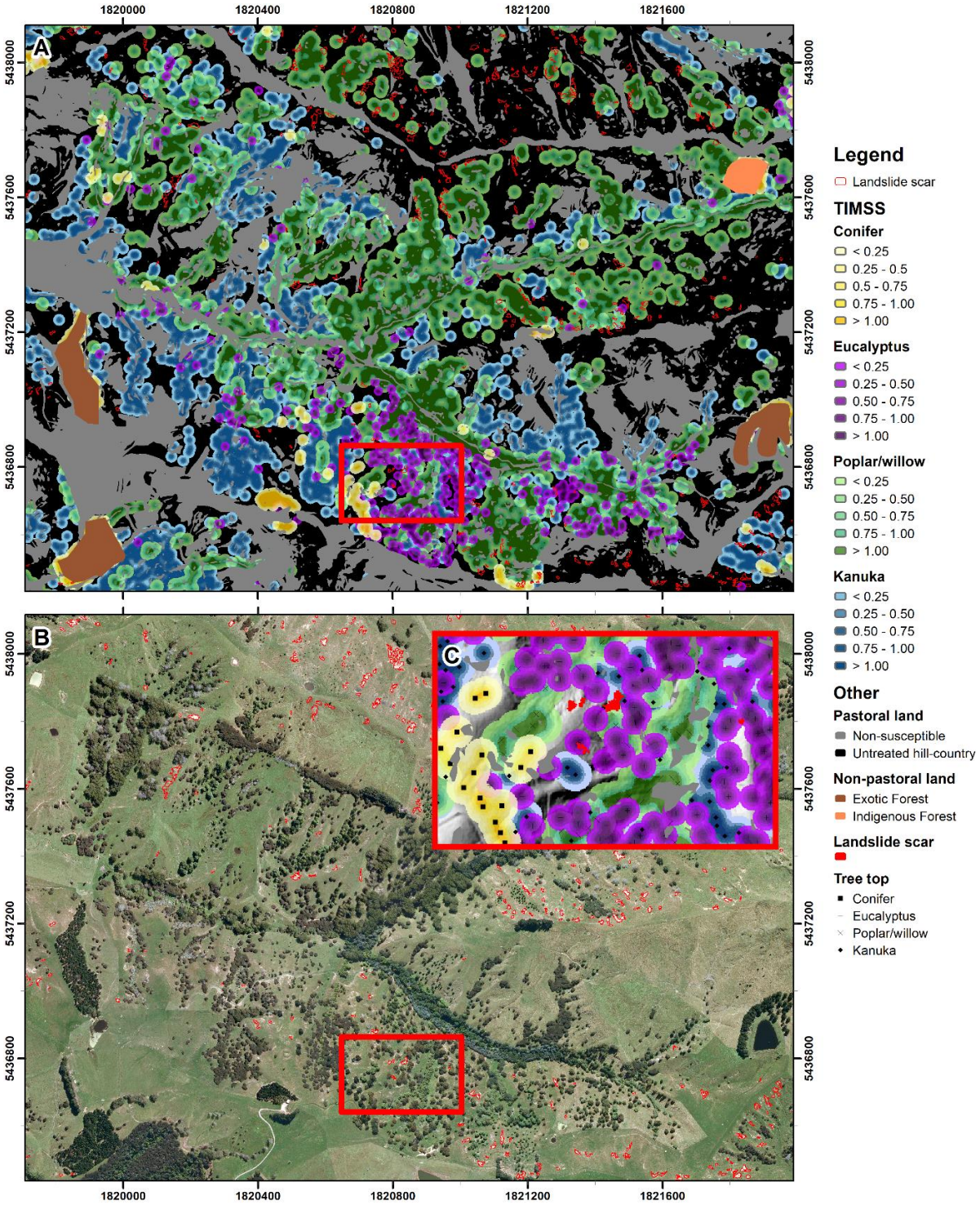

Figure 3.12. A: For an area at Site 2, empirical tree influence models on stability for the four species classes: conifer, eucalyptus, poplar/willow and kānuka, non-susceptible pastoral land (defined by slope threshold of 17.5 °), and untreated pastoral hill country; B: Regional multispectral orthophotos (2010) showing landslide scars mapped in imagery. Red frames in A and B show extent of Insert C: Illustration of landslide causation: though trees contribute to slope stability, they do not always prevent landslide erosion – a reflection of a multivariate problem. Note, the influence of more than 1 tree at a given location is assumed to be additive, which is why values exceed 1. Map projection is New Zealand Transverse Mercator (NZTM).

The discussion thus focuses on the shape and maximum distance of the TIMSS curves (Figure 3.10). Root distribution data from extractions and/or models are limited for comparison purposes. Yet, we found very similar relationships expressed in the TIMSS to existing root distribution models for similar species (Abernethy and Rutherfurd, 2001; Sakals and Sidle, 2004; Schwarz et al., 2016, 2012). The model developed by Sakals and Sidle (2004) to assess the spatial variability of root cohesion based on a calibration of measured root cohesion from a Douglas-fir stand of 20 root systems found the relationship between normalized root densities and root influence radii to be sigmoidal in shape, differing slightly between two age groups of trees. This suggests the TIMSS have potential transferability to other species and environmental settings, where the representation of individual trees for landslide susceptibility modelling is desired, for example, in agroforestry landscapes (Hairiah et al., 2020; van Noordwijk et al., 2019).

A further comparison can be made to the root-bundle model calibrated by Schwarz et al. (2016) using two root distribution datasets of fully excavated poplars from Gisborne and samples from 20 trenches at a site near Palmerston North, New Zealand, planted in a range of high densities (89–237 sph) according to a Nelder planting design (Phillips et al., 2014). The results were used in slope stability calculations to quantitatively evaluate the mechanical stabilization effects of spaced trees on pastoral hill country. The maximum lateral root spread was reported as 13.3 m for 2-year-old poplar species in the Gisborne site and estimated as only 4.2 m for the high-density stands at the Palmerston North site. The modelled spatial root reinforcement curve in the root-bundle model used a Weibull survival function, which is similar to the non-linear logistic regressions fitted for the TIMSS. However, it is clear there are significant differences between the maximum effective distance of poplars/willows modelled by Schwarz et al. (2016) and that observed in the TIMSS, which can be explained by considering: i) the influence of different environmental conditions as demonstrated by lateral root growth of 1–2-year-old trees at the flat, irrigated site with free draining alluvial soils exceeding that of the 10-year-old trees on 5–20° slopes at the Palmerston North site with silt-

loam soils featuring various mottles and concretions in the sub-soil; ii) different tree densities and sampling methods (full excavations versus trenches), may have also contributed to the large difference found between their two sites; iii) the hydrological influence was not quantified by Schwarz et al. (2016), which may partly explain the differences from the maximum distance observed in the TIMSS; and iv) the average age of poplars and willows in our study area in the Wairarapa will likely exceed the age of trees for which root data is available for comparison purposes (e.g. McIvor et al., 2009, 2008; Schwarz et al., 2016).

Most of the poplar and willow trees mapped at Sites 1 and 2 were planted in the 1980s and 1990s, with a mean tree height of 13.7 m (Figure 3.11). While there are no published data of root densities of fully mature, scattered trees, a comparison with the largest dataset of full excavations of poplars, documented by McIvor et al. (2009, 2008) can further help with an interpretation of the TIMSS. Based on their observations of 'Veronese' poplar clones aged between 5 and 12 years, they found maximum lateral root distance extended up to 14 m. At 14 m, the poplar and willow TIMSS is 0.2. The remaining difference in $f(r)$ where $14 < r < 21$ may be attributable to both the younger age of excavated trees by (McIvor et al., 2009) and the hydrological influence of trees that modifies water infiltration and soil moisture content (Gonzalez-Ollauri and Mickovski, 2017; Phillips and Marden, 2005; Stokes et al., 2014; Zillgens et al., 2007). Even though these excavations were undertaken for young trees, they do support the observation that mature poplars and willow trees have a maximum effective distance on slope stability of about 20 m. Further experimental research and root data collection of fully mature poplar and willow trees are required to confirm the findings of this study. However, as was found by Schwarz et al. (2016), the challenge associated with measurements taken from excavations is the high variability in root distributions within single species due to varying environmental constraints. McIvor et al. (2009) found soil depth and associated water storage capacity to be likely limiting factors for growth and root development. There were also indications that terrain morphology influenced the root morphology with roots extending further uphill on steeper slopes.

Excavations of mature kānuka trees by Watson et al. (1995) found a mean maximum root length of 3.6 m and a maximum root length of 6.1 m for the 32-year-old age group. Adopting a correction factor of 0.35 delineated crowns per stem, the kānuka TIMSS can be interpreted accordingly (Table 3.3). Thus, the maximum effective distance of 17 m is due to the influence of approximately 3 stems, and the kānuka in the study area are largely mature trees that are several decades old so will likely have more developed root systems than that documented by Watson et al. (1995). The same study also excavated three *Pinus radiata* aged 25 years and found a mean maximum root length of 9.1 m. Once more, adopting a correction factor of 0.34, the conifer TIMSS with a maximum effective distance of 17 m can be interpreted as the effect of approximately 3 stems. A further important consideration is that the tensile strength of fine roots differs across species classes, and is a limiting factor for *Pinus radiata*, whose mean live-root tensile strengths are only 40% and 50% of kānuka and 'Veronese' poplar (*Populus deltoides x nigra*) root strengths, respectively (Watson and Marden, 2004).

However, in the absence of comparable data, the maximum distance of influence presents some initial interpretational difficulty; and yet, the data presented here are based on empirical observations of the spatial relationship between trees and landslide erosion. Several factors need to be considered when interpreting the results such as the respective contributions of the hydrological and mechanical processes by which vegetation modifies slope stability. The TIMSS represent the mean spatial distribution of the combined mechanical and hydrological influence imparted on the soil during the rainfall events that triggered the landslides between 2005 and 2010. More detailed analysis of antecedent soil moisture conditions leading up to the storms of 2005, 2006, and 2009 may shed light on the respective roles of mechanical and hydrological processes of trees, particularly given that, with the exception of the March 2005 storm, the remainder were during the winter month of July where interception and evapotranspiration are less relevant due to leaf fall. Yet, despite being the only deciduous species class, the poplar-willow TIMSS outperforms the other three classes in terms of the

magnitude of influence beyond 4 m, which supports the fact that the mechanical mechanism of poplar and willow species is significant due to the high tensile strengths of the roots.

3.4.3 Implications for Land Management in Pastoral Hill Country

There has been strong emphasis on biological erosion control in New Zealand's pastoral hill country – either through space-planted trees or blanket afforestation, because of its relative low cost and its effectiveness (G. Douglas et al., 2013b; Phillips and Marden, 2005). In more recent times, erosion mitigation has been made a component of Farm Environment Plans (FEP), which are comprehensive plans undertaken by regional councils, farmers or other industry groups that integrate soil conservation into land management practices and farming operations (Basher et al., 2016; L Basher et al., 2008; Basher, 2013; Collins et al., 2014; Douglas et al., 2008; Dymond et al., 2016; Manderson et al., 2007; Phillips et al., 2008; Phillips and Marden, 2000). Yet, little is known about the effectiveness of individual trees and stands and the overall effectiveness of these measures at landscape scales. Both the rural SVM tree species classification produced for New Zealand's pastoral hill country and the derived TIMSS can be applied at farm to landscape scales to inform on which species are either pre-existing in the landscape or have been successfully established in the context of FEPs (Figure 3.12). Furthermore, through integration into high-resolution landslide susceptibility modelling, it is now possible to both i) quantify the mitigation effectiveness of individual trees and compare species and ii) inform on where to prioritize future mitigation, given the spatial probability of landslide occurrence, which can be modified by the presence or absence of trees. Mitigation effectiveness is a multivariate problem, as it is dependent on site-specific conditions, which vary with, for example, slope gradient, soil, and rock type. Therefore, including the four TIMSS as covariates within a landslide susceptibility assessment can provide a statistical measure for

the respective contributions of each layer to slope stability. Furthermore, allometric functions could also be used to scale the TIMSS, e.g., according to tree height or area of tree canopy.

The tree densities listed in Table 3.6 provide an initial indication of how widely soil conservation practices have been adopted in the study area, and the spatially explicit representation of added slope stability due to trees provides further detail (Figure 3.12). An average of 3.2 poplar and willow trees/ha (total of 109,000 trees), 1.2 eucalyptus/ha (41,000 trees) and 1.9 coniferous species/ha (66,000 trees) in pastoral hill country (slopes > 17.5°) reflects the work carried out by landowners and soil conservators over the past several decades. However, these numbers are also indicative of large areas of untreated land with elevated levels of landslide susceptibility. To treat the remaining 212.5 km^2 (56%) of untreated pastoral hill country (TIMSS = 0) in the study area, an additional 950,000 poplars/willows would need to be planted if using a regular grid of 15 x 15 m (44 sph), which falls within the recommended planting density of 30–60 sph (e.g., Douglas et al., 2011; Wilkinson, 1999). A planting density of 44 sph would result in TIMSS values >0.5, which would achieve significantly more reduction in landslide erosion than values <0.5. However, landslide susceptibility assessments incorporating the species-specific TIMSS should be used to inform on mitigation plans and planting densities in untreated terrain, since not all pastoral hill country is equally susceptible to landsliding. Variation in morphological (e.g., slope gradient; Figure 3.6), geological, and hydrological geo-environmental variables can influence the potential for landslide occurrence (Budimir et al., 2015; Reichenbach et al., 2018; Süzen and Kaya, 2012; van Westen et al., 2008).

Yet, the large amount of mature kānuka in the study area, particularly on hillslopes, has reduced the propensity for landsliding in many areas (Table 3.6): 50% of kānuka trees growing on pastoral land are found on slopes >25°; the slope value of the 0.75 quantile is 31°. Given that the mean slope of landslide scars is 32.2° (SD = 5.1°), kānuka is the most abundant form of woody vegetation on highly susceptible slopes. Kānuka are better suited to these growing

conditions than poplars and willows (Allen et al., 1992). Indeed, the 0.5 and 0.75 quantiles of slope values for poplars and willows on pastoral land are 18° and 25°, respectively, and are evidence that these unrooted poles are more likely to be planted on lower, more hospitable slopes that favour tree establishment. Thus, more planting to reinforce susceptible slopes is required to reach a recommended planting density of 25–160 sph (G. Douglas et al., 2013a; Hawley and Dymond, 1988; Schwarz et al., 2016; Wilkinson, 1999). According to the TIMSS, poplars and willows have the greatest influence on slope stability, but many other factors and potential co-benefits must also be considered when deciding on which species to plant (Benavides et al., 2009; Dominati et al., 2014; England et al., 2020; Kemp et al., 2018; Norton et al., 2020).

3.5 Conclusion

We developed a rural tree species classification of individual tree crowns using freely available high resolution multi-spectral imagery, with an overall accuracy of 92.6%. Native kānuka is the dominant woody vegetation species in pastoral hill country of the study area with an average of 24.1 sph, and thus provides a valuable soil conservation function as the most abundant species on susceptible slopes. Of exotic species that were planted for erosion and sediment control, poplars and willows make up 51% (109,000 trees) in pastoral hill country at a mean density of 3.2 trees/ha.

The novel approach demonstrated in this paper advances the method first introduced by Hawley and Dymond (1988) by developing tree influence models on slope stability (TIMSS) for four dominant tree species in New Zealand's pastoral hill country. The method uses inductive inference to infer tree influence by assessing the spatial relationship between trees and landslide erosion. This approach requires a large landslide inventory (we used >43,000 features) and many widely spaced trees (86,000) in a silvopastoral landscape. The results can both challenge and validate understanding of the role of trees on slope stability, which is

typically quantified using physical root reinforcement models. The TIMSS have largely confirmed the shape and distribution of spatial root distribution models, with influence on slope stability declining rapidly with distance from trees as a sigmoid curve. Poplars and willows have the greatest maximum effective distance (20 m), and the tree influence decreases more slowly with increasing distance compared to the other three species classes. The spatial application of TIMSS has shown that 43.8% of the pastoral hill country in the study area (165.3 km^2) has increased slope stability due to the presence of trees on slopes. An additional 950,000 poplars/willows at 44 sph would be required to mitigate landslide erosion on the remaining 212.5 km^2 (56.2%) of untreated pastoral hill country in the study area. However, not all pastoral hill country is equally prone to landslide erosion. Therefore, tree influence models should be integrated into multi-variate landslide susceptibility modelling in silvopastoral and agroforestry landscapes to support the development of targeted mitigation plans.

4

4 QUANTIFYING EFFECTIVENESS OF TREES FOR LANDSLIDE EROSION CONTROL

Raphael I. Spiekermann[1,2], Hugh G. Smith[2], Sam McColl[1], Lucy Burkitt[1], Ian Fuller[1]

Geomorphology (Elsevier), Vol. 396(107993), 1. January 2022, p. 1-16
Submitted 20 June 2021
Accepted 11 October 2021
Available online 15 October 2021, reprinted with permission of Elsevier.
https://doi.org/10.1016/j.geomorph.2021.107993

This publication presents a landslide susceptibility model developed using binary logistic regression for silvopastoral landscapes, which for the first time includes spatial distribution models for individual trees of different vegetation types. Models were trained and tested using the landslide inventory introduced in Chapter 3, consisting of 43,000 landslide scars mapped across an 843 km^2 area. In addition, the effect of highly skewed continuous tree variables on the maximum likelihood estimator is investigated by testing different sampling strategies aimed at reducing positive skewness. With an adequate sample size, highly skewed continuous predictor variables were found to not result in an inflation of effect size. Using two farms in the study area, the application of the landslide susceptibility model is illustrated by quantifying the reduction in shallow landslide erosion due to trees.

[1] School of Agriculture and Environment, Massey University, Palmerston North, New Zealand

[2] Manaaki Whenua – Landcare Research, Palmerston North, New Zealand

4.1 Introduction

Accurately quantifying the effectiveness of trees for hillslope stability remains a key challenge for erosion control research. Irrespective of tree species, methods to quantify the effect of trees on landslide erosion generally use 1) empirical- (e.g., Douglas et al. 2013a), 2) physical- (e.g., Schwarz et al. 2016), or 3) statistical-based approaches (e.g., Reichenbach et al. 2014). Quantitative empirical studies have demonstrated and/or modelled that widely spaced trees on hillslopes reduce landslide erosion by 70–95% within 10 m of tree stems compared with untreated control sites (G. Douglas et al., 2013a; Douglas et al., 2009; Hawley and Dymond, 1988; Hicks, 1989b, 1989a, 1992; McIvor et al., 2011, 2015; Phillips et al., 2008; Thompson and Luckman, 1993). Yet, such univariate methods do not account for variation in environmental factors and tree densities. Physical models can include root reinforcement modelling to quantify increases in soil shear strength for a given slope (e.g., Schwarz et al. 2010c, 2016). Such approaches are well suited to assessing effectiveness of trees at the hillslope scale but are less practical at regional scales due to the data requirements relating to the physical parameters of the soil which can be highly variable is hilly or steep landscapes (Holcombe et al., 2012; Masi et al., 2021). For larger areas, simplified assumptions must be made (Salvatici et al., 2018), which can result in poorer performance of physical models compared with statistical methods (e.g., Cervi et al. 2010). Therefore, both deterministic and probabilistic approaches that integrate root reinforcement models in slope stability calculations have largely had homogenous protection forests as the object of their investigation (e.g., (Alessio Cislaghi et al., 2017). Probabilistic approaches deal with the variability inherent in input parameters by considering the probability distributions. For example, SlideforMap generates hypothetical landslides of varying sizes to compute slope stability using semi-random samples over pre-defined ranges for soil cohesion, internal friction angle and soil depth (van Zadelhoff et al., 2021). A further novelty of SlideforMap is the inclusion of root reinforcement based on

individual tree detection with application at landscape to regional scales. While integrating the influence of individual trees in slope stability calculations has been held in the domain of physical modelling, this study aims to develop a statistical approach for assessing effectiveness of individual trees in silvopastoral landscapes.

Landslide susceptibility can be defined as the likelihood of future landslide occurrence for a given areal unit given local geo-environmental attributes (Brabb, 1984). Statistical landslide susceptibility models do not attempt to model the physical processes that control slope stability. Rather, and in the absence of geotechnical soil data, statistical models use readily available surrogate data and thus have less stringent data requirements compared with physical models. A key input parameter that influences the accuracy of statistical susceptibility models, especially for evaluating the influence of single trees, is the quality of vegetation data. In most existing statistical models, land use or land cover data (LULC) are used to capture the varying effect of vegetation composition. These data are frequently prepared through visual interpretation of aerial photography and are rarely available at the scale required to quantify the effect of individual trees (Reichenbach et al., 2018; Spiekermann et al., 2021). Therefore, in hill country, where shallow landslide erosion is a dominant geomorphic process (Smith et al., 2021), we address the methodological and knowledge gap related to statistical modelling at landscape scale to quantify the reduction in landslide erosion due to individual trees at landscape scales.

In this context of silvopastoral landscapes, previous studies have been limited by scale (e.g., hillslope) or method (e.g., univariate analyses). There is a need for spatially explicit modelling to assess the impact of differing tree species and planting densities on landslide erosion while accounting for varying environmental conditions, such as slope gradient, lithology, or soil type. To enable such assessments, high resolution vegetation data are a prerequisite. Automated processing of satellite imagery and airborne LiDAR data is continually increasing the spatial and temporal resolution of land cover products, creating opportunities to map the location of individual trees in the landscape (Brandt et al., 2020; Gómez et al., 2016; Weinstein et al.,

2021). However, beyond mapping trees, the challenge for landslide susceptibility models is the spatial representation of trees as predictor variables in the model: Representing individual trees as points/pixels, mapping tree canopies, or using an arbitrary radius to define an area of influence of a tree fail to acknowledge the spatial variation in the distribution and strength of roots as well as the hydrological interactions between trees and soil. While root distribution models have been used for physical, process-based modelling, the cost of data collection is prohibitive and not suited to landscapes with a diverse range of tree species. A solution to this problem was recently proposed by Spiekermann et al. (2021), whereby the average extent and spatial pattern of individual trees on slope stability is inferred by considering the relationship between the location of trees and landslides. The recent availability of the tree influence models (TIMSS) provides an opportunity to create greatly improved landslide susceptibility models for silvopastoral landscapes. Thereby, the increase in slope stability due to individual trees can be quantified, and, inversely, the reduction in landslide susceptibility and erosion. Accounting for the influence of individual trees has been a gap in the statistical landslide susceptibility and risk literature. In this study, we address this gap by using high resolution data at landscape scale to quantify the reduction in landslide erosion due to individual trees while accounting for local environmental conditions.

Method development for landslide susceptibility modelling is a comprehensive research field that most commonly focuses on generating suitable datasets (e.g., van Westen et al. 2008, Chang et al. 2019, Smith et al. 2021), model development (e.g., Van Den Eeckhaut et al. 2006, Hong et al. 2017, Huang and Zhao 2018), sampling methods (Conoscenti et al., 2016; Heckmann et al., 2014), model performance and validation (e.g., (Petschko et al., 2014; Rossi et al., 2010; Steger et al., 2016b; Xiao et al., 2020), and uncertainty and error evaluation (e.g., Steger et al. 2016a, 2017). All these research objectives have the aim of obtaining reliable landslide susceptibility maps to improve management decisions aimed at reducing landslide risk. We address a knowledge gap related to the integration of individual trees into landslide susceptibility models – specifically for silvopastoral environments. This study is the first of its

kind that aims to quantify the reduction in susceptibility to shallow landslide erosion due to the influence of individual trees. We integrate the TIMSS (Spiekermann et al., 2021) of four different tree types for statistical landslide susceptibility assessments using binary logistic regression models. Furthermore, we investigate whether including highly skewed, continuous TIMSS variables in logistic regression modelling has implications for estimation of effect size. Following model development, two farms from the Wairarapa region, New Zealand, are used to illustrate how the landslide susceptibility model can be used to quantify effectiveness of trees for landslide erosion control.

4.2 Data and Methods

4.2.1 Study Area

The study area is an 843 km^2 area in the Wairarapa in the south-east of the North Island of New Zealand (Figure 4.1). Most of the study area (92%) is used for pastoral farming and is underlain by predominantly Neogene-aged massive, poorly bedded mudstone and alternating sandstone and mudstone (Lee and Begg, 2002). Soils commonly have a dense subsoil zone of low permeability formed in loess that is the failure plane for many landslides (De Rose, 2013). A band of coquina limestone forms the central and south-western part of the study area (Figure 3.1). The terrain has low to moderate relief (<150 m) that is intensely dissected, with narrow ridge and spur crests, hillslopes mostly between 15° and 35°, and narrow valley floors. This topography is locally referred to as “hill country”. Significant areas of colluvium (landslide debris) have accumulated along the base of many hillslopes, and in mid- and upper-slope hollows. Mean annual rainfall is 1100 mm, characterised by winter maxima and summer droughts. Long duration, low intensity rainfall is typical with low daily rainfall totals (De Rose, 2013). However, landslide-generating storms have occurred frequently since climatic records began in the 1880s. Most of these storms do not have particularly high storm or daily rainfall

totals (100–200 mm) but often occur when antecedent moisture conditions are high (Basher et al., 2018; De Rose, 2013).

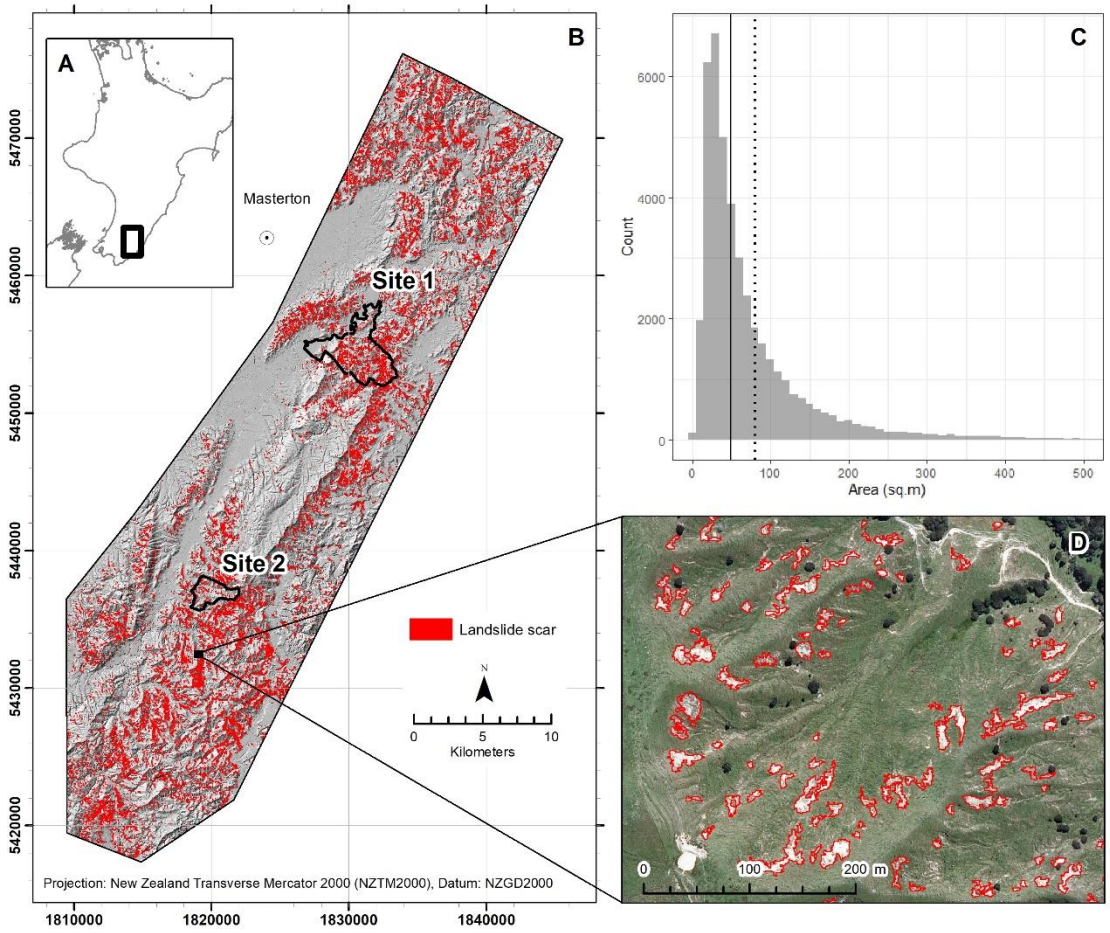

Figure 4.1. A: Location of study area in the lower North Island, New Zealand; B: Shallow landslide inventory 2005–2009 used to train landslide susceptibility models; C: Histogram of landslide scar size (bin width = 10 m^2), including vertical lines of median (49 m^2) and mean (81 m^2); D: Extent of black frame within study area showing a sample of mapped shallow landslides.

Two farms (Sites 1 and 2) were selected from within the study area in the Wairarapa hill country to quantify the effectiveness of trees on slope stability (Figure 4.1). Both farms have a history of landslide and soil erosion research activity (Basher et al., 2018; De Rose, 2013; G. Douglas et al., 2013a; Lambert et al., 1984; Spiekermann et al., 2021). Site 1 is a 1,700-ha sheep and beef farm located east of Masterton in a region of steep pastoral hill country. The original native vegetation was cleared between 1860 and 1890 (Lambert et al., 1984). A major rainfall storm event led to widespread landsliding in 1977 (Crozier et al. 1980, Glade 1998, De Rose 2013; Figure 4.2). Preventative measures were largely non-existent before the event. Soil

conservation works in the form of space-planted poplar, willow, and eucalyptus trees began in the 1980s. While planting has been sustained since commencement, the density of trees on hillslopes differs greatly across the farm, with some hillslopes devoid of tree cover (Table 4.1). Site 1 is thus representative of a "moderate" level of tree cover for New Zealand's pastoral hill country farms.

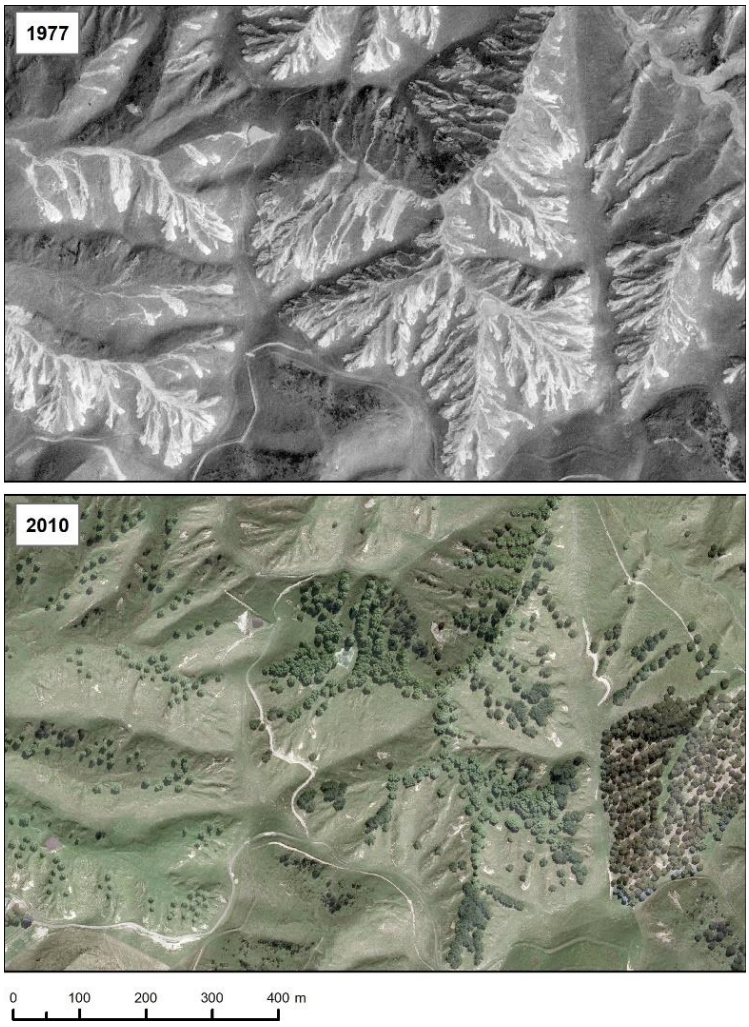

Figure 4.2. Susceptibility to landslide erosion is temporally dynamic, as exemplified by a small area within site 1 (see Figure 4.1 for location). High density of shallow landslides in 1977 led to extensive space-planting of poplar, willow, and eucalyptus trees (2010).

Site 2 is a 462-ha sheep and beef farm located at the upper catchment of the Waikoukou Stream and has had a great deal of soil and water conservation implemented since 1956. The main objectives of these conservation works were to intensively plant slopes and gullies prone to severe erosion using poplars, willows, and protected seedlings of other species. According to farm plan documents (Wairarapa Catchment Board 1956), the early European land cover

likely consisted of light bush, kānuka, and fern, with heavier podocarp species in the wider valleys. Several remnants of kānuka (naturally regenerated following initial clearance) remain distributed across the farm. Overall, there is a higher tree density (by species and in total) compared with Site 1 (Table 4.1).

Table 4.1. Stem counts and densities by tree type at Sites 1 and 2

	Site 1			Site 2		
Tree type	Count	Percent	Stems per ha	Count	Percent	Stems per ha
Eucalyptus	708	9%	0.4	2247	16%	4.9
Kānuka	1900	25%	1.1	7797	57%	16.9
Conifer	352	5%	0.2	1048	8%	2.3
Poplar/Willow	4545	61%	2.7	2703	20%	5.9
Total	7506	100%	4.4	13795	100%	29.9

4.2.2 Landslide Inventory

Shallow landslides are the most dominant mass movement process in the study area. This is due to a high-energy geomorphic environment that is predisposed to landsliding with soft sedimentary rocks, steep and highly dissected slopes, and frequent high-intensity rainfall events that regularly trigger many thousands of shallow landslides (Crozier, 2018; Smith et al., 2021). These favourable natural conditions for landslide erosion are compounded by historic changes to land cover with the removal of indigenous forest in the late 1800s to early 1900s for pastoral farming (Glade, 2003). Shallow landslides are commonly small features (50–100 m^2; Figure 4.1) involving soil and regolith less than 1.5 m deep with long narrow debris tails (Basher, 2013; Betts et al., 2017; Crozier, 1996; Glade, 1998). The triggering mechanism is assumed to be rising pore water pressure due to sustained rainfall reducing the internal friction of soil particles until the gravitational forces ultimately overcome the resistance of the soil.

The landslide inventory used in this study is described by Spiekermann et al. (2021), which we refer to for description of mapping methodology. The shallow landslide dataset consists of 43,069 landslide scars (Figure 4.1) that were mapped in regional orthophotos from 2010 (RGB, 0.4 m GSD) and are used in this study to fit and test the landslide susceptibility models. The

landslides were triggered by several storms. Two of the storm events, in March 2005 and July 2006, affected the entire study area, with a median recorded rainfall of 175 mm (range: 130 – 382 mm) and 204 mm (range: 172 – 321 mm) over 48 and 72 hrs, respectively. Three further storms, in late July 2006 (149 mm; 48 hrs), October 2006 (130 mm; 48 hrs), and June 2009 (197 mm; 24 hrs), were more localised to the south. The median scar area is 49 m^2 and the mean is 82.1 m^2, which is consistent with findings of previous studies (Betts et al., 2017; De Rose, 2013; Smith et al., 2021).

4.2.3 Predictor Variables

To develop the statistical model of landslide susceptibility, key predictor variables of shallow landslide erosion were generated from existing datasets. Selection of predictor variables was based on an understanding of the geomorphic process being assessed, i.e., all selected factors have direct physical process relevance for slope stability. Moreover, since the objective is to investigate the effect of trees on landslide susceptibility, we aimed to keep the model simple by keeping the number of predictor variables to a minimum. Therefore, we include the topographic variables of slope gradient, aspect (northernness, easternness), tree cover using the four TIMSS, and lithology (Table 4.2).

Table 4.2. Predictor variables used in landslide susceptibility model [n.= numerical; c. = categorical data. For lithology, the percentage of study area and number of landslide scars is given for each category.

Data	**Model inputs**
Topography [n.]	Slope gradient [°]; northernness (cosine transformation of slope aspect), easternness (sine transformation of slope aspect).
TIMSS [n.]	Tree influence models for following vegetation types: eucalyptus, kānuka, conifer, poplar/willow.
Lithology [c.]	Argillite – crushed [0.2%, 48]; Undifferentiated floodplain alluvium [8.5%, 249]; Gravels [0.9%, 229]; Greywacke [1.9%, 178], Limestone [9.9%, 1,252]; Loess [28.7%, 6665]; Mudstone or fine siltstone – banded [6.6%, 4,204]; Mudstone or fine siltstone – jointed [19.8%, 15,204]; Mudstone or fine siltstone – massive [15.0%, 10,533]; Sandstone or coarse siltstone – banded [0.1%, 2]; Sandstone or coarse siltstone – massive [8.3%, 4494]; Unconsolidated to moderately consolidated clays [0.2%, 11].

Slope gradient is the most influential environmental predictor variable used in landslide susceptibility modelling (Carrara et al. 1991, 1995, Chung and Fabbri 2003, Budimir et al. 2015, Reichenbach et al. 2018) – particularly in combination with variables pertaining to the mechanical properties of soil and lithology (Betts et al., 2017; Reichenbach et al., 2018). The reason for its effective explanatory power is directly related to the physics of mass movement. Slope gradient controls the stresses and resistance acting on a slope to maintain stability (Wu and Sidle, 1995), with increasing shear stress and decreasing resistance for higher slope gradients.

Slope aspect is frequently used as a predisposing factor in landslide susceptibility assessments (e.g., Salter et al. 1983, Galli et al. 2008, Ruff and Czurda 2008, van Westen et al. 2008). It has been suggested that contrasting microclimate between slopes of different aspect can produce asymmetric valley morphology through control of slope weathering and erosional and depositional processes (Burnett et al., 2008). The direction of incoming weather events may also create a 'shadow effect', impacting some slopes more than others (Liu and Shih, 2013). Crozier et al. (1980) undertook statistical analyses of the distribution of landslides triggered in the winter of 1977 in the Wairarapa and found a strong preference for northerly aspects (61.6% of slips on N, NW, and NE octants). Similarly, another Wairarapa-based study (Gao and Maro, 2010) reports a preference for northerly aspects, which they suggest is a product of deeper weathering from increased solar radiation and wetting and drying cycles experienced by north-facing (southern hemisphere) slopes. Wetting and drying cycles also initiate cracking, resulting in reduced soil cohesion (He et al., 2020) and allowing water to penetrate down to the less permeable bedrock which acts as the surface of rupture (Brooks et al., 2002). The effect of aspect can also be related to structural geology (e.g., dip direction and dip angle of bedding planes; Ruff and Czurda 2008). Crozier et al. (1980) suggested that preference of landsliding on a particular slope aspect can be temporally dynamic. They found weakest conditions at the bedrock/regolith interface on southerly slopes, and north to west-facing slopes were less disturbed. They therefore postulate that following removal of the original forest cover for

pastoral farming, mass movement processes may have initially favoured southern slopes, providing a more extensive, weaker, and undisturbed regolith on north-facing slopes – which was more severely affected in recent times (e.g., the 1977 landslide-triggering rainfall event documented by Crozier et al., 1980 and Gao and Maro, 2010; see Figure 4.2). Indeed, landslide susceptibility is not static reality, but is temporally dynamic (Gorsevski et al. 2006; Figure 4.2). We therefore include slope aspect in the model to test whether a similar preference can be observed today, or if a change is apparent.

The topographic variables were derived from a 1-m digital elevation model constructed from airborne light detection and ranging (LiDAR) data from 2013. Since the landslides were triggered before the LiDAR surveys, a median filter with 3-m radius was used to remove minor surface roughness produced by the landslide scars to approximate the terrain surface before failure.

Lithology is commonly an important factor in shallow landslide susceptibility modelling since the material type directly influences soil properties such as hydraulic conductivity and texture (Smith et al., 2021). Crozier et al. (1980) found fewer shallow landslides in areas of alluvium, limestone, and sandstone compared with less permeable formations of mudstone and alternating sedimentary rocks. This observation corresponds well to patterns in our landslide inventory (cf. Figure 4.1a and Figure 4.3a), showing a much lower density in limestone terrain. Thus, we hypothesize that lithology is an important predisposing factor. We used lithological data (near-surface rock type) from the NZ Land Resource Inventory, which was derived from 1:250,000 time-stratigraphic geological maps, using stereo aerial photograph interpretation and field verification to aid mapping at a scale of 1:50,000 (Newsome et al. 2008; Figure 4.3a). Lithology was converted from vector format to a grid at 1-m GSD. We accept that both boundary and material type errors will result from using lithological data of much lower resolution than for terrain attributes. To ensure sufficient samples were gathered across all material types to safely infer the relationship, we remove material types that are represented in less than 1% of combined presence and absence points (minimum 861 samples of balanced

dataset). This led to the removal of four material types: “Argillite – crushed”, “Gravels”, “Sandstone or coarse siltstone – banded”, and “Unconsolidated to moderately consolidated clays” (see Table 4.2), which reduced the landslide inventory by 290 to 42,778 scars.

Finally, we include the TIMSS (Spiekermann et al., 2021), which we use to quantify the reduction in landslide susceptibility due to the presence of trees in pastoral hill country (Figure 4.3b). TIMSS can be defined as spatial representations of the average influence of individual trees on slope stability and were developed for different tree genera based on an empirical relationship between distance from tree and reduction in soil surface eroded.

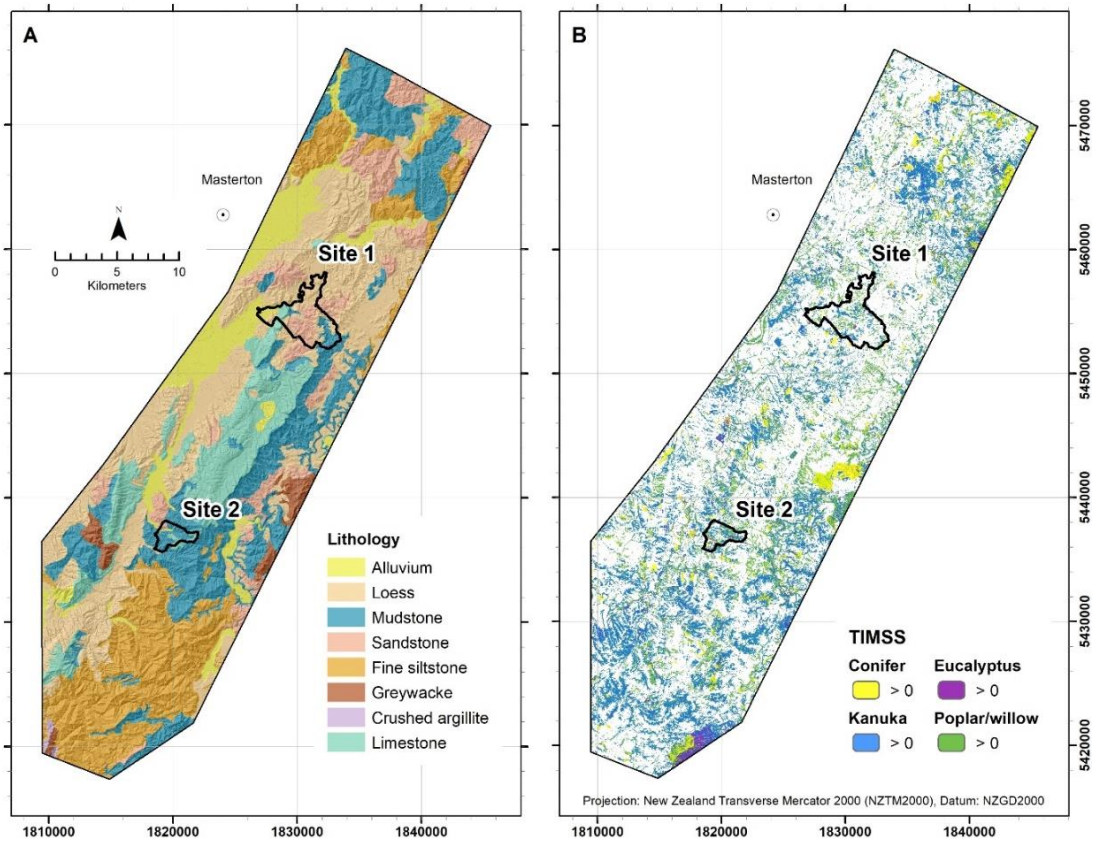

Figure 4.3. Insert A: Lithology of study area; Insert B: Tree influence models on slope stability (TIMSS) showing location of different tree types within silvopastoral hill country of study area.

The TIMSS were fit using least-squares logistic regression. Therefore, the models are sigmoidal in shape reaching an asymptotic value denoting the average maximum effective distance of a tree, i.e., the point at which the tree has no observable influence on slope stability due to mechanical and hydrological processes (Cohen and Schwarz, 2017; de Jesús Arce-

Mojica et al., 2019; Istanbulluoglu and Bras, 2005; Kim et al., 2013; Phillips and Marden, 2005; Schmidt et al., 2001; Schwarz et al., 2010c; Spiekermann et al., 2021). While TIMSS are normalized to 0–1, where 1 is equal to the maximum influence on slope stability of an individual tree of a particular vegetation type, a spatial unit (here, a 1-m pixel) may exceed 1 due to the additive contributions from multiple trees.

TIMSS are available for the dominant tree types in the study area, which include eucalyptus, kānuka, poplar/willow and coniferous tree species. Poplars (*Populus* spp.) and willows (*Salix* spp.) have been a cost-effective option for promoting slope stability in New Zealand's pastoral hill country. They are easily established from large unrooted poles and rapidly develop extensive root systems (Phillips et al., 2014). Willows and many poplar varieties are tolerant of periodically saturated soils and have comparatively high transpiration rates during the growing season (Wilkinson, 1999). As with poplars and willows, eucalyptus (*Eucalyptus* spp., e.g., *Eucalyptus globulus*) establish rapidly in cool temperate climates. They are more tolerant to dry soil conditions and summer droughts, but are overall less abundant in the study area (Spiekermann et al., 2021). Unlike poplars and willows, coniferous tree species are mostly found in forestry blocks or used as shelter belts. While the roots of conifers (mostly *Pinus radiata*) are not as strong as kānuka, poplars and willows, they have been shown to root deeply (> 2m) (Watson et al., 1995). Kānuka (*Kunzea* spp.) are commonly found in dense groves and are the most abundant tree species in the study area. As with most indigenous species in New Zealand, kānuka are slower growing, have shallower root systems, but higher tensile strength than exotic species (Phillips et al., 2011b; Watson and Marden, 2004). Since many local environmental factors such as soil and climate influence the development of tree root architecture, root systems between and within tree species vary considerably – particularly as a function of plant density as neighbouring plants compete for available resources (nutrients, water, light) (Danjon et al., 2013). However, due to the paucity of species-specific data on root

architecture, we use the TIMSS to represent the average influence of an individual tree on slope stability for the four dominant tree types in the study area, assuming an additive function where more than one tree contributes to slope stability at a given point in the landscape. Further details of the development of TIMSS are given in Spiekermann et al. (2021).

4.2.4 Landslide Susceptibility Model

Binary logistic regression

We integrate the TIMSS of four different tree types developed by Spiekermann et al. (2021) into a binary logistic regression model (BLR) to quantify the effectiveness of trees in terms of the reduction in the spatial probability of landslide occurrence. Development of the BLR method is attributed to Cox (1958) and Walker and Duncan (1967) and is the most common statistical method used for landslide susceptibility modelling (Lombardo and Mai, 2018; Reichenbach et al., 2018). It has been shown to produce comparatively low error rates (Brenning, 2005; Smith et al., 2021). We adopt BLR since the effect size of the predictor variables can be quantitatively evaluated using odds ratios. As discussed by Lombardo and Mai (2018), pseudo-quantitative methods that use frequency ratios or expert-knowledge to determine weights for pre-disposing factors (e.g., Persichillo et al., 2017) are not based on underlying probability distributions and are therefore unable to represent the probability of landslide occurrence, which limits the statistical interpretation of the models.

BLR is well suited to landslide susceptibility modelling since it models the probability of a binary response variable ($Y = 0|1$), which corresponds to the absence/presence of landslides. Independent variables can be both numerical and categorical, and as with all regression analyses, the variability of Y is explained in terms of covariates $\mathrm{x}_1, \ldots, \mathrm{x}_i$. In BLR, the linear function takes on the form:

$$logit\ (\mathrm{Y}) = \log\left(\frac{p}{1-p}\right) = \beta_0 + \beta_1 \mathrm{x}_1 + \ \ldots\ + \beta_i \mathrm{x}_i \qquad (1)$$

where y is the dependent variable, i.e., landslide occurrence, x_i is the *i*-th explanatory variable, β_0 is a constant, β_i is the *i*-th regression coefficient, and logit is the link function used to convert log-odds ($\pm\infty$) to probability. The logistic function is sigmoidal in shape and always yields values between 0 and 1. The probability of landslide occurrence can thus be formulated as:

$$p(Y = 1) = \frac{1}{1+exp^{-(\beta_0 + \beta_1 \mathrm{x}_1 + \ \ldots\ + \beta_i \mathrm{x}_i)}} \qquad (2)$$

The maximum likelihood estimator is used to fit optimal coefficients for all predictor variables. The maximum likelihood function iteratively fits model coefficients so that p yields values close to 1 where $Y = 1$, and values close to 0 where $Y = 0$ until model convergence is reached. In the context of landslide susceptibility, the probabilities from logistic regression correspond to the predisposition of a given mapping unit to landsliding and are thus often referred to as spatial probabilities with no regard for temporal probability. Logistic regression modelling was performed using the caret package (Kuhn, 2008) within the open-source statistical software R (R Core Team 2021); The raster package was used for model predictions (Hijmans, 2021).

Logistic regression assumes independence of the predictor variables. We used the *car* package in R (Fox and Weisberg, 2010) to test for multicollinearity by quantifying the variance inflation factor (VIF) for all continuous variables. Variable selection is carried out using a preliminary model with full sample size. A predetermined VIF threshold is commonly used to select variables for removal from the model. While a threshold of 10 is more common (Heckmann et al., 2014; O'Brien, 2007; Smith et al., 2021), we use a more stringent threshold of 2 that has also been used by other authors (e.g., Van Den Eeckhaut et al., 2006). Additionally, all variables were removed with a test-statistic for the Wald test (z-statistic) of less than 2, which means the effect size is not significantly different from 0 (95% confidence

level) and removal will not significantly affect model fit. All subsequent models use the same variables following removal of insignificant predictor variables.

Sampling design

Landslide susceptibility modelling using logistic regression relies on points in the landscape representing presence and absence of landslides. Though we expect our observations to be correlated, the following steps were taken to increase independence in our observations: each landslide scar was represented by a single centroid pixel (landslide initiation point – LIP) before extracting spatial data to both landslide presence and absence points. This is a common method aimed at reducing spatial autocorrelation between observations (Atkinson and Massari, 2011; Lombardo and Mai, 2018; Petschko et al., 2014; Van Den Eeckhaut et al., 2006). In addition, and before generating absence points, we created a mask to ensure spatial independence of landslides and non-landslides by buffering all landslide polygons by 7.3 m. This distance denotes the 90th percentile of the radius r of the landslide scar inventory, assuming a circular shape. Absence points thus needed to be separated by a distance of $2r$, or 14.5 m. Random absence points were generated in R using the QGIS implementation *qgisprocess* package, an update to the *RQGIS* package (Muenchow et al., 2017).

As noted by Knevels et al. (2020) and Heckmann et al. (2014), the implications of the method used to generate absence points are seldom adequately considered. To evaluate the sensitivity of our model to the selection of absence data, we test the hypothesis that different sampling methods for absence points render significantly different effect sizes for the tree variables. The rationale for doing so is that in silvopastoral landscapes trees are relatively sparsely distributed across the landscape and – by implication – the randomly generated absence points are more likely to fall in open pasture. Since shallow landslides are predominantly triggered in open pasture, the implication is that both presence and absence points mostly have TIMSS values of 0 (Figure 4.A1; Table 4.3). Therefore, all four TIMSS variables have very high positive skewness in the distribution of both presence and absence

samples (Table 4.3). While the maximum likelihood estimator is tolerant of highly skewed continuous predictors with large sample sizes, the effect sizes of the variables can be inflated (Alkhalaf and Zumbo, 2017).

The following sampling design is used for presence and absence selection:

a. *Spatially restricted sampling to twice the effective distance* ($2xED$) *of TIMSS*: We created masks at twice the effective distance from trees for each of the TIMSS, which corresponds to 26 m for eucalyptus, 34 m for conifers and kānuka, and 40 m for poplar and willow trees. This has the effect of creating more even *spatial* odds for presence and random absence points to be located within or beyond the effective distance of trees. This approach reduces the skewness of the TIMSS variables (Table 4.3). We further hypothesised that this sampling strategy will increase the ability of the maximum likelihood estimator to produce consistent effect sizes. A consequence of masking to $2xED$ was a reduction in the size of the study area by 45.7% to 458 km^2. Landslide presence points within $2xED$ amounted to 26,038. Following Knevels et al. (2020), we randomly generated absence points using a 5:1 absence-presence ratio within the same mask, then resampled $n = 100$ times with a 1:1 landslide presence-absence ratio to account for random variability in the absence samples.

b. *Random sampling across the entire study area (All)*: Absence points were randomly generated to create five times the number of landslide points (213,890). As with sample design A, we resampled $n = 100$ times with a 1:1 landslide presence-absence ratio to produce balanced datasets of 42,778 presence and absence points. To compare like-for-like with sample design A ($2xED$), we reduced the sample size to 26,038 presence and absence points.

c. *Combined TIMSS vs class-specific*: To quantify the total effect of trees on landslide susceptibility, the sum of the four TIMSS was included as a single tree factor in

separate model runs. This had the effect of reducing the positive skewness associated with the TIMSS of each tree type (Table 4.3). Effect size and model performance were compared with those of class-specific TIMSS.

d. *Effect of sample size*: To determine the number of samples required for optimal model performance, we tested model performance for different sample sizes (Heckmann et al., 2014; Petschko et al., 2014; Smith et al., 2021). By reducing the sample size, the average distance between observations increases. This results in greater independence in observations but can come at a cost of not adequately sampling from the diversity of predictor variables in the study area. Small sample sizes lead to greater model variability, which is reversed with increasing sample size. We investigated the point at which spatial autocorrelation was minimized without the cost of poorer model performance. Additionally, we evaluated the effect of sample size on estimation of coefficients and odds ratios. We posit that if effect sizes are not significantly altered with decreasing sample sizes, we may conclude that spatial autocorrelation is not inflating variables when fitting a model using full sample size. We expect model variability to eventually plateau with increasing sample size. The following ten sample sizes were selected: 50, 100, 250, 500, 1000, 2000, 4000, 8000, 16000, and full sample size of 26038 presence and absence points. The varied sample sizes were also used to contrast sampling design A (no spatial restrictions), and B ($2xED$), albeit for a single randomly sampled equal number of absence points.

Table 4.3. Comparison of skewness and sampling frequency of TIMSS variables dependence on sampling strategy (all vs 2xED) using single random selection of absences (1:1)

	Eucalyptus	Kānuka	Poplar/willow	Conifer	All TIMSS
Skewness (1:1 all)	9.9	3.5	2.8	10.0	2.7
Skewness (1:1 2xED)	7.3	2.5	1.9	7.0	1.9
Presence samples > 0 (%)	1.1%	10.2%	15.6%	0.5%	16.0%
Absence samples > 0 (%)	1.7%	10.8%	16.4%	2.5%	17.6%
Presence and absence > 0 (%)	2.8%	21.0%	32.1%	2.5%	33.6%
2xED absence samples > 0 (%)	3.3%	18.7%	28.3%	3.9%	30.5%
2xED presence and absence > 0 (%)	5.1%	35.5%	54.0%	4.7%	56.9%
Mean (Presence >0)	0.29	0.36	0.37	0.34	0.62
Mean (Absence >0)	0.45	0.56	0.58	0.77	1.02
Mean (2xED Absence >0)	0.47	0.55	0.57	0.77	1.02

Model prediction performance

To test model prediction performance of each model, we used k-fold ($k = 5$) cross validation (CV). Samples were randomly partitioned into k folds, whereby $k - 1$ folds are used to train the model and the remaining fold used to test the predictive ability of the model using selected performance measures. This is repeated until each of the five folds has been used for model testing. To ensure the performance measures are not influenced by a particular data partitioning, this process is repeated 10 times. Moreover, we use 100 balanced datasets, each with a different set of randomly selected absence points for 10 repeats of k-fold CV, yielding a total of 5000 coefficient estimates and performance metrics.

Receiver operator curves (ROC) are used to estimate model performance by plotting the true positive rate (sensitivity) against false positive rate (1 – specificity) for each model run across all potential cut-offs. The area under the ROC (AUROC) summarizes a model's prediction performance for balanced samples as it does not depend on the cut-off used to calculate classification accuracy (Hosmer and Lemeshow, 2000). An AUROC score of 1 would mean the model can perfectly discriminate between presence and absence of landslides in its

predictions; a value of 0.5 corresponds to no discriminatory power and is equal to that achieved by pure chance. Since a subset of the randomly generated absence points are likely to be located in terrain susceptible to landsliding (i.e., with values similar to those of presence points), an AUC score of 1 is highly unlikely. A good AUC score is considered to be between 0.8 and 0.9; an excellent score is > 0.9 (El Khouli et al., 2009). Model performance metrics and regression coefficients are stored for each of the four sampling methods (A-D). The optimum sampling strategy is determined by comparing performance metrics (median AUROC) and exploring implications for number and density of landslide samples on model variability.

Following selection of the optimal sampling strategy, spatial predictions of susceptibility are made for the two case study sites. The susceptibility values indicate where landsliding can be expected in future, i.e., the values are the probability of belonging to a class associated with unstable terrain (where $Y = 1$). We classified these spatial probabilities of landslide occurrence into three susceptibility classes of low, medium, and high (Lombardo and Mai, 2018; Petschko et al., 2014). The classes correspond to the 5, 20 and, 80 percentiles of the probability distribution extracted at 42,778 LIPs.

Quantifying effectiveness of biological erosion control

As with previous studies that investigated the importance of specific factors in explaining landslide occurrence (Knevels et al., 2020; Schmaltz et al., 2017), we calculated odds ratios (OR) for each of the TIMSS covariates to compare the effectiveness of different tree species in reducing the spatial probability of landslide occurrence. Odds were obtained by exponentiating both sides of equation (1) so that:

$$odds = \frac{p}{1-p} = e^{\beta_0 + \beta_1 x_1 + \ldots + \beta_i x_i} \qquad (3)$$

Thus, for a unit increase in covariate x_i, the odds of a spatial unit being susceptible to landsliding increase by a factor e^{β_i}, as expressed by odds ratios:

$$OR = \frac{odds(x+1)}{odds(x)} = \frac{e^{\beta_0 + \beta_1 x_1 + \ldots + \beta_i (x_i+1)}}{e^{\beta_0 + \beta_1 x_1 + \ldots + \beta_i x_i}} = e^{\beta_i} \qquad (4)$$

As the TIMSS variables are on the same normalized scale with a value of 1 denoting the maximum tree influence of an individual tree of a vegetation type on slope stability, a direct comparison is possible without rescaling. Besides comparing OR of the four TIMSS variables, we ran predictions for Sites 1 and 2 iteratively dropping a TIMSS variable to explore the impact of the different tree types in reducing landslide susceptibility. We then illustrate how the landslide susceptibility model can be used to quantify the reduction in shallow landslide erosion due to trees present in the landscape.

4.3 Results

4.3.1 Variable Importance, Estimation of Effect Sizes, and Model Performance

Multicollinearity tests showed all continuous variables to have a VIF <3, with the kānuka and poplar/willow TIMSS variables the only factors with a VIF slightly above 2. Thus, all continuous variables were retained in the model. Two lithologies, "Mudstone or fine siltstone – banded" and "Mudstone or fine siltstone – jointed", were removed from the BLR model as the coefficients were not significantly different from 0 and, thus, did not contribute to an improved model fit. Therefore, these two lithologies effectively became the reference category. The remaining six lithologies had coefficients that are significantly less than 0, which means the odds of shallow landsliding are significantly reduced (Table 4.4). Thus, the most susceptible lithology in the study area are "Mudstone or fine siltstone – banded" and "Mudstone or fine siltstone – jointed", closely followed by "Mudstone or fine siltstone – massive" and "Sandstone/coarse siltstone – massive".

The effectiveness of trees at reducing landslide erosion was quantified using odds ratios, which can be interpreted as factors of change in the odds of a spatial unit being susceptible to shallow landslide erosion. Results show the chosen sampling strategy has very little impact on variation in effect sizes, which is evidenced by minor variations in the odds ratios of the species-specific TIMSS (Figure 4.4). Interestingly, the $2xED$ sampling strategy did not drastically change the effect sizes of TIMSS predictor variables. There is a notable difference in odds ratios of the TIMSS across vegetation types. Sampling from all available presence and absence points (All), median odds ratios for eucalyptus (0.04) and conifer (0.04) TIMSS were significantly less than that of the poplar/willow (0.33) and kānuka (0.32) TIMSS (Figure 4.4). Merging all TIMSS into a single tree variable resulted in a median odds ratio of 0.28 (using unrestricted sampling strategy (All)), which is comparable to that of poplar/willow and kānuka. The merged TIMSS also results in less variation in estimation of effect size compared to the species-specific TIMSS. However, results show that both merging TIMSS into a single tree variable and using $2xED$ sampling led to a reduction in median AUROC (Figure 4.5).

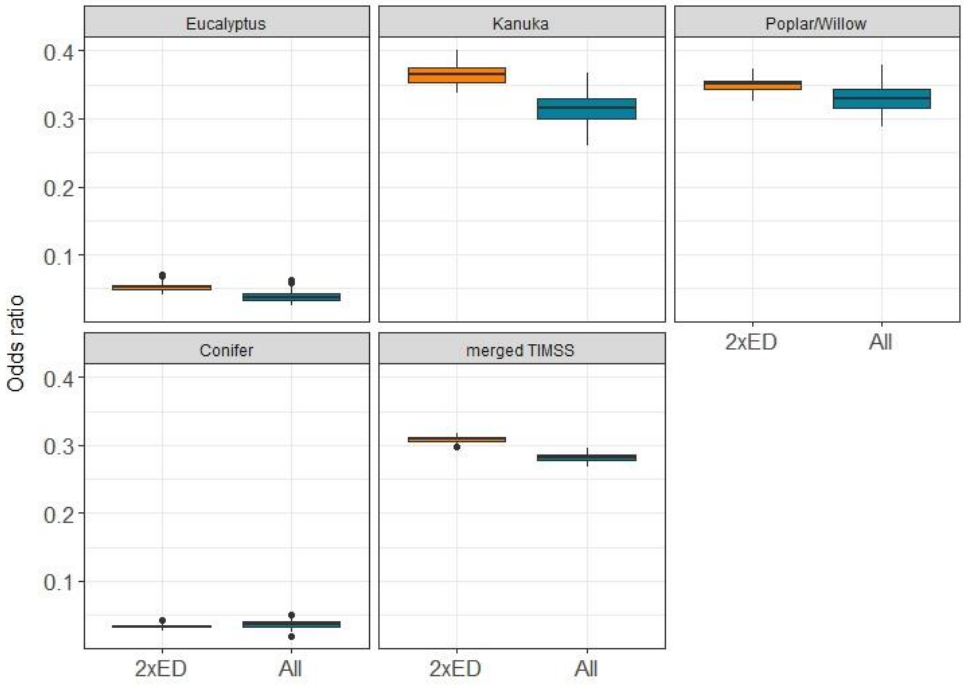

Figure 4.4. Comparison of odds ratio of species-specific TIMSS variables and merged TIMSS from 100 BLR models using balanced sample sizes of 26,038 presence and absence points and two different spatial sampling methods (2xED vs All).

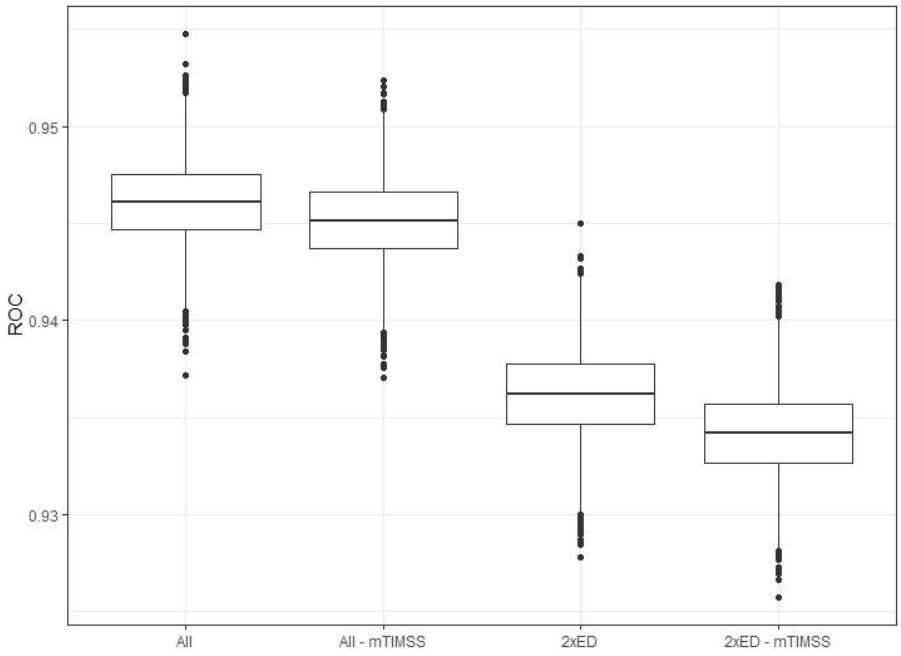

Figure 4.5. Boxplots showing AUROC of four different logistic regression models using 10x 5-fold CV with 100 balanced resamples of presence and absence points sampled from: 1) all available landslide presence and absence points; 2) as (1) but with merged TIMSS predictors; 3) landslide presence and absence points within twice the effective distance to trees (2xED); and 4) as (3) but with merged predictors.

As expected, model performance increased greatly with increasing sample size, plateauing above a sample size of 1000 (Figure 4.6b, Figure 4.6c). The larger range in ROC scores with reduced sample sizes suggests deficient model performance with less than 1000 presence/absence points. While this holds true for both sampling strategies (All vs. $2xED$), randomly sampling from the entire dataset of presences and absences consistently produced higher median ROC scores and less variance. Odds ratios of the TIMSS fluctuate more with reduced sample sizes and are not significantly altered with increasing sample sizes beyond 1000 presence/absence points (Figure 4.6a).

The final model used for predictions adopted a sampling strategy using all presence and absence points – again generating 100 balanced sets of all LIPs (42,778) and equal number of absence points, randomly sampled from 5x the number of scars. Again, 5-fold cross-validation using 10 repeats on each of the 100 balanced datasets was used to quantify model performance (Figure 4.7). Median AUROC of the 5000 train-test cycles was 0.946, and an IQR of 0.002 (Figure 4.7a). The model with the highest median AUROC of the 100 sets was selected for

predictions, which had a median AUROC of 0.948 and an accuracy of 88.7% using a cut-off of 0.5 (Figure 4.7b). The very low IQR of AUROC suggests model performance is not dependent on the selection of absence points. Variable coefficients and OR of the final model are shown in Table 4.4. Eucalyptus and conifer TIMSS have the lowest OR at 0.04, followed by kānuka and poplar/willow with 0.29 and 0.34, respectively. The low 95% confidence intervals indicate high precision of the odds ratios. The spatial distribution of the ORs is shown in Figure 4.8.

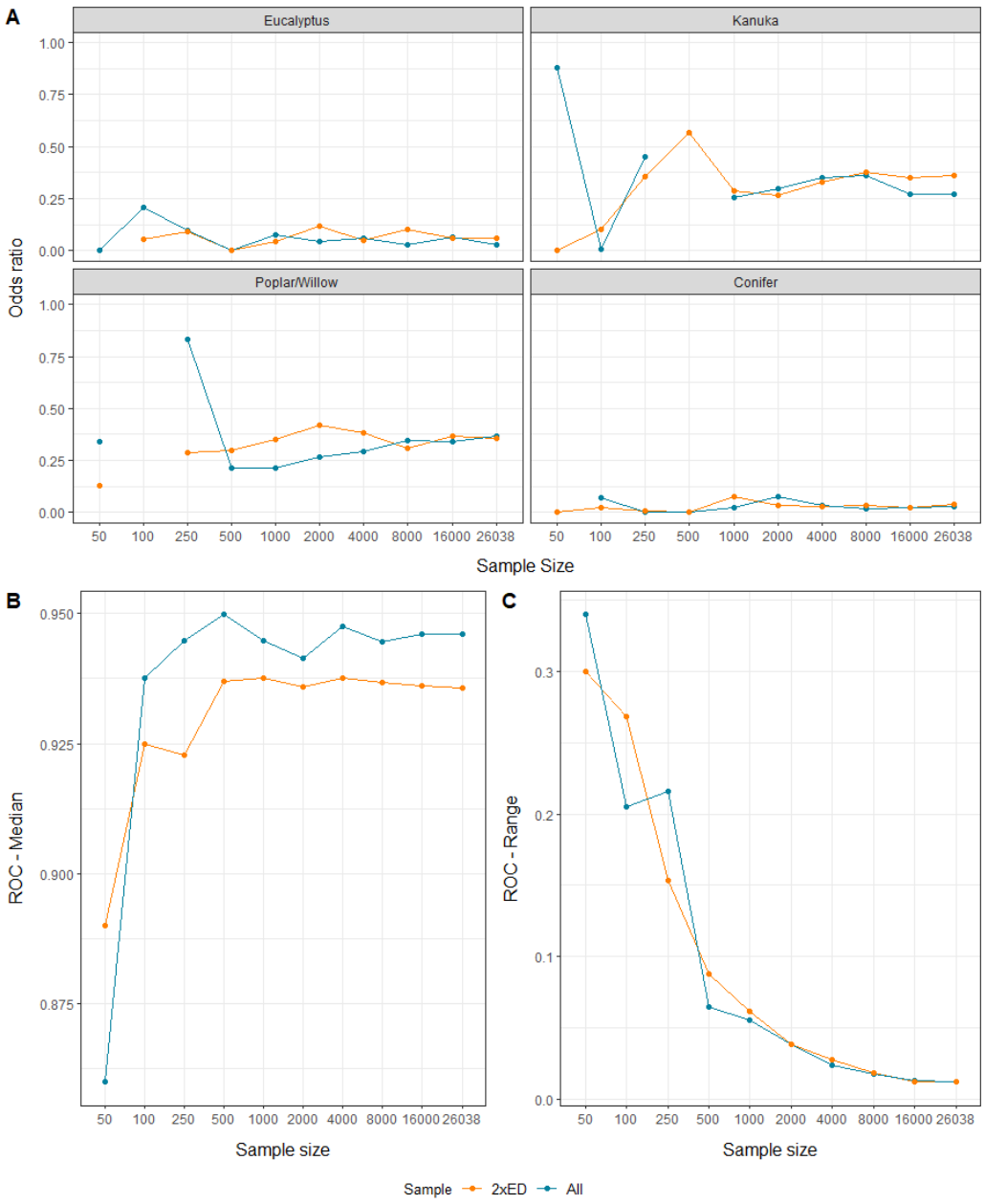

Figure 4.6. A) Dependence of odds ratio of TIMSS variables on sample size; Data gaps are values > 1. B) and C) Area under ROC (median, range) with increasing sample size, contrasting sampling strategies based on single random sample and 20 x 5-fold CV.

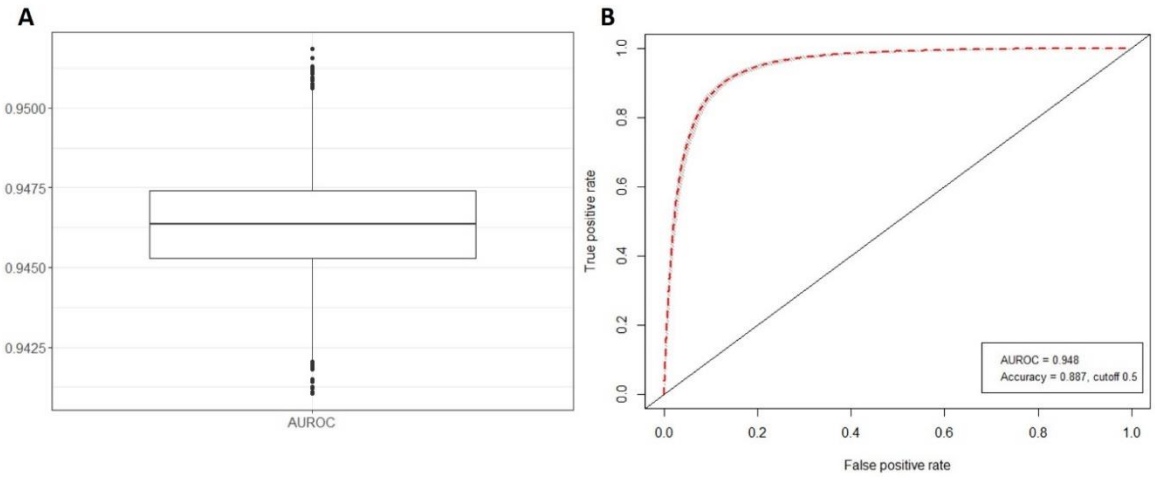

Figure 4.7. A: Boxplot of AUROC based on 100 balanced sets of all landslide scars (42,778) and equal number of randomly selected absence points, each using 10 x 5-fold cross-validation (total of 5000 resamples). Best of the 100 final models was selected using greatest median AUROC score for predictions. B: The ROC of the final model selected for predictions – ROC of 50 folds (grey), final model (red dash; AUROC 0.948).

Table 4.4. Coefficients, associated standard errors, z-statistics, and odds ratios of predictor variables of final model. Colour codes represent topographic (grey), TIMSS (green), and lithology (blue) variables. p-value of Wald's test and likelihood ratio test < 0.001 for all variables. Note, inputs to the model were not standardized to allow easier interpretation with knowledge of units (Table 4.1)

term	β	std. error	z statistic	OR (95% CI)
(Intercept)	-6.941	0.058	-119.6	
Slope	0.284	0.002	137.2	1.33 (1.32,1.33)
Northernness	0.698	0.017	41.0	2.01 (1.94,2.08)
Easternness	0.209	0.016	13.1	1.23 (1.19,1.27)
Eucalyptus	-3.325	0.159	-20.9	0.04 (0.03,0.05)
Kānuka	-1.228	0.067	-18.2	0.29 (0.26,0.33)
Poplar/Willow	-1.077	0.054	-19.9	0.34 (0.31,0.38)
Conifer	-3.195	0.170	-18.8	0.04 (0.03,0.06)
Alluvium (1 vs 0)	-0.591	0.118	-5.0	0.55 (0.44,0.7)
Greywacke (1 vs 0)	-2.390	0.112	-21.4	0.09 (0.07,0.11)
Limestone (1 vs 0)	-1.261	0.051	-24.5	0.28 (0.26,0.31)
Loess (1 vs 0)	-0.588	0.031	-18.8	0.56 (0.52,0.59)
Mudstone/fine siltstone – massive (1 vs 0)	-0.165	0.030	-5.4	0.85 (0.8,0.9)
Sandstone/coarse siltstone – massive (1 vs 0)	-0.220	0.039	-5.6	0.8 (0.74,0.87)

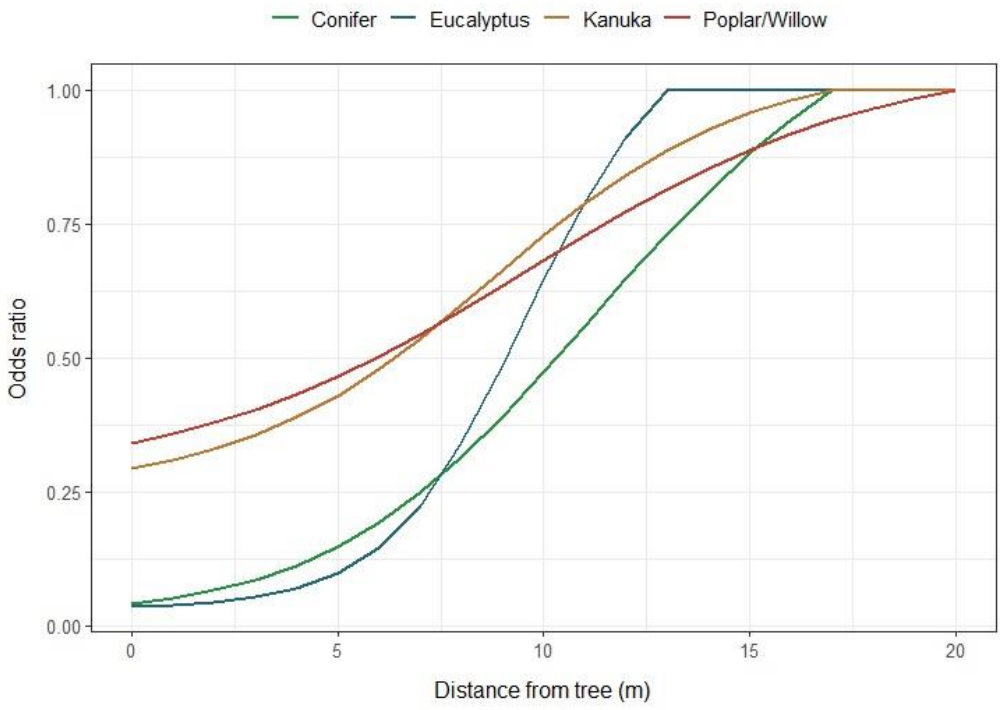

Figure 4.8. Spatial distribution of odds ratio for each tree type as a function of distance from tree. Odds ratios are calculated using the exponential function of the regression coefficient multiplied with the TIMSS values at increasing distance from a tree. An odds ratio of 1 means there is no change to outcome (= maximum effective distance of an individual tree), and an odds ratio less than 1 is associated with lower odds of outcome.

4.3.2 Quantifying Effectiveness of Biological Erosion Control

For Sites 1 and 2, we illustrate how the landslide susceptibility model can be used to quantify the reduction in landslide erosion due to trees present on the farms. Here, landslide erosion refers to source scar erosion only, not necessarily erosion along the transition zone. We classified the spatial probabilities of the landslide susceptibility map into the three distinct classes based on thresholds related to the percentage of observed landslides falling within each susceptibility class of low (<0.32), medium (0.32 – 0.72) and high (>0.72) corresponding to the 5, 20 and 80 percentiles (Figure 4.9). Thus, assuming the same triggering events occur in the future, 80% of landsliding can be expected to be triggered in the "high" class, a further 15% in the "medium" class, and remaining 5% in the "low" class. Using the final BLR model (Figure 4.7b), landslide susceptibility predictions were made for Sites 1 and 2 with and without the

TIMSS variables (Figure 4.10). Moreover, we iteratively removed a TIMSS variable to explore the impact of the different tree types in reducing landslide susceptibility (Figure 4.11).

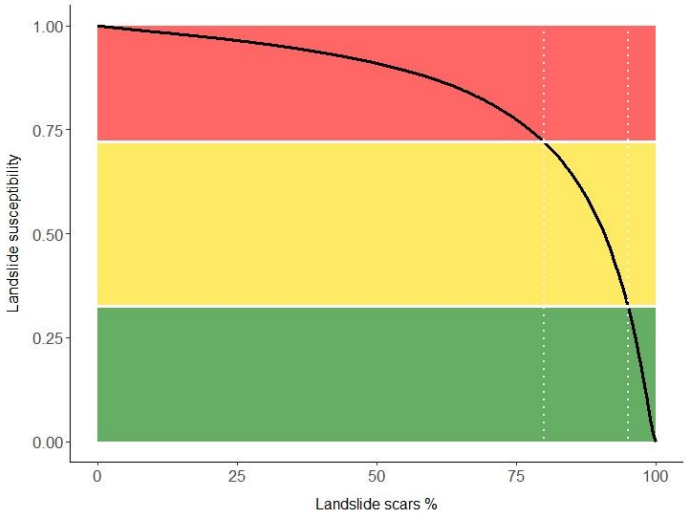

Figure 4.9. Cumulative percentage of landslide scars in three susceptibility classes defined according to 5th and 20th percentiles of probability values at landslide initiation points. The class thresholds correspond to probability values of 0.32, and 0.72.

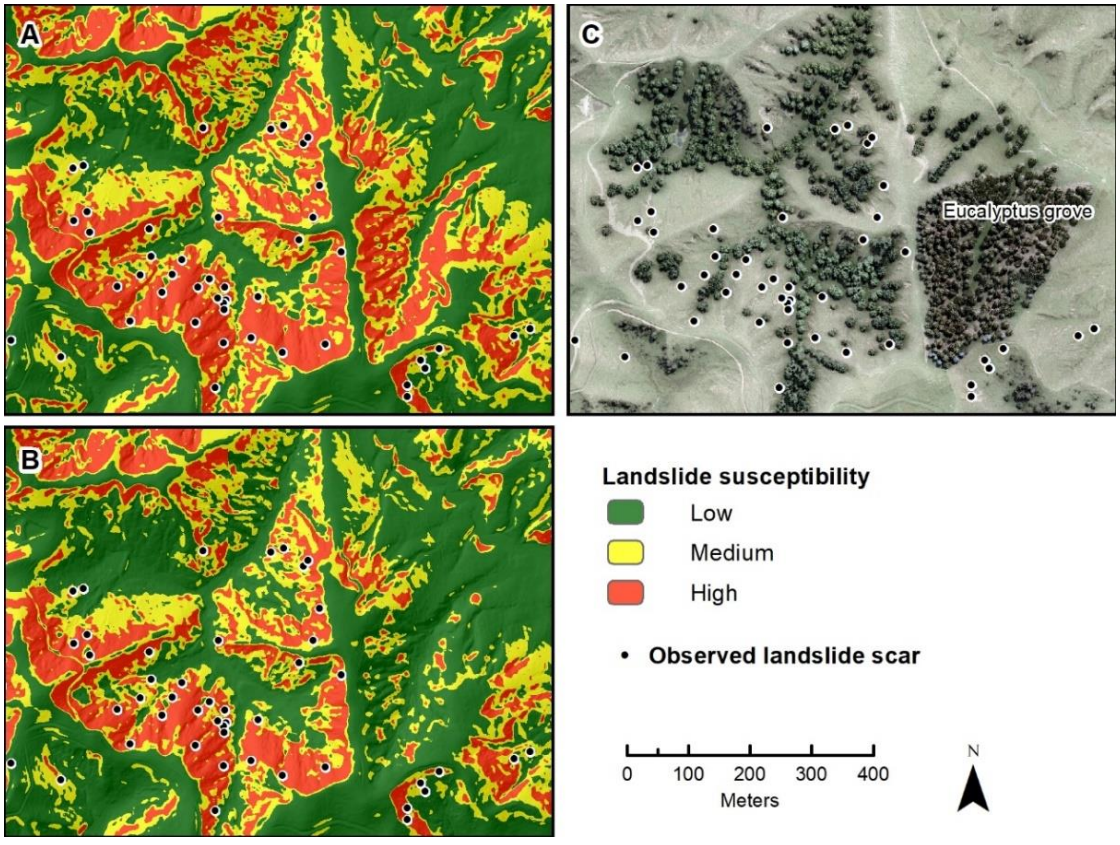

Figure 4.10. Landslide susceptibility for a small area within Site 1: A) Landslide susceptibility with no trees; B) Landslide susceptibility with trees present in 2013; C) distribution of trees – mainly poplars/willows, and eucalyptus species. Note, the eucalyptus grove in the southeast of insert C has led to a much greater reduction in landslide susceptibility compared with the poplars and willows to the west, which were largely planted in areas of low susceptibility.

Sites 1 and 2 have similar distributions of landslide susceptibility across the three classes following removal of tree cover, with 15.0% of Site 1 classified as highly susceptible compared to 14.7% at Site 2 (Figure 4.11). Due to current levels of tree cover, the proportion of the sites with highly susceptible land has reduced to 12.1% at Site 1 and 7.3% at Site 2. There is less change in the medium class at Site 1 with a reduction from 17.7% to 16.2%, compared with a reduction from 24.2% to 18.2% at Site 2. At both sites, poplars and willows have contributed most to the reduction, followed by kānuka and eucalyptus. This is not only a function of the abundance, but also due to the efficiency of poplars/willows using wide spacings. While kānuka is the most abundant species in terms of stem count, it is more often concentrated in dense groves. Poplars/willows are distributed more evenly across the susceptibility classes at both sites. This may be because willows are frequently used for riparian planting to stabilize banks in areas of low landslide susceptibility, but it may also indicate a lack of targeted erosion control of highly susceptible slopes. Eucalyptus species at Site 2 are also more efficient than conifers, contributing to an 11% reduction in the high class due to an average density of 5.1 stems/ha. In contrast, kānuka has reduced susceptibility in the high class by 16.1% due to an average density of 31.1 stems/ha. Thus, wider spacings between trees results in more efficient use of plant material.

Accounting for the rate of landslide erosion across different susceptibility classes (Figure 4.9), and assuming the triggering mechanism of observed landslides is the same in the future, landslide erosion has been reduced by 16.6% at Site 1 and 42.9% at Site 2 due to all existing vegetation. While these reductions have been aggregated for each site, the results are scale dependent (e.g., local/paddock vs. farm/catchment). Within each site there is much spatial variation depending on where pre-existing vegetation is located and where plantings have been concentrated in the past.

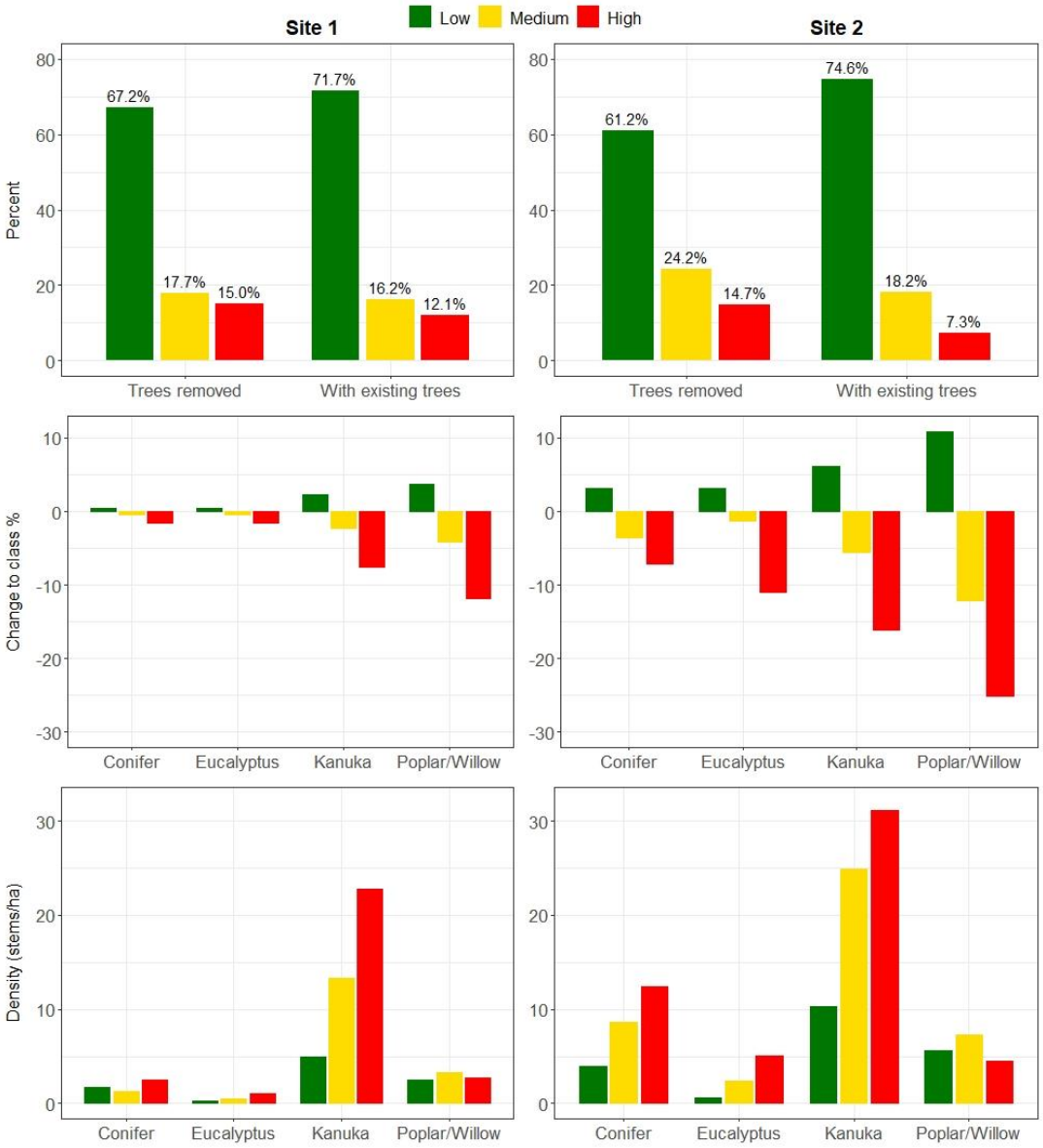

Figure 4.11. For Sites 1 (left column) and 2 (right column): percentage of landslide susceptibility classes (low, medium, and high) with and without trees; contribution of different tree types to change (%) in landslide susceptibility; density (stems/ha) of different species across susceptibility classes.

4.4 Discussion

4.4.1 Highly Skewed Predictor Variables for Logistic Regression

Spatially restricted sampling increased the proportion of both presence and absence points with a TIMSS value > 0 – in all cases reducing the positive skew (Table 4.3). However, due to the difference in abundance across the tree classes within the study area, the positive skewness remained high for both eucalyptus (9.9 down to 7.3) and conifer (10.0 to 7.0) compared with kānuka (3.5 to 2.5) and poplar/willow TIMSS (2.8 to 1.9). This is simply a reflection of the proportion of samples in proximity to conifers and eucalyptus species in the study area (for species abundance see Spiekermann et al., 2021). Since the positive skewness associated with eucalyptus and conifer TIMSS remains high regardless of sampling strategy used, the risk of inflated effect size is not significantly reduced. Yet, Alkhalaf and Zumbo (2017) found that highly skewed continuous predictors are only problematic when samples sizes are small. Given that we use very large sample sizes (total of 85,556 using all LIPs and equal number of absence points), we can assume that the highly skewed eucalyptus and conifer TIMSS predictors will not affect the estimation and inferences.

However, we further tested this by creating domain-specific models by iteratively sampling presence and absence points according to tree type, i.e., restricting sample selection to $2xED$ of the conifer class, followed by eucalyptus class. This significantly reduced the sample size (conifer domain: 1477 LIPs; eucalyptus domain: 3092), but also reduced the positive skewness (conifer domain 2.15; eucalyptus domain 2.49). Interestingly, the estimate of effect size was not significantly altered due to the reduction in positive skewness (OR: conifer TIMSS 0.07; eucalyptus TIMSS 0.09). Thus, we conclude that the estimates produced using all available LIPs are valid and robust.

4.4.2 Effect Sizes and Model Performance

In terms of differences in effect size, the BLR found a notable difference in OR across tree type, including the spatial distribution surrounding trees (Table 4.4; Figure 4.8). In particular, the lower odds in landslide occurrence associated with *Pinus radiata* contradict knowledge of the root strengths of these species. Watson and Marden (2004) found mean live-root tensile strengths for *Pinus radiata* to be only 40% and 50% of kānuka and 'Veronese' poplar (*Populus deltoides x nigra*) root strengths, respectively. In part, this apparent discrepancy may be explained by the greater density of planted conifers compared with poplar/willows and may also be due to differences in age distributions. Furthermore, a value of 1 in the conifer and kānuka TIMSS corresponds to the influence of approximately 3 stems on average, since these species are more difficult to delineate, given crown morphology and tree density (see Spiekermann et al., 2021). However, some uncertainty and error from the landslide mapping and species classification will be propagated through to the measure of effect size for different tree types. We note that in the process of mapping landslides, scars (or portions thereof) may have been obscured by the canopy cover. This source of error may lead to an overestimation of effect size of trees, which would likely be more pronounced for smaller landslide inventories. Additionally, the influence of trees on slope stability is dependent on the age of the tree and the extent of the root systems. This study uses a fixed representation of tree influence on slope stability for four tree types, which does not change as a function of allometric relationships to above-ground metrics such as tree height.

To determine whether spatial autocorrelation was present and resulting in inflated effect sizes of the TIMSS variables, we compared resulting ORs based on nine different sample sizes (100 – 26,038). With samples >1000 presence and absence points, estimates became relatively stable while the range in AUROC of repeated train-tests using cross-validation dropped below 0.1 (Figure 4.6c). Since estimates of effect sizes were not significantly altered with smaller sample sizes, we may conclude that spatial autocorrelation is not inflating variables when fitting

models using the full sample size. Furthermore, including all available data to train the model results in an improvement in model performance without affecting statistical inferences.

The performance of the final model has an AUROC of 0.95, which equates to an accuracy of 88.7% using a cut-off of 0.5 for binary classification (Figure 4.7b). Given the relatively simple model with few predictor variables, a comparably high AUROC score was achieved, which is not uncommon when LiDAR data are used for detailed topographic representation (e.g., Petschko et al., 2014; Knevels et al., 2020). The detailed representation of land cover through integration of individual trees improved model performance – albeit subtle with an increase in AUROC from 0.937 to 0.948. Thus, models with different predictor variables can be similar in terms of their performance, but the implications can be significant for the geomorphic plausibility of spatial predictions and land management decisions (Steger et al., 2016a).

Further improvements in performance by including additional predictor variables (e.g., curvature or surface roughness) are likely to be incremental, since a proportion of randomly generated absence points will always be located on slopes susceptible to landslide erosion. In our two case studies, these highly susceptible areas equated to approximately 7.3% and 12.1 % (Figure 4.11). Sensitivity using the final model was calculated to be 0.859, and specificity 0.903, which means the rate of false positives was lower than that of false negatives. Therefore, false positives are inherently unavoidable using this method to create absences for binary logistic regression.

Besides the TIMSS variables, the topographic and lithology predictors are important factors to consider. Slope gradient has an OR of 1.33, which means that for an increase in 1 degree, the odds of landslide occurrence increase by a factor of 1.33, and since the increase is exponential, an increase of 10 degrees increases the odds by a factor of 17.06. Northern aspect doubles the odds of landsliding compared with southern aspect, whereas an east-west gradient was less important, though landslide susceptibility increases slightly on eastern aspects (Table

4.3). In terms of lithology, greywacke and limestone are the least susceptible lithologies with ORs of 0.09 and 0.28, respectively. These ORs are to be interpreted with reference to the two reference lithologies “Mudstone or fine siltstone – banded” and “Mudstone or fine siltstone – jointed”, i.e., with all else equal, the odds of landsliding on limestone are a tenth of that on mudstone.

Statistical models have previously been used to evaluate variable importance and effect sizes of differing land covers to explain landslide occurrence, albeit not at the level of individual trees. For example, Knevels et al. (2020) examined differences across LULC classes. The authors found broad-leaf and mixed forests were less susceptible to landslides than conifer forests. Moreover, forests were in general far less likely to experience landsliding compared to non-forested areas (odds ratio of 0.03). A similar forest effect, albeit of lower magnitude (odds ratio of 0.21) has been found elsewhere (Schmaltz et al., 2017). These results are supported by many additional studies that found substantial differences in landslide occurrence across different land cover classes (Basher, 2013; Glade, 2003, 1998; Marden et al., 2014; Papathoma-Köhle and Glade, 2013; Phillips et al., 2018; Song et al., 2008). Persichillo et al. (2017) investigated the effect of land use changes on the occurrence of shallow landslides using multi-temporal land-use maps. Other studies have combined assessments of historic land cover dynamics to inform future scenarios (Pisano et al., 2017; Reichenbach et al., 2014; Torizin et al., 2018). Concluding that land cover significantly alters landslide risk, they encourage the use of multi-temporal landslide inventories aligned with concurrent LULC data. Indeed, landslide susceptibility is no static reality, but is temporally dynamic (Gorsevski et al., 2006).

4.4.3 Implications for Land Management

The landslide susceptibility model developed here can be used to improve targeting of erosion mitigation measures. An interesting observation from the case studies is that landsliding is highly concentrated to certain areas of the landscape. Indeed, 80% of future landsliding is

predicted to be found within 12.1% (206 ha) and 7.3% (34 ha) of Sites 1 and 2, respectively (Figure 4.11). This points towards the potential for smarter targeting of erosion control. Conversely, implementing tree planting in less susceptible terrain (e.g., the medium class) will not be as efficient in terms of reduction in landslide erosion on a per tree basis since only 15% of landslides are expected to occur in terrain of medium susceptibility. Yet, the feasibility of treatment is likely to be reduced in areas of high susceptibility due to unfavourable conditions for plant growth (e.g., shallow soils, increased moisture stress, exposure to wind gusts, etc.).

Recently, national-scale assessments aimed at quantifying on-farm mitigation in New Zealand assumed a 70% reduction in sediment yield across all farms that had a farm environmental plan involving widely spaced plantings of trees (Monaghan et al., 2021; Neverman et al., 2019) – which assumes space planting of all slopes (Hawley and Dymond, 1988). Such assumptions are commonly used in models to inform policy development at regional to national scale (Basher et al., 2020; McDowell et al., 2020; Monaghan et al., 2021). Using high resolution data, this study, while limited to two farms, has undertaken a spatially explicit quantification of the reduction in landslide erosion due to trees actually present in the landscape. Both farms have a history in soil conservation – Site 1 since the 1980s, Site 2 since the 1950s. The results shed some doubt on the previously assumed effectiveness of tree planting in the context of farm environment plans, since mitigation effectiveness is very much dependent on the scale of plantings (both number and density) and the targeting of susceptible land. In the absence of spatially explicit assessments that evaluate the reduction in landsliding due to actual mitigation measures, the assumptions made by such national-scaled models may provide misleading expectations to policy planners and practitioners alike when not interpreted with good knowledge of the assumptions.

4.5 Conclusion

We developed a landslide susceptibility model using binary logistic regression for silvopastoral landscapes. For the first time, the influence of individual trees of different vegetation types is integrated into a statistical landslide susceptibility model. Model performance was very good, with a median AUROC of 0.95 in the final model used for predictions, which equates to an accuracy of 88.7%. The effect of highly skewed continuous variables on the maximum likelihood estimator was investigated by testing different sampling strategies aimed at reducing positive skewness. With an adequate sample size, we found that highly skewed continuous predictor variables do not result in an inflation of effect size.

The effectiveness of trees at reducing landslide erosion was quantified using odds ratios, which can be interpreted as factors of change in the odds of a spatial unit being susceptible to shallow landslide erosion. The odds ratio for poplar/willow trees indicated that the odds of shallow landslides were reduced by a factor of 0.34 close to the base of poplar/willow trees, whereas at a distance of 20 m from the tree, the average tree had no measurable effect on landslide susceptibility. Eucalyptus had a lower odds ratio (greater effect) at close proximity with an OR of 0.04 at tree stem, but reaching an odds ratio of 1 at 13 m. Kānuka had a similar spatial pattern to poplar/willows, but is more difficult to interpret as individual trees are more difficult to delineate, which means the effect is a function of multiple stems (approximately 3 stems).

We illustrated application of the landslide susceptibility model by quantifying the reduction in shallow landslide erosion due to trees, for two case study sites, and also evaluated reductions achieved by tree type. Future landslide erosion was reduced by 16.6% at Site 1 and 42.9% at Site 2 due to all existing vegetation. The effectiveness of individual trees on reducing landslide erosion was shown to be less a function of species than that of targeting highly susceptible areas with adequate plant densities. We found 80% of landslides are triggered in 12.1% and 7.3% of

Sites 1 and 2, respectively, suggesting there is great potential for smarter targeting of erosion control by decision-makers in land management. The high-resolution spatial information provided by the landslide susceptibility map can be used to support the development of landslide erosion mitigation measures.

4.6 Supplementary Material

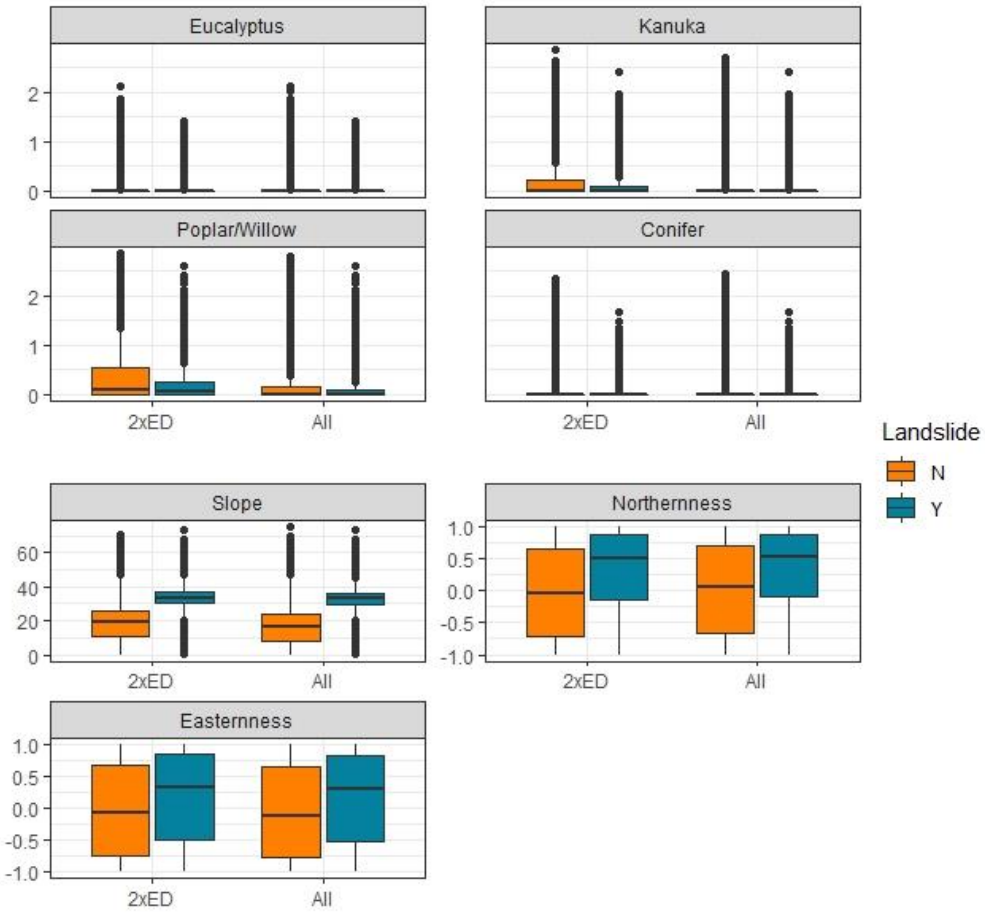

Figure 4.A1. Boxplot diagrams for numerical variables in landslide susceptibility model showing differences in median and interquartile range for landslide presence and absence (5x) for the two different sampling approaches (all vs 2xED). N= Landslide absence points; Y = Landslide presence points.

5

5 Development of a Morphometric Connectivity Model to Mitigate Sediment Derived from Storm-Driven Shallow Landslides

Raphael I. Spiekermann[1,2], Hugh G. Smith[2], Sam McColl[1], Lucy Burkitt[1], Ian Fuller[1]

Ecological Engineering (Elsevier), Vol. 180, Issue 106676
Submitted 8 February 2022
Accepted 27 April 2022
Available online 4 May 2022, reprinted with permission of Elsevier.
https://doi.org/10.1016/j.ecoleng.2022.106676

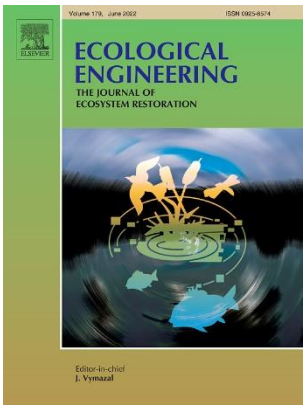

This publication investigates determinants of sediment connectivity for a landslide-triggering storm event in 1977 in the Wairarapa, New Zealand. As a global first, a morphometric landslide connectivity model is developed to predict the likelihood of sediment delivery to streams following landslide initiation. A range of connectivity scenarios are explored by defining a set of sinks and simulating varying rates of sediment generation during flood events of increasing magnitude. Furthermore, the influence of coalescing landslide deposits in determining sediment delivery is assessed. By coupling landslide susceptibility and connectivity predictions in a modular form, the cost effectiveness of targeted versus non-targeted approaches to shallow landslide mitigation are quantified. The cost-effectiveness of targeted mitigation of landslide-derived sediment is found to be approximately 10-fold greater than a non-targeted approach.

[1] School of Agriculture and Environment, Massey University, Palmerston North, New Zealand

[2] Manaaki Whenua – Landcare Research, Palmerston North, New Zealand

5.1 Introduction

Shallow landslides are an important mass wasting process and source of sediment in steep terrain and can have significant downstream impacts on freshwater and marine environments (Broeckx et al., 2016; Dymond et al., 2017b; Glade, 2003; Jia et al., 2021; Rahn, 2005; Ziemer et al., 1991). In New Zealand, much pastoral farmland is predisposed to shallow landslide erosion reflecting steep and highly dissected slopes underlain by soft sedimentary rocks (Basher, 2013). Following European settlement, deforestation of a large part of the country for pastoral farming has accelerated landslide erosion rates (Fuller and Rutherfurd, 2021; Glade, 2003). Shallow translational landslides occur within the material above the bedrock, i.e., the regolith which includes soil, saprolite, colluvium and deposits of tephra and loess (Crozier, 1996; Phillips et al., 2021). They are small, shallow rapid failures that have been identified as the most common type of mass movement in the New Zealand landscape (Basher, 2013; Smith et al., 2021; Spiekermann et al., 2022). Shallow landslides have also been referred to as earth flows (e.g., Crozier 1996) or mud flows (Geertsema et al., 2010) reflecting movement as liquified material (Cruden and Varnes, 1996). Periodic high-intensity rainfall events regularly trigger large numbers and high densities of shallow landslides (Crozier, 2018). The landslide deposits of shallow landslide scars (50–100 m^2; Betts et al. 2017) are typically long and narrow and may coalesce with adjacent landslide deposits to transport and deposit fine sediment in freshwater streams below (Bessette-Kirton et al., 2020; Kasai and Yamada, 2019; Mondini et al., 2011). In the long-term, shallow landslides can seriously degrade the soil resource (De Rose et al., 1993; Lambert et al., 1984) and, as an important source of sediment, contribute to the degradation of freshwater quality and marine receiving environments (Davies-Colley, 2013; Hicks et al., 2011).

The importance of shallow landslides as a contributor to catchment sediment budgets is spatially and temporally variable as a function of i) the predisposition of the terrain to

landsliding, ii) the frequency and magnitude of both the triggering mechanism (e.g., rainfall) and the response (i.e., the landslides), and iii) sediment connectivity that determines off-slope sediment delivery rates. Sediment connectivity describes both the potential and proficiency of a catchment to facilitate the conveyance of sediment between its components (Heckmann and Vericat, 2018), that is, the transfer of sediment from a source to sink via sediment detachment and transport (Bracken et al., 2015; Najafi et al., 2021a). There are a variety of landforms and scales where connected sediment transfer takes place. These include on hillslopes, between hillslopes and channels, and within channels (Brierley et al., 2006; Fuller and Death, 2018). Connectivity is an important concept as it can help anticipate downstream impacts of hillslope erosion. When considered as a functional, process-based framework (Bracken et al., 2015), it can help increase understanding of how erosion and sediment delivery to streams can have severe downstream effects on water quality and ecosystem health (Dymond et al., 2017b). Moreover, consideration of connectivity is essential from a sediment management perspective, for example prioritizing erosion mitigation on hillslopes to reduce sediment delivery to streams or to improve sediment continuity in catchments (Simoni et al., 2017). Therefore, this study is concerned with sediment connectivity in terms of lateral linkages that drive the supply of materials from slopes to the channel network (Brierley et al., 2006).

Silvopastoralism has been widely adopted as a sustainable land management and soil conservation tool in New Zealand (Benavides et al., 2009; Mackay-Smith et al., 2021; Wall et al., 1997). A primary objective in integrating trees into pastoral hill country is the prevention of hillslope erosion and delivery of sediment to streams (Basher et al., 2020; Spiekermann et al., 2022, 2021; Thompson and Luckman, 1993), since high sediment connectivity can have detrimental outcomes on riverine and estuarine habitats by reducing the diversity, types, and abundance of fauna (Fuller and Rutherfurd, 2022). The introduction of sediment standards into New Zealand's National Policy Statement for Freshwater Management (NPS-FM) has required regional authorities to manage freshwater in a way that considers the effects of land-use, including the effects on receiving estuarine environments (New Zealand Government, 2020a).

From a sediment mitigation perspective, both potential landslide source areas and mobilisation of sediment from source to channel need to be assessed to support targeted erosion control through tree planting. In general, targeting mitigation actions to critical source areas greatly increases the cost-effectiveness of measures (Doody et al., 2012; McDowell, 2014; McDowell et al., 2018). Cislaghi and Bischetti (2019) proposed a modular approach to couple slope stability modelling and connectivity. Similar methods have been used for modelling sediment delivery from debris flows (Burton and Bathurst, 1998), surface erosion (Najafi et al., 2021b; Poeppl et al., 2019; Zhao et al., 2020), and large wood recruitment to streams (Lucía et al., 2015; Rigon et al., 2012). These approaches adopt either physical or statistical models to predict slope stability, followed by a prediction of run-out length to determine the degree of connectivity. While landslide connectivity models have been categorised by various authors (e.g., Rickenmann 2005b, Cislaghi and Bischetti 2019, Najafi et al. 2021a), the most common methods use either a limiting criterion (e.g., involving critical slope and deposition zone; e.g., Bathurst et al., 1997 or Dymond et al., 2006), or some variation of an empirically fitted relationship between landslide volume and runout length (e.g., Cislaghi and Bischetti, 2019), which may be extended to include additional factors influencing run-out distance such as travel angle or fall height (Bessette-Kirton et al., 2020; Corominas, 1996). Other approaches to identify erosion source and deposition areas include the use of repeat digital elevation models (Croke et al., 2013; Heckmann and Vericat, 2018; Scheip and Wegmann, 2022), mathematical graph theory (Heckmann and Schwanghart, 2013), and a two-parameter friction model (Wichmann et al., 2009).

The index of connectivity (IC) developed by Borselli et al. (2008) and further developed by Cavalli et al. (2013) has been widely adopted. Najafi et al. (2021a) reviewed the IC and discussed its limitations, which relate to the interpretation of the index as well as the lack of quantitative validation. However, the IC has been successfully used as a predictor of muddy flood-affected sites (de Walque et al., 2017) and sediment transfer between sediment sources (e.g., landslides, debris flows, sheet, and rill erosion) and water channels (e.g., Najafi et al.

2021b, Martini et al. 2022). Najafi et al. (2021a) also made an important distinction between structural and functional connectivity concepts. The IC aims to represent structural sediment connectivity based on (high-resolution) topographic influences on sediment flux. Since the IC fails to represent process-specific characteristics of sediment source and transport, inconsistencies can arise when comparing IC values to process-specific modelling (Cislaghi and Bischetti, 2019; Poeppl et al., 2019; Zhao et al., 2020). Thus, the IC is a useful tool for representing structural connectivity but is less well suited for modelling functional connectivity (Martini et al., 2022).

Against this background, we follow a modular approach proposed by Cislaghi and Bischetti (2019) for shallow landslides by coupling a landslide susceptibility model with a connectivity model. Since the use of universal empirical relationships between scar size and run-out distance is known to perform poorly because it disregards multiple factors that determine connectivity (Cislaghi and Bischetti, 2019; Corominas, 1996), we develop the first statistical connectivity model for shallow landslides using binary logistic regression. The advantages of this approach are its limited data requirements, which consist of a high-resolution DEM for generating morphometric predictors and mapped landslide scars and deposits used to fit the model.

In addition, we consider a range of sediment delivery scenarios by defining a series of sinks and short- to long-term sediment stores in recognition of the observed variation in run-out behaviour – from insipient failures to strong, stiff plastic flows and – in their most fluid state, a slurry flow of material (Crozier, 1996). This allows a preliminary investigation of temporal dynamics in connectivity and considers the potential for deposited material to be reworked during subsequent rainfall events, for example, increased recruitment of sediment by overland flow across saturated soils adjacent to streams. A further objective of this paper is to assess sediment delivery from shallow landslides under different land management scenarios at the scale of widely spaced individual trees. We quantify sediment delivery reductions compared to a pasture-only baseline using the following conditions: 1) existing tree cover, 2) targeted mitigation to slopes with high landslide susceptibility and high sediment connectivity, and 3)

complete tree cover using a 15 x 15 m grid of poplar trees. Predictions are made for 50 pastoral farms in the Wairarapa hill country to quantify the reductions in sediment delivery from shallow landslides under the different land management scenarios. We also 1) provide an assessment of cost effectiveness based on the number of trees required to achieve the respective outcomes, 2) quantify the cost-effectiveness of targeted versus non-targeted erosion control, and 3) discuss the implications for land management.

5.2 Data and Methods

5.2.1 Study Area

An inventory comprising shallow landslide scars and deposits mapped across a 700-ha area of steep pastoral farmland east of Masterton in the Wairarapa of New Zealand (Figure 5.1) forms the basis of the present study. The study area is part of a 1700 ha sheep and beef farm, which has been the focus of many previous studies on soil erosion (e.g., Crozier et al. 1980, Lambert et al. 1984, Rosser and Ross 2011b, De Rose 2013, Basher et al. 2018, Spiekermann et al. 2021, 2022). The layer of indigenous vegetation was cleared for pastoral farming between 1860 and 1890 (Lambert et al., 1984). Besides small patches of naturally regenerating *Leptospermum scoparium* (mānuka) and *Kunzea* spp. (kānuka) visible in historic imagery, woody vegetation was largely absent in the study area until the 1980s when soil conservation works began to populate hillslopes with widely spaced poplar, willow, and eucalyptus trees. The morphology is best characterised by its steep, highly dissected terrain with narrow ridge and spur crests, hillslopes mostly between 15° and 35° that are underlain by highly erodible Neogene-aged sedimentary rocks. These consist mostly of massive, poorly bedded sandstone and coarse siltstone, partially overlain by a loess mantle. Brown loamy soils (Waitataura_14a.1) are most common in the study area and are moderately well drained (Lilburne et al., 2012). However, a dense subsoil zone of slow permeability provides a failure plane for shallow

landslides (De Rose, 2013). Gley soils (Taihape_10a.1; Lilburne et al., 2012) are commonly found on the lower slopes and valley bottoms. A large gully has formed in the northern section of the study area within an area of massive mudstone. To the west of the gully, an area largely devoid of landslides is part of a band of coquina limestone that extends farther to the south-west of the study area. Mean annual rainfall is approximately 1100 mm, with wet winters and dryer summers the norm.

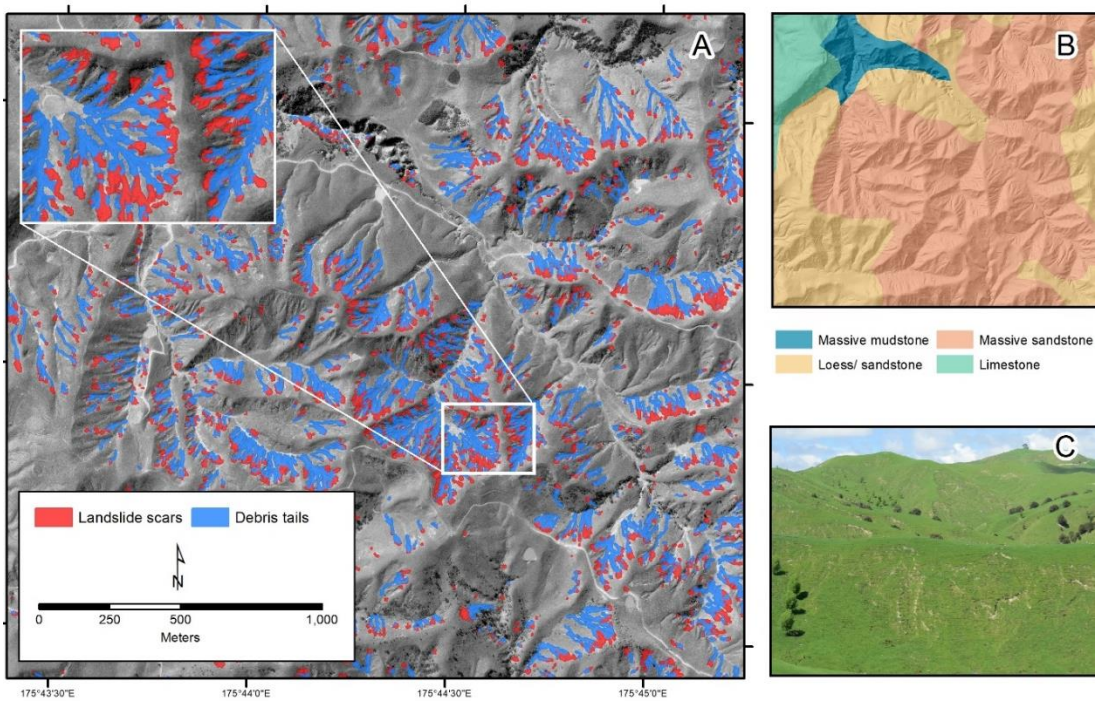

Figure 5.1. Insert A: 1977 imagery with landslide scars and deposits; Insert B: Lithology; Insert C: Landscape photo within study area showing steep, deeply dissected terrain (Source: Ebony Davison). Note: Location of study area in New Zealand is shown in Figure 5.3.

5.2.2 Data and Data Preparation

Landslide inventory

Beginning 18/09/1977, a rainfall event lasting five days (with 137 mm rainfall recorded at the nearest weather station – Gladstone) caused very extensive shallow landsliding in the Wairarapa hills (De Rose, 2013). Wet winter months preceding the rainfall event contributed to high antecedent soil moisture conditions. An aerial survey captured photography at a scale of 1:25000 shortly after the event, on 10/10/1977, which allowed scars and landslide deposits

to be identified and differentiated (Figure 5.1). Mapping was enhanced by producing raster objects via the multiresolution segmentation algorithm in eCognition using the panchromatic image from 1977, the DEM and slope grids as inputs (see

Supplementary Material 5.A5) Scars and landslide deposits were classified based on the brightness (mean and standard deviation) of image objects and a slope gradient threshold of 30° aimed at removing most false positives. Image objects adjacent and at lower elevation to mapped scars were classified as landslide deposits while increasing thresholds for mean slope and brightness to allow for greater variation caused by conglomerates of turf and sediment in image objects. The process of landslide deposit classification was done iteratively to allow landslide deposits to expand downslope. Manual refinement of the classification was performed across the entire study area by selecting and removing falsely classified objects. The ruleset description can be viewed in the supplementary material. The final landslide inventory includes 2002 scars and 1216 landslide deposits. Of these scars, 446 have no obvious landslide deposit, which suggests these may represent incipient failures or intact rafts of turf. A further 571 scars had a single deposit, whereas the remaining 985 scars have landslide deposits that coalesced with adjacent landslide deposits.

Landslide connectivity scenarios

In this study, landslide connectivity is operationalized through a simple definition: A shallow landslide is defined as connected when its landslide deposit intersects with a pre-defined sink, which we refer to as a connectivity target. This definition results in a binary classification of landslide scars as “connected” (LC) or “unconnected” (LU), and therefore lends itself to a statistical investigation of the factors that determine connectivity based on a Bernoulli distribution. In addition, this study aims to investigate the dependence of connectivity on the definition of the connectivity target by assessing changes to the Bernoulli distribution as well as change in effect size of variables. Therefore, we define a set of six connectivity targets using a LiDAR-derived stream network and the topographic wetness index (TWI). The varying

connectivity targets are designed to test the effect of different catchment hydrological conditions on sediment delivery. This allows exploration of how timing of landslides either within-storm or differences in soil wetness between storms may affect sediment delivery.

The first connectivity target is defined by a stream network that was generated using the 1-m DEM, following the standard procedure of filling terrain depressions with the Fill Sinks XXL function (proposed for LiDAR DEM processing by Wang and Liu, 2006) and a flow algorithm (Quinn et al., 1991). A stream initiation value of 6400 m^2 was set, which was identified as a suitable threshold in mudstone terrain for permanent, intermittent, and ephemeral streams (Storey and Wadhwa, 2009). The streams were buffered by 5 m and the polygon used to represent the first of six targets. We refer to this connectivity target as "Streams".

The remaining five connectivity targets were defined using the TWI, which is a measure for accumulated water or soil saturation (Moore et al., 1991, 1988), calculated as:

$$TWI = \ln\left(\frac{SCA}{sg}\right)$$

where SCA is the specific catchment area, and sg is slope gradient in radians. We set the minimum slope in the filled DEM to 0.01 radians to avoid division by zero during TWI calculation (Kopecký et al., 2021). Slope was calculated using the 3rd degree polynomial with 10 parameters (Haralick, 1983), which is the slope algorithm that performed best when used to predict measured soil moisture as a component of TWI (Kopecký et al., 2021). Targets were then defined using TWI thresholds based on the distribution of TWI values in the study area (Figure 5.1b). The thresholds used to represent potential zones of saturated soils correspond to the 75, 80, 85, 90, and 95th percentiles of the TWI distribution in the study area. A lower cut-off corresponds to a larger hypothesized zone of saturated soils, which has the effect of increasing the ratio of scar connectivity (Figure 5.2c; Table 4.2). TWI zones unconnected from the stream network were removed. Therefore, the TWI-based connectivity targets are upslope extensions to the stream network. While the transport capacity of sediment in these TWI zones is unknown, we expect sediment delivery to decrease with increasing size of the TWI

connectivity target, as there are more opportunities for deposition to occur on footslopes and floodplains during the overland flow phase between landslide deposition and subsequent erosion/transport through the TWI-defined saturated area to the stream channel. Thus, while an increasing proportion of landslide deposits intersect the larger connectivity targets, the average proportion of source material that is ultimately delivered into the stream channel is reduced compared to landslide deposits delivering directly to the stream channel.

We differentiate these two aspects of sediment delivery by quantifying the landslide connectivity ratios (the proportion of landslides connecting to target) and sediment delivery ratios (SDR) for each respective target. The SDRs were based on the scar area/volume of connecting landslides. For the *Streams* target, we assumed that, on average, connected landslides delivered 50% of mobilised sediment to sink (Jones and Preston, 2012; Reid and Page, 2002). For sediment deposited to the *Streams* target, sediment transport in the channel network is accelerated by in-stream processes.

We consider SDR to be both a function of 1) the LCR (number of landslide deposits connecting to target) and 2) the capacity to maintain sediment transport from source (landslide scar) to sink (stream). Therefore, we assume the rate of delivery to the water channel is reduced by increments of 5% with each successive TWI-based connectivity target (TWI-p.95: 45% – TWI-p.75: 25%) to reflect the hypothesized reduction in transport capacity from the initial landslide deposition and subsequent transport of sediment to stream channel by overland flow – either within or post rainfall event. In the absence of empirical evidence to support this assumption, this approach is aimed at modelling the reduction in recruitment and transport capacity in areas of increasing distance from the water channel to explore the dependence on assumptions related to sink definition and transport capacity. Besides distance, the roughness in surface morphology of footslopes and toeslopes may impede particles being entrained in overland flow. SDRs thus describe the proportion of all mobilised material entering the watercourse or to an area where overland flow is likely to allow sediment transport to continue, albeit at a reduced rate. The TWI-based connectivity targets are, thus, designed to characterize

potential increases in SDR through surface runoff erosion post rainfall event (Xiong et al., 2022). In addition, we compute sediment yields for the landslide triggering event, assuming soil bulk density is 1.4 t m^{-3} and an average scar depth of 1 m (Crozier, 1996).

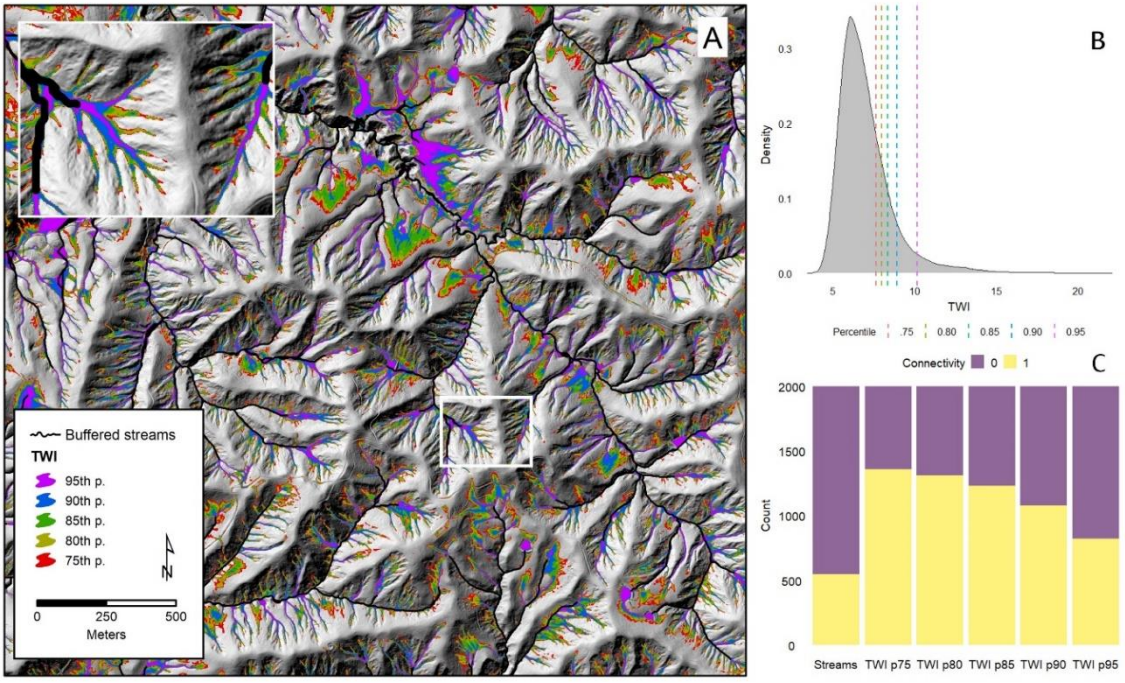

Figure 5.2. Insert A: Stream network and TWI-based sinks set using percentiles from the distribution shown in Insert B; Insert C: Number of landslide scars connected (1) and unconnected (0) based on intersection of landslide deposits with respective sinks.

Explanatory variables

The most common approach for estimating sediment delivery from landslides to streams is to develop empirical relationships between soil volume and run-out distance, which may be further refined by considering the vertical drop (Rickenmann, 1999). Therefore, an important explanatory variable that determines runout-distance is the initial soil-involved landslide volume (Cislaghi and Bischetti, 2019; Corominas, 1996; Crozier, 1996). We include landslide scar area (ScarArea) as an explanatory variable in the models. Scar area is a reasonable substitute for volume, since shallow landslides tend to have small depth to area ratios (Betts et al., 2017). To test the influence of multi-source landslide deposits on the mobility of sediment material, we also include the total area of all scars (SumScAr) contributing to any given landslide deposit as a second variable related to the volume of source material.

The LiDAR digital terrain model (DTM) from Greater Wellington Regional Council was used at 1-m resolution to generate a set of fourteen morphometric explanatory variables to investigate their importance as predictors of connectivity (Table 5.1). Because landslides were triggered in 1977 prior to the LiDAR survey, a median filter with 3-m radius was used to remove minor surface roughness produced by the shallow landslide scars (ca. 1 m depth; Betts et al., 2017) to approximate the terrain surface prior to failure. Each landslide scar was converted to a centroid point (forced inside polygon) and morphometric variables were extracted at the location of points. The variables were standardised (centred around the mean and scaled by the standard deviation) prior to fitting models to allow comparison of coefficient estimates.

Flow Accumulation is the accumulated count of cells flowing into any given cell (m^2). Flow accumulation is therefore a measure for topographic location with respect to catchment and a proxy for (potential) surface runoff. Due to the high positive skewness, a log-transformation of flow accumulation was used. *Distance to Channel* is the overland flow distance (m), whereas the *Vertical Distance to Channel* is the altitude difference (m) to a pre-defined channel network (see section 2.2.2). *Slope Height* (standardized) and *Valley Depth* are relative measures for slope position (Böhner and Selige, 2006). *Valley Depth* is the normalized difference between slope height and valley depth. *Easternness* uses the sine transformation of slope aspect (dx); *Northernness* the cosine transformation (dy) since aspect is a circular variable. *Slope gradient* is the gradient at the centroid of the scar (°; Zevenbergen and Thorne 1987); Crozier (1996) found a significant correlation ($P < 0.05$) between the surface angle of rupture and runout distance. We include the *Downslope Distance Gradient* (Hjerdt et al., 2004), $\tan \alpha_d = d/L_d$, where L_d is the horizontal distance to the point with an elevation d meters below the elevation of the starting cell, following the steepest-direction flow path. The gradient aims to quantify topographic controls on local hydrology – specifically groundwater table gradients that are less dependent on local surface slope. We hypothesize that the *Downslope Distance Gradient* is important for sediment delivery as it captures landform-scaled slope gradient in contrast to local

surface slope. In consideration of raster resolution (1 m) and topography, we selected a d-value of 50 m. *Gradient Difference* is the unitless difference between $\tan \alpha_d$ and local surface gradient (Hjerdt et al., 2004). The *Topographic Positioning Index* compares the elevation of each cell in a DTM to the mean elevation of a specified neighbourhood around that cell (Guisan et al., 1999). Thus, high values correspond with local high points such as ridges, low values with local low points such as valley bottoms.

Table 5.1. Morphometric explanatory variables used in connectivity model. All variables are continuous and calculated at 1-m resolution

	Morphometric explanatory variable	**Algorithm**	**Parameterization**
1	Log-transformed flow accumulation (LogFA)	Package: RSAGA, Library: ta_channels, Module: 0	Method: Multiple Flow Direction (MFD) Convergence = 1
2	Distance to channel (DisOvrlnd)	Package: RSAGA, Library: ta_channels, Module: 4	Method: MFD
3	Vertical distance to channel (VDis)	Package: RSAGA, Library = ta_channels, Module = 4	
4	Slope Height (SlopeSH)	Package: RSAGA, Library = ta_morphometry, Module = 14	w = 0.5 t = 15 e = 2
5	Valley depth (SlopeVD)	Package: RSAGA, Library = ta_morphometry, Module = 14	w = 0.5 t = 15 e = 2
6	Easternness	Package: qgisprocess: grass7:r.slope.aspect	
7	Northernness	Package: qgisprocess, grass7:r.slope.aspect	
8	Slope gradient (Slope)	Package: RSAGA, Library: ta_morphometry, Module: 0	
9	Downslope distance gradient (Gradient)	Package: RSAGA, Library: ta_morphometry, Module: 9	d = 50
10	Gradient difference (GradientDif)	Package: RSAGA, Library: ta_morphometry, Module: 9	d = 50
11	Topographic Position Index (TPI)	Package: RSAGA, Library: ta_morphometry, Module: 18	r_min = 3 r_max = 30
12	Topographic Wetness Index (TWI)	Package: RSAGA, Library: ta_hydrology, Module: 20	
13	Topographic ruggedness index (TRI)	Package: RSAGA, Library: ta_morphometry, Module: 16	r = 10
14	Vector Ruggedness Measure (VRM)	Package: RSAGA, Library: ta_hydrology, Module: 17	r = 4

The *Topographic Wetness Index* is a measure of water accumulation or soil saturation (Moore et al., 1988), which may influence sediment viscosity of the mobilised material, and also the propensity for surface runoff generation. The *Topographic Ruggedness Index* is a measure of topographic heterogeneity within a defined radius (r = 10 m; Riley et al. 1999) and is hypothesized to influence the downslope depositional rate (Crozier, 1996). Similarly, the *Vector Ruggedness Measure* decomposes slope and aspect into 3-dimensional vectors and calculates the resultant vector magnitude within a user-specified moving rectangular window (r = 4 m; Sappington et al. 2007). Each of these variables was processed in R (R Core Team 2021) using the packages RSAGA (v. 1.3.0; Brenning et al. 2018) or qgisprocess (v.0.0.0.9; Dunnington 2021) and extracted to points using the raster package (v.3.4-13; Hijmans 2021).

5.2.3 The Landslide Connectivity Model

Binary logistic regression with LASSO

The statistical evaluation of landslide connectivity aims to test the importance of the selected morphometric variables in determining sediment delivery from hillslopes to streams. For each of the six connectivity targets (Section 2.2.2), an equal number of connected and unconnected landslide points were selected. Depending on the connectivity target, the number of connected landslides differ between the minimum of 546 connected to the Streams target and a maximum of 1388 for the TWI-75 target (Table 5.2). As the area of the zone defined as the target increases, the degree of landslide connectivity increases. Therefore, where the ratio of Landslide-Connected to Landslide-Unconnected (LC:LU) <1, we selected all connected landslide points and an equal number of randomly sampled unconnected landslide points, and vice versa where the ratio LC:LU >1. These balanced sets of landslide points constitute the binary response variable (LU=0, LC=1) with the corresponding independent explanatory variables (Table 5.1).

We developed the connectivity models using logistic regression, which models the probability of a binary response variable ($Y = 0|1$) with a Bernoulli distribution. Logistic

regression uses the maximum likelihood estimator to determine parameters β_0 and β_1 to find optimum probability values given a set of predictor variables x_i. Variable selection was automated with the *Least Absolute Shrinkage Selection Operator* (lasso; Tibshirani 1996). The advantage of the lasso method is that variable selection and coefficient estimation is performed simultaneously to generate a model that optimizes for performance while avoiding over-fitting. This is achieved by minimizing the negative log-likelihood function (Akalin et al., 2020; Hastie et al., 2001) :

$$-\ln(L) = -\sum_{i=1}^{n}[-ln\left(1 + e^{(\beta_0+\beta_1 x_1+\cdots\beta_i x_i)} + y_i(\beta_0 + \beta_1 x_1 + \cdots \beta_i x_i)\right)$$

by adding a penalty term that forces coefficients to be shrunk towards 0, where p is the number of variables in the model:

$$-\ln(L) \; + \; \lambda\sum_{j=1}^{p}|\beta_j|$$

The penalty term is determined by the parameter λ which controls the sparsity of the estimator, i.e., the number of coefficients shrunk to 0. The optimal tuning parameter is found by testing a range of values in a cross-validation to reduce out-of-sample error. Lasso regression was implemented in R using the caret (Kuhn, 2008) and glmnet (Friedman et al., 2010) packages. The raster package was used for model predictions (Hijmans, 2021).

Sampling design and model evaluation

To test the consistency of variable selection, estimation of coefficients, and model performance across the six connectivity targets, we repeatedly sampled from the landslide dataset to generate 100 balanced datasets, whereby $n = \min\{LC, LU\}$ (Table 5.2). This process is repeated for each of the six connectivity scenarios resulting in 600 models. Each model was tuned to determine the optimal λ value (range 0.001 – 0.1 by 0.001 increments) using k-fold cross validation ($k = 10$). Samples were randomly partitioned into k folds, whereby $k - 1$

folds were used to train the model and the remaining fold used to test the predictive ability of the model. This was repeated until each of the ten folds was used for model testing.

Since logistic regression results in predicted probabilities of class association, a probability cut-off needs to be selected for binary classification and model validation. The selection of cut-off can be varied depending on the purpose of the model which may influence the tolerance of certain true positive or false positive rates. For this reason, the area under receiver operator curves (AUROC) is commonly used to estimate model performance as it is a threshold-independent performance measure (Brenning, 2005). Receiver operator curves plot the true positive rate (sensitivity) against false positive rate (1 – specificity) across all potential cut-offs (0-1). The AUROC is therefore a suitable measure to summarize a model's prediction performance for balanced samples as it does not depend on the cut-off used to calculate classification accuracy (Hosmer and Lemeshow, 2000). An AUROC score of 1 would mean the model can perfectly discriminate between connected and unconnected landslides in its predictions; a value of 0.5 corresponds to no discriminatory power and is equal to that achieved by pure chance. A good AUROC score is considered to lie between 0.8 and 0.9; an excellent score > 0.9 (El Khouli et al., 2009; Safari et al., 2016).

Variable importance is assessed using inclusion rate and the size of standardized coefficient estimate values. Based on results of k-fold cross-validation, the model with the highest median AUROC was selected from the 100 repetitions for each of the six targets and used to quantify model fit and prediction skill. Model fit was estimated by quantifying AUROC and maximum accuracy using predictions on the entire unbalanced dataset of 2002 landslide scars. Maximum accuracy uses the probability threshold (= cut-off) that renders a binary classification with the highest accuracy. Given that the datasets are unbalanced across all six targets (Table 5.2), the optimal cut-off can deviate from 0.5. The predictive skill was quantified through AUROC for each of the ten folds using cross-validation and evaluated using boxplots.

Generating accurate predictions of landslide size is an active research field – both in the domain of physical-process-based modelling (e.g., Bellugi et al. 2015a, 2015b) and statistical modelling (Lombardo et al., 2021). Moreover, coalescing landslides were hypothesized to be an important determinant of landslide connectivity and were therefore investigated by inclusion of the total area of all scars contributing to a given landslide deposit (SumScAr). However, given the challenges associated with forecasting landslide size, location, and density, we investigate how well morphometric variables can predict connectivity without knowledge of the size of mobilised source material. The scar size variables are thus removed to both test the sensitivity of the models to the size of mobilised source material and investigate the extent to which morphometric variables can predict connectivity without prior knowledge of scar size or density. We refer to the two model runs as "scar-size models" and "morphometric models". Spatial predictions of connectivity (Section 5.2.4) for the land management scenarios are based on the morphometric model which includes only topographic effects.

5.2.4 Land Management Scenario Modelling

Landslide susceptibility

We followed a modular approach to couple potential source areas through landslide susceptibility and sediment delivery through connectivity models (Cislaghi and Bischetti, 2019). We use the landslide susceptibility model developed by Spiekermann et al. (2022), which is based on a landslide inventory of approximately 43,000 scars that were triggered between 2005 and 2009. Landslide scars were mapped in the Wairarapa pastoral hill country overlapping the study area (Figure 5.3). Predictor variables include slope gradient, aspect, lithology, and tree influence models on slope stability (TIMSS) that represent the influence of individual trees for four different vegetation types). TIMSS were developed for different tree types based on an empirical relationship between distance from tree and reduction in soil surface eroded. The models are spatial representations of this relationship (1-m pixel),

following a sigmoidal shape until reaching an asymptotic value denoting the distance at which the tree has no observable influence on slope stability (Spiekermann et al., 2022, 2021). TIMSS are normalized to 0–1 but can exceed values of 1 due to the additive contributions from multiple trees. TIMSS are produced for the dominant tree types in the study area, which include eucalyptus, kānuka, poplar/willow and coniferous tree species. Binary logistic regression was used to develop the susceptibility model and model performance using k-fold cross-validation was excellent (AUROC of 0.95).

Coupling landslide connectivity and susceptibility

We integrated predictions of landslide connectivity and susceptibility using a modular approach. First, spatial predictions were reclassified into three classes, “Low”, “Medium”, and “High”. Class thresholds were determined by ranking landslide scars in decreasing order by their probability values. The probability values associated with the 5^{th} and 15^{th} percentiles were then selected. For the landslide susceptibility classification (Spiekermann et al., 2022), these values correspond to 0.32 and 0.72, which means that 80% of landslide scar points had probability values >0.72, 15% had values between 0.32 and 0.72 and the remaining 5% had probability values <0.32 (Spiekermann et al., 2022).

The same procedure was used for the predicted probabilities of landslide connectivity using the connected landslide scars and ranking these in descending order by their probability values. Similarly, the high connectivity class can be interpreted as being the zone where 80% of connected landslides were triggered, which we refer to as the connectivity rate. An intersection of the two reclassified spatial predictions resulted in a matrix of nine classes describing both the likelihood of landsliding to occur in future and the potential for sediment to be delivered to the respective target.

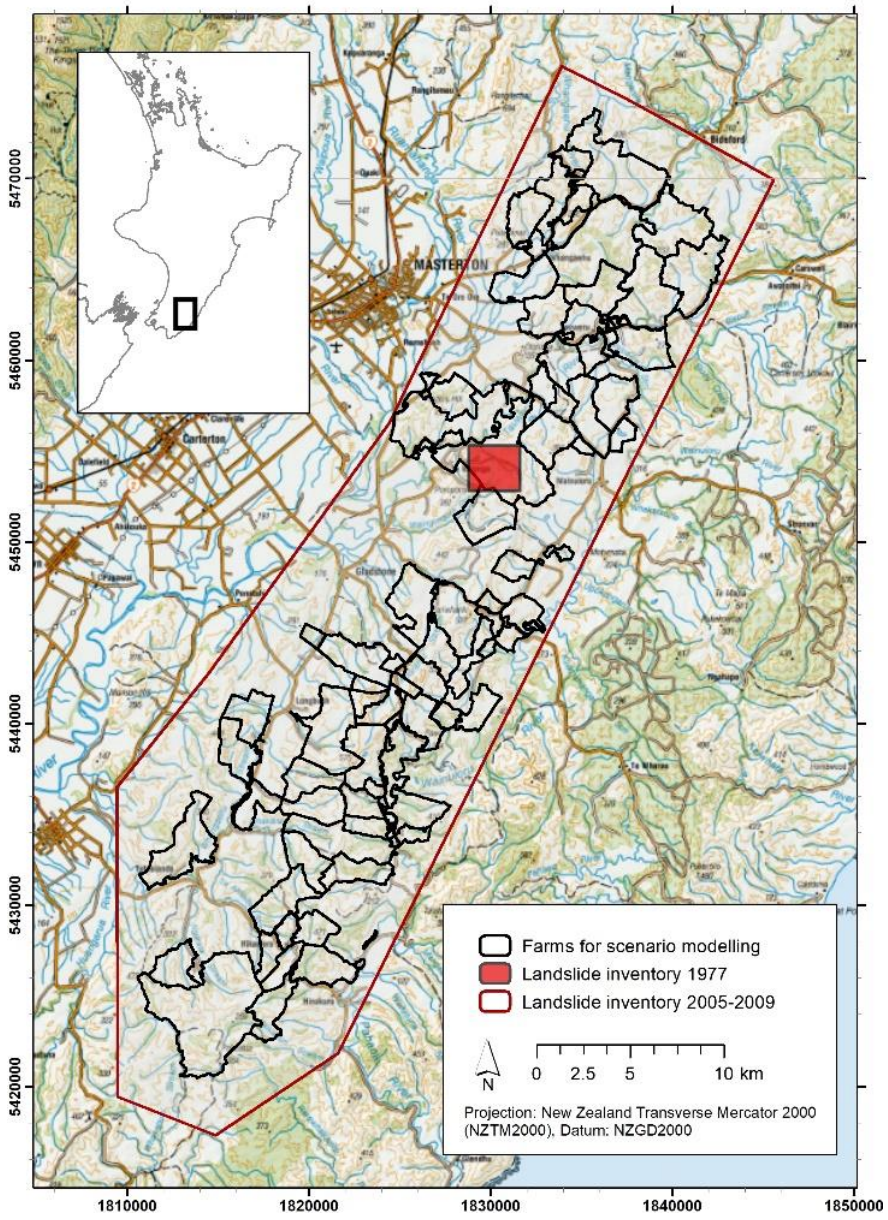

Figure 5.3. Location of study area of the 1977 landslide inventory used for the connectivity model, the extended study area of the 2005-09 landslide inventory used by the landslide susceptibility model, and the location of 50 farms selected for the land management scenarios.

Landslide connectivity ratios (LCR) were computed for each of the connectivity classes (i = 3) for the six morphometric models based on the number of landslides connecting (LC_j) to each jth target (j = 6) of the total number of landslides in the inventory (L_N). The class-specific connectivity rate (CR_i) is 0.8 for the high connectivity class, 0.15 for medium, and 0.05 for the low class:

$$LCR_{ij} = \frac{LC_j}{L_N} \times CR_i$$

SDRs were calculated for each connectivity class i in a similar way based on the volume of connected scars (LCV_j) relative to total landslide scar volume (L_V), for the class-specific proportion of the connected scar volume (that differs with target j) (CP_{ij}). For example, for $j = \text{Streams}$, 0.77 of the volume of material from connected scars (LCV_j) was sourced from the high class, 0.19 from the medium class and 0.04 from the low class. The target-specific delivery rate (DR_j: 0.5 for Streams, 0.45 for TWI-95, etc.; section 2.2.2) must also be considered, as follows:

$$SDR_{ij} = \frac{LCV_j}{L_V} \times CP_{ij} \times DR_j$$

These SDRs are used to calculate class-specific event sediment yields (ESY_{ij}; t/km^2/yr) for each of the jth targets ($j = 6$) as follows:

$$ESY_{ij} = \frac{SDR_{ij} \times LCV_j}{A_{ij}} \times \rho$$

As mentioned in section 2.2.2, we here assume soil bulk density ρ is 1.4 t m^{-3}. A_{ij} refers to the area occupied by class i using modelled predictions of landslide connectivity based on the jth target. The total event sediment yield is the sum of the delivered class-specific loads across the study area divided by the total mapped aera $A = 7$ km^2.

Land management scenarios

To quantify the reduction in sediment delivery from shallow landslides compared to a pasture-only baseline (S_0), we developed land management scenarios to estimate the expected reductions under the following conditions: 1) actual woody vegetation as at 2013 (WV), 2) targeted mitigation to slopes with high landslide susceptibility and high potential for sediment delivery (S_1), and 3) complete tree cover using a 15 x 15 m grid of poplar trees (S_2). Under these scenarios, the layout and/or density of trees changes, which directly impacts on the likelihood of landslide occurrence, whereas predictions of connectivity are static due to the

dependence on morphometric determinants only. The baseline is represented by a pasture-only scenario, which is achieved by setting the TIMSS variables to 0 in the landslide susceptibility model. This baseline scenario thus corresponds to the landslide susceptibility in 1977 – a landscape exhibiting a very sparse woody vegetation cover (see study area description in section 2.1). Scenarios 1 and 2 are constructed using the poplar/willow TIMSS based on a regular grid of points representing tree locations at 15 m spacings. Values of the TIMSS model are applied as a function of distance (1-m radial increments), ranging from 1 at the tree location to 0.06 at a radius of 20 m from the simulated tree (Spiekermann et al., 2021). The resulting raster grid at 1-m spatial resolution accounts for the additive effect of the nearest four trees at any given point. Scenario 1 applies this grid across the entire farm, whereas for Scenario 2 the grid is only applied to slopes classified as both highly susceptible and with high landslide connectivity, which we refer to as targeted mitigation zones.

Predictions are made for 50 farms (>300 ha) in the Wairarapa hill country (Figure 5.3) to quantify the reductions in sediment delivery from shallow landslides under the three scenarios using the buffered stream network (*Streams*) as connectivity target. Reductions in landslide erosion and sediment delivery are based on changes to the distribution of landslide susceptibility classes (CC, %) for each farm f:

$$CC_f = \frac{(S_x - S_0)}{S_0} * 100$$

where S_x are the proportions of the nine susceptibility/connectivity classes of scenarios S_1 and S_2, and S_0 the baseline. We assume that future landsliding will follow the same pattern as in the past, such that the majority (80%) of landslides will occur in the *high* susceptibility zone, and so forth. Therefore, a reduction in the area occupied by the *high* susceptibility zone equates to a reduction in future landslide erosion and sediment delivery. The reduction in sediment delivery (SD_{red}) considers the rate (based on counts) of landsliding LR_i and connectivity CR_i in each of the classes $i = \{0.8, 0.15, 0.05\}$:

$$SD_{red} = CC_{\%} \times LR_i \times CR_i$$

Based on the size of the farm, and the mitigation zones associated with S_1 and S_2, we calculate the number of poplar trees required to effect the modelled change. We use an average cost of $33 per plant, which is an estimate from the Greater Wellington Regional Council based on 3-m planting material, 1.7-m Dynex protection sleeve, labour and helicopter delivery (D. Boone, personal communication, November 2, 2021). We quantify the cost-effectiveness of targeted erosion control and discuss the implications for land management.

5.3 Results

5.3.1 Landslide Connectivity Models with Scar Size Variables

The variable inclusion rate (%; Figure 5.4a) and coefficient estimates (median; Figure 5.4b) from the lasso regression model for each of the six targets suggest that the scar size variables (*ScarArea*, *SumScAr*), which represent the volume of mobilised source material, are the most important factors that determine landslide connectivity. These variables were selected in 591 of the 600 models and the effect sizes were also the greatest. The results presented here further show that besides the size of individual landslide scars (*ScarArea)*, the coalescing of multiple landslides (*SumScAr*) in highly dissected hilly terrain is also an important determinant of sediment connectivity (Figure 5.4). There is a notable difference in the coefficient estimates of scar size variables with respect to connectivity target. For *Streams*, *TWI-p.95* and *TWI-p.90*, which represent the targets at greater distance from slopes, the individual scar size (m^2) was not as important a factor in determining connectivity as the sum of all scars (m^2) contributing to a coalescing landslide deposit; and vice versa for the remaining three connectivity targets. This indicates that when multiple scars contribute mobilised sediment to a common landslide

deposit, transportation and delivery of sediment is enhanced and can be deposited at greater distance from source. While there is an overall significant difference between individual scar sizes of connected and unconnected landslides, the difference is accentuated for *TWI-p.80 – TWI-p.75* (Table 5.2). Where *Streams* are set as the connectivity target, the average *SumScAr* (m^2) is almost three times greater for connected landslides (952 m^2) compared to unconnected landslides (330 m^2). On average, 6.3 individual scars contribute material to a coalescing landslide deposit compared with 2.2 for unconnected. This indicates that accounting only for the individual landslide scar size can result in underestimation of the runout distance given that landslide derived material from multiple sources can contribute to the transport of debris downslope.

Table 5.2. Number and scar size (mean, standard deviation) of connected and unconnected landslide scars, as well as fraction ground eroded by connected and unconnected landslide scars.

	Streams	**TWI-p.75**	**TWI-p.80**	**TWI-p.85**	**TWI-p.90**	**TWI-p.95**
Landslide scars - connected (LC)	546	1388	1311	1227	1078	809
Landslide scars - unconnected (LU)	1456	614	691	775	924	1193
Mean (SD) scar size – LC (m^2)	156 (229)	127 (176)	129 (180)	133 (184)	137 (192)	145 (204)
Mean (SD) scar size – LU (m^2)	82 (105)	47 (401)	52 (52)	55 (56)	62 (68)	74 (96)
Fraction ground eroded - LC (%)	0.122	0.252	0.242	0.232	0.211	0.122
Fraction ground eroded - LU (%)	0.171	0.041	0.052	0.061	0.082	0.171

Besides landslide scar size, distance is an important determinant of connectivity. Both *DisOvrlnd* and *VDis* had high inclusion rates and coefficient estimates – most notably for the *Streams* target, where *DisOvlrnd* was more important than *VDis* with a median coefficient of -1.31. Here, connectivity was found to be greater on north-facing slopes. Also noteworthy is the inverse relationship to *SlopeSH*, which may indicate higher connectivity of landslides occurring at mid-slope – where greater proximity to the stream network was more important than vertical drop. Other morphometric variables, such as *TWI*, *Slope*, *GradientDif*, *TWI* and *TRI*, were frequently shrunk to 0 and rarely included for the five TWI-based targets. Furthermore, while other morphometric variables had higher inclusion rates (*TPI*, *Gradient*), they were less important given their low median coefficient estimates. The full distribution of coefficient

estimates across the 100 models as well as the estimates of the best performing model are shown in Figure. 5.A1 (Supplementary Material).

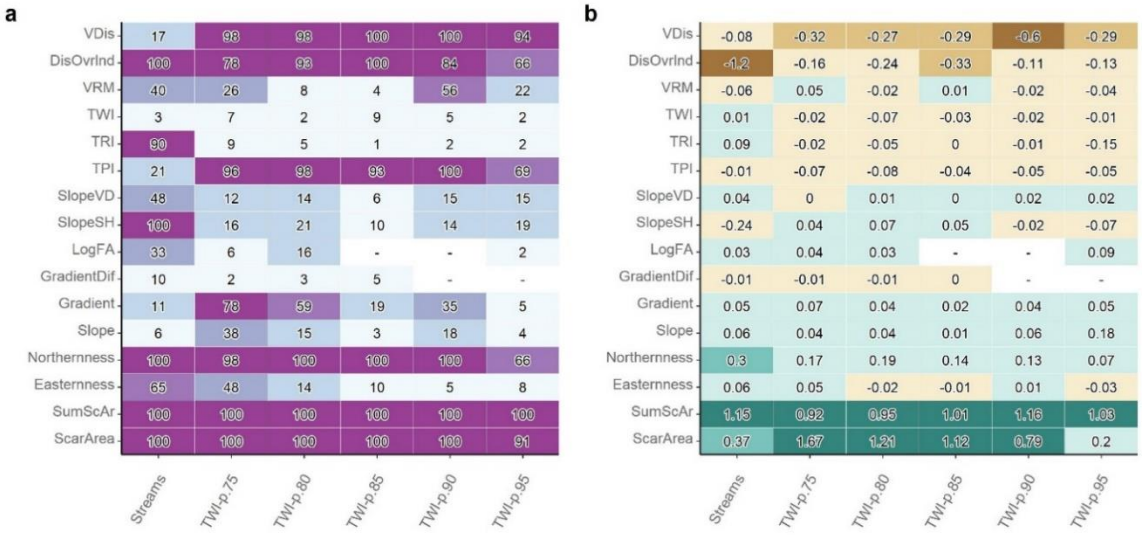

Figure 5.4. Insert a): Heat-map displaying the inclusion rate of variables for all 6 connectivity targets including the scar size variables. The numbers indicate how often variables were selected for the models out of 100 estimates. Note that the sum of scar area is the only variable included consistently across all connectivity targets. Darker colours show variables selected more frequently. Grey boxes with a dash indicate which variables were never selected for the models. Insert b): Heat-map displaying estimates of coefficients (median of non-zero estimates) for all six connectivity-targets. Grey boxes are equivalent to coefficients of zero and were never selected for the models.

Model performance of the 100 repetitions using 10-fold cross-validations was very good for the scar-size models, and generally decreased with increasing size of the connectivity target, from a median AUROC of 0.87 for *Streams* to 0.81 for *TWI-p.75* (Figure 5.5a). This means the models were best at classifying landslides as connected or unconnected when the 5 m buffered stream network was set as the connectivity target. It may reflect the importance of the combined scar size (*SumScAr*) in determining connectivity to streams and the lack of connectivity of individual scars. While only 150 of 571 landslides (26%) with 1:1 scar-desposit ratio connected, 396 of 985 (40%) with converging landslide deposits connected to target.

Model performance was further evaluated for the best of the 100 models considering both model fit and predictive skill. Model fit was excellent across all six scar-size models, with AUROCs ranging between 0.81 and 0.88, which corresponds to a maximum accuracy of 81.6% (Streams) and 75.7% (*TWI-p.80*; Figure 5.6). Predictive skill is shown in the boxplots in Figure 5.6. While AUROC scores are generally high, a small number of train-test iterations resulted

in low AUROC scores causing large variation in predictive skill. TWI-*p.80*, *TWI-p.90* and *TWI-p.95* show the greatest variation in AUC, which points to greater uncertainty with these models. Yet in all but 4 of the 60 train-test iterations, cross-validation results across all six scar-size connectivity models had scores >0.75, which suggests these models can predict sediment delivery with a fair degree of certainty (Safari et al., 2016).

Variation in coefficient estimates is another indication for robustness in model fit, which was greatest for the scar size variables, as well as DisOvrlnd and VDis (Figure 5.A2) However, these are the variables with the highest inclusion rate, which likely impacts on the variability of coefficient estimates. Along with the scar size variables, these two distance variables were the most important in terms of effect size. TPI had both a high inclusion rate in the TWI-based models and low variability in the estimates of effect size. The red dots in Figures 5.A2 and 5.A3 signify the coefficient values used in the best-ranked models used for spatial predictions.

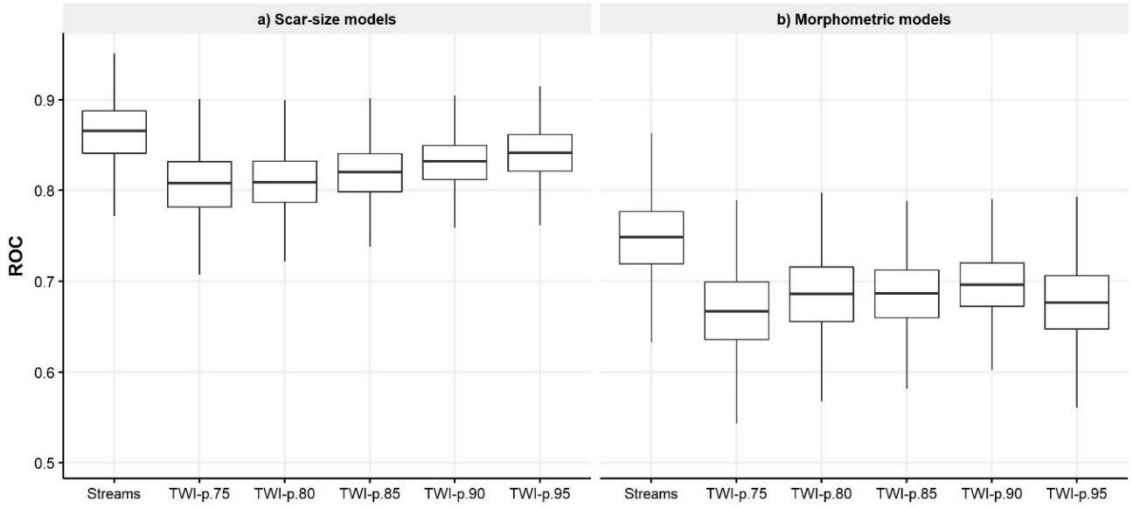

Figure 5.5. Model performance (AUROC) by a) scar-size connectivity models and b) morphometric connectivity models for each of the targets. Boxplots include 100 model repetitions, each with 10-fold cross-validation.

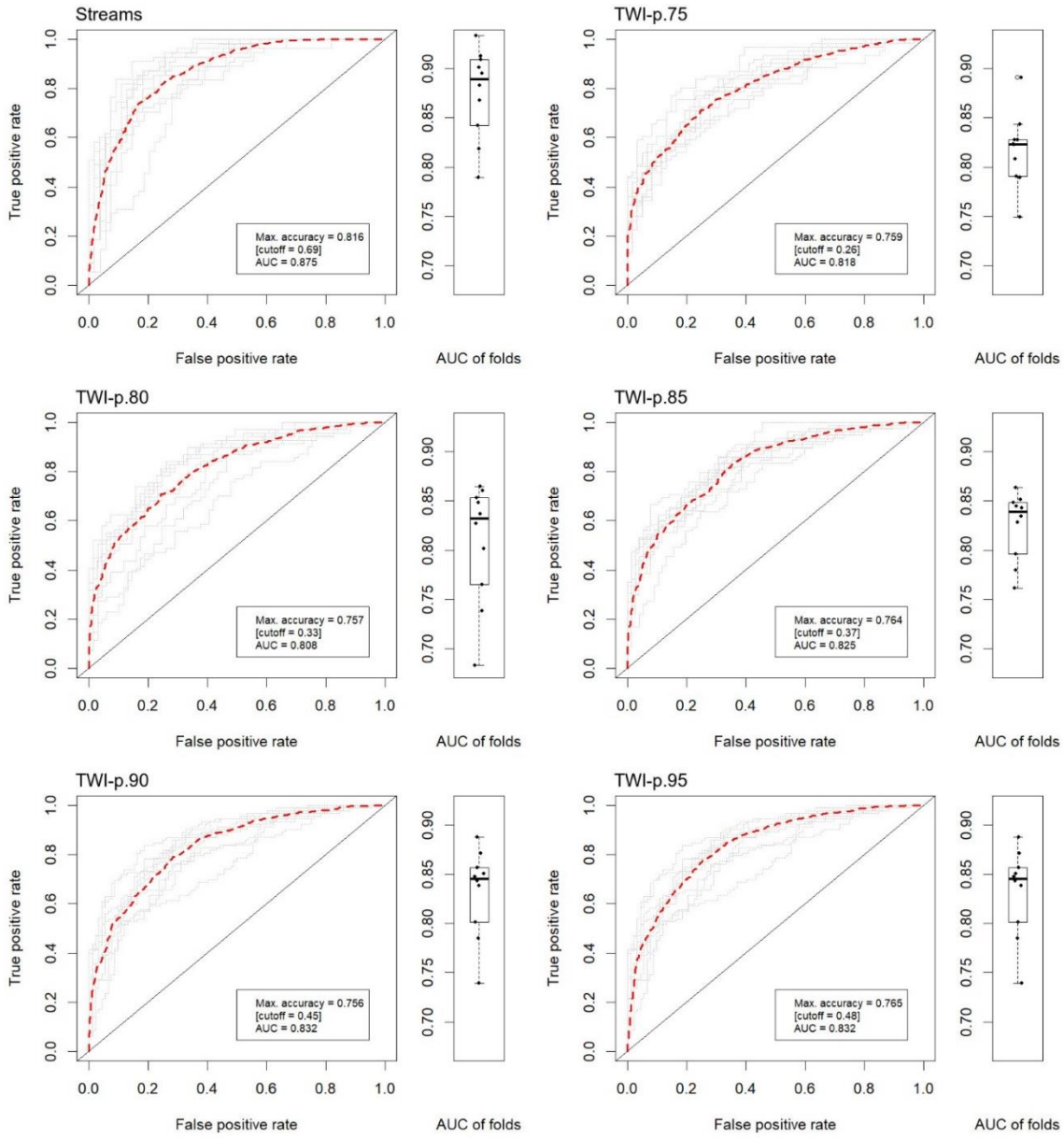

Figure 5.6. ROC plots for best of 100 models including scar size variables based on six different connectivity targets. The grey dashed lines are ROC-curves based on validation using 10-fold CV. The red dashed line is the ROC curve based on model predictions of entire unbalanced dataset (2002 scars). Maximum accuracy is calculated using the cut-off that renders the highest accuracy for the entire dataset.

5.3.2 Morphometric Landslide Connectivity Models

The morphometric landslide connectivity models isolate the role of local topography in determining sediment connectivity. The result of removing the two scar size variables (*ScarArea*, *SumScAr*) promotes the importance of all fourteen morphometric variables included in the models. The inclusion rate is overall high, with *Northernness*, *TPI*, *Gradient*, *VDis*, *DisOvrlnd*, and *VRM* most often selected across all six targets (Figure 5.7a). *TWI*, *Slope*,

GradientDif, and *LogFA* were included less often and when included had small coefficient estimates. In terms of effect size, *VDis*, *DisOvrlnd*, *Northernness* and *Gradient* were the most important variables in determining connectivity (Figure 5.7b).

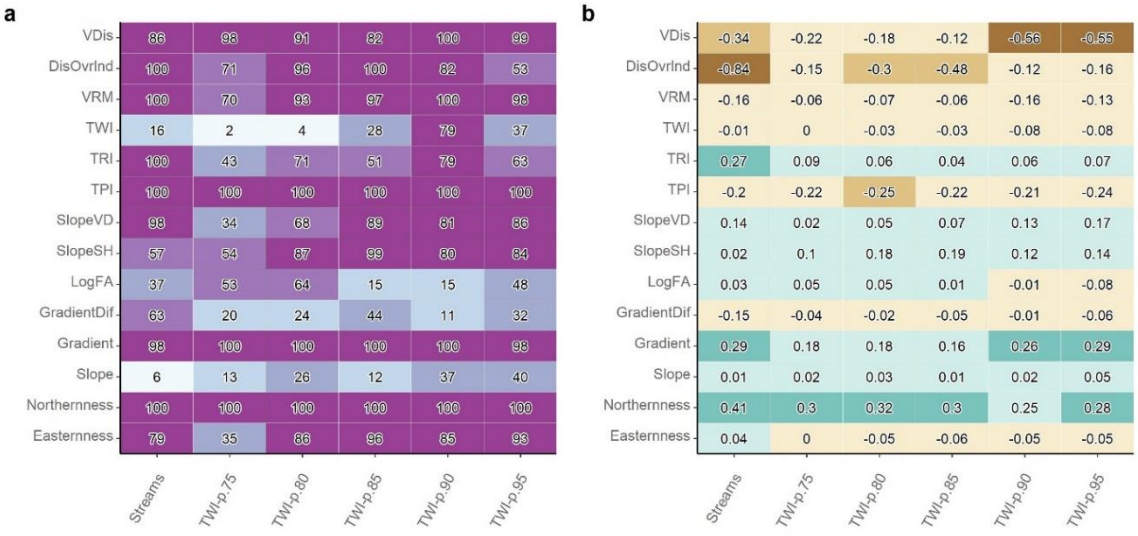

Figure 5.7. Insert a): Heat-map displaying the inclusion rate of variables for all 6 connectivity targets excluding the scar size variables. The numbers indicate how often variables were selected for the models out of 100 estimates. Note that the exclusion of scar size variables increases inclusion rate of morphometric variables. Darker colours show variables selected more frequently. Grey box with a dash indicates the variable was never selected for the models. Insert b): Heat-map displaying estimates of coefficients (median of non-zero estimates) for all six connectivity-targets. The grey box is equivalent to a coefficient of zero and was never selected for the models.

However, the removal of scar size variables comes at a cost in terms of model performance (Figure 5.5b), which is to be expected given the importance of these variables in the scar-size models. Across the 100 repetitions, the *Streams* connectivity model performed best, with a median AUROC of 0.75. The TWI-based models performed less well, with median AUROC ranging between 0.67 and 0.69. Of the 100 repetitions, the best-performing *Streams* connectivity model had a model fit with an AUROC of 0.76 and accuracy of 75.7% (Figure 5.8). Of the six models, the *TWI-p.75* connectivity model reveals the worst model fit with an AUROC of 0.67. The remaining four TWI connectivity models have an AUROC of approximately 0.70. In terms of predictive skill, the *Streams* connectivity model outperforms the five TWI models with a median AUROC of 0.77 from 10-fold cross-validation. The range in AUROC from 0.67 to 0.84 suggests potential for both good and poor predictions. Of the TWI connectivity models, the *TWI-p.80* model shows greatest predictive skill with a median

AUROC of 0.72. However, three of ten folds tested poorly (<0.66), which indicates high model uncertainty for predictions of connectivity.

As with the scar-size connectivity models, the greatest variation in effect size is found with *DisOvrlnd* and *VDis* (Figure 5.A3). The least variation is found in the morphological *TWI-p.90* connectivity model. However, this is explained by the well-balanced dataset of connected to unconnected landslides (Table 5.2), which means resampling from the unconnected would result in very similar datasets across the 100 model runs compared to the other five targets used. This approach is still meaningful in that it is much like a repeated cross-validation (100 x 10-fold CV). *DisOvrlnd* is the most important variable for predicting connectivity to *Streams* and, while still important for the TWI-models, its effect is less pronounced. As with the scar-size connectivity models, north-facing slopes are generally more likely to connect to water ways than south-facing slope. This may be due to topographic differences and variation in soil properties that influence properties such as clay content.

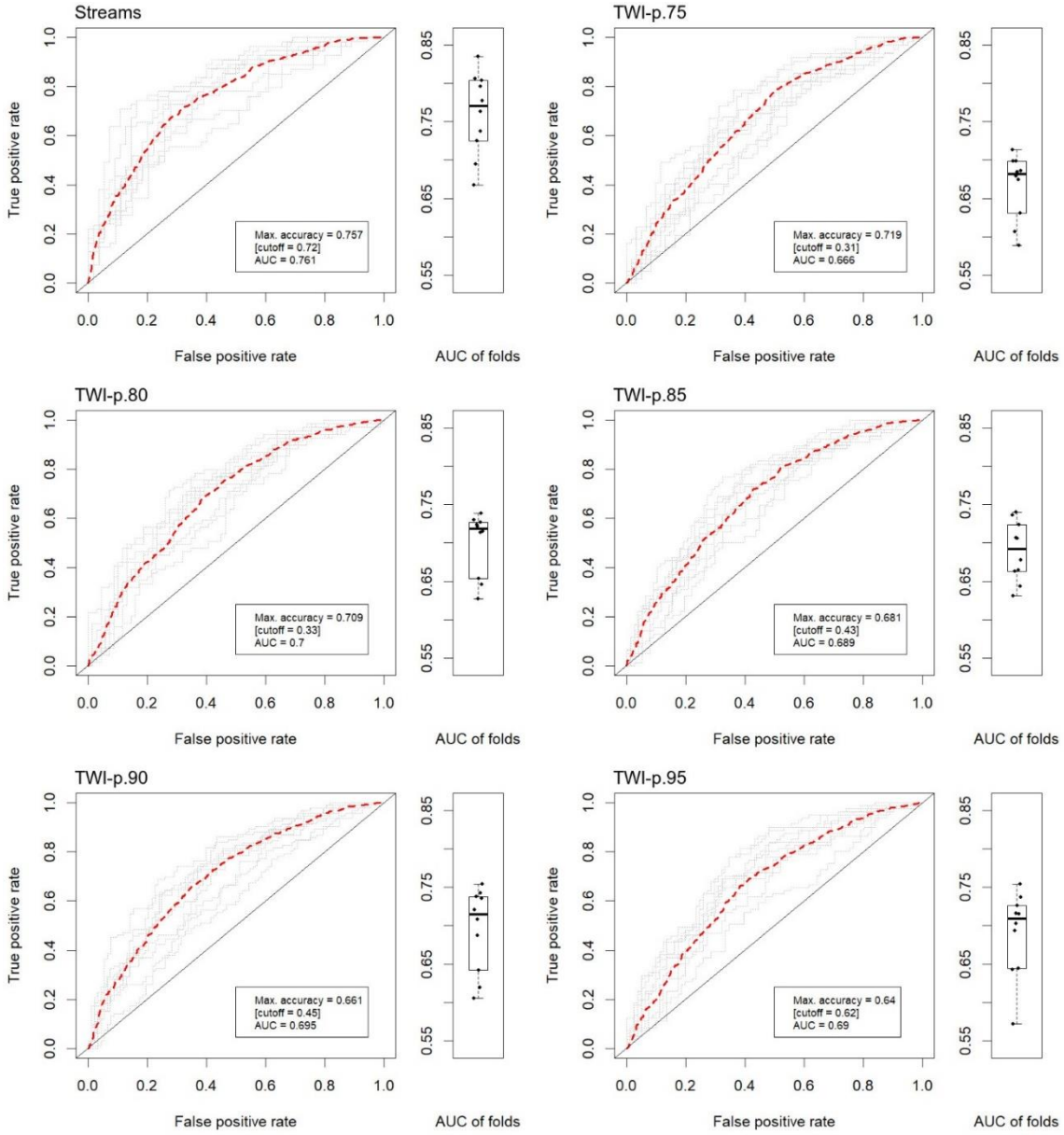

Figure 5.8. ROC plots for best of 100 models including only morphometric variables based on six different connectivity targets. The grey dashed lines are ROC-curves based on validation using 10-fold CV. The red dashed line is the ROC curve based on model predictions of entire unbalanced dataset (2002 scars). Maximum accuracy is calculated using the cut-off that renders the highest accuracy for the entire dataset.

5.3.3 Quantifying the Reduction of Sediment Delivery at Farm Scale

The spatial predictions of landslide connectivity were reclassified into three classes using probability thresholds. These were obtained by ranking all connected scars (Table 5.2) in descending order and extracting the probability values at the 80th and 95th percentiles. Thus,

80% of scars connecting to streams have probability values >0.42 and 95% > 0.25. The probability values were reclassified into three classes describing the likelihood of sediment delivery using these thresholds. The “high” connectivity class represents the area where 80% of connected scars are located; the “moderate” is representative of terrain where 15% of all connected scars were triggered; and finally, the “low” class where the remaining 5% of all connected scars were triggered (Table 5.3).

Increases in model accuracy increases the refinement of spatial predictions. This has implications from an erosion and sediment mitigation perspective. A connectivity model with poor performance may have large uncertainties in spatial predictions, which reflects in the difficulty to classify units as potentially connected/ unconnected. This in turn increases the proportion of land that requires biological mitigation due to the uncertainty.

A landslide susceptibility or connectivity model with greater accuracy can classify spatial units as stable/unstable or connected/unconnected with much greater certainty. This in turn enables more precise targeting of erosion and sediment mitigation. Observable differences in the spatial predictions of landslide connectivity predictions across the six different morphometric models are thus both functions of varying target definition and inherent model uncertainties (Figure 5.9).

Hillslope-channel coupling of landslides is largely dependent on the run-out distance of landslide deposits and the proximity to the connectivity target. The spatial definition of the connectivity target determines the distance landslide-derived material must be transported to enter the channel network. Therefore, the landslide connectivity ratio (LCR), i.e., the proportion of connected landslide scars, is lowest for the 5 m buffered streams (0.27), and highest for the *TWI-p.75* zone (0.69; Table 5.3). Since the size of connected landslides are on average larger than unconnected scars (Table 5.2), the SDR does not equal the LCR (Table 5.3). Further, we assume the proportion of mobilised sediment retained on the hillslope increases for each of the successive connectivity targets.

Estimated SDRs ranges from 0.21 for the *Streams* connectivity target, increasing to 0.29 for the *TWI-p.90* target before dropping back to 0.21 for the TWI-p.75 target. Assuming highly saturated soils enabled surface runoff to continue during and post storm event, sediment delivery was also 21% for the *TWI-p.75* scenario. The highest sediment delivery ratio of 0.29 was found for the *TWI-p.90* scenario.

Assuming an average scar depth of 1 m and soil with bulk density of 1.4 (Crozier, 1996), the equivalent sediment yield for the 1977 rainfall event was 3548 t/km^2 for the *Streams* connectivity target and 7564 t/km^2 using the *TWI-p.75* connectivity scenario (Table 5.3). The resulting sediment yield is much greater despite the delivery ratio not changing (0.21 for both Streams and *TWI-p.75*), likely reflecting the larger proportion of landslides connecting to the connectivity target. However, at 9033 t/km^2, the highest sediment yield is found for the *TWI-p.85* scenario. The results suggest sediment yield is a function of the landslide connectivity ratio and the capacity of sediment to be entrained when mobilised material is not delivered directly to the channel network.

Table 5.3. Landslide connectivity ratios, landslide delivery ratios, and event sediment yields for the three connectivity classes and six targets.

Connectivity class		Streams	TWI-p.75	TWI-p.80	TWI-p.85	TWI-p.90	TWI-p.95
Landslide connectivity ratio	Low	0.01	0.03	0.03	0.03	0.03	0.02
	Medium	0.04	0.10	0.10	0.09	0.08	0.06
	High	0.22	0.55	0.52	0.49	0.43	0.32
	Total	0.27	0.69	0.65	0.61	0.54	0.40
Sediment delivery ratio	Low	0.01	0.01	0.01	0.02	0.02	0.01
	Medium	0.04	0.03	0.03	0.05	0.06	0.04
	High	0.16	0.18	0.20	0.21	0.21	0.21
	Total	0.21	0.21	0.25	0.28	0.29	0.26
Event sediment yield(t/km^2)	Low	383	1299	1711	2237	2298	1068
	Medium	2771	3605	4412	6522	6799	3742
	High	6564	13527	13620	13885	12568	8523
	Total	3548	7564	8366	9033	8545	6027

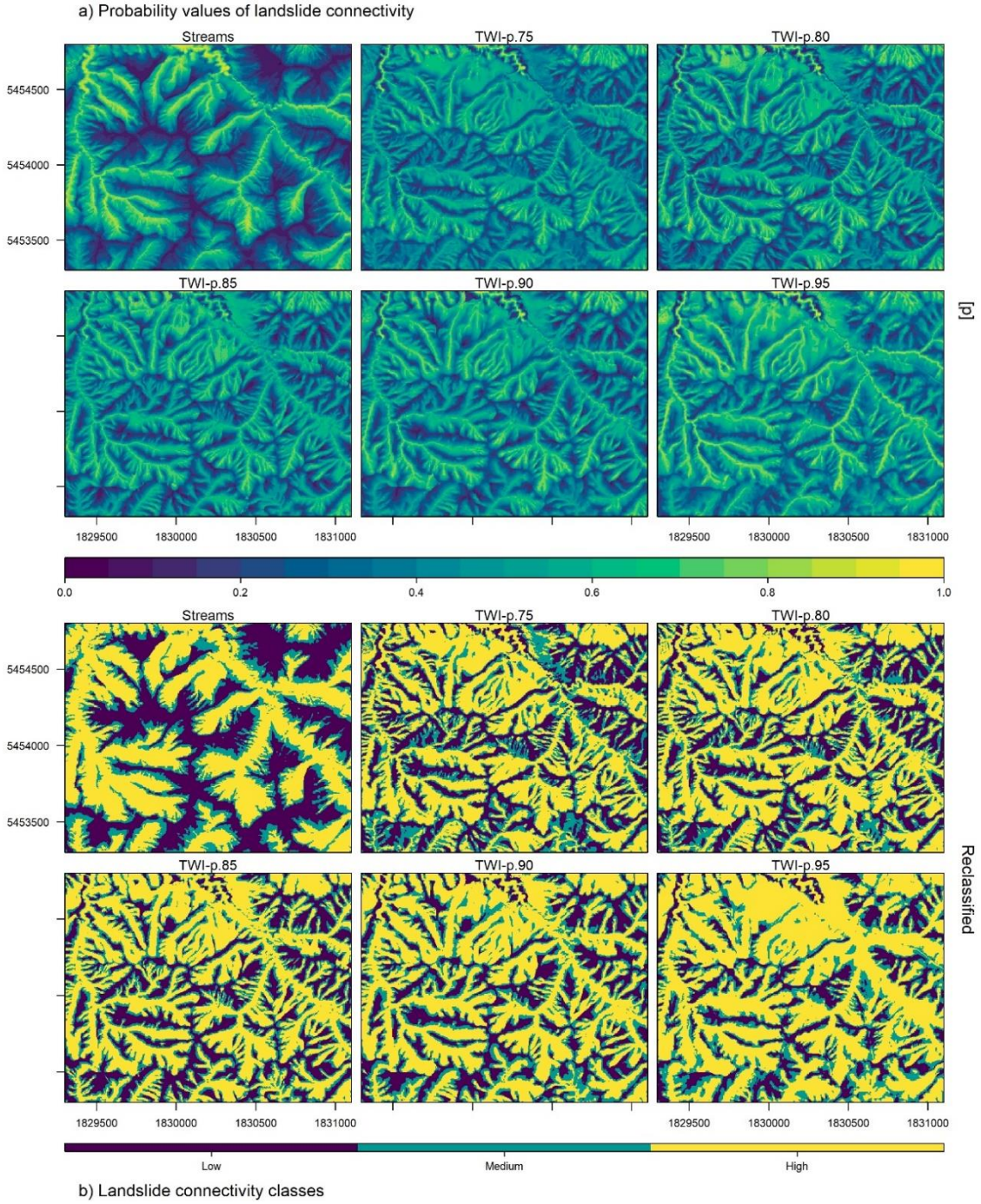

Figure 5.9. a) For a sample area (1800 m by 1500 m), probability values of connectivity and b) reclassified connectivity into three classes expressing the likelihood of sediment delivery according to the probability distribution of connected scars (see Figure 5.A*4). Projection: New Zealand Transverse Mercator 2000 (NZTM2000).*

5.3.4 Land Management Scenario Modelling

Scenario modelling across 50 farms (with a median farm size of 608 ha) shows that, under the treeless baseline scenario, only 6.5% (2400 ha) of the total area is both highly susceptible to shallow landsliding and has high potential for sediment delivery to the stream network

(Figure 5.10a). However, due to the actual tree cover (WV), this class now represents just 4.7% of the total area (Figure 5.10b). The change in class distribution from a pasture-only scenario (Figure 5.11a) to that of 2013 (Fig. 11b) has led to an estimated reduction in sediment delivery of 23.8% across the 50 farms (Table 5.4). Targeted mitigation of the 6.5% of highly susceptible and connected land using a 15 x 15 m grid of poplars (Figure 5.11c, 511e) has potential to reduce sediment delivery by 33.6% compared with the baseline scenario. The maximum reduction in sediment delivery using the same 15 m-spaced trees covering all farmland is 56.1%. Under these scenarios, the sediment yield for the storm event of 1977 would have been reduced from 3548 t/km^2 (equivalent to the pasture-only scenario S_0) to 2703 t/km^2 due to actual vegetation (WV), 2356 t/km^2 for S_1 (targeted) and 1557 t/km^2 for S_2 (maximum; Table 5.3).

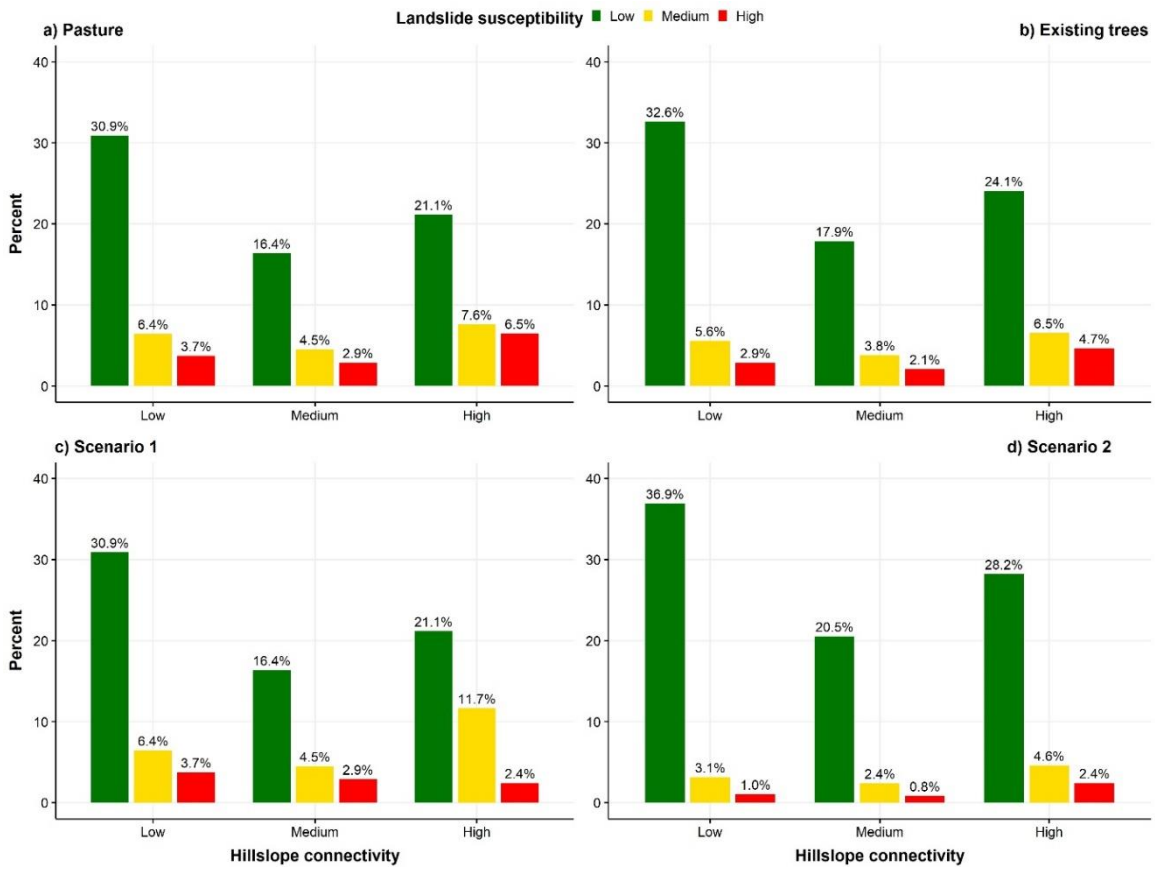

Figure 5.10. Landslide susceptibility and connectivity distribution of combined farms (total area 36,500 ha).

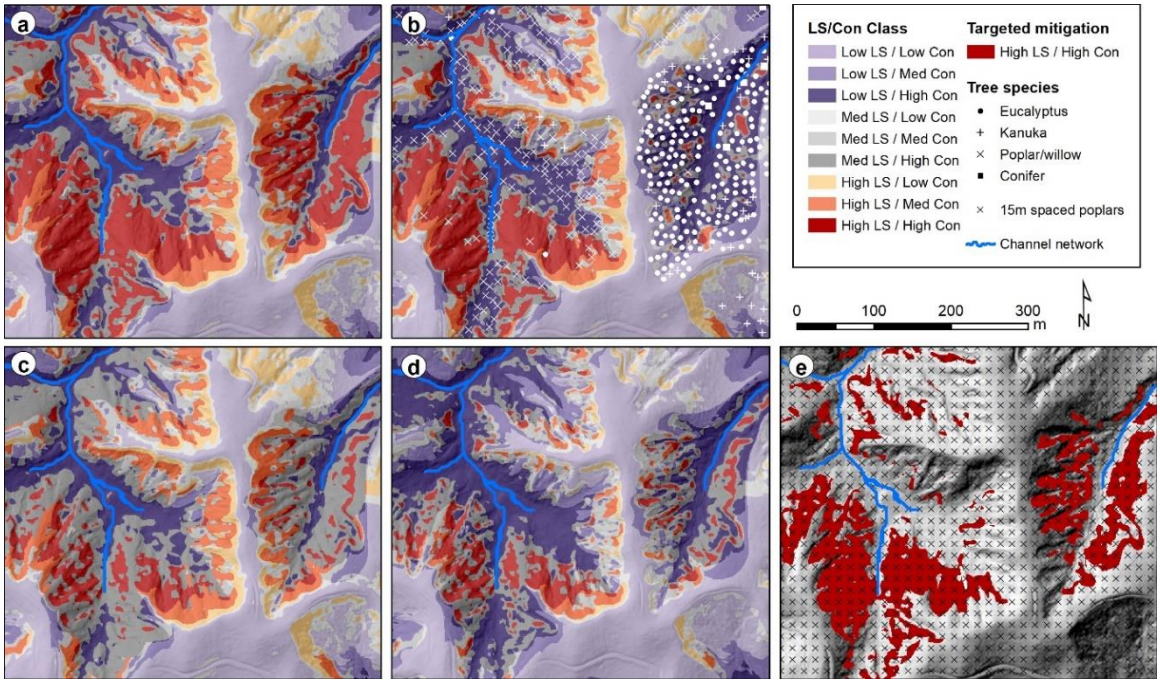

Figure 5.11. Landslide susceptibility and connectivity maps under a) pasture, b) actual tree cover (2013), c) targeted mitigation to terrain shown in e), and d) full tree cover using 15x15 m grid of poplar trees shown in e).

5.4 Discussion

5.4.1 Sediment Delivery by Landslides

Empirical investigation of runout behaviour, mobility and connectivity of shallow landslides typically includes a quantification of the source material deposited into streams (i.e., the sediment-delivery ratio - SDR). SDRs of shallow landslides can vary significantly and are dependent on soil mass, topography (e.g., slope geometry, surface roughness), soil type (e.g., clay content, saturated water content that produces liquid behaviour in soils) and available zone of accumulation prior to entering a water course (Bathurst et al., 1997; Bessette-Kirton et al., 2020; Cavalli et al., 2013; Cislaghi and Bischetti, 2019; Crozier, 1996). Estimates for sediment delivery ratios can be used to inform process-specific contributions to long-term (e.g., Dymond et al. 2016b) or event-scale sediment budgets (e.g., Page et al. 1994).

Reid and Page (2002) investigated connectivity of landslide deposits to streams in the Waipaoa catchment (East Coast of North Island, NZ) and found 65% of landslides connected

to streams, with an overall sediment delivery ratio of 0.45. In contrast, Jones and Preston (2012) estimated a sediment delivery ratio ranging from 0.12 to 0.28 in the same catchment. Furthermore, through field measurements, Preston (2008) quantified SDRs ranging between 0.23 and 0.28. These estimates by Jones and Preston (2012) and Preston (2008) are similar to our findings despite the different geomorphological setting (SDR 0.21; Table 5.3). Empirical investigation during landslide-triggering events and process-based modelling could help alleviate the current paucity of knowledge related to transport capacity of sediment following landslide initiation. In this regard, the timing of landsliding with respect to storm duration is an important consideration in terms of transport capacity during the event (Preston, 2008). The scenarios using TWI-based connectivity targets aim to address this knowledge gap by quantifying SDRs based on assumptions of increased delivery and reworking of the deposited mass during the rainfall event. However, these TWI-based connectivity targets can also be used to characterize potential increases in SDR through surface runoff erosion post-event (Xiong et al., 2022). Under these assumptions, our results show the SDR could potentially increase to 0.43 (Table 5.3). However, field measurements or use of high-resolution repeat LiDAR are required to corroborate these findings (Scheip and Wegmann, 2022).

The SDRs equate to an event sediment yield of between 3548 t km^{-2} and 9033 t km^{-2} (Table 5.3). To put this into context, the study area drains into the Taueru River, which – based on sediment gauging data – has an average annual sediment yield of 358 t km^{-2} (Hicks et al., 2019). However, this estimate of sediment yield for the Taueru is based on a sediment monitoring period from May 1968 – May 1981 (at Te Weraiti). It therefore includes the effect of the 1977 storm event and subsequent contribution of sediment from landslides, which can impact on sediment loads for several years (Basher et al., 2011). Even so, by comparing the event sediment yields (Table 5.3) with average annual estimates, it is evident that shallow landslides are the dominant source of sediment in the Taueru Catchment. Multi-temporal mapping in the same study area confirms that landsliding is a regular occurrence in these landscapes: Over the course

of 128 years (1882-2010), the cumulative scar area comprised 22% of the planform area of the study site (60 ha), which equates to 2% of the land surface per decade (De Rose, 2013).

The relative importance of shallow landslides to long-term sediment loads can differ significantly – even within the same catchment (Hicks et al., 2000). Shallow landsliding was found to be the dominant erosion process in the Te Arai sub-catchment (Hicks et al., 2000), which comprises 23% of the Waipaoa Catchment. However, for the Waipaoa Catchment as a whole, landslides contribute only about 15±5% of the long-term suspended sediment load in the Waipaoa River (Reid and Page, 2002) – increasing to ~48% during extreme events (Page et al., 1999). Other erosion processes in other parts of the catchment are more significant sediment sources (Hicks et al., 2000; Reid and Page, 2002), particularly the extensive gully systems (Michael Marden et al., 2018), but also streambank erosion (De Rose and Basher, 2011). Landslides were also determined to be the most important contributor to the sediment load of the Manawatū catchment (Dymond et al., 2016). However, such estimates are very sensitive to the universal SDR used (0.50), which is known to vary depending on morphological setting (Dickinson and Wall, 1977). Indeed, Burns (1979) suggested that each potential sediment source has unique delivery potential, which can be quantified in terms of probability with respect to the stream and catchment divide. Our approach overcomes these limitations by having developed statistical connectivity models using a suite of morphometric variables to predict the likelihood of a landslide delivering sediment to a predefined sink and can therefore be considered an integration of functional and structural connectivity (Najafi et al., 2021a). Yet, how the predictions translate into SDRs requires further research but could be based on an empirical relationship between probability values of landslide connectivity and observed estimates of SDR. While the model is limited by the landslide inventory which characterises a single event for a 7-km^2 area, future development will also aim to increase the landslide scar-deposit inventory so that soil characteristics (e.g., texture) can be included in the model. In addition, it would be important to determine sensitivity of predicted reductions in landslide

susceptibility and connectivity to the choice of statistical model (e.g., a generalised additive model or a random forest model).

The scenarios presented here are based on past observations of both landslide occurrence from the years 2005–2010 and sediment delivery from the 1977 event. Predicted rates of sediment delivery and reductions associated with actual tree cover and mitigation scenarios compared to a pasture baseline assume the mechanisms of failure and delivery will be similar in future. Validation of the landslide susceptibility model shows a shift in terms of probability distribution of the 1977 landslide inventory compared with the larger, more recent landslide inventory from 2005 to 2009 used to generate the susceptibility model (Figure 5.12). Only 70.5% of landslides triggered in 1977 are located in the high susceptible class. The high class used for scenario modelling is defined by a probability threshold of 0.72 that represents the 80th percentile of landslide scars ranked in descending order in the landslide inventory of 2005–2009. By extracting the landslide susceptibility values at the scar locations from 1977, the equivalent 80th percentile probability threshold of 1977 landslide scars is 0.60. The results of the validation suggest that historic landslides were occurring more frequently on what is considered "moderately susceptible terrain" by a present-day susceptibility model. This may reflect differences in the triggering mechanism, that is, long-duration (low-intensity) rainfall with high antecedent conditions in 1977 versus the high intensity rainfall events of 2005–2009 (Crozier et al., 1980; Spiekermann et al., 2021). However, it may also be an indication of terrain resistance (Crozier and Preston, 1999; Jones and Preston, 2012). The location of more recent failures likely reflects the erosional history of the landscape where undisturbed regolith close to spurs and crests has little lateral support due to previous failures lower on the slope (Preston, 2008). Topographic controls on surface and sub-surface flow and water content not only impact landslide occurrence, but also have implications for the behaviour of debris runout. As the landslide mass proceeds downslope, its mobility will increase due to greater surface water flows resulting from convergence in flow paths and larger drainage area. This has the effect of increasing the liquid fraction of the landslide deposit, which reduces internal friction, resulting

in greater run-out down-slope (Scheip and Wegmann, 2022). If, because of terrain event resistance (Jones and Preston, 2012), landslide failures are occurring increasingly on steeper upper slopes, the likelihood of fluidised flow may be reduced due to lower soil water content these areas of initiation. In addition, results show the importance of landslide density in determining sediment delivery, and in this regard are similar to findings elsewhere (e.g., Bessette-Kirton et al. 2020). Landslide deposits formed from multiple source areas that coalesce were more likely to deliver to the stream network than single source landslide deposits. Further research is needed to examine the relationship between i) landslide-triggering rainfall magnitude, ii) topographic controls on landslide initiation, iii) evolution of terrain resistance, and iv) type of debris runout, i.e., fluidised with internal friction removed, intact sliding of a landslide mass or incipient failure.

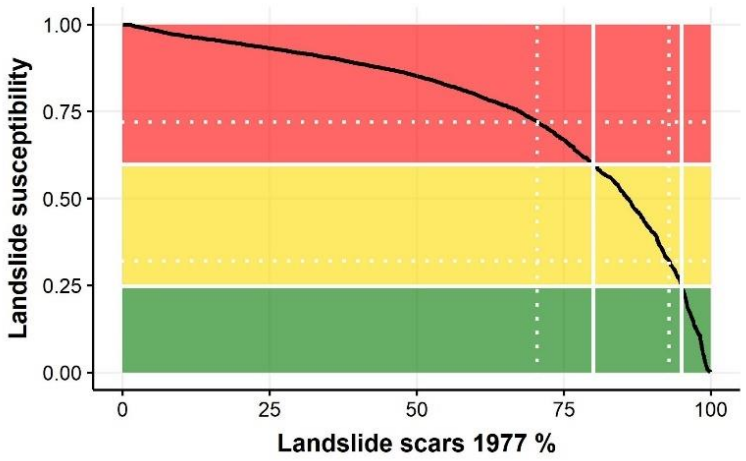

Figure 5.12. Validation of the landslide susceptibility model based on historic landslides. White lines locate the probability thresholds at the 80th and 95th percentiles in the count of landslides ranked in descending order according to landslide susceptibility values. Dotted lines show the cut-offs used to classify landslide susceptibility into three classes of Low, Medium, and High susceptibility according to the probability distribution in the landslide inventory from 2005-2009 (Spiekermann et al., 2022).

5.4.2 Smarter Targeting of Erosion and Sediment Mitigation

Scenario modelling results provide clear evidence that the cost-effectiveness of targeted mitigation S_1 is greatly increased compared to a non-targeted approach. A targeted approach

involves prioritizing mitigation on slopes with high landslide susceptibility and high potential for sediment delivery. On average, just 3 trees/ha of farm are required to mitigate the 2,400 ha of highly susceptible and connected terrain across the 50 farms. The median area of this zone requiring mitigation is 36 ha across the 50 farms, which would require an investment of approximately $53,000 to achieve the median reduction of 33.6%. Thus, the average investment required on a per hectare basis amounts to $2.82 per 1% reduction in sediment delivery from shallow landslides. This compares to S_2, which represents a random approach to targeting, i.e., mitigation is implemented proportional to the area occupied by the landslide susceptibility/connectivity classes. The average investment to achieve a 1% reduction in sediment delivery is thus substantially greater ($26.2/ha; Table 5.4).

Table 5.4. Overall reduction in sediment delivery to streams across 50 farms (35,900 ha) relative to baseline (S0).

	Existing vegetation	Scenario 1	Scenario 2
Reduction (%)	23.8	33.6	56.1
Tree count	738,818	105,307	1,629,381
Area treated (ha)	12,480	2369	36,661
Farm-average trees/ha	20.2	2.9	44.4
Average cost for 1% reduction ($/ha)	na	2.82	26.2

For example, if a 10% reduction is desired (compared to baseline) for a 500-ha farm, the investment would amount to $14,100 – assuming all trees survive. To achieve a 10% reduction on the same farm using a non-targeted approach, an investment of approximately $131,000 would be required. There is thus an order of magnitude difference in terms of cost-effectiveness between a targeted versus non-targeted approach. However, it is important to consider the variation in terms of reduction in sediment delivery achieved and the cost of doing so across the 50 farms (Figure 5.13). The mean cost for a 1% reduction is $2.82/ha for Scenario 1 (SD: $1.37; range: $0.21-$7.92); The mean for Scenario 2 is $26.20/ha (SD: 3.69; range: $17.54 – $38.94).

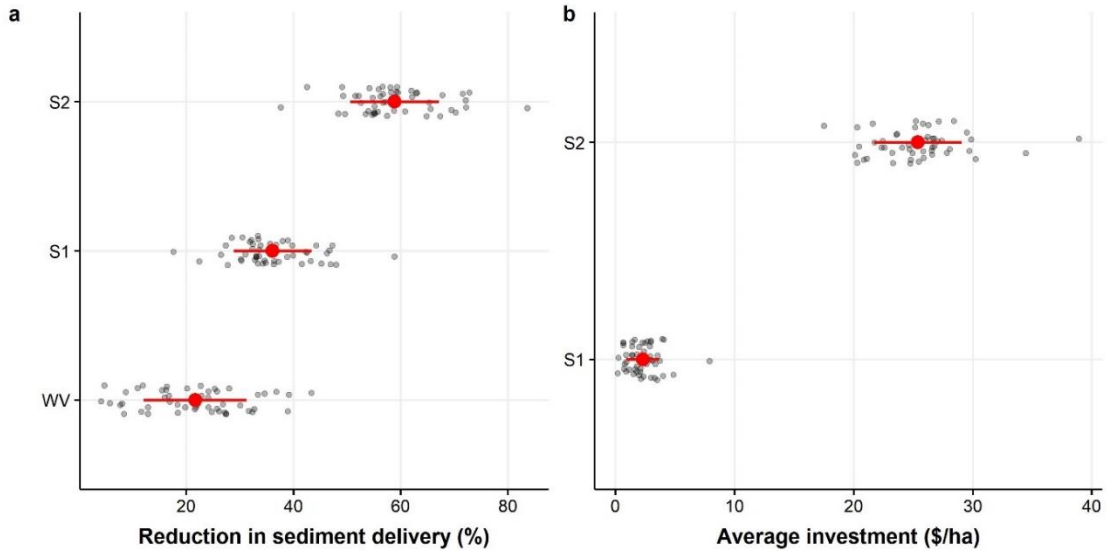

Figure 5.13. Insert a). Modelled reduction in sediment delivery to the stream network (%) for actual woody vegetation (WV; 2013), targeted mitigation (S1) and maximum possible with full tree cover (S2). Red strip charts correspond to the mean of sediment reductions (point) from 50 farms and 1 SD (line); Insert b). The farm-average investment required on a per hectare basis to achieve a 1% reduction in sediment delivery.

Due to the actual tree cover in the Wairarapa hill country, sediment delivery from shallow landsliding is 23.8% less, compared with a pasture-only scenario. In fact, the importance of already existing vegetation is similar to what could be achieved using a targeted approach (33.6% reduction). However, the estimated number of trees in the landscape is substantially different. Approximately 34% of land across the 50 properties have added protection due to the presence of trees. However, many of these trees are not providing a direct benefit in terms of slope stability (e.g., when located on floodplains), but are likely adding value to the farm enterprise elsewhere (e.g., through shelter provision, additional income from honey, carbon, or forestry). In terms of future erosion and sediment control works, the cost-effectiveness is substantially increased by targeting highly susceptible and connected slopes.

5.5 Conclusion and Outlook

This study developed and tested statistical approaches to modelling sediment mobility from shallow landslides by coupling slope stability and sediment connectivity models. The method demonstrates a useful integration of functional and structural connectivity. We have

demonstrated the development and application of the first morphometric connectivity model to enable targeted mitigation of landslide-derived sediment. The model has very limited data requirements: 1) an inventory of landslide scars and deposits and 2) a high-resolution (LiDAR) DEM. An important outcome of the lasso regression is the potential consequence of over-reliance on individual landslide scar size as a predictor of connectivity. Without considering contributions of landslide-derived material from multiple sources to the transport of delivery downslope, the run-out distance is likely to be underestimated for shallow landslides. This result speaks in favour of a morphometric model given the difficulty in predicting the location, size, and density of future shallow landslides. However, removal of scar size variables comes at a cost in terms of model performance. For the *Streams* connectivity model, the median AUROC was reduced from 0.88 to 0.75 across 100 repetitions.

To simulate the variation in sediment delivery based on a range in storm magnitude, we defined six different sediment connectivity targets. Sediment delivery ratios from the landslide triggering event of 1977 ranged between 0.21 and 0.29, depending on the definition of sink. However, the connectivity scenarios show that sediment yields can change significantly depending on the degree to which sediment recruitment from lower slopes is possible during a storm event. When accounting only for direct deposition into streams, the event sediment yield was estimated at 3548 t/km^2 (Table 5.3). However, when assuming continued sediment recruitment at reduced rate by overland flow across saturated soils as well as post-event reworking of deposited material, the maximum sediment yield was estimated at 9033 t/km^2. This estimate of event sediment yield is approximately 2.5 times greater than estimates only considering landslide deposits connecting to streams directly and challenges previous assumptions related to sediment delivery ratios and the importance of shallow landsliding for sediment budgets.

We selected 50 farms to quantify the reduction in sediment delivery based on contrasting mitigation options: 1) targeting critical source areas of sediment and 2) a non-targeted approach to tree planting. The cost-effectiveness of these different mitigation options suggests there is an

order of magnitude difference between a targeted versus non-targeted approach in terms of the ratio of investment to reduction in sediment delivery achieved. An important outcome of the landslide susceptibility and connectivity modelling is that in total only 6.5% (2,370 ha) of farmland is the potential source of approximately two-thirds of landslide-derived sediment across the 50 farms (Figure 5.11). Due to existing vegetation, this area has already been reduced to 4.7% (1,720 ha). Further reductions in future sediment delivery can be achieved by increasing slope stability on these highly susceptible and connected slopes through additional biological mitigation. For a farm of 500 ha, the average cost to achieve a 10 percent reduction in landslide-derived sediment is $14,100 for targeted mitigation and $131,000 for non-targeted (Table 5.4). To achieve the maximum reduction possible for a targeted approach to mitigation using a 15-m grid of poplar poles on the same farm (500 ha), the cost is estimated as $47,000 for targeted mitigation and $440,000 for non-targeted to achieve the same result of 33.6% reduction in sediment delivery. However, further research is required to test the feasibility of treatment across different landslide susceptibility classes. Shallow landslides are more likely to occur on steep slopes where establishment of biological controls (e.g., poplar poles) is more challenging due to reduced soil moisture, exposure to wind gusts, and shallower soils.

In terms of future research needs, increasing landslide scar-deposit inventories across a range of environments could allow statistical connectivity models to include soil characteristics (e.g., soil type, depth, etc.). Furthermore, there is currently a lack of understanding regarding the relationship between triggering mechanism, topographic controls, and terrain resistance (Jones and Preston, 2012) and debris run-out behaviour of shallow landslides. Our results show that both scar size and the density of landslide occurrence are very important as determinants of sediment delivery since coalescing landslide deposits are much more likely to deliver sediment, which is corroborated by related research (e.g., Scheip and Wegmann 2022). Therefore, future landslide susceptibility models should provide predictions on the intensity of landslides (Lombardo et al., 2020, 2018), their size (Lombardo et al., 2021) and probability of landslide deposits coalescing. While the morphometric connectivity model was developed to

support land management decisions and increase effectiveness of erosion and sediment mitigation, there is equally great potential to include the spatial predictions of connectivity in sediment budget modelling at catchment scale.

5.6 Supplementary Material

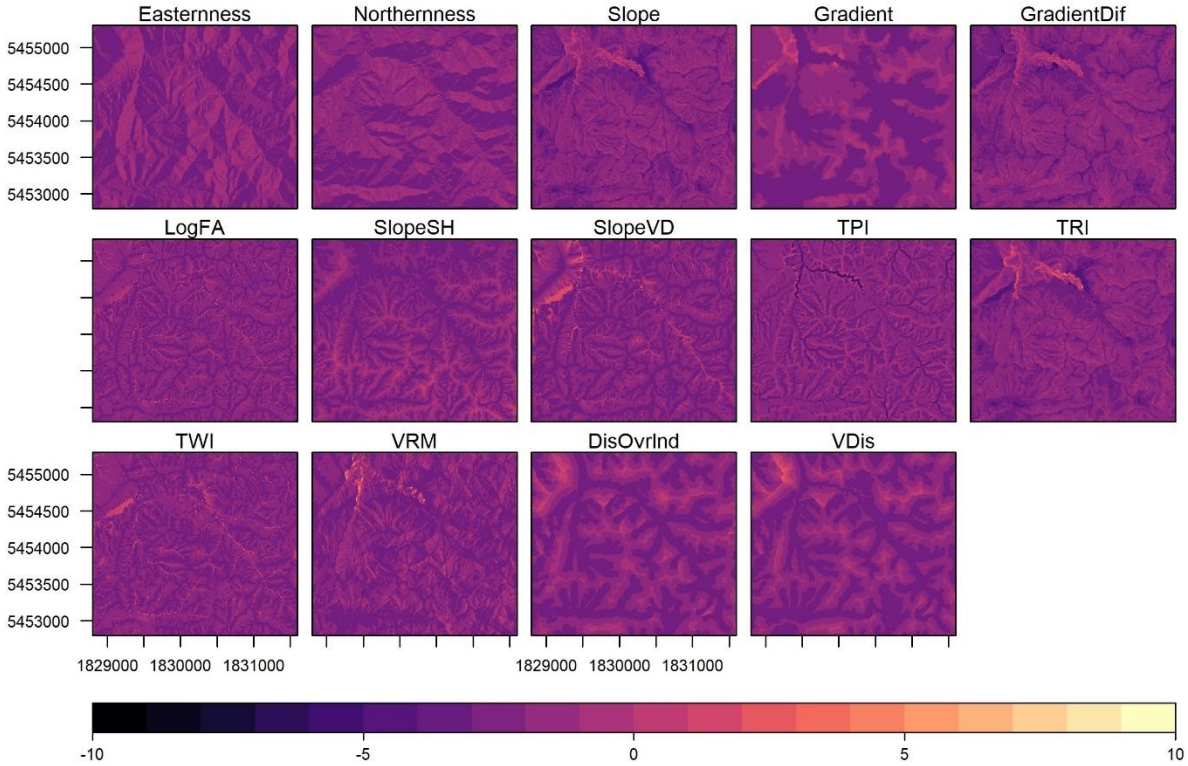

Figure 5.A1. Standardized morphometric explanatory variables (see section 2.2.3 for variable description).

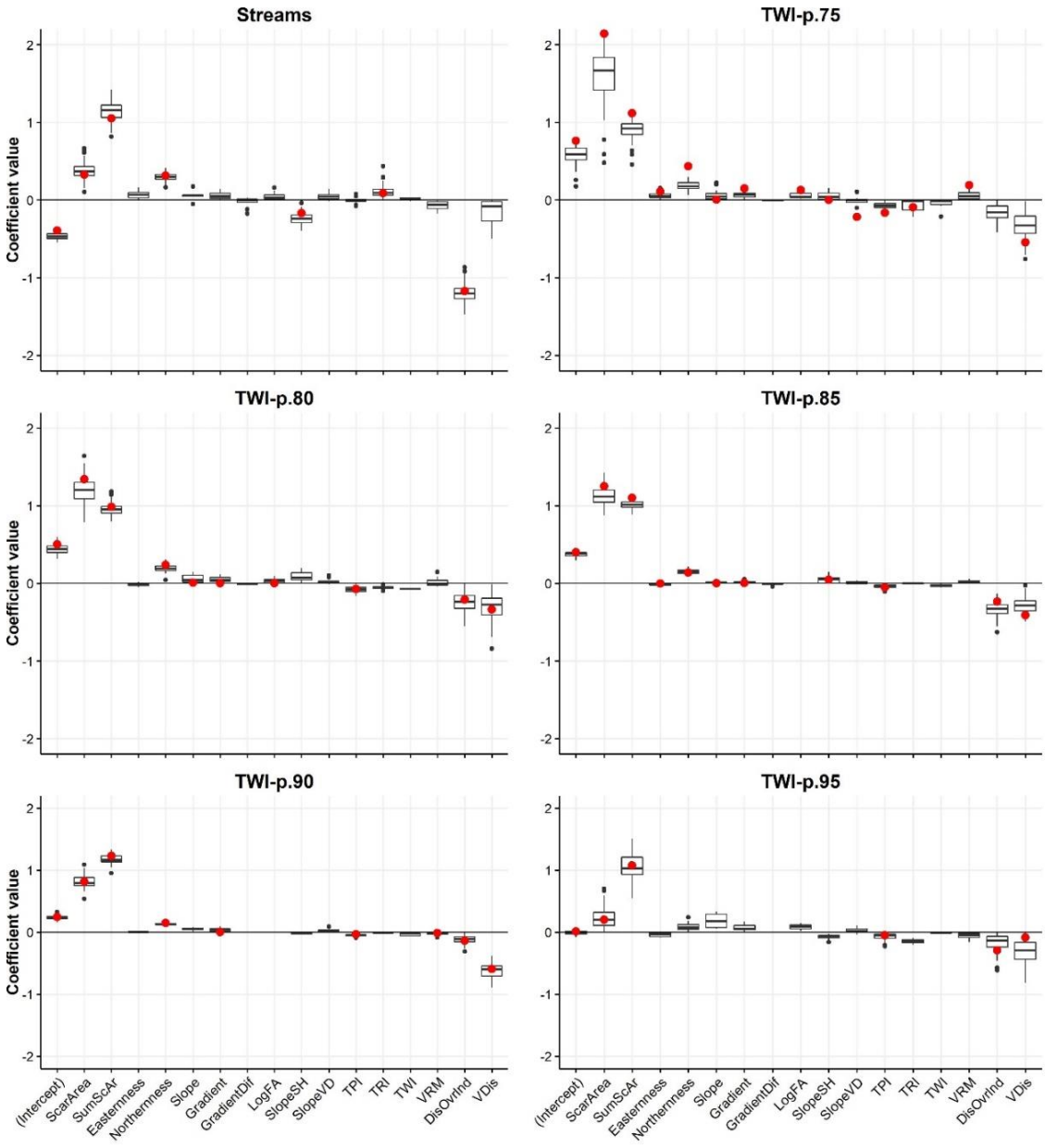

Figure 5.A2. Lasso regression coefficient estimates from 100 final models to predict landslide connectivity for each of the six connectivty targets using both scar size and morphometric variables.

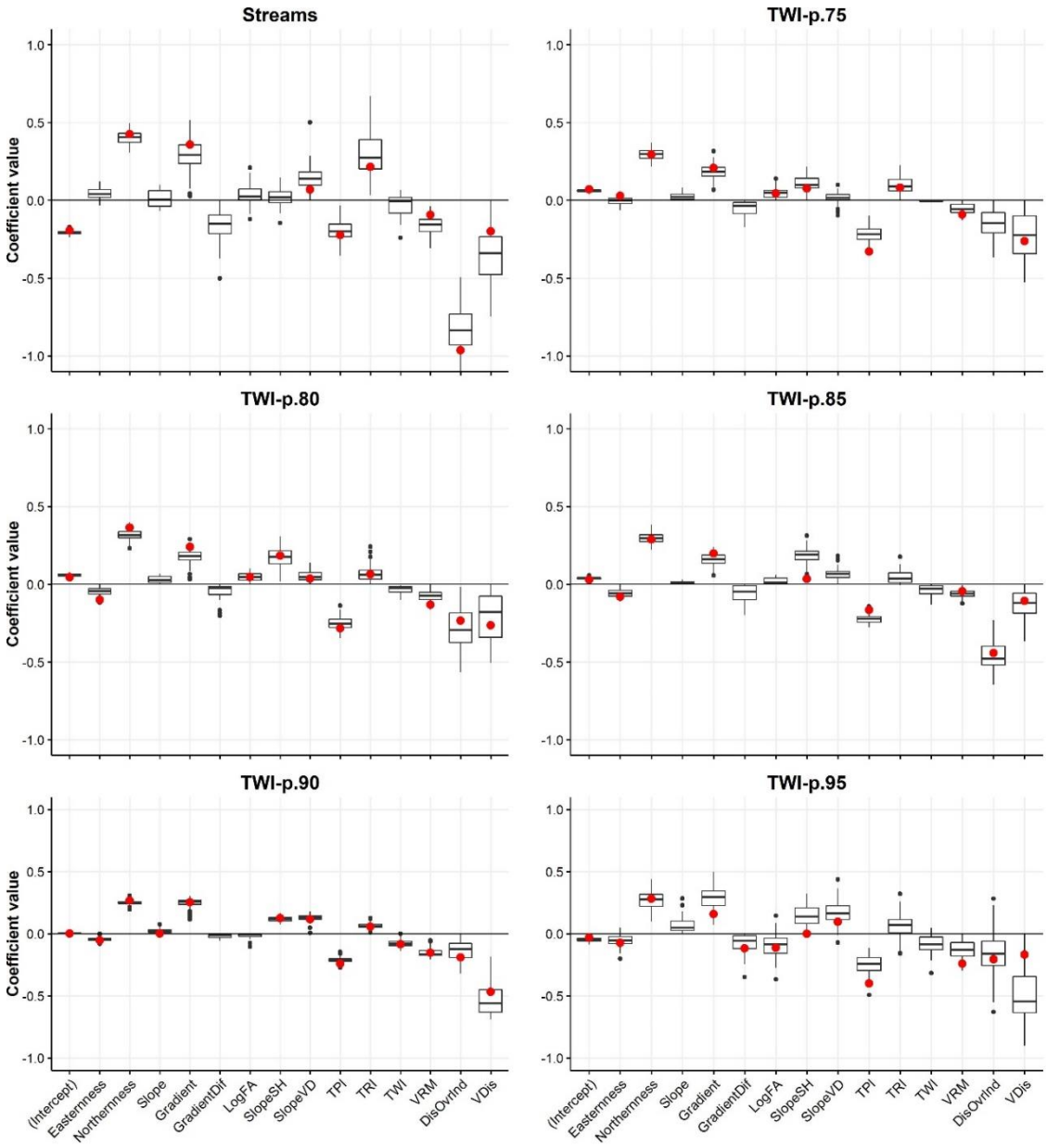

Figure 5.A3. Lasso regression coefficient estimates from 100 final models to predict landslide connectivity for each of the six connectivty targets using both scar size and morphometric variables.

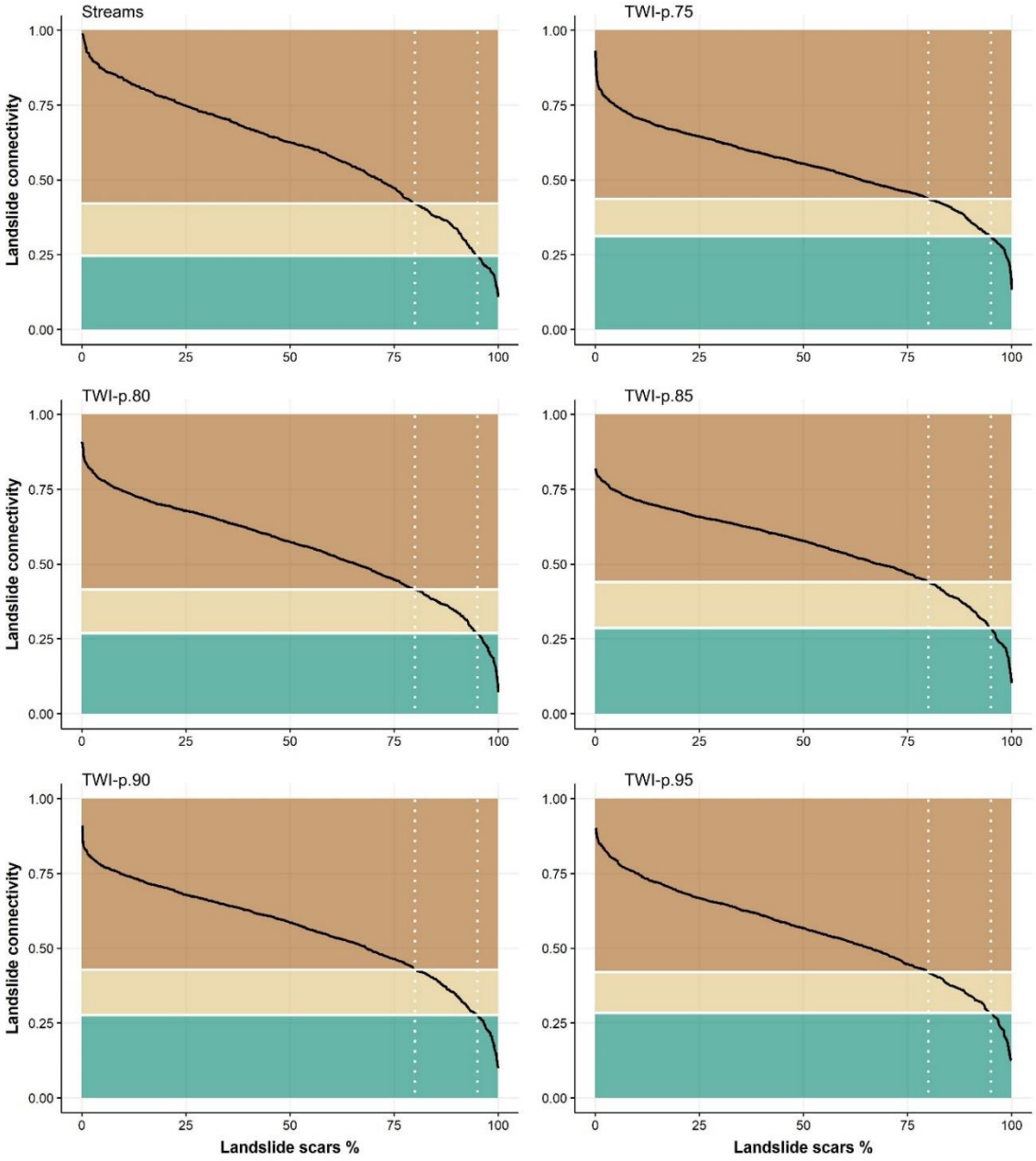

Figure 5.A4. For the six morphometric connectivity targets, cumulative percentage of connected landslide scars in three connectivity classes defined according to 5, 20, and 80 percentiles (dotted vertical lines) of probability values ranked in descending order. The class probability thresholds correspond to the intersection of vertical lines with the curve.

5.A5 Rule-set description from eCognition for classifying landslide scars and tails

Inputs:

Panchromatic imagery from 1977 (img_77, scale: 1:25000).

1-m LiDAR DEM, Greater Wellington Regional Council

Classes: scars, deposit

Process: Main:

Landslide-mapping

Segmentation

multiresolution segmentation: 25 [shape:0.3 compct.:0.7] creating 'top level'

multiresolution segmentation: at top level: 40 [shape:0.3 compct.:0.7] creating 'above'

Classification

assign class: with Mean img_77 > 185 and Mean slope > 30 and Standard deviation img_77 < 12 at top level: scars

assign class: with Mean img_77 > 182 and Mean diff. to darker neighbors img_77 > 25 and Mean slope > 30 and Standard deviation img_77 < 15 at top level: scars

assign class: 3x: unclassified with Mean img_77 > 160 and Mean slope > 20 and (Mean diff. to dem, scars < 0 or Mean diff. to dem, tails < 0) at top level: deposit

assign class: unclassified with Mean img_77 > 145 and Mean diff. to darker neighbors img_77 > 35 and Mean slope > 30 and Standard deviation img_77 < 15 at top level: scars

assign class: 3x: unclassified with Mean img_77 > 130 and Mean slope > 20 and (Mean diff. to dem, deposit < 0 or Mean diff. to dem, scars < 0) at top level: deposit

Copy and refine

copy image object level: at top level: copy creating 'copy above' above

!!Manual refinement!!

merge region: scars, deposit at copy above: merge region

export results

export vector layer: scars, deposit at top level: export object shapes to landslides_1977

PART III

SYNTHESIS AND OUTLOOK

6

6 SYNTHESIS

6.1 Introduction

The research presented in this thesis aimed to address the paucity of data and understanding related to the effectiveness of silvopastoral systems on mitigating *shallow landsliding* in pastoral hill-country at scales ranging from slope through farm and landscape scales. In addition, geospatial methods were developed to quantify the effect of a discontinuous tree cover in mitigating landslide-derived *sediment delivery* to streams. Spatially explicit models were developed to assess the impact of differing tree species, planting densities, and individual tree location, on rainfall-triggered landslides and sediment delivery while accounting for varying environmental conditions, such as slope gradient and lithology. In pursuit of these objectives, this research has contributed to the on-going development of statistically based spatial modelling of landslide susceptibility and sediment connectivity. The conceptual framing that underpins the research comprises a triangular relationship between i) airborne remote sensing of the environment, ii) statistically based geospatial modelling that iii) aims to evaluate and inform land management decisions related to biological erosion and sediment mitigation (Figure 1.1). The research is thus situated in an interdisciplinary setting that spans geomorphology, remote sensing, and agroforestry systems science. In fact, this thesis exemplifies the *Science of Geography* in practice, since the focus is on studying human-landscape interactions through spatial analyses and modelling.

The literature review in Chapter 2 summarized the scientific literature of the key components that are relevant to this research, providing a robust context and justification of the pathway chosen for further developing the ideas, concepts and methods described in Chapters 3-5. Indeed, Chapters 3-5 pursued the stated objectives (see Chapter 1.2) of the thesis following

a logically coherent rationale and conceptual design, beginning with the development of methods to generate inventories of landscape features that became the object of investigation – namely individual trees and shallow landslide scars. These inventories then formed the basis for the three subsequent spatial models.

The first of these models is documented in Chapter 3, with the development of the tree influence models on slope stability (TIMSS). Using a subset of the tree and landslide scar inventories (i.e., all widely spaced trees located on hillslopes in proximity to landslide scars), an empirically derived individual tree effect on slope stability was established. This method, which is based on a spatial relationship (i.e., Euclidean distance), was adopted for four different tree types including coniferous species, poplar/willow, kānuka, and eucalyptus.

The resulting TIMSS were subsequently used to integrate individual tree effects in a statistical landslide susceptibility model (Chapter 4). The high positive skewness associated with the TIMSS data raised important questions related to the reliability and robustness in estimation of coefficients using binary logistic regression. This is directly a result of the sampling method adopted in statistically based spatial modelling approaches for binary classifications, which is exacerbated in silvopastoral landscapes for two reasons: 1) landslides are more likely to occur in open pasture, that is, at a distance to trees; and 2) the dominant land cover in silvopastoral systems is pasture. Given these two known facts, and that a balanced sampling approach commonly adopted for binary logistic regression requires 50% of samples to represent the location of previous landslide scars and 50% to represent randomly generated landslide absence points, most samples are located outside the sphere of influence of trees. This resulted in most presence and absence points having TIMSS values equal to 0, which produced the high positive skewness in the distribution. Chapter 4 is therefore primarily devoted to testing whether the high positive skewness associated with the TIMSS variables produces (un)reliable estimates of effect size; and at a more fundamental level, whether a statistical approach to modelling slope stability in silvopastoral landscapes is indeed feasible. Having established that high positive skewness does not result in inflation of effect size, the statistical landslide

susceptibility model was subsequently used to quantify the effectiveness of trees present on two selected farms.

Since Chapter 4 is focussed on quantifying reductions in landslide occurrence compared to a treeless pasture baseline, Chapter 5 aims to develop a methodology to quantify reductions in landslide-derived sediment delivery to streams. This requires an ability to link hillslope processes to channels, which was achieved through incorporation of sediment connectivity. Specifically, a morphometric landslide connectivity model was trained and tested using a sample of landslide scars and deposits mapped in historic aerial photography for an area in the Wairarapa of New Zealand. By coupling i) landslide susceptibility, which provides information pertaining to where landslide occurrence is expected, and ii) landslide connectivity, which produces spatial predictions for the probability of sediment delivery to adjacent stream, Chapter 5 quantified the effect of trees on reducing sediment delivery through comparisons to a treeless baseline scenario. The following section considers how this thesis has made contributions to advancing science-based knowledge. Chapter 7 concludes with a summary of how each of the stated research objectives defined in Chapter 1.2 have been addressed.

6.2 Contribution to Science

While the research documented in this thesis has addressed many knowledge gaps related to the effectiveness of silvopastoral systems on landslide occurrence and sediment yields, there are also equally important methodological contributions made pertaining to advances in statistically based spatial modelling. The statistical landslide susceptibility model developed in Chapter 4 is a global first in terms of integrating individual tree effects. Understanding limitations associated with previous attempts to capture vegetation effects on slope stability – both in statistical and physically-based models, will give prominence to the contribution of this thesis to advancing science.

6.2.1 Limitations of Tree Effects in Previous Statistical Landslide Susceptibility Models

Previous statistical landslide susceptibility models were limited by their spatial representation of trees as predictor variables. Most models include land use or land cover data available at coarse scales (Knevels et al., 2021, 2020; Reichenbach et al., 2014; Smith et al., 2021). An example of this is the use of the Land Cover Data Base (LCDB) of New Zealand, which has been used for regional-scaled modelling of landslide susceptibility (Smith et al., 2021). At this scale, different types of vegetation cover (e.g., grasslands, deciduous hardwoods and mānuka/kānuka) are mapped at a minimum areal unit of 1 ha. However, these regional-scaled data are inadequate for capturing individual tree effects in silvopastoral systems (Figure 6.1).

Other authors include higher resolution variables derived from remotely-sensed (satellite) imagery to represent physical vegetation characteristics (Wang et al., 2022). An example is the use of the Normalized Difference Vegetation Index (NDVI), which is based on spectral reflectance measurements acquired in the red (visible) and near-infrared regions of the electromagnetic spectrum (Arabameri and Pourghasemi, 2019). High values of NDVI (close to 1) represent areas of dense green vegetation, and negative values indicate either an absence of vegetation or moisture-stressed vegetation (Gessesse and Melesse, 2019). However, inclusion of NDVI-based variables can be problematic due to the lack of a clear relationship between the index and the physical properties of vegetation that affect slope stability (Reichenbach et al., 2018). For example, deciduous trees outside the growing season can have NDVI values less than green pasture. Thus, the rationale for including higher resolution vegetation variables such as NDVI in a landslide susceptibility model is not adequately justified.

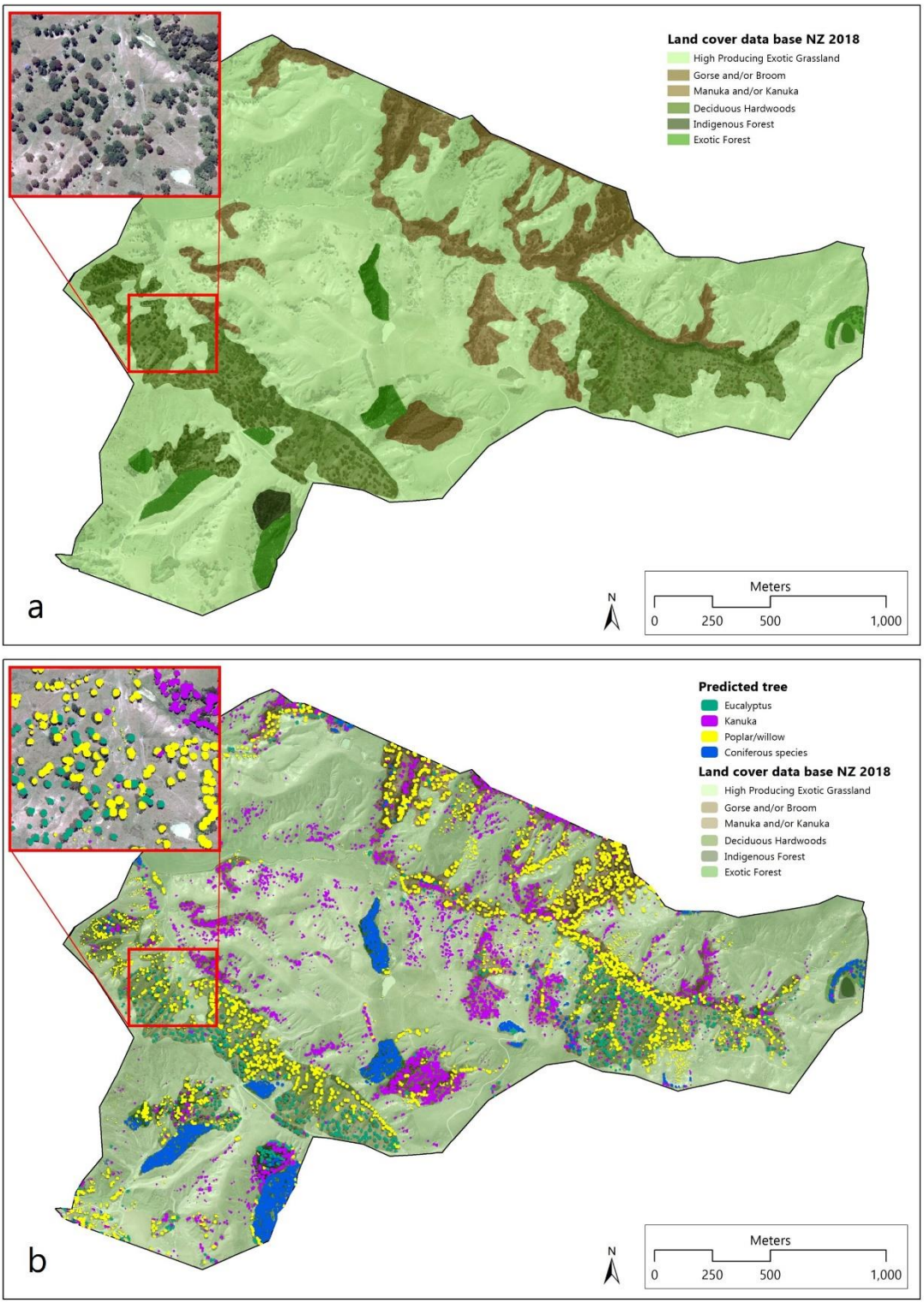

Figure 6.1. Implications of land cover data available at different scales: a) Regionally scaled land cover data are useful for regional landslide susceptibility modelling, but inadequate for capturing individual tree effects; b) LiDAR data enables individual trees to be identified and tree canopies can be classified using high resolution imagery (see Chapter 3).

Of particular relevance for silvopastoral systems is the failure of such metrics that reflect properties of tree canopies (NDVI) to account for the spatial variation in the distribution and strength of roots and the hydrological interactions between trees and soil at the scale of the individual tree. Characteristics of individual tree canopies can reflect differences in vegetation composition, which can be useful for tree species classifications (Fassnacht et al., 2016) or relating canopy dimensions to above-ground biomass (Lau et al., 2019). Yet, the relationship between tree canopy and slope stability is more complex – primarily due to the nature of root system architecture and differences in root strength across vegetation species, which is not reflected by greenness in the canopy. Thus, tree effects on slope stability are spatially more heterogenous than the more uniform tree canopy might suggest. While simple above ground measures of vegetation can improve on coarse-scaled land cover data, the significance of above-ground measures of vegetation with respect to slope stability needs to carefully be established (Reichenbach et al., 2018).

6.2.2 Current Limitations with Physical Approaches to Quantifying Tree Effects

Chapter 2 reviewed empirical evidence of the mechanisms by which trees stabilise slopes, including the mechanical processes via root systems. Furthermore, recent developments in root reinforcement models were discussed, including data requirements and assumptions. Since many abiotic (e.g., light, temperature, rainfall) and biotic (e.g., other trees, organisms in soil) factors influence the development of both tree crown and root system architecture (Iwasa et al., 1985; Lindh et al., 2018; Pierret et al., 2007), the hydrological and mechanical processes of a tree can vary considerably between and within tree species (Hales et al., 2009; Masi et al., 2021; Schmidt et al., 2001). This is particularly true when tree densities are such that competition for limited available resources (nutrients, water, light) is increased (Danjon et al., 2013). In their review of root systems of mixed-tree systems, Kumar and Jose (2018) found evidence that two

or more tree species located in close proximity can cause reduced lateral spread of roots and/or increase root penetration at greater soil depths. Trees with similar root growth habit are more likely to have interlocking root systems that increase competitive interactions, whereas mixing tree species with different growth habits can result in temporal or spatial complementarity in use of above and below ground resource (Kumar and Jose, 2018). This is due to phenotypic plasticity, which enables roots to respond to effects arising from i) variation in the abiotic environment (soil nutrients, water, light), ii) the presence of neighbouring trees, and/or iii) herbivory (Callaway et al., 2003).

There is currently a paucity of species-specific data on root system architecture from widely spaced trees such as those found in agroforestry systems (Kumar and Jose, 2018). Most root extraction work aimed at characterising root system architecture of trees has been undertaken in forest stands (Hales, 2018), which means there is less data available to inform the development of root reinforcement models in silvopastoral systems or to calibrate root growth models (Schlüter et al., 2018). Knowledge of root systems in silvopastoral settings is limited to individual species of certain age classes (Marden et al., 2018; Phillips et al., 2014; Stone and Kalisz, 1991). This lack of data has direct implications for estimating the magnitude of lateral root reinforcement in fully mature adult trees, since the quantitative estimates rely on knowledge of the spatial distribution of the roots (Cohen and Schwarz, 2017). Moreover, the data requirements for developing estimates for species-specific, spatially distributed root reinforcement (kPa) are not insignificant (Schwarz et al., 2010c). In fact, due to variability within root systems, it was found a minimum of four trees must be excavated to obtain sufficient root information to reduce the error associated with root reinforcement estimates to a level acceptable by geotechnical guidelines (Giadrossich et al., 2020). These requirements can change according to species and site specifics.

Therefore, the limiting factor to further develop root reinforcement models in silvopastoral systems is the lack of species-specific root data, which includes:

- Data pertaining to the strength and behaviour of different root diameter classes within the root-soil matrix (Schwarz et al., 2010a);
- Morphological data pertaining to the root system architecture, including the number of roots in different diameter classes with increasing distance from tree trunk;
- Root data of trees that grow in different environmental settings (e.g., substrate characteristics), spacings, and mixed-species vs. monoculture silvopastoral systems.

Given the current lack of observational data, were root reinforcement models to be used in a mixed-tree silvopastoral system, important assumptions in the model parameterisation would need to be made, particularly relating to total and maximum root lengths (Stone and Kalisz, 1991). While these data limitations mean root reinforcement modelling in silvopastoral landscapes remains a challenge, the advantages of physically-based modelling may justify future investment in data collection. These physical approaches quantify both the mechanical reinforcement provided by root systems and the hydrological effects of trees on regulating soil moisture. Advantages of root reinforcement modelling include the ability to quantify the added contribution to soil strength as a measure of force (kPa) and consider how the margin of stability will change given a scenario such as a rainfall event or change in land cover (Schwarz et al., 2016). A further key advantage is the use of allometric relationships between above and below-ground biomass. Thus, as advances in technology increase the ability to characterise above-ground properties of trees (Gunawardena et al., 2015), the main barrier to improved estimates of mechanical reinforcement of slopes by silvopastoral trees is the prohibitive cost associated with empirical data collection.

6.2.3 Overcoming Data Limitations

Given the current limitations discussed in the above two sections, this thesis developed Tree Influence Models on Slope Stability (TIMSS) and integrated these into a landslide susceptibility model (Figure 6.2). The TIMSS represent the average influence of an individual tree on slope

stability for the four most abundant tree types in the study area, fulfilling the following four criteria:

- Individual tree effects from different vegetation types (e.g., coniferous, poplar/willow) are captured.
- Hydrological and mechanical effects are accounted for.
- Values are spatially distributed as a function of distance from tree (trunk).
- Contributions of neighbouring trees to slope stability are considered additive.

The method used to generate the TIMSS is novel, building on that developed by Hawley and Dymond (1988). The approach adopted in Chapter 3 to generate a two-dimensional spatial representation of individual tree influence is a departure from previous methods that quantify and model tree effects using physical measurements of force (kPa). While measurements of force are a requirement for physical models, measurement units are largely irrelevant to statistical models.

However, a critique of the TIMSS method could include the lack of physical basis, as the TIMSS rely solely on patterns observed at landscape scale to infer what the physical parameters must be that render the relationships between the objects of interest, namely trees and landslide scars. This raises the question of plausibility, to which there are two helpful responses: The first is by way of a practical justification. Given the data scarcity with respect to root system architecture of adult trees, which have been established in an environment with negligible competition from neighbours, a validation of the TIMSS is only possible with reference to the limited root data available from widely spaced trees (see Chapter 3). Both extracted root systems of younger trees (e.g., McIvor et al., 2009) and equivalent spatially distributed root reinforcement models (e.g., Schwarz et al., 2016) were similar to the TIMSS in terms of the sigmoidal shape of the curves (Fig. 3.10) despite the unit of measurement not being the same.

Secondly, the method of inquiry used follows a logical form guided by material induction theory (Norton, 2021). Based on a set of warranting facts, material inductive inference allows conclusions to be drawn that amplify pre-existing knowledge of the system (Norton, 2021). The

warranting facts in this case can be summarised in the following statement: *"Trees modify slope stability due to mechanical and hydrological mechanisms".* Based on the assumption that these effects must manifest in such a way that can be observed at landscape scale, Chapter 3 developed the geospatial methods to determine whether landslide scars occur preferentially close to or remote from trees. The resulting TIMSS therefore infer the extent to which individual trees increase slope stability. The TIMSS raise some interesting questions, particularly related to the average maximum effective distance of an individual tree (e.g., 20 m for poplar/willow). Further destructive sampling of mature trees within silvopastoral systems would be required to test the veracity of the TIMSS models. Besides the mechanical processes, the TIMSS implicitly reflect hydrological processes of trees that regulate soil moisture. This could also help explain the average maximum effective distances of up to 20 m.

However, a reduction of a tree to observations of the behaviour of its components (e.g., foliage, root system) cannot reveal the full extent of its properties – let alone a tree interacting within its environment composed of biotic and abiotic components. These properties that most natural systems have in addition to the sum of properties of the components are referred to as *emergent properties* of irreducible systems (Jorgensen, 2016). This concept of emergent properties promoted by *Systems Ecology Science* poses a challenge to physically-based models that follow an inherently reductionist approach to studying tree effects on slope stability. The TIMSS, which are based on empirical data of tree effects (in fact, based on measurements of the process of interest), have the potential to stimulate a scientific discourse on the role and effectiveness of a discontinuous tree cover located on hillslopes in a silvopastoral landscape.

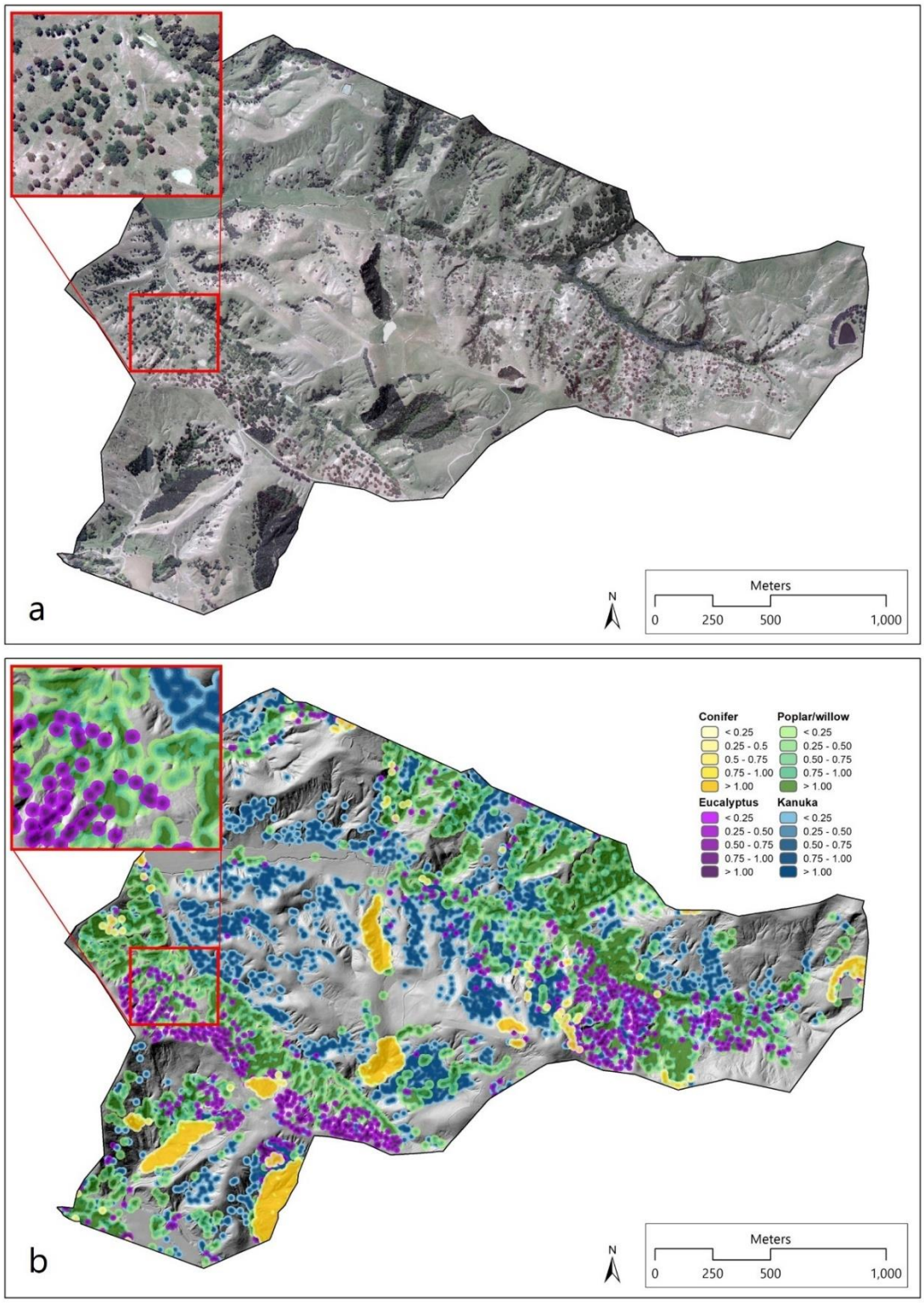

Figure 6.2. The discontinuous tree cover shown in the orthophoto from 2013 (Greater Wellington Regional Council) (a) can be captured in landslide susceptibility models through use of the tree influence models on slope stability (TIMSS) shown in map (b).

6.3 A Landslide Erosion and Sediment Management Framework

Frameworks for effective land management have been widely proposed (e.g., Christodoulou and Nakos, 1990; Foran and Wardle, 1995; McDowell et al., 2018; Owens, 2009; Stankey, 1985; Steiner and Osterman, 1988; Trodahl et al., 2017). Qualitative, systematic frameworks for evaluation of effectiveness following implementation of control measures have been designed in other disciplines (e.g., van der Fels-Klerx et al., 2014). However, a similar framework to support the planning, implementation, and evaluation of erosion and sediment mitigation is currently lacking and would be useful to help define and quantify effectiveness. Therefore, a simple framework is proposed in Figure 6.3. While the focus here is on biological mitigation of shallow landslides, the framework could equally be applied to other erosion processes.

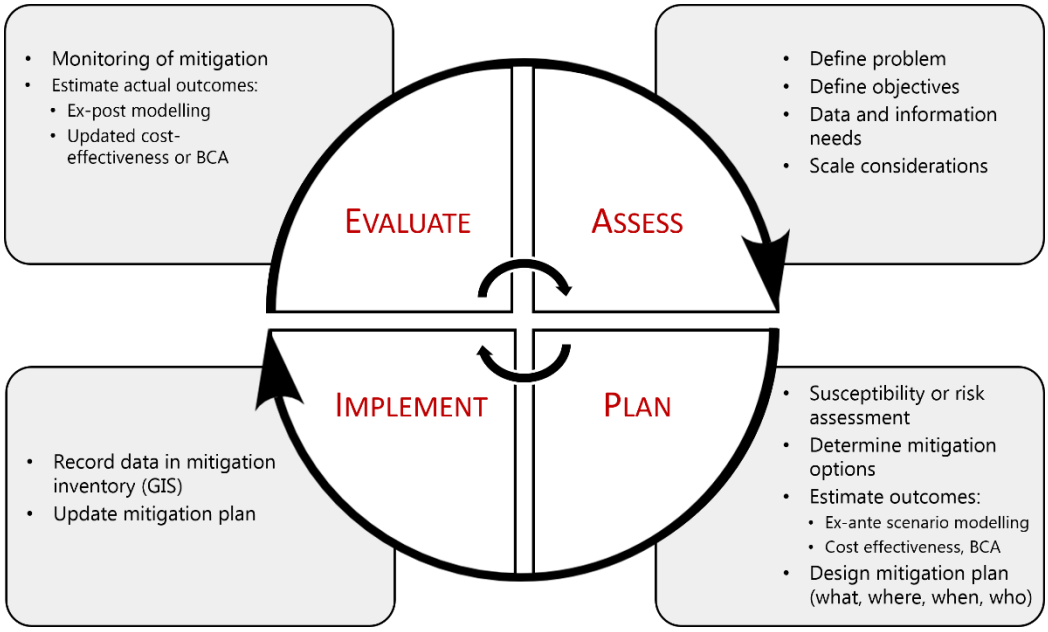

Figure 6.3 Management framework for erosion and sediment mitigation

There are four distinct phases that define the framework: *(1) Assess, (2) Plan, (3) Implement, and (4) Evaluate*. The assessment phase begins with the problem definition and setting objectives. The general objective is to design and implement cost-effective, targeted erosion control measures to conserve soil and meet water quality targets. Resources (data, information) are collated that can help make the connection between catchment erosion sources, sediment loads in rivers, and sediment-related water quality. Scale considerations are important at this point and can have implications in terms of availability and utility of data and information (Figure 6.4). In its essence, this first phase sets the scene to help determine which areas in the catchment, farm, or slope are prone to erosion and/or potential sources of sediment to subsequently inform the mitigation plan.

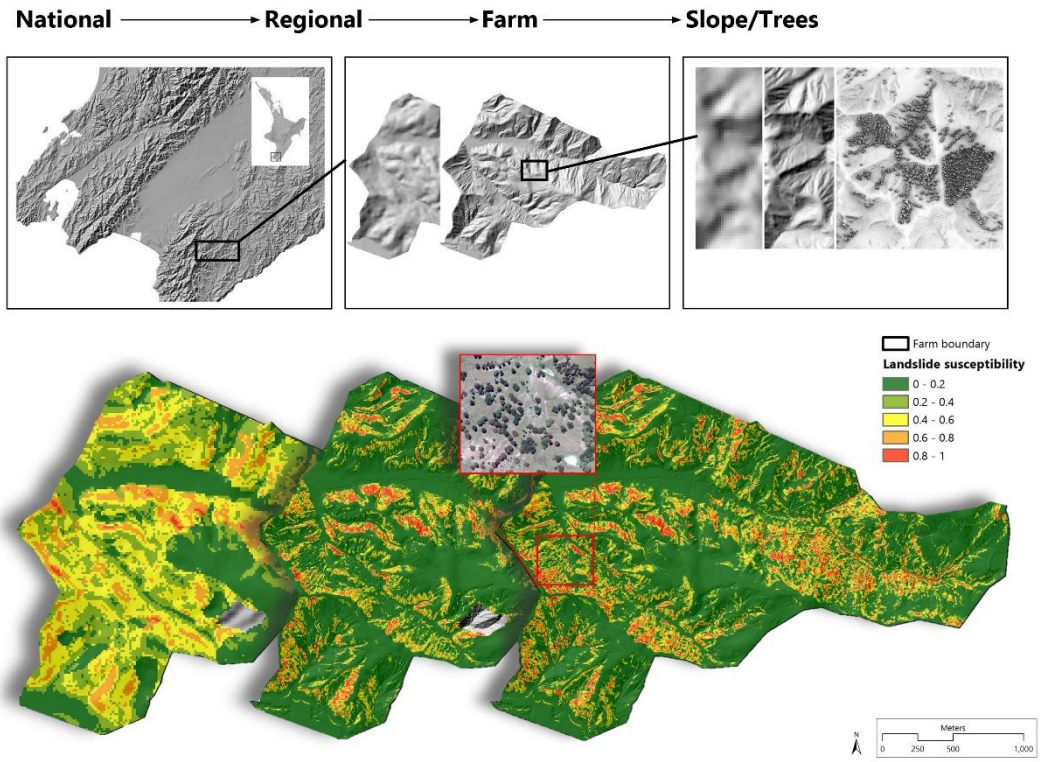

Figure 6.4 Scale considerations: Different data products available at different scales can serve different purposes to support decision-making for erosion and sediment mitigation. Shown above are shaded relief maps of digital elevation models (DEMs) at different scales: from left to right: 15-m (based on topographic contour lines), LiDAR-based 5-m and 1-m ground-sampling-distance (GSD). Below are landslide susceptibility models using topographic variables derived from the differently scaled DEMs (15m, 5m, 1m) shown above. The 15m and 5m DEM based models using LCDB are based on Smith et al. (2021), the 1m model using TIMSS based on Spiekermann et al. (2022). Other issues determined by the scale of data used for modelling include its impact on the accuracy/ performance of models, as well as requirements of computing power.

The planning phase is focused on decision-support and entails careful preparation of a strategy for mitigation measures to address the problem and pursue the objectives set out in Phase 1 (the *why*). This phase also includes a spatial assessment of erosion and sediment-related risks. The strategy should include information regarding what form of mitigation will be implemented where, when, and by whom. This plan needs to be based on an understanding of what effect the proposed mitigation is likely to have with respect to the defined objectives. This can involve ex-ante scenario modelling using a range of mitigation options (see Figure 5.11) and use of cost-effectiveness or benefit-cost analyses. The information delivered in this phase will ensure mitigation decisions are made to maximize the benefit, with respect to the problem and objectives defined in the previous phase.

The third phase is focused on implementation of biological mitigation and capturing data in a GIS database. This record of mitigation measures forms the basis for the fourth phase, which is focused on monitoring and evaluating outcomes. In contrast to the second phase, where possible outcomes based on a range of options are evaluated through scenario modelling, the *Evaluate* phase considers mitigation that was *actually* implemented through ex-post scenario modelling (Figure 5.11). The objective here is to quantify the performance of implemented erosion control at scales of interest (e.g., farm or catchment). Components of this final phase include quantifying survival and/or growth rates of the planted trees, which can be undertaken in the field and/or remotely through use of airborne or satellite imagery. Since mitigation plans are not always implemented as intended, and to account for tree mortality, ex-post scenario modelling allows the performance of established mitigation measures to be quantified. Since erosion and sediment mitigation requires a long-term management strategy, the framework is inherently cyclical in nature.

6.4 Landslide Risk in Silvopastoral Systems

The management framework for erosion and sediment mitigation introduced above proposed a spatial susceptibility or risk assessment as a component of the second management phase *Plan* (Figure 6.3). Landslide susceptibility is generally considered a component of landslide risk (Guzzetti et al., 2006). While this thesis has not aimed to undertake a landslide risk assessment, consideration of a risk lens can help i) improve land management outcomes with respect to shallow landslides and ii) explore future development opportunities that a risk framework enables. Quantitative risk assessments are more holistic than susceptibility alone as they consider the vulnerability of valued elements (resources) at risk with respect to landslide hazard, which describes a magnitude-frequency relationship between the landslide response and its temporal occurrence.

Risk assessments aim to quantify the potential impact of a specific phenomenon or hazard scenario (Crawford et al., 2018; Pondard and Daly, 2011; Wagenaar et al., 2019). Landslide risk is nested within an array of concepts within disaster risk science (Birkmann et al., 2013; Crawford et al., 2018; Crozier and Glade, 2004). The concept of disaster risk – first introduced by the United Nations Disaster Relief Organization (UNDRO, 1980), has been widely used in landslide risk frameworks (e.g. Dai, Lee, and Ngai 2002; Lateltin et al. 2005) and applications (e.g. Bell and Glade, 2004; Sterlacchini et al., 2007). Risk assessments commonly assess risks of natural hazards to infrastructure or human life and are aimed at increasing understanding of risks to improve decision making in spatial planning as well as the identification of targeted mitigation measures (Kienberger et al., 2016; Spiekermann et al., 2015b). Evaluating and quantifying the effectiveness of an implemented measure in terms of reducing risk is a component of the risk analysis process. While risk analysis tools are generally used to determine optimal risk-reducing measures (Wagenaar et al., 2019), a retrospective evaluation (i.e., ex-post) of the performance of the mitigative measures is rarely undertaken (Holcombe et al., 2012).

The framework provides guidance to quantify the potential and actual reductions in risk due to biological mitigation. There are commonly two primary objectives (next to secondary objectives such as shade and shelter) to planting trees on hillslopes, namely i) conservation of soil resources by limiting hillslope erosion; and ii) reducing delivery of landslide-generated sediment to stream networks in pursuit of a particular objective (e.g., to preserve and/or improve downstream aquatic ecology and sustain recreational use) (Benavides et al., 2009; Kemp et al., 2018).

Given these two objectives of tree planting, the framework identifies two closely related risks:

1) Risk of soil loss and pasture production due to rainfall-triggered landsliding for a given period.

2) Risk of long-term landslide-derived sediment yields exceeding a pre-defined target, causing damage to downstream freshwater quality and aquatic ecosystems.

As with other risk frameworks (Bell and Glade, 2004; Birkmann et al., 2013; Crawford et al., 2018; Crozier and Glade, 2004), risk (R) can be defined as:

$$R = H_L \times E \times V$$

where R is a function of landslide hazard (H_L), elements at risk (E), and vulnerability (V). H_L is the product of the conditional probability of a rainfall-triggered landslide response of a given magnitude in a given period $P(M_t)$, and the spatial probability of landslide occurrence $P(S_L)$, also referred to as landslide susceptibility (Figure 6.5). The elements at risk E are either i) on-site elements related to loss of soil productivity and fertility – and therefore loss of pasture and livestock production (Li et al., 2011; Moir et al., 2000), and/or ii) off-site elements related to downstream impacts on freshwater environments (e.g., impact of fine sediment on freshwater habitats) and receiving environments (Fuller and Death, 2018).

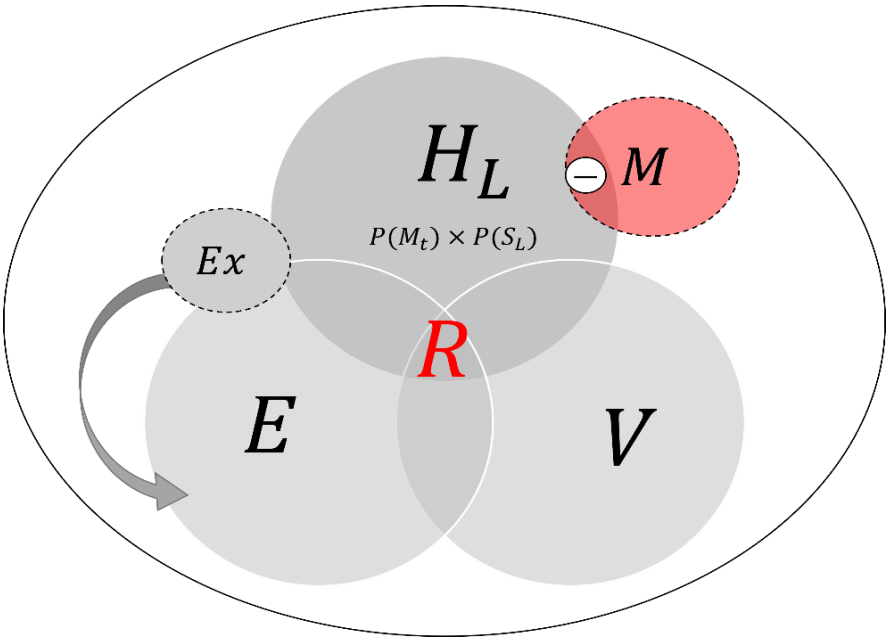

Figure 6.5. Illustrative diagram of the relationship between components that constitute the risk framework used for quantifying the performance of biological erosion and sediment control with respect to shallow landslides. Risk R to landslide erosion and sediment delivery to streams is considered a function of hazard H_L, elements at risk E, and vulnerability V. H_L is modified by mitigation M. The elements at risk E are the productivity and fertility of soils, and/or freshwater environments, and V is the sensitivity of elements at risk to disturbances in the form of landsliding. Exposure Ex is the coupling of hillslope and waterways through hillslope connectivity.

V is either i) the sensitivity of soil to erosion and its ability to recover its productive value (B. J. Rosser and Ross, 2011; Trustrum et al., 1984), or ii) sensitivity of freshwater and estuarine environments to additional sediment input (e.g., affected by the stability and resilience of the stream geomorphology and ecology) (Fuller and Death, 2018). For assessing risk to aquatic health, a further important consideration is exposure (Ex), which is the coupling of hillslope and streams through hillslope connectivity (Figure 6.5). Connectivity differs spatially depending on land cover, topography, soil composition, water content and size of landslides (Poeppl et al., 2019). Landslide susceptibility $P(S_L)$ is modified by the presence or absence of woody vegetation on slopes, that is, biological erosion mitigation M. The risk framework is designed to support the quantification of M as a reduction in landslide occurrence $P(S_L)$ and, by extension, R. This thesis developed a statistical landslide susceptibility model to determine changes in $P(S_L)$ due to M. However, the quantification of risk demands knowledge of magnitude-frequency relationships, that is, data on rainfall storm events with a range of occurrence probabilities, each triggering a different landslide response of a given magnitude. These data and the derived magnitude-frequency relationships allow the identification and quantification of the 'elements at risk' to a given magnitude of erosion response.

In terms of quantification of risk for the two different definitions provided, the first relates to loss of soil and productivity. Therefore, risk reduction can be quantified in monetary terms if the pre-event productivity of the soil is known (e.g., dry matter production of pasture; Li et al., 2011) as well as its trajectory for recovery (Trustrum et al., 1984). However, the second definition of risk is more difficult to monetize (Iftekhar and Polyakov, 2021), particularly since the downstream impacts associated with sediment are so varied and the temporal component less well understood (e.g., time until recovery). Therefore, catchment sediment yield ($t/km^2/yr$) with respect to a target value is an appropriate unit for quantifying risk to freshwater quality and aquatic ecosystems. Depending on the vulnerability of elements at risk to additional sediment input and the characteristics of the geomorphic system (e.g., its transport capacity),

sediment yields that exceed a certain threshold may constitute a risk to a given catchment, whereas yields below the threshold can be sustained in the long-term (Fuller and Death, 2018).

In consideration of the two definitions of risk and the broad objectives of landslide mitigation to combat these risks, biological mitigation performance can be defined as follows:

A soil conservation perspective (on-site impacts) with respect to shallow landslide erosion:

1) The performance of biological mitigation is the degree to which *pasture and livestock production losses* have been averted due to the hydrological and mechanical influence of the woody vegetation on slope stability within a given area and for a given period.

A freshwater health perspective (off-site impacts) with respect to landslide-derived sediment delivery to streams:

2) The performance of biological mitigation is the degree to which long-term *catchment sediment yields* have been reduced to a pre-defined target (sustainable threshold), thus avoiding (further) degradation of freshwater channels and receiving environments.

These two definitions are important to consider in setting objectives (Phase 1 "*Assess*" of management framework; Figure 6.3) as they have implications for the development of the mitigation plan (Figure 6.6). Depending on the risk perspective, mitigation measures will likely be prioritized differently. For example, sediment mitigation implemented on a farm in the upper catchment has, in theory, greater impact on downstream aquatic ecosystem health than mitigation measures on a farm in the lower catchment. Furthermore, results from Chapter 5 indicate that the extent of tree planting required on a given farm will be halved when pursuing freshwater objectives compared to a focus on soil conservation only. This is due to the spatial variation in hillslope-channel coupling. Chapter 5 made predictions of landslide susceptibility and connectivity across several farms for a treeless baseline scenario, two planting scenarios (targeted, non-targeted), as well as the actual tree cover. Reductions in landslide susceptibility and connectivity due to the tree cover were used to quantify expected relative reductions in future landslide occurrence and sediment delivery for each of the scenarios. While the

vulnerability of elements at risk were not quantified in this thesis, knowledge of the sensitivity of soils and aquatic ecosystems to further disturbances by erosion and sediment would enable a meaningful and quantifiable characterisation of the achieved reductions to be made. Furthermore, a hazard assessment would allow mitigation performance to be quantified with respect to the magnitude of the landslide response for a given rainfall event with a particular occurrence probability. Thus, the benefit of a risk assessment is in enabling quantitative responses to the following questions:

- Have the achieved reductions in future landslide occurrence avoided further land degradation to create a sustainable land management system and pastoral farm enterprise? Specifically, given a pre-defined risk tolerance of X% in reduction of pasture dry matter production due to shallow landsliding over a 50-year period, has the catchment-wide landslide mitigation plan been successful?
- Have the reductions in future sediment delivery achieved a sustainable equilibrium between sediment delivery and transport capacity?

The risk framework has both retrospective and predictive components. Implemented biological erosion mitigation can be quantified using ex-post modelling to determine its effectiveness at reducing landslide risk. This is illustrated using predictions for landslide susceptibility under different scenarios in Figure 6.6. Equally, a risk assessment can identify priority areas for erosion and sediment control and ex-ante scenario modelling can be undertaken to predict the potential reduction in landslide risk. This points to the fact that there is an important temporal component to risk since risk evolves and is dynamic in nature (Glade and Crozier, 2005; Gorsevski et al., 2006; Spiekermann et al., 2015b). Adapting to evolving risks is an important component of risk management, particularly considering predicted climate change impacts (Basher et al., 2020; Monaghan et al., 2021). This dynamic is incorporated in the erosion and sediment management framework (Figure 6.3).

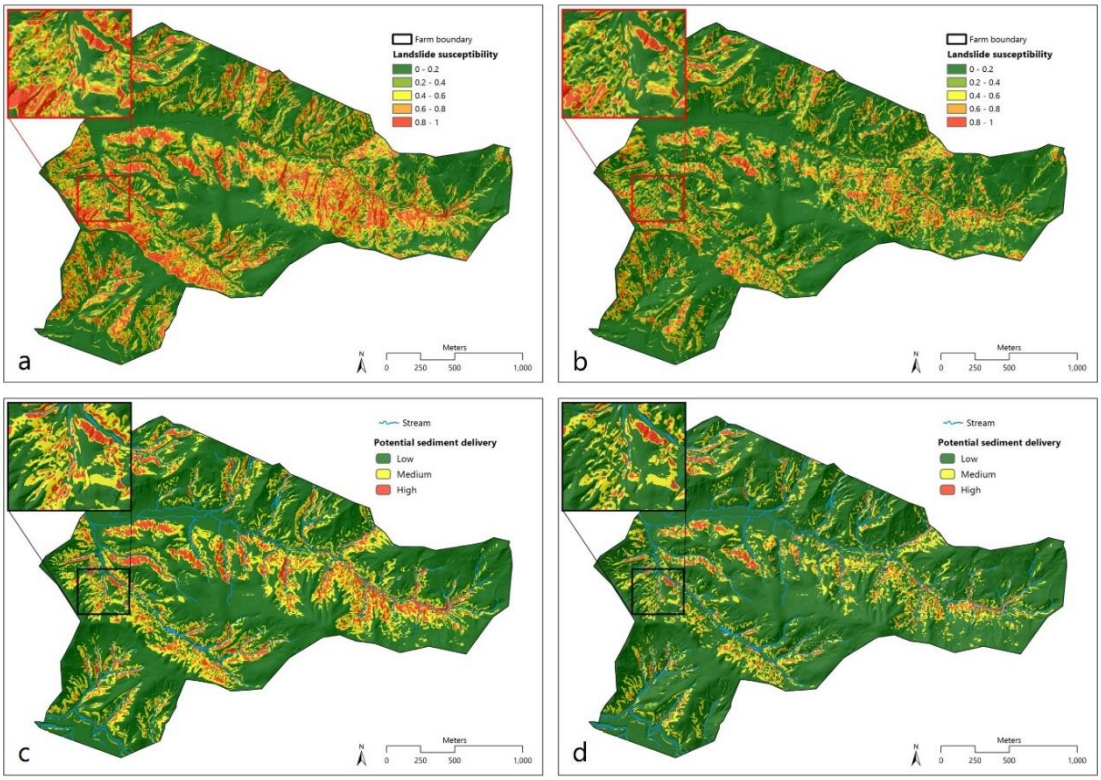

Figure 6.6. For a given farm, landslide susceptibility (a,b) and potential sediment delivery (c, d) under a treeless scenario (a,c) and with actual tree cover as at 2013 (b,d). Consideration of elements at risk can have significant implications in terms of where biological mitigation should be prioritised.

Implicit in the risk framework are factors that must be considered when quantifying mitigation effectiveness. The first of these concerns the establishment of trees. Trees become effective at reducing landslide erosion once successfully established with mature root systems. However, various factors can lead to mortality of trees following planting, and include disturbance by livestock, soil conditions, exposure to wind gusts, and summer droughts (Douglas et al., 2016; Wilkinson, 1999). Additionally, there are many co-benefits of trees in silvopastoral systems, which were elaborated in Chapter 2.1. Examples include shade, shelter, supplementary fodder, timber supply, replenishing soil fertility, and cultural benefits (Gebrewahid et al., 2019; Mackay-Smith et al., 2021; Wilkinson, 1999).

6.5 Summary

It is important to consider that different remote sensing products and spatial datasets can be used to inform landslide erosion and sediment control at different scales. For example, the value of regional-scale data for landslide susceptibility modelling (Figure 6.1) lies in the ability to immediately identify where erosion hotspots are located within the region, accounting for variation in lithology, topography, and land cover. It provides a data-driven approach for prioritization of resource for erosion and sediment mitigation. Thus, differences in scale are complementary in this process of identifying potential sediment source areas (Figure 6.4), beginning with nationally available datasets through to inclusion of LiDAR-derived products for improving both model performance and spatial refinement in predictions. A notable benefit of LiDAR products in silvopastoral landscapes is the resolution of the data that enables individual tree effects on slope stability to be captured. Due to the high resolution of spatial models, the effectiveness of silvopastoral trees in terms of reductions in future landsliding and sediment delivery can be quantified (see Chapters 4 and 5).

The discussion of current limitations of statistical and physically based slope stability models in silvopastoral landscapes (see Section 6.2) suggests future method advancement is less restricted by know-how (e.g., machine-learning algorithms), and much more impeded by inadequacy of data. For physically-based approaches, the limiting factor remains root data for calibrating root reinforcement models specifically for silvopastoral environments. For statistical modelling, the challenge is similarly present in adequately characterizing individual tree effects through time, i.e., as a tree grows following establishment through to full maturity. In developing the TIMSS, this thesis has made significant contributions towards capturing individual tree effects in landscapes with discontinuous tree cover. Indeed, as a global first, a landslide susceptibility model was successfully developed integrating the individual tree effects through inclusion of the TIMSS as predictor variables, which allowed the effectiveness of silvopastoral systems on slope stability to be quantified at a range of scales. In this thesis,

effectiveness was quantified at the scale of individual farms (see Chapters 4 and 5). The same would be possible at scales of individual slopes or paddocks, through to catchment scale. A second global first was the development of a morphometric landslide connectivity model to predict the likelihood of sediment delivery to streams following landslide initiation (Chapter 6).

Moreover, this thesis has demonstrated how landslide susceptibility and connectivity models can be integrated to mitigate landslide-derived sediment. The models also enable the development of mitigation scenarios, which can be helpful in estimating outcomes (long-term reductions in landslide-derived sediment yields), but also for contrasting the cost-effectiveness of different approaches. Chapter 5 undertook scenario modelling to quantify targeted versus non-targeted approaches to mitigation, and found a targeted approach resulted in a 10-fold increase in cost-effectiveness of measures (Table 5.4). These results underscore the importance of targeted erosion and sediment mitigation to achieve freshwater quality targets.

7 CONCLUSION

The research undertaken in this thesis aimed to increase understanding of silvopastoral systems with respect to mitigating landslide erosion and sediment delivery to streams. Chapters 3-5 delivered on this aim by developing methods to quantify the performance of biological mitigation in terms of both i) soil conservation by estimating reductions in landslide occurrence (Chapter 4), and ii) with respect to outcomes that impact aquatic ecosystems by estimating reductions in sediment delivery to streams (Chapter 5). Sediment delivered to streams from landslides contributes to the degradation of freshwater and receiving environments by smothering benthic habitats and increasing turbidity, light attenuation, and sediment-bound contaminants. While the geospatial methods developed are complementary to in-stream approaches that monitor water quality through time, they are clearly distinct. In-stream monitoring of water clarity, turbidity and/or suspended sediment remain i) highly challenging in the short-term due to the lag-time required for biological mitigation to take effect, ii) challenging in the long-term due to conflation of multiple possible explanatory factors, such as the presence of legacy sediment (e.g., previous landslide events) or effects of historic land use change, and, iii) compounded by the nature of point sampling to represent a complexity of up-stream erosion, transport and deposition processes.

Yet, New Zealand's National Policy Statement for Freshwater Management (NPS-FM) requires long-term monitoring of visual clarity at measurement sites as the method to monitor and quantify outcomes (New Zealand Government, 2020a). To meet catchment targets with respect to freshwater quality and aquatic ecosystem health, Freshwater Farm Plans (FFPs) are to be used as the mechanism to identify adverse effects on freshwater and plan mitigation measures to avoid and remedy these effects. Responding to these challenges, the methods developed in this thesis provide a spatially explicit, high-resolution modelling approach that

capture individual tree effects on slope stability and are therefore designed for application in silvopastoral landscapes. The methods enable both i) the ex-post quantification of previously implemented biological landslide mitigation (aimed at increasing slope stability to reduce the occurrence of future landsliding) and ii) ex-ante quantitative estimates of future reductions in landslide-derived sediment yields for a given biological mitigation plan. The research presented in this thesis not only developed novel methods to respond to the demand for (spatial) guidance on the sediment risks related to freshwater but also demonstrated application by quantifying the performance of mitigation actions.

The conclusions and key findings with respect to the stated objectives of this thesis are as follows:

1. In Chapter 3, remote sensing techniques were developed for i) rapid acquisition of large quantities of landslide data comprising tens of thousands of individual landslides, and ii) delineation and classification of individual tree canopies. The study demonstrates the advantages of semi-automated object-based image analysis (OBIA) for mapping shallow landslides at landscape scale. The classification of individual trees is the first of its kind in New Zealand, making use of freely available high resolution multi-spectral imagery and LiDAR data, achieving an overall accuracy of 93%. Native kānuka was found to be the most abundant woody vegetation on slopes within the Wairarapa study area, fulfilling an important soil conservation function.

2. These landslide and tree inventories were subsequently used to test the hypothesis that individual tree effect on slope stability can be ascertained by examining the spatial relationship between landslides and trees. The emerging patterns showed that this was indeed possible, and the resulting spatially-distributed tree influence models (TIMSS) at 1-m resolution largely confirm the sigmoidal shape and distribution of physically-based root reinforcement models. The TIMSS formed the basis for the modelling

undertaken in the following chapters aimed at quantifying the performance of trees in silvopastoral landscapes.

3. Chapter 4 was largely devoted to developing a statistical landslide susceptibility model for application in silvopastoral landscapes. This required the incorporation of the TIMSS as predictor variables to account for individual tree effects on slope stability. High positive skewness associated with the TIMSS (that are continuous variables with value range 0-1) presented a potential challenge to the maximum likelihood estimator in logistic regression modelling, since high skewness is known to inflate the coefficient estimates in certain situations (i.e., given an inadequate sample size). This potential barrier to statistical modelling approaches was rigorously tested by adopting a range of sampling approaches aimed at reducing skewness. The results showed that the maximum likelihood estimator produced consistent estimates of effect size. With an adequate sample size, highly skewed continuous predictor variables do not result in an inflation of effect size. Therefore, the TIMSS were included in the landslide susceptibility model, and subsequently used to address the fourth stated objective of this thesis. Moreover, with a median AUROC of 0.95 in the final model, performance was very good and equates to an accuracy of 89% when classifying the probability values into a binary classification using a probability threshold (cut-off) of 0.5.

4. The application of the landslide susceptibility model in Chapters 4 and 5 demonstrate a data-driven approach to improve targeting of erosion control from landscape to slope scales. Chapter 4 undertook an ex-post assessment of slope stability for two case study sites to quantify the performance of silvopastoral trees in reducing future landslide occurrence. The assessment was based on the actual tree cover (as at 2013) and included a breakdown of reductions in landslide erosion achieved by tree type, made possible by the tree classification developed in Chapter 3. Future landslide erosion was reduced by 17% at Site 1 and 43% at Site 2 due to the actual tree cover. The difference in reductions across these two sites underscores the importance of targeting highly

susceptible areas and doing so with adequate tree densities. An important finding is the high degree of refinement in spatial predictions of landslide susceptibility enabled by the LiDAR DEM derivatives and TIMSS. Based on observing where past landslides have occurred, the majority (80%) of future landslides are expected to be triggered in areas that currently occupy 12% and 7% of Sites 1 and 2, respectively. This strongly suggests that there is great potential for improved targeting of erosion control by decision-makers in land management, also increasing the economic feasibility. The high-resolution spatial information provided by the landslide susceptibility maps can be used to support the development of landslide erosion mitigation plans.

5. The primary objective of Chapter 5 was the development of a morphometric landslide connectivity model to inform on the likelihood of sediment delivery to adjacent streams in the event of a rainfall-triggered shallow landslide. Using lasso logistic regression, the determinants of sediment connectivity were investigated using an inventory of landslide scars and deposits from a storm event in 1977 in the Wairarapa. A range of connectivity scenarios were proposed by defining a set of six connectivity targets (sinks). The implications of target definition were subsequently explored by simulating varying rates of sediment generation during flood events of increasing magnitude. Sediment delivery ratios (SDRs) from the landslide triggering event of 1977 ranged between 0.21 and 0.29, depending on the definition of sink. These SDRs correspond to event sediment yields 3548 t/km^2 when accounting only for direct deposition into streams, and 9033 t/km^2 when assuming continued sediment recruitment at reduced rate by overland flow across saturated soils as well as post-event reworking of deposited material. Further responding the Objective 4 of the thesis, the landslide susceptibility and connectivity predictions were coupled in modular form to enable ex-ante modelling of different mitigation scenarios.

6. Fifty farms were selected to quantify the reduction in sediment delivery based on contrasting mitigation options: 1) targeting critical source areas of sediment and 2) a

non-targeted approach to tree planting. The cost-effectiveness assessment of these different mitigation options suggests there is an order of magnitude difference between a targeted versus non-targeted approach in terms of the ratio of investment to reduction in sediment delivery achieved. In monetary terms, the average cost for a 500 ha farm to achieve a 10% reduction in landslide-derived sediment is $14,100 for targeted mitigation and $131,000 for non-targeted tree planting.

A key finding in integrating landslide susceptibility and connectivity modelling is that, with a shift in focus from soil conservation to freshwater management, the area requiring biological mitigation through tree planting has greatly been reduced. In total, only 6.5% (2370 ha) of the 36,000 ha of farmland assessed represents the potential source of approximately two-thirds of landslide-derived sediment across the 50 farms. Due to existing tree cover, this area requiring tree planting has already been reduced to 4.7% (1720 ha).

7. The seventh and final objective relates to an observed need for a landslide erosion and sediment risk management framework. An erosion and sediment management framework (Figure 6.3) was proposed in Chapter 6, which is complemented by a risk framework (Figure 6.5). In combination, these frameworks provide guidance for planning, implementing, and monitoring erosion and sediment mitigation in silvopastoral landscapes. Their main objective is to initiate a reflective response to land management, considering what the objectives are at each point in time and across different spatial scales.

To summarise, the research undertaken in this study has contributed to science-based knowledge of human-landscape interactions. The findings summarized here can contribute to combat further degradation of land and aquatic environments. Moreover, if the methods developed in this thesis were to find widespread application, outcomes for soil conservation and freshwater quality could be greatly improved, both in terms of cost and effect.

8

8 OUTLOOK

The research undertaken in this thesis has advanced knowledge of the effectiveness of silvopastoral systems in mitigating landslide erosion and sediment delivery to streams through use of remote sensing and spatial modelling. An implicit by-product to this scientific endeavour is a refined understanding of the limits to the current state of knowledge. While knowledge of the world is advanced, the realisation of its limitations give rise to further questions that warrant further investigation. This thesis concludes with a view to future research opportunities, which extend beyond simply improving and further refining existing methodologies developed.

In the context of outcomes of silvopastoral systems pertaining to slope stability, method development towards improved mapping and classification of individual trees is an important step to enable monitoring and quantification of impacts. Recent advances in tree crown segmentation using convolutional neural networks show individual trees can be accurately mapped in aerial photography without the need of LiDAR data (Brandt et al., 2020; Skole et al., 2021). While the TIMSS provide a means to statistically model individual tree effects on slope stability in silvopastoral landscapes, they are limited by the absence of a relationship to above-ground biomass (e.g., crown size), which would provide a basis for determining the magnitude and distance of a tree's influence. Therefore, each tree is assumed to have the same (average) influence on slope stability – with the only point of difference based on vegetation class (e.g., poplar/willow vs coniferous species).

Therefore, future research should focus on the development of spatially distributed root reinforcement models for silvopastoral trees that are based on allometric relationships between below- and above-ground biomass (e.g., tree height). While LiDAR data provides very accurate estimates of tree height, the acquisition of the data is expensive and, therefore, less suited for monitoring land cover changes through time at regional scale. A potential step-change is a very

recent study that has demonstrated how deep-learning methods applied to aerial photography can be used to estimate individual tree heights at national scale (Li et al., 2022). While LiDAR data is required to train such models, the deep-learning methods show promise in terms of building multi-temporal inventories of individual trees at national scale. Tree inventories alongside root data form the basis of spatially-distributed root reinforcement models and need to be developed with root data specific to silvopastoral systems, since the lack of competition will result in different above and below ground tree architecture (Callaway et al., 2003; Kumar and Jose, 2018; Nair et al., 2021).

Since root-reinforcement models are generally integrated as a sub-model in physically-based slope stability models, there is currently no example of a statistical model that includes a root reinforcement model as an explanatory variable. Yet, a comparison of statistical and physical approaches to landslide susceptibility modelling at the individual tree scale would provide insights into the strengths and limitations of each method. While both methods are concerned with slope stability, the underpinning theoretical frameworks are different – each with its own set of assumptions. A comparison of the spatial predictions of physical and statistical models would enable implications for land managers to be considered. For example, would mitigation measures differ in terms of their spatial targeting, and how do estimates for mitigation performance compare?

The landslide connectivity model developed in Chapter 5 predicts the probability that a landslide will connect to an adjacent stream. The predictions are based on a binary distribution (connected/unconnected). While this is initially adequate for informing biological mitigation planning, assumptions need to be made with respect to the mass of sediment delivered to sink. This is important for improving estimates of event-based and long-term sediment loads (Dymond et al., 2016). Therefore, future research should focus on developing multi-variate models that improve on existing run-out models to predict the mass of sediment delivered to stream. Since the findings of this research show a strong dependence on coalescing landslide

deposits, the ability to predict landslide densities with respect to storm rainfall magnitude would further enhance estimates of sediment delivery.

Regarding future research needs in the context of silvopastoral systems in New Zealand, most research has focused on poplar, willow, and radiata pine systems (Kemp et al., 2018). Soil conservation has been the main driver of silvopastoralism in steep, erosion-prone terrain (Benavides et al., 2009), with most studies attempting to quantify the effects of the trees on pasture production (Devkota et al., 2009; Guevara-Escobar et al., 1997; Sloan et al., 2014; Wall et al., 2006, 1997). However, silvopastoral systems are highly multifunctional, and additional benefits, including animal welfare (e.g., Betteridge et al., 2012), biodiversity, carbon sequestration, hydrological impacts, and soil nutrient effects (e.g., Guevara-Escobar et al., 2000), have received less attention.

An example of an additional benefit is the potential increased pasture production under tree canopies. This phenomenon has been found in various landscapes around the globe (Frost and McDougald, 1989; Moreno and Pulido, 2008; Peri et al., 2016), including a recent two-year study in New Zealand that found a 108% increase in green dry matter production under fully mature kānuka trees compared to paired areas of open pasture in the same paddock at two sites (Mackay-Smith et al., 2022a). This increase was associated with 116% and 49% more plant-available P and soil organic matter under the tree canopies, respectively, as well as a significant increase in soil porosity. Moreover, there is evidence that livestock prefer to graze the understorey of widely spaced kānuka trees compared to open pasture (Mackay-Smith et al., 2022b), which may result in a positive feedback loop in improving soil fertility as livestock deposit nutrients and organic matter in these tree-pasture locations. Thus, a tree-pasture system is a potentially transformational management practice to overcome key trade-offs between production, environmental, and cultural outcomes. Yet further fundamental research is required to advance understanding of the underlying mechanisms, that is, the tree-functional traits in interaction with livestock and soil that result in beneficial emergent properties in the silvopastoral system.

Given the challenges associated with a changing climate – particularly with respect to expected increases in the frequency and magnitude of rainfall events, silvopastoral systems have the potential to respond to these challenges by building resilient socio-ecological landscapes that safeguard and enhance the sustained economic viability of pastoral farms in New Zealand. The research presented in this thesis has made an important step in this direction by developing methods and demonstrating application of spatial modelling that informs cost-effective, targeted biological mitigation for reducing landslide erosion and sediment delivery to streams.

9

9 BIBLIOGRAPHY

Abad, L., Hölbling, D., Spiekermann, R., Prasicek, G., Dabiri, Z., Argentin, A.-L., 2022. Detecting landslide-dammed lakes on Sentinel-2 imagery and monitoring their spatio-temporal evolution following the Kaikōura earthquake in New Zealand. Sci. Total Environ. 820, 153335. https://doi.org/10.1016/j.scitotenv.2022.153335

Abernethy, B., Rutherfurd, I.D., 2001. The distribution and strength of riparian tree roots in relation to riverbank reinforcement. Hydrol. Process. 15, 63–79. https://doi.org/10.1002/hyp.152

Akalin, A., Franke, V., Uyar, B., Ronen, J., 2020. Computational Genomics with R. Berlin, Germany.

Aleotti, P., Chowdhury, R., 1999. Landslide hazard assessment: Summary review and new perspectives. Bull. Eng. Geol. Environ. 58, 21–44. https://doi.org/10.1007/s100640050066

Alkhalaf, A., Zumbo, B.D., 2017. The impact of predictor variable(s) with skewed cell probabilities on wald tests in binary logistic regression. J. Mod. Appl. Stat. Methods 16, 40–80. https://doi.org/10.22237/jmasm/1509494640

Allen, R.B., Partridge, T.R., Lee, W.G., 1992. Ecology of Kunzea ericoides (A. Rich.) J. Thompson (kanuka) in east Otago, New Zealand. New Zeal. J. Bot. 30, 135–149. https://doi.org/10.1080/0028825X.1992.10412894

Ammer, C., Wagner, S., 2005. An approach for modelling the mean fine-root biomass of Norway spruce stands. Trees - Struct. Funct. 19, 145–153. https://doi.org/10.1007/s00468-004-0373-4

Arabameri, A., Pourghasemi, H.R., 2019. Spatial Modeling of Gully Erosion Using Linear and Quadratic Discriminant Analyses in GIS and R, in: Pourghasemi, H.R., Gokceoglu, C. (Eds.), Spatial Modeling in GIS and R for Earth and Environmental Sciences. Elsevier, pp. 299–321. https://doi.org/10.1016/B978-0-12-815226-3.00013-2

Atkinson, P.M., Massari, R., 2011. Autologistic modelling of susceptibility to landsliding in the Central Apennines, Italy. Geomorphology 130, 55–64. https://doi.org/10.1016/j.geomorph.2011.02.001

Barnes, G., 2016. Soil mechanics: principles and practice, Fourth edi. ed. Macmillan Education/Palgrave, London SE - xxiv, 560 pages : illustrations ; 25 cm.

Basher, L., Betts, H., Lynn, I., Marden, M., McNeill, S., Page, M., Rosser, B., 2018. A preliminary assessment of the impact of landslide, earthflow, and gully erosion on soil carbon stocks in New Zealand. Geomorphology 307, 93–106. https://doi.org/10.1016/j.geomorph.2017.10.006

Basher, L, Botha, N., Dodd, M., Douglas, G., Lynn, I., Marden, M., McIvor, I., Smith, W., 2008. Hill country erosion: A review of knowledge on erosion processes, mitigation options, social learning and their long term effectiveness in the management hill country erosion. A Rep. Prep. Minist. Agric. For.

Basher, Les, Botha, N., Dodd, M.B., Douglas, G.B., Lynn, I., Marden, M., McIvor, I., 2008. Hill country erosion: a review of knowledge on erosion processes, mitigation options, social learning and their long-term effectiveness in the management of hill country erosion.

Basher, L., Moores, J., McLean, G., 2016. Scientific basis for erosion and sediment control practices in New Zealand.

Basher, L., Spiekermann, R., Dymond, J., Herzig, A., Hayman, E., Ausseil, A.G., 2020. Modelling the effect of land management interventions and climate change on sediment loads in the Manawatū–Whanganui region. New Zeal. J. Mar. Freshw. Res. 54, 490–511. https://doi.org/10.1080/00288330.2020.1730413

Basher, L.R., 2013. Erosion Processes and Their Control in New Zealand. Ecosyst. Serv. New Zeal. Cond. Trends 363–374.

Basher, L.R., Hicks, D.M., Clapp, B., Hewitt, T., 2011. Sediment yield response to large storm events and forest harvesting, Motueka River, New Zealand. New Zeal. J. Mar. Freshw. Res. 45, 333–356. https://doi.org/10.1080/00288330.2011.570350

Bast, A., Wilcke, W., Graf, F., Lüscher, P., Gärtner, H., 2014. The use of mycorrhiza for eco-engineering measures in steep alpine environments: Effects on soil aggregate formation and fine-root development. Earth Surf. Process. Landforms 39, 1753–1763. https://doi.org/10.1002/esp.3557

Bates, D.M., Watts, D.G., 1988. Nonlinear regression analysis and its applications, Wiley series in probability and mathematical statistics. Applied probability and statistics. Wiley, New York SE - xiv, 365 pages : illustrations ; 24 cm.

Bathurst, J.C., Burton, A., Ward, J.T., 1997. Debris Flow Run-Out and Landslide Sediment Delivery Model Tests. J. Hydraul. Eng. 123, 410–419. https://doi.org/10.1061/(ASCE)0733-9429(1997)123:5(410)

Bell, R., Glade, T., 2004. Quantitative risk analysis for landslides - Examples from Bíldudalur, NW-Iceland. Nat. Hazards Earth Syst. Sci. 4, 117–131. https://doi.org/10.5194/nhess-4-117-2004

Bellugi, D., Milledge, D.G., Dietrich, W.E., McKean, J.A., Perron, J.T., Sudderth, E.B., Kazian, B., 2015a. A spectral clustering search algorithm for predicting shallow landslide size and location. J. Geophys. Res. Earth Surf. 120, 300–324. https://doi.org/10.1002/2014JF003137

Bellugi, D., Milledge, D.G., Dietrich, W.E., Perron, J.T., McKean, J., 2015b. Predicting shallow landslide size and location across a natural landscape: Application of a spectral clustering search algorithm. J. Geophys. Res. Earth Surf. 120, 2552–2585. https://doi.org/10.1002/2015JF003520

Benavides, R., Douglas, G.B., Osoro, K., 2009. Silvopastoralism in New Zealand: Review of effects of evergreen and deciduous trees on pasture dynamics. Agrofor. Syst. 76, 327–350. https://doi.org/10.1007/s10457-008-9186-6

Bergin, D.O., Kimberley, M.O., Marden, M., 1995. Protective value of regenerating tea tree stands on erosion-prone hill country, East Coast, North Island, New Zealand. New Zeal. J. For. Sci. 25, 3–19.

Bessette-Kirton, E.K., Coe, J.A., Schulz, W.H., Cerovski-Darriau, C., Einbund, M.M., 2020. Mobility characteristics of debris slides and flows triggered by Hurricane Maria in Puerto Rico. Landslides 17, 2795–2809. https://doi.org/10.1007/s10346-020-01445-z

Betts, H., Basher, L., Dymond, J., Herzig, A., Marden, M., Phillips, C., 2017. Development of a landslide component for a sediment budget model. Environ. Model. Softw. 92, 28–39. https://doi.org/10.1016/j.envsoft.2017.02.003

Birkmann, J., Cardona, O.D., Carreño, M.L., Barbat, A.H., Pelling, M., Schneiderbauer, S., Kienberger, S., Keiler, M., Alexander, D., Zeil, P., Welle, T., 2013. Framing vulnerability, risk and societal responses: The MOVE framework. Nat. Hazards 67, 193–211. https://doi.org/10.1007/s11069-013-0558-5

Blaschke, T., 2010. Object based image analysis for remote sensing. ISPRS J. Photogramm. Remote Sens. 65, 2–16. https://doi.org/10.1016/j.isprsjprs.2009.06.004

Blaschke, T., Hay, G.J., Kelly, M., Lang, S., Hofmann, P., Addink, E., Queiroz Feitosa, R., van der Meer, F., van der Werff, H., van Coillie, F., Tiede, D., 2014. Geographic Object-Based Image Analysis - Towards a new paradigm. ISPRS J. Photogramm. Remote Sens. 87, 180–191. https://doi.org/10.1016/j.isprsjprs.2013.09.014

Board, W.C., 1956. Farm conservation scheme.

Böhner, J., Selige, T., 2006. Jürgen Böhner 1 & Thomas Selige 2 1 115, 13–28.

Borselli, L., Cassi, P., Torri, D., 2008. Prolegomena to sediment and flow connectivity in the landscape: A GIS and field numerical assessment. Catena 75, 268–277. https://doi.org/10.1016/j.catena.2008.07.006

Brabb, E.E., 1984. Innovative approaches to landslide hazard and risk mapping, in: 4th International Symposium on Landslides. Toronto, Canada, pp. 307–324.

Bracken, L.J., Croke, J., 2007. The concept of hydrological connectivity and its contribution to understanding runoff-dominated geomorphic systems. Hydrol. Process. 21, 1749–1763. https://doi.org/10.1002/hyp.6313

Bracken, L.J., Turnbull, L., Wainwright, J., Bogaart, P., 2015. Sediment connectivity: A framework for understanding sediment transfer at multiple scales. Earth Surf. Process. Landforms 40, 177–188. https://doi.org/10.1002/esp.3635

Brandt, M., Romankiewicz, C., Spiekermann, R., Samimi, C., 2014. Environmental change in time series - An interdisciplinary study in the Sahel of Mali and Senegal. J. Arid Environ. 105, 52–63. https://doi.org/10.1016/j.jaridenv.2014.02.019

Brandt, M., Tucker, C.J., Kariryaa, A., Rasmussen, K., Abel, C., Small, J., Chave, J., Rasmussen, L.V., Hiernaux, P., Diouf, A.A., Kergoat, L., Mertz, O., Igel, C., Gieseke, F., Schöning, J., Li, S., Melocik, K., Meyer, J., Sinno, S., Romero, E., Glennie, E., Montagu, A., Dendoncker, M., Fensholt, R., 2020. An unexpectedly large count of trees in the West African Sahara and Sahel. Nature 587, 78–82. https://doi.org/10.1038/s41586-020-2824-5

Brenning, A., 2005. Spatial prediction models for landslide hazards: Review, comparison and evaluation. Nat. Hazards Earth Syst. Sci. 5, 853–862. https://doi.org/10.5194/nhess-5-853-2005

Brenning, A., Bangs, D., Becker, M., 2018. RSAGA: SAGA Geoprocessing and Terrain Analysis.

Brierley, G., Fryirs, K., Jain, V., 2006. Landscape connectivity: The geographic basis of

geomorphic applications. Area 38, 165–174. https://doi.org/10.1111/j.1475-4762.2006.00671.x

Broeckx, J., Vanmaercke, M., Bălteanu, D., Chendeş, V., Sima, M., Enciu, P., Poesen, J., 2016. Linking landslide susceptibility to sediment yield at regional scale: application to Romania. Geomorphology 268, 222–232. https://doi.org/10.1016/j.geomorph.2016.06.012

Brooks, S.M., Crozier, M.J., Preston, N.J., Anderson, M.G., 2002. Regolith stripping and the control of shallow translational hillslope failure: Application of a two-dimensional coupled soil hydrology-slope stability model, Hawke's Bay, New Zealand. Geomorphology 45, 165–179. https://doi.org/10.1016/S0169-555X(01)00153-2

Budimir, M.E.A., Atkinson, P.M., Lewis, H.G., 2015. A systematic review of landslide probability mapping using logistic regression. Landslides 12, 419–436. https://doi.org/10.1007/s10346-014-0550-5

Bunting, P., Lucas, R., 2006. The delineation of tree crowns in Australian mixed species forests using hyperspectral Compact Airborne Spectrographic Imager (CASI) data. Remote Sens. Environ. 101, 230–248. https://doi.org/10.1016/j.rse.2005.12.015

Burnett, B.N., Meyer, G.A., McFadden, L.D., 2008. Aspect-related microclimatic influences on slope forms and processes northeastern Arizona. J. Geophys. Res. Earth Surf. 113, 1–18. https://doi.org/10.1029/2007JF000789

Burns, R.G., 1979. An improved sediment delivery model for piedmont forests, Vol. 3. School of Forest Resources, University of Georgia in cooperation with Environmental Resources Center, Georgia Institute of Technology, Atlanta.

Burton, A., Bathurst, J.C., 1998. Physically based modelling of shallow landslide sediment yield at a catchment scale. Environ. Geol. 35, 89–99. https://doi.org/10.1007/s002540050296

Callaway, R.M., Nadkarni, N.M., Mahall, B.E., 1991. Facilitation and Interference of Quercus Douglasii on Understory Productivity in Central California. Ecology 72, 1484–1499. https://doi.org/10.2307/1941122

Callaway, R.M., Pennings, S.C., Richards, C.L., 2003. Phenotypic plasticity and interactions among plants. Ecology 84, 1115–1128. https://doi.org/10.1890/0012-9658(2003)084[1115:PPAIAP]2.0.CO;2

Carrara, A., Cardinali, M., Detti, R., Guzzetti, F., Pasqui, V., Reichenbach, P., 1991. GIS

techniques and statistical models in evaluating landslide hazard. Earth Surf. Process. Landforms 16, 427–445. https://doi.org/https://doi.org/10.1002/esp.3290160505

Carrara, A., Cardinali, M., Guzzetti, F., Reichenbach, P., 1995. GIS Technology in Mapping Landslide Hazard, in: Carrara, A., Guzzetti, F. (Eds.), Geographical Information Systems in Assessing Natural Hazards. Springer Netherlands, Dordrecht, pp. 135–175. https://doi.org/10.1007/978-94-015-8404-3_8

Cavalli, M., Trevisani, S., Comiti, F., Marchi, L., 2013. Geomorphometric assessment of spatial sediment connectivity in small Alpine catchments. Geomorphology 188, 31–41. https://doi.org/10.1016/j.geomorph.2012.05.007

Cervi, F., Berti, M., Borgatti, L., Ronchetti, F., Manenti, F., Corsini, A., 2010. Comparing predictive capability of statistical and deterministic methods for landslide susceptibility mapping: A case study in the northern Apennines (Reggio Emilia Province, Italy). Landslides 7, 433–444. https://doi.org/10.1007/s10346-010-0207-y

Chang, K.T., Merghadi, A., Yunus, A.P., Pham, B.T., Dou, J., 2019. Evaluating scale effects of topographic variables in landslide susceptibility models using GIS-based machine learning techniques. Sci. Rep. 9, 1–21. https://doi.org/10.1038/s41598-019-48773-2

Christodoulou, M., Nakos, G., 1990. An approach to comprehensive land use planning. J. Environ. Manage. 31, 39–46. https://doi.org/10.1016/S0301-4797(05)80013-1

Chung, C.J.F., Fabbri, A.G., 2003. Validation of spatial prediction models for landslide hazard mapping. Nat. Hazards 30, 451–472. https://doi.org/10.1023/B:NHAZ.0000007172.62651.2b

Cislaghi, A., Bischetti, G.B., 2019. Source areas, connectivity, and delivery rate of sediments in mountainous-forested hillslopes: A probabilistic approach. Sci. Total Environ. 652, 1168–1186. https://doi.org/10.1016/j.scitotenv.2018.10.318

Cislaghi, A., Bordoni, M., Meisina, C., Bischetti, G.B., 2017. Soil reinforcement provided by the root system of grapevines: Quantification and spatial variability. Ecol. Eng. 109, 169–185. https://doi.org/10.1016/j.ecoleng.2017.04.034

Cislaghi, Alessio, Chiaradia, E.A., Bischetti, G.B., 2017. Including root reinforcement variability in a probabilistic 3D stability model. Earth Surf. Process. Landforms 42, 1789–1806. https://doi.org/10.1002/esp.4127

Cohen, D., Schwarz, M., 2017. Tree-root control of shallow landslides. Earth Surf. Dyn. 5, 451–477. https://doi.org/10.5194/esurf-5-451-2017

Cohen, D., Schwarz, M., Or, D., 2011. An analytical fiber bundle model for pullout mechanics of root bundles. J. Geophys. Res. Earth Surf. 116, 1–20. https://doi.org/10.1029/2010JF001886

Cohen, J., 1960. A Coefficient of Agreement for Nominal Scales. Educ. Psychol. Meas. 20, 37–46. https://doi.org/10.1177/001316446002000104

Collins, A., Mackay, A., Basher, L., Schipper, L., Carrick, S., Manderson, A., Cavanagh, J., Clothier, B., Weeks, E., Newton, P., 2014. Phase 1: looking back, Future requirements for soil management in New Zealand. Palmerston North.

Commandeur, P.R., Pyles, M.R., 1991. Modulus of elasticity and tensile strength of Douglas-fir roots. Can. J. For. Res. 21, 48–52. https://doi.org/10.1139/x91-007

Conoscenti, C., Rotigliano, E., Cama, M., Caraballo-Arias, N.A., Lombardo, L., Agnesi, V., 2016. Exploring the effect of absence selection on landslide susceptibility models: A case study in Sicily, Italy. Geomorphology 261, 222–235. https://doi.org/10.1016/j.geomorph.2016.03.006

Cooper, G., 2015. without any more new farm plans or works implementation from 2014 onwards ' 0, 1–5.

Coppin, N.J., Richards, I.G., 1990. Use of vegetation in civil engineering, Construction Industry Research and Information Association. Butterworths, London SE - xvii, 292 pages : illustrations ; 24 cm.

Corominas, J., 1996. The angle of reach as a mobility index for small and large landslides. Can. Geotech. J. 33, 260–271. https://doi.org/10.1139/t96-005

Cox, D.R., 1958. The Regression Analysis of Binary Sequences. J. R. Stat. Soc. Ser. B 20, 215–232. https://doi.org/10.1111/j.2517-6161.1958.tb00292.x

Crawford, M.H., Crowley, K., Potter, S.H., Saunders, W.S.A., Johnston, D.M., 2018. Risk modelling as a tool to support natural hazard risk management in New Zealand local government. Int. J. Disaster Risk Reduct. 28, 610–619. https://doi.org/10.1016/j.ijdrr.2018.01.011

Croke, J., Fryirs, K., Thompson, C., 2013. Channel-floodplain connectivity during an extreme flood event: Implications for sediment erosion, deposition, and delivery. Earth Surf. Process. Landforms 38, 1444–1456. https://doi.org/10.1002/esp.3430

Crozier, M.J., 2018. Reprint of "A proposed cell model for multiple-occurrence regional landslide events: Implications for landslide susceptibility mapping." Geomorphology 307,

3–11. https://doi.org/10.1016/j.geomorph.2018.02.001

Crozier, M.J., 2005. Multiple-occurrence regional landslide events in New Zealand: Hazard management issues. Landslides 2, 247–256. https://doi.org/10.1007/s10346-005-0019-7

Crozier, M.J., 1996. Runout behaviour of shallow, rapid earthflows. Zeitschrift Fur Geomorphol. Suppl. 35–48.

Crozier, M.J., Eyles, R.J., Crozier, M.J., McConchie, J.A., Owen, R.C., 1980. Distribution of landslips in the Wairarapa hill country. New Zeal. J. Geol. Geophys. 23, 575–586. https://doi.org/10.1080/00288306.1980.10424129

Crozier, M.J., Glade, T., 2004. Landslide Hazard and Risk: Issues, Concepts and Approach, in: Glade, T., Anderson, M., Crozier, M.J. (Eds.), Landslide Hazard and Risk. John Wiley & Sons, Ltd, pp. 1–40.

Crozier, M.J., Preston, N.J., 1999. Modelling changes in terrain resistance as a component of landform evolution in unstable hill country, in: Hergarten, S., Neugebauer, H.J. (Eds.), Process Modelling and Landform Evolution. Springer-Verlag, Berlin/Heidelberg, pp. 267–284. https://doi.org/10.1007/BFb0009730

Cruden, D.M., Varnes, D.J., 1996. Landslide types and processes, in: Landslides: Investigation and Mitigation, Transportation Research Board Special Report 247, Washington D.C. pp. 36–75.

Dai, F.C., Lee, C.F., Ngai, Y.Y., 2002. Landslide risk assessment and management: An overview. Eng. Geol. 64, 65–87. https://doi.org/10.1016/S0013-7952(01)00093-X

Dalponte, M., Bruzzone, L., Gianelle, D., 2012. Tree species classification in the Southern Alps based on the fusion of very high geometrical resolution multispectral/hyperspectral images and LiDAR data. Remote Sens. Environ. 123, 258–270. https://doi.org/10.1016/j.rse.2012.03.013

Dalponte, M., Coomes, D.A., 2016. Tree-centric mapping of forest carbon density from airborne laser scanning and hyperspectral data. Methods Ecol. Evol. 7, 1236–1245. https://doi.org/10.1111/2041-210X.12575

Danjon, F., Stokes, A., Bakker, M.R., 2013. Root systems of woody plants. Plant Roots Hidden Half, Fourth Ed. 431–456. https://doi.org/10.1201/b14550-34

Davies-Colley, R.J., 2013. River Water Quality in New Zealand : An Introduction and Overview. River Water Qual. 432–447.

de Jesús Arce-Mojica, T., Nehren, U., Sudmeier-Rieux, K., Miranda, P.J., Anhuf, D., 2019. Nature-based solutions (NbS) for reducing the risk of shallow landslides: Where do we stand? Int. J. Disaster Risk Reduct. 41. https://doi.org/10.1016/j.ijdrr.2019.101293

De Rose, R.C., 2013. Slope control on the frequency distribution of shallow landslides and associated soil properties, North Island, New Zealand. Earth Surf. Process. Landforms 38, 356–371. https://doi.org/10.1002/esp.3283

De Rose, R.C., Basher, L.R., 2011. Measurement of river bank and cliff erosion from sequential LIDAR and historical aerial photography. Geomorphology 126, 132–147. https://doi.org/10.1016/j.geomorph.2010.10.037

De Rose, R.C., Trustrum, N.A., Blaschke, P.M., 1993. Post-deforestation soil loss from steepland hillslopes in Taranaki, New Zealand. Earth Surf. Process. Landforms 18, 131–144.

de Walque, B., Degré, A., Maugnard, A., Bielders, C.L., 2017. Artificial surfaces characteristics and sediment connectivity explain muddy flood hazard in Wallonia. Catena 158, 89–101. https://doi.org/10.1016/j.catena.2017.06.016

Devkota, N.R., Kemp, P.D., Hodgson, J., Valentine, I., Jaya, I.K.D., 2009. Relationship between tree canopy height and the production of pasture species in a silvopastoral system based on alder trees. Agrofor. Syst. 76, 363–374. https://doi.org/10.1007/s10457-008-9192-8

Dickinson, W.T., Wall, G.J., 1977. The relationship between source-area erosion and sediment yield. Hydrol. Sci. Bull. 22, 527–530. https://doi.org/10.1080/02626667709491755

Dodd, M.B., McGowan, A.W., Power, I.L., Thorrold, B.S., 2005. Effects of variation in shade level, shade duration and light quality on perennial pastures. New Zeal. J. Agric. Res. 48, 531–543. https://doi.org/10.1080/00288233.2005.9513686

Dominati, E.J., Mackay, A., Lynch, B., Heath, N., Millner, I., 2014. An ecosystem services approach to the quantification of shallow mass movement erosion and the value of soil conservation practices. Ecosyst. Serv. 9, 204–215. https://doi.org/10.1016/j.ecoser.2014.06.006

Doody, D.G., Archbold, M., Foy, R.H., Flynn, R., 2012. Approaches to the implementation of the Water Framework Directive: Targeting mitigation measures at critical source areas of diffuse phosphorus in Irish catchments. J. Environ. Manage. 93, 225–234. https://doi.org/10.1016/j.jenvman.2011.09.002

Dorren, L., Schwarz, M., 2016. Quantifying the Stabilizing Effect of Forests on Shallow Landslide-Prone Slopes, in: Renaud, F.G., Sudmeier-Rieux, K., Estrella, M., Nehren, U. (Eds.), Ecosystem-Based Disaster Risk Reduction and Adaptation in Practice. Advances in Natural and Technological Hazards Research. Springer International Publishing Switzerland, pp. 255–270. https://doi.org/10.1007/978-3-319-43633-3

Douglas, G., Dymond, J., McIvor, I., 2008. Monitoring and reporting of whole farm plans as a tool for affecting land use change. Agresearch, Palmerston North, N.Z.

Douglas, G., McIvor, I.R., Manderson, A.K., Koolaard, J.P., Todd, M., Braaksma, S., Gray, R.A.., 2013a. Reducing shallow landslide occurrence in pastoral hill country using wide-spaced trees. L. Degrad. Dev. 24, 103–114. https://doi.org/10.1002/ldr.1106

Douglas, G., Wall, A.J., Dodd, M.B., Hawke, M.F., McIvor, I.R., 2013b. Balancing pastoral and plantation forestry options in New Zealand and the Role of Agroforestry. 22nd Int. Grasslands Congr.

Douglas, G.B., McIvor, I.R., Lloyd-West, C.M., 2016. Early root development of field-grown poplar: effects of planting material and genotype. New Zeal. J. For. Sci. 46, 1–14. https://doi.org/10.1186/s40490-015-0057-4

Douglas, G.B., Mcivor, I.R., Manderson, A.K., Todd, M., Braaksma, S., Gray, R.A., 2009. Effectiveness of space-planted trees for controlling soil slippage on pastoral hill country, Nutrient management in a rapidly changing world. Palmerston North.

Douglas, G.B., Walcroft, A.S., Hurst, S.E., Potter, J.F., Foote, A.G., Fung, L.E., Edwards, W.R.N., Van Den Dijssel, C., 2006a. Interactions between Widely Spaced Young Poplars (Populus spp.) and Introduced Pasture Mixtures. Agrofor. Syst. 66, 165–178. https://doi.org/10.1007/s10457-005-6641-5

Douglas, G.B., Walcroft, A.S., Hurst, S.E., Potter, J.F., Foote, A.G., Fung, L.E., Edwards, W.R.N., Van Den Dijssel, C., 2006b. Interactions between widely spaced young poplars (Populus spp.) and the understorey environment. Agrofor. Syst. 67, 177–186. https://doi.org/10.1007/s10457-005-3394-0

Douglas, G.B., Walcroft, A.S., Wills, B.J., Hurst, S.E., Foote, A.G., Trainor, K.D., Fung, L.E., 2001. Resident pasture growth and the micro-environment beneath young, widespaced poplars in New Zealand. Proc. New Zeal. Grassl. Assoc. 131–138. https://doi.org/10.33584/jnzg.2001.63.2441

Duncan, J.M., Wright, S.G., Brandon, T.L., 2014. Soil Strength and Slope Stability, 2nd ed. Wiley.

Dunnington, D., 2021. qgisprocess: Use 'QGIS' Processing Algorithms.

Dymond, J.R., Ausseil, A.-G., Shepherd, J.D., Buettner, L., 2006. Validation of a region-wide model of landslide susceptibility in the Manawatu–Wanganui region of New Zealand. Geomorphology 74, 70–79. https://doi.org/10.1016/j.geomorph.2005.08.005

Dymond, J.R., Davies-Colley, R.J., Hughes, A.O., Matthaei, C.D., 2017a. Predicting improved optical water quality in rivers resulting from soil conservation actions on land. Sci. Total Environ. 603–604, 584–592. https://doi.org/10.1016/j.scitotenv.2017.06.116

Dymond, J.R., Davies-Colley, R.J., Hughes, A.O., Matthaei, C.D., 2017b. Predicting improved optical water quality in rivers resulting from soil conservation actions on land. Sci. Total Environ. 603–604, 584–592. https://doi.org/10.1016/j.scitotenv.2017.06.116

Dymond, J.R., Herzig, A., Basher, L., Betts, H.D., Marden, M., Phillips, C.J., Ausseil, A.G.E., Palmer, D.J., Clark, M., Roygard, J., 2016. Development of a New Zealand SedNet model for assessment of catchment-wide soil-conservation works. Geomorphology 257, 85–93. https://doi.org/10.1016/j.geomorph.2015.12.022

Dymond, J.R., Zörner, J., Shepherd, J.D., Wiser, S.K., Pairman, D., Sabetizade, M., 2019. Mapping physiognomic types of indigenous forest using space-borne SAR, optical imagery and air-borne LiDAR. Remote Sens. 11. https://doi.org/10.3390/rs11161911

Ekanayake, J.C., Marden, M., Watson, A.J., Rowan, D., 1997. Tree roots and slope stability: A comparison between pinus radiata and känuka. New Zeal. J. For. Sci. 27, 216–233.

El Khouli, R.H., Macura, K.J., Barker, P.B., Habba, M.R., Jacobs, M.A., Bluemke, D.A., 2009. Relationship of temporal resolution to diagnostic performance for dynamic contrast enhanced MRI of the breast. J. Magn. Reson. Imaging 30, 999–1004. https://doi.org/10.1002/jmri.21947

England, J.R., O'Grady, A.P., Fleming, A., Marais, Z., Mendham, D., 2020. Trees on farms to support natural capital: An evidence-based review for grazed dairy systems. Sci. Total Environ. 704, 135345. https://doi.org/10.1016/j.scitotenv.2019.135345

Fassnacht, F.E., Latifi, H., Stereńczak, K., Modzelewska, A., Lefsky, M., Waser, L.T., Straub, C., Ghosh, A., 2016. Review of studies on tree species classification from remotely sensed data. Remote Sens. Environ. 186, 64–87. https://doi.org/10.1016/j.rse.2016.08.013

Fassnacht, F.E., Neumann, C., Forster, M., Buddenbaum, H., Ghosh, A., Clasen, A., Joshi, P.K., Koch, B., 2014. Comparison of Feature Reduction Algorithms for Classifying Tree Species With Hyperspectral Data on Three Central European Test Sites. IEEE J. Sel. Top.

Appl. Earth Obs. Remote Sens. 7, 2547–2561. https://doi.org/10.1109/JSTARS.2014.2329390

Fischer, J., Stott, J., Law, B.S., 2010. The disproportionate value of scattered trees. Biol. Conserv. 143, 1564–1567. https://doi.org/10.1016/j.biocon.2010.03.030

Foran, B., Wardle, K., 1995. Transitions in land use and the problems of planning: A case study from the mountainlands of New Zealand. J. Environ. Manage. 43, 97–127. https://doi.org/10.1016/S0301-4797(95)90101-9

Fox, J., Weisberg, S., 2010. An R Companion to Applied Regression, 2nd ed. SAGE Publications.

Friedman, J., Hastie, T., Tibshirani, R., 2010. Regularization Paths for Generalized Linear Models via Coordinate Descent. J. Stat. Softw. 33, 1–22. https://doi.org/10.18637/jss.v033.i01

Frost, W.E., McDougald, N.K., 1989. Tree canopy effects on herbaceous production of annual rangeland during drought. J. range Manag. 42, 281–283.

Fuller, I.C., Death, R.G., 2018. The science of connected ecosystems: What is the role of catchment-scale connectivity for healthy river ecology? L. Degrad. Dev. 29, 1413–1426. https://doi.org/10.1002/ldr.2903

Fuller, I.C., Rutherfurd, I.D., 2022. Geomorphic Responses to Anthropogenic Land-Cover Change in Australia and New Zealand, in: Shroder, J. (Jack) F.B.T.-T. on G. (Second E. (Ed.), Treatise on Geomorphology. Elsevier, Oxford, pp. 584–619. https://doi.org/10.1016/B978-0-12-818234-5.00104-8

Fuller, I.C., Rutherfurd, I.D., 2021. Geomorphic Responses to Anthropogenic Land-Cover Change in Australia and New Zealand, in: Reference Module in Earth Systems and Environmental Sciences. Elsevier. https://doi.org/https://doi.org/10.1016/B978-0-12-818234-5.00104-8

Galli, M., Ardizzone, F., Cardinali, M., Guzzetti, F., Reichenbach, P., 2008. Comparing landslide inventory maps. Geomorphology 94, 268–289. https://doi.org/https://doi.org/10.1016/j.geomorph.2006.09.023

Gao, J., Maro, J., 2010. Topographic controls on evolution of shallow landslides in pastoral Wairarapa, New Zealand, 1979-2003. Geomorphology 114, 373–381. https://doi.org/10.1016/j.geomorph.2009.08.002

Gebrewahid, Y., Teka, K., Tewolde-berhan, S., Birhane, E., Eyasu, G., Meresa, E., 2019.

Dispersed trees on smallholder farms enhance soil fertility in semi-arid Ethiopia.

Geertsema, M., Schwab, J.W., Jordan, P., Millard, T.H., Rollerson, T.P., 2010. Hillslope processes, in: Pike, R.G., Redding, T.E., Moore, R.D., Winkler, R.D., Bladon, K.D. (Eds.), Compendium of Forest Hydrology and Geomorphology in British Columbia. Volume 1 of 2. B.C. Min. For. Range, For. Sci. Prog., Victoria, B.C. and FORREX Forum for Research and Extension in Natural Resources, Kamloops, B.C., pp. 213–273.

Genet, M., Stokes, A., Fourcaud, T., Norris, J.E., 2010. The influence of plant diversity on slope stability in a moist evergreen deciduous forest. Ecol. Eng. 36, 265–275. https://doi.org/10.1016/j.ecoleng.2009.05.018

Gessesse, A.A., Melesse, A.M., 2019. Temporal relationships between time series CHIRPS-rainfall estimation and eMODIS-NDVI satellite images in Amhara Region, Ethiopia, in: Melesse, A.M., Abtew, W., Senay, G. (Eds.), Extreme Hydrology and Climate Variability. Elsevier, pp. 81–92. https://doi.org/10.1016/B978-0-12-815998-9.00008-7

Giadrossich, F., Cohen, D., Schwarz, M., Ganga, A., Marrosu, R., Pirastru, M., Capra, G.F., 2019. Large roots dominate the contribution of trees to slope stability. Earth Surf. Process. Landforms 44, 1602–1609. https://doi.org/10.1002/esp.4597

Giadrossich, F., Schwarz, M., Cohen, D., Cislaghi, A., Vergani, C., Hubble, T., Phillips, C., Stokes, A., 2017. Methods to measure the mechanical behaviour of tree roots: A review. Ecol. Eng. 109, 256–271. https://doi.org/10.1016/j.ecoleng.2017.08.032

Giadrossich, F., Schwarz, M., Cohen, D., Preti, F., Or, D., 2013. Mechanical interactions between neighbouring roots during pullout tests. Plant Soil 367, 391–406. https://doi.org/10.1007/s11104-012-1475-1

Giadrossich, F., Schwarz, M., Marden, M., Marrosu, R., Phillips, C., 2020. Minimum representative root distribution sampling for calculating slope stability in pinus radiata d.Don plantations in New Zealand. New Zeal. J. For. Sci. 50, 1–12. https://doi.org/10.33494/nzjfs502020x68x

Gilchrist, A.N., deZ Hall, J.R., Foote, A.G., Bulloch, B.T., 1993. Pasture growth around broad-leaved trees planted for grassland stability, in: Proceedings of the XVII International Grassland Congress. Rockhampton, Australia, pp. 2062–2063.

Glade, T., 2003. Landslide occurrence as a response to land use change: A review of evidence from New Zealand. Catena 51, 297–314. https://doi.org/10.1016/S0341-8162(02)00170-4

Glade, T., 1998. Establishing the frequency and magnitude of landslide-triggering rainstorm events in New Zealand. Environ. Geol. 35, 160–174.

Glade, T., Crozier, M. J., 2005. The Nature of Landslide Hazard Impact, in: Glade, Thomas, Anderson, M., Crozier, Michael J. (Eds.), Landslide Hazard and Risk. John Wiley & Sons, Ltd, pp. 43–74.

Goff, J.R., 1997. A chronology of natural and anthropogenic influences on coastal sedimentation, New Zealand. Mar. Geol. 138, 105–117. https://doi.org/10.1016/S0025-3227(97)00018-2

Gómez, C., White, J.C., Wulder, M.A., 2016. Optical remotely sensed time series data for land cover classification: A review. ISPRS J. Photogramm. Remote Sens. 116, 55–72. https://doi.org/10.1016/j.isprsjprs.2016.03.008

Gonzalez-Ollauri, A., Mickovski, S.B., 2017. Hydrological effect of vegetation against rainfall-induced landslides. J. Hydrol. 549, 374–387. https://doi.org/10.1016/j.jhydrol.2017.04.014

Gordon, A.M., Newman, S.M., Coleman, B.R.W., Thevathasan, N.V., 2018. Temperate Agroforestry: An Overview, in: Gordon, Andrew M., Newman, Steven M., Coleman, Brent R.W. (Eds.), Temperate Agroforestry Systems. CAB International, pp. 1–6.

Gorsevski, P. V., Gessler, P.E., Boll, J., Elliot, W.J., Foltz, R.B., 2006. Spatially and temporally distributed modeling of landslide susceptibility. Geomorphology 80, 178–198. https://doi.org/10.1016/j.geomorph.2006.02.011

Graf, F., Frei, M., Böll, A., 2009. Effects of vegetation on the angle of internal friction of a moraine. For. Snow Landsc. Res. 82, 61–77.

Green, M.O., 2013. Catchment sediment load limits to achieve estuary sedimentation targets. New Zeal. J. Mar. Freshw. Res. 47, 153–180. https://doi.org/10.1080/00288330.2012.757241

Gregory, P.J., 2006. Plant roots: growth, activity, and interaction with soils. Blackwell Pub., Oxford.

Guevara-Escobar, A., Kemp, P.D., Hodgson, J., Mackay, A.D., Edwards, W.R.N., 1997. Case study of a mature Populus deltoides-pasture system in a hill environment. Proc. New Zeal. Grassl. Assoc. 185, 179–185. https://doi.org/10.33584/jnzg.1997.59.2239

Guevara-Escobar, A., Mackay, A.D., Hodgson, J., Kemp, P.D., 2002. Soil properties of a widely spaced, planted poplar (<emph type="2">Populus

deltoides</emph>)–pasture system in a hill environment. Soil Res. 40, 873–886.

Guisan, A., Weiss, S.B., Weiss, A.D., 1999. GLM versus CCA spatial modeling of plant species distribution. Plant Ecol. 143, 107–122. https://doi.org/10.1023/A:1009841519580

Gunawardena, A.R., Nissanka, S.P., Dayawansa, N.D.K., Fernando, T.T., 2015. Estimation of above ground biomass in Horton Plains National Park, Sri Lanka using Optical, thermal and RADAR remote sensing data. Trop. Agric. Res. 26, 608. https://doi.org/10.4038/tar.v26i4.8123

Guzzetti, F., Carrara, A., Cardinali, M., Reichenbach, P., 1999. Landslide hazard evaluation: a review of current techniques and their application in a multi-scale study, Central Italy. Geomorphology 31, 181–216.

Guzzetti, F., Galli, M., Reichenbach, P., Ardizzone, F., Cardinali, M., 2006. Landslide hazard assessment in the Collazzone area, Umbria, central Italy. Nat. Hazards Earth Syst. Sci. 6, 115–131. https://doi.org/10.5194/nhess-6-115-2006

Hairiah, K., Widianto, W., Suprayogo, D., Van Noordwijk, M., 2020. Tree roots anchoring and binding soil: Reducing landslide risk in Indonesian agroforestry. Land 9, 1–19. https://doi.org/10.3390/LAND9080256

Hales, T.C., 2018. Modelling biome-scale root reinforcement and slope stability. Earth Surf. Process. Landforms 43, 2157–2166. https://doi.org/10.1002/esp.4381

Hales, T.C., Ford, C.R., Hwang, T., Vose, J.M., Band, L.E., 2009. Topographic and ecologic controls on root reinforcement. J. Geophys. Res. Earth Surf. 114, 1–17. https://doi.org/10.1029/2008JF001168

Hamza, O., Bengough, A.G., Bransby, M.F., Davies, M.C.R., Hallett, P.D., 2007. Mechanics of root-pullout from soil: A novel image and stress analysis procedure, in: Eco-and Ground Bio-Engineering: The Use of Vegetation to Improve Slope Stability : Proceedings of the First International Conference on Eco-Engineering 13-17 September 2004, Developments in Plant and Soil Sciences TA - TT -. Dordrecht : Springer Netherlands, pp. 213–221. https://doi.org/10.1007/978-1-4020-5593-5_20 LK - https://landcareresearch.on.worldcat.org/oclc/5665207311

Haralick, R.M., 1983. Ridges and valleys on digital images. Comput. Vision, Graph. Image Process. 22, 28–38. https://doi.org/10.1016/0734-189X(83)90094-4

Harvey, A.M., 2002. Effective timescales of coupling within fluvial systems. Geomorphology 44, 175–201. https://doi.org/10.1016/S0169-555X(01)00174-X

Harvey, A.M., 2001. Coupling between hillslopes and channels in upland fluvial systems: implications for landscape sensitivity, illustrated from the Howgill Fells, northwest England. Catena 42, 225–250.

Hastie, T., Tibshirani, R., Friedman, J., 2001. The Elements of Statistical Learning. Math. Intell. 27, 83–85. https://doi.org/10.1198/jasa.2004.s339

Hathaway, R.L., Van Kraayenoord, C.W.S., Directorate, N.Z.W. and S., Authority, N.Z.N.W. and S.C., 1987. Plant Materials Handbook for Soil Conservation. Volume 1, Principles and Practices, Water & soil miscellaneous publication. National Water and Soil Conservation Authority.

Hawke, M.F., 1991. Pasture production and animal performance under pine agroforestry in New Zealand. For. Ecol. Manage. 45, 109–118. https://doi.org/10.1016/0378-1127(91)90210-M

Hawley, J.G., Dymond, J.R., 1988. How much do trees reduce landsliding? J. Soil Water Conserv. 43, 495–498.

He, L.P., Yu, J.Y., Hu, Q.J., Cai, Q.J., Qu, M.F., He, T.J., 2020. Study on crack propagation and shear behavior of weak muddy intercalations submitted to wetting-drying cycles. Bull. Eng. Geol. Environ. 79, 4873–4889. https://doi.org/10.1007/s10064-020-01842-7

Heckmann, T., Cavalli, M., Cerdan, O., Foerster, S., Javaux, M., Lode, E., Smetanová, A., Vericat, D., Brardinoni, F., 2018. Indices of sediment connectivity: opportunities, challenges and limitations. Earth-Science Rev. 187, 77–108. https://doi.org/10.1016/j.earscirev.2018.08.004

Heckmann, T., Gegg, K., Gegg, A., Becht, M., 2014. Sample size matters: Investigating the effect of sample size on a logistic regression susceptibility model for debris flows. Nat. Hazards Earth Syst. Sci. 14, 259–278. https://doi.org/10.5194/nhess-14-259-2014

Heckmann, T., Schwanghart, W., 2013. Geomorphic coupling and sediment connectivity in an alpine catchment - Exploring sediment cascades using graph theory. Geomorphology 182, 89–103. https://doi.org/10.1016/j.geomorph.2012.10.033

Heckmann, T., Vericat, D., 2018. Computing spatially distributed sediment delivery ratios: inferring functional sediment connectivity from repeat high-resolution digital elevation models. Earth Surf. Process. Landforms 43, 1547–1554. https://doi.org/10.1002/esp.4334

Hicks, D.L., 1992. Impact of soil conservation on storm-damaged hill country grazing lands in New Zealand. Aust. J. Soil Water Conserv. 5, 34–40.

Hicks, D.L., 1989a. Storm damage to bush, pasture and forest : a comparison from Cyclone Bola, Division of Land and Soil Sciences technical record PN. DSIR Division of Land and Soil Sciences, Palmerston North SE - 5, [5] leaves : illustrations ; 31 cm.

Hicks, D.L., 1989b. Farm conservation measures' effect on hill country erosion: an assessment in the wake of Cyclone Bola, Division of Land and Soil Sciences technical record PN. NZ Dept. of Scientific and Industrial Research, [Palmerston North, N.Z.] SE - 8, [1] leaves : ill. ; 30 cm.

Hicks, D.M., Gomez, B., Trustrum, N.A., 2000. Erosion thresholds and suspended sediment yields, Waipaoa River Basin, New Zealand. Water Resour. Res. 36, 1129–1142. https://doi.org/10.1029/1999WR900340

Hicks, D.M., Hill, J., Shankar, U., 1996. Variation of suspended sediment yields around New Zealand: The relative importance of rainfall and geology. IAHS-AISH Publ. 236, 149–156.

Hicks, D.M., Semadeni-Davies, A., Haddadchi, A., Shankar, U., Plew, D., 2019. Updated sediment load estimator for New Zealand. NIWA Client Rep. 2018341CH.

Hicks, D.M., Shankar, U., Mckerchar, A.I., Basher, L., Lynn, I., Page, M., Jessen, M., 2011. Suspended sediment yields from New zealand rivers. J. Hydrol. New Zeal. 50, 81–142.

Hijmans, R.J., 2021. raster: Geographic data analysis and modeling.

Hjerdt, K.N., Mcdonnell, J.J., Seibert, J., Rodhe, A., 2004. A new topographic index to quantify downslope controls on local drainage 40, 1–6. https://doi.org/10.1029/2004WR003130

Hölbling, D., Betts, H., Spiekermann, R., Phillips, C., 2016. Semi-automated landslide mapping from historical and recent aerial photography. Proc. 19th Agil. 2016 Conf. Geogr. Inf. Sci. 14–17.

Holcombe, E., Smith, S., Wright, E., Anderson, M.G., 2012. An integrated approach for evaluating the effectiveness of landslide risk reduction in unplanned communities in the Caribbean, Natural Hazards. https://doi.org/10.1007/s11069-011-9920-7

Hong, H., Ilia, I., Tsangaratos, P., Chen, W., Xu, C., 2017. A hybrid fuzzy weight of evidence method in landslide susceptibility analysis on the Wuyuan area, China. Geomorphology 290, 1–16. https://doi.org/10.1016/j.geomorph.2017.04.002

Hoogmoed, M., Cunningham, S.C., Thomson, J.R., Baker, P.J., Beringer, J., Cavagnaro, T.R., 2012. Does afforestation of pastures increase sequestration of soil carbon in Mediterranean climates? Agric. Ecosyst. Environ. 159, 176–183.

https://doi.org/10.1016/j.agee.2012.07.011

Hooke, J., 2003. Coarse sediment connectivity in river channel systems: A conceptual framework and methodology. Geomorphology 56, 79–94. https://doi.org/10.1016/S0169-555X(03)00047-3

Hooke, J., Souza, J., 2021. Challenges of mapping, modelling and quantifying sediment connectivity. Earth-Science Rev. 223, 103847. https://doi.org/10.1016/j.earscirev.2021.103847

Hosmer, D.W., Lemeshow, S., 2000. Assessing the Fit of the Model, in: Applied Logistic Regression. John Wiley & Sons, Inc., Hoboken, NJ, USA, pp. 143–202. https://doi.org/10.1002/0471722146.ch5

Huang, Y., Zhao, L., 2018. Review on landslide susceptibility mapping using support vector machines. Catena 165, 520–529. https://doi.org/10.1016/j.catena.2018.03.003

Hubble, T.C.T., Docker, B.B., Rutherfurd, I.D., 2010. The role of riparian trees in maintaining riverbank stability: A review of Australian experience and practice. Ecol. Eng. 36, 292–304. https://doi.org/https://doi.org/10.1016/j.ecoleng.2009.04.006

Huntsinger, L., Johnson, M., Stafford, M., Fried, J., 2010. Hardwood rangeland landowners in California from 1985 to 2004: Production, ecosystem services, and permanence. Rangel. Ecol. Manag. 63, 324–334. https://doi.org/10.2111/08-166.1

Huntsinger, L., Oviedo, J.L., 2014. Ecosystem services are social-ecological services in a traditional pastoral system: The case of California's mediterranean rangelands. Ecol. Soc. 19. https://doi.org/10.5751/ES-06143-190108

Hürlimann, M., McArdell, B.W., Rickli, C., 2015. Field and laboratory analysis of the runout characteristics of hillslope debris flows in Switzerland. Geomorphology 232, 20–32. https://doi.org/10.1016/j.geomorph.2014.11.030

Iftekhar, M.S., Polyakov, M., 2021. Economics of Ecological Restoration. Oxford Res. Encycl. Environ. Sci. 1–24. https://doi.org/10.1093/acrefore/9780199389414.013.751

Istanbulluoglu, E., Bras, R.L., 2005. Vegetation-modulated landscape evolution: Effects of vegetation on landscape processes, drainage density, and topography. J. Geophys. Res. Earth Surf. 110, 1–19. https://doi.org/10.1029/2004JF000249

Iwasa, Y., Cohen, D., Leon, J.A., 1985. Tree height and crown shape, as results of competitive games. J. Theor. Biol. 112, 279–297. https://doi.org/10.1016/S0022-5193(85)80288-5

Jansson, M.B., 1988. A Global Survey of Sediment Yield. Geogr. Ann. Ser. A, Phys. Geogr. 70, 81–98. https://doi.org/10.1080/04353676.1988.11880241

Jennings, S.B., Brown, N.D., Sheil, D., 1999. Assessing forest canopies and understorey illumination: Canopy closure, canopy cover and other measures. Forestry 72, 59–73. https://doi.org/10.1093/forestry/72.1.59

Jia, G., Alvioli, M., Gariano, S.L., Marchesini, I., Guzzetti, F., Tang, Q., 2021. A global landslide non-susceptibility map. Geomorphology 389, 107804. https://doi.org/10.1016/j.geomorph.2021.107804

Joffre, R., Rambal, S., Ratte, J.P., 1999. The dehesa system of southern Spain and Portugal as a natural ecosystem mimic. Agrofor. Syst. 45, 57–79. https://doi.org/10.1023/a:1006259402496

Jonckheere, I., Fleck, S., Nackaerts, K., Muys, B., Coppin, P., Weiss, M., Baret, F., 2004. Review of methods for in situ leaf area index determination Part I. Theories, sensors and hemispherical photography. Agric. For. Meteorol. 121, 19–35. https://doi.org/10.1016/j.agrformet.2003.08.027

Jones, H., Clough, P., Höck, B., Phillips, C., 2008. Economic costs of hill country erosion and benefits of mitigation in New Zealand : Review and recommendation of approach Economic costs of hill country erosion and benefits of mitigation in New Zealand : Review and recommendation of approach.

Jones, K.E., Preston, N.J., 2012. Spatial and temporal patterns of off-slope sediment delivery for small catchments subject to shallow landslides within the Waipaoa catchment, New Zealand. Geomorphology 141–142, 150–159. https://doi.org/10.1016/j.geomorph.2011.12.037

Jorgensen, S., 2016. Introduction to Systems Ecology, NV-1 onl. ed, Applied Ecology and Environmental Management ; v. 4. CRC Press, Hoboken. https://doi.org/10.1201/b11877

Kanungo, D.P., Arora, M.K., Sarkar, S., Gupta, R.P., 2009. Landslide Susceptibility Zonation (LSZ) Mapping - A Review. J. Asian Earth Sci. 2, 81–105.

Kasai, M., Yamada, T., 2019. Topographic effects on frequency-size distribution of landslides triggered by the Hokkaido Eastern Iburi Earthquake in 2018. Earth, Planets Sp. 71. https://doi.org/10.1186/s40623-019-1069-8

Kemp, P.D., Hawke, M.F., Knowles, R.L., 2018. Temperate agroforestry systems in New Zealand., in: Temperate Agroforestry Systems. CABI, Wallingford, pp. 224–236.

https://doi.org/10.1079/9781780644851.0224

Kienberger, S., Spiekermann, R., Tiede, D., Zeiler, I., Bussink, C., 2016. Spatial risk assessment of opium poppy cultivation in Afghanistan: integrating environmental and socio-economic drivers. Int. J. Digit. Earth. https://doi.org/10.1080/17538947.2016.1250828

Kim, D., Im, S., Lee, C., Woo, C., 2013. Modeling the contribution of trees to shallow landslide development in a steep, forested watershed. Ecol. Eng. 61, 658–668. https://doi.org/10.1016/j.ecoleng.2013.05.003

Knevels, R., Brenning, A., Gingrich, S., Heiss, G., Lechner, T., Leopold, P., Plutzar, C., Proske, H., Petschko, H., 2021. Towards the use of land use legacies in landslide modeling: Current challenges and future perspectives in an austrian case study. Land 10, 1–28. https://doi.org/10.3390/land10090954

Knevels, R., Petschko, H., Proske, H., Leopold, P., Maraun, D., Brenning, A., 2020. Event-based landslide modeling in the styrian basin, Austria: Accounting for time-varying rainfall and land cover. Geosci. 10, 1–29. https://doi.org/10.3390/geosciences10060217

Kopecký, M., Macek, M., Wild, J., 2021. Topographic Wetness Index calculation guidelines based on measured soil moisture and plant species composition. Sci. Total Environ. 757, 143785. https://doi.org/10.1016/j.scitotenv.2020.143785

Korhonen, L., Korhonen, K.T., Rautiainen, M., Stenberg, P., 2006. Estimation of forest canopy cover: A comparison of field measurement techniques. Silva Fenn. 40, 577–588. https://doi.org/10.14214/sf.315

Kuhn, M., 2008. Building predictive models in R using the caret package. J. Stat. Softw. 28, 1–26.

Kumar, B.M., Jose, S., 2018. Phenotypic plasticity of roots in mixed tree species agroforestry systems: review with examples from peninsular India. Agrofor. Syst. 92, 59–69. https://doi.org/10.1007/s10457-016-0012-2

Laio, F., 2006. A vertically extended stochastic model of soil moisture in the root zone. Water Resour. Res. 42, 1–10. https://doi.org/10.1029/2005WR004502

Lambert, M.G., Trustrum, N.A., Costall, D.A., 1984. Effect of soil slip erosion on seasonally dry wairarapa hill pastures. New Zeal. J. Agric. Res. 27, 57–64. https://doi.org/10.1080/00288233.1984.10425732

Lateltin, O., Haemmig, C., Raetzo, H., Bonnard, C., 2005. Landslide risk management in

Switzerland. Landslides 2, 313–320. https://doi.org/10.1007/s10346-005-0018-8

Lau, A., Calders, K., Bartholomeus, H., Martius, C., Raumonen, P., Herold, M., Vicari, M., Sukhdeo, H., Singh, J., Goodman, R.C., 2019. Tree biomass equations from terrestrial LiDAR: A case study in Guyana. Forests 10, 1–18. https://doi.org/10.3390/f10060527

Lee, J.M., Begg, J.G., 2002. Geology of the Wairarapa area: scale 1:250,000, Geological. ed. Institute of Geological & Nuclear Sciences.

Leenaars, J.G.B., Claessens, L., Heuvelink, G.B.M., Hengl, T., Ruiperez González, M., van Bussel, L.G.J., Guilpart, N., Yang, H., Cassman, K.G., 2018. Mapping rootable depth and root zone plant-available water holding capacity of the soil of sub-Saharan Africa. Geoderma 324, 18–36. https://doi.org/10.1016/j.geoderma.2018.02.046

Legros, F., 2002. The mobility of long-runout landslides. Eng. Geol. 63, 301–331. https://doi.org/10.1016/S0013-7952(01)00090-4

Levia, D.F., Germer, S., 2015. A review of stemflow generation dynamics and stemflow-environment interactions in forests and shrublands. Rev. Geophys. https://doi.org/10.1002/2015RG000479

Lexartza-Artza, I., Wainwright, J., 2009. Hydrological connectivity: Linking concepts with practical implications. Catena 79, 146–152. https://doi.org/10.1016/j.catena.2009.07.001

Li, F.Y., Snow, V.O., Holzworth, D.P., 2011. Modelling the seasonal and geographical pattern of pasture production in New Zealand. New Zeal. J. Agric. Res. 54, 331–352. https://doi.org/10.1080/00288233.2011.613403

Li, S., Brandt, M., Fensholt, R., Kariryaa, A., Igel, C., Gieseke, F., Nord-Larsen, T., Oehmcke, S., Carlsen, A.H., Junttila, S., Tong, X., D'Aspremont, A., Ciais, P., 2022. Digital twinning of all forest and non-forest trees at national level via deep learning. available Res. Sq. PREPRINT. https://doi.org/https://doi.org/10.21203/rs.3.rs-1661442/v1

Liang, W.L., Kosugi, K., Mizuyama, T., 2011. Soil water dynamics around a tree on a hillslope with or without rainwater supplied by stemflow. Water Resour. Res. 47, 1–16. https://doi.org/10.1029/2010WR009856

Lilburne, L.R., Hewitt, A.E., Webb, T.W., 2012. Soil and informatics science combine to develop S-map: A new generation soil information system for New Zealand. Geoderma 170, 232–238. https://doi.org/https://doi.org/10.1016/j.geoderma.2011.11.012

Lindh, M., Falster, D.S., Zhang, L., Dieckmann, U., Brännström, Å., 2018. Latitudinal effects on crown shape evolution. Int. J. Bus. Innov. Res. 17, 8149–8158.

https://doi.org/10.1002/ece3.4275

Liu, J.K., Shih, P.T.Y., 2013. Topographic correction of Wind-Driven rainfall for landslide analysis in central Taiwan with validation from Aerial and satellite optical images. Remote Sens. 5, 2571–2589. https://doi.org/10.3390/rs5062571

Lombardo, L., Mai, P.M., 2018. Presenting logistic regression-based landslide susceptibility results. Eng. Geol. 244, 14–24. https://doi.org/10.1016/j.enggeo.2018.07.019

Lombardo, L., Opitz, T., Ardizzone, F., Guzzetti, F., Huser, R., 2020. Space-time landslide predictive modelling. Earth-Science Rev. 209, 103318. https://doi.org/10.1016/j.earscirev.2020.103318

Lombardo, L., Opitz, T., Huser, R., 2018. Point process-based modeling of multiple debris flow landslides using INLA: an application to the 2009 Messina disaster. Stoch. Environ. Res. Risk Assess. 32, 2179–2198. https://doi.org/10.1007/s00477-018-1518-0

Lombardo, L., Tanyas, H., Huser, R., Guzzetti, F., Castro-Camilo, D., 2021. Landslide size matters: A new data-driven, spatial prototype. Eng. Geol. 293. https://doi.org/10.1016/j.enggeo.2021.106288

Lucas, M., Schlüter, S., Vogel, H.J., Vetterlein, D., 2019. Roots compact the surrounding soil depending on the structures they encounter. Sci. Rep. 9, 1–13. https://doi.org/10.1038/s41598-019-52665-w

Lucía, A., Comiti, F., Borga, M., Cavalli, M., Marchi, L., 2015. Dynamics of large wood during a flash flood in two mountain catchments. Nat. Hazards Earth Syst. Sci. 15, 1741–1755. https://doi.org/10.5194/nhess-15-1741-2015

Mackay-Smith, T.H., Burkitt, L., López, I.F., Janet, R., 2022a. Kānuka as a silvopastoral tree for low producing hill country, in: Christensen, C.L., Horne, D.J., Singh, R. (Eds.), Adaptive Strategies for Future Farming. Occasional Report No. 34. Farmed Landscapes Research Centre, Massey University., Palmerston North, New Zealand, pp. 1–4.

Mackay-Smith, T.H., Burkitt, L., Reid, J., López, I.F., Phillips, C., 2021. A Framework for Reviewing Silvopastoralism: A New Zealand Hill Country Case Study. Land 10, 1–28. https://doi.org/https://doi.org/10.3390/land10121386

Mackay-Smith, T.H., Burkitt, L.L., López, I.F., Reid, J.I., 2022b. The impact of a kānuka silvopastoral system on surface runoff and sediment and nutrient losses in New Zealand hill country. CATENA 213, 106215. https://doi.org/10.1016/j.catena.2022.106215

Manderson, A.K., Mackay, A.D., Palmer, A.P., 2007. Environmental whole farm management

plans: Their character, diversity, and use as agri-environmental indicators in New Zealand. J. Environ. Manage. 82, 319–331. https://doi.org/10.1016/j.jenvman.2005.05.020

Manning, A.D., Gibbons, P., Lindenmayer, D.B., 2009. Scattered trees: A complementary strategy for facilitating adaptive responses to climate change in modified landscapes? J. Appl. Ecol. 46, 915–919. https://doi.org/10.1111/j.1365-2664.2009.01657.x

Marden, M., 2012. Effectiveness of reforestation in erosion mitigation and implications for future sediment yields, East Coast catchments, New Zealand: A review. N. Z. Geog. 68, 24–35. https://doi.org/10.1111/j.1745-7939.2012.01218.x

Marden, Michael, Fuller, I.C., Herzig, A., Betts, H.D., 2018. Badass gullies: Fluvio-mass-movement gully complexes in New Zealand's East Coast region, and potential for remediation. Geomorphology 307, 12–23. https://doi.org/10.1016/j.geomorph.2017.11.012

Marden, M., Herzig, A., Basher, L., 2014. Erosion process contribution to sediment yield before and after the establishment of exotic forest: Waipaoa catchment, New Zealand. Geomorphology 226, 162–174. https://doi.org/10.1016/j.geomorph.2014.08.007

Marden, M., Lambie, S., Rowan, D., 2018. Root system attributes of 12 juvenile indigenous early colonising shrub and tree species with potential for mitigating erosion in New Zealand. New Zeal. J. For. Sci. 48, 1–19. https://doi.org/10.1186/s40490-018-0115-9

Marden, M., Phillips, C., Rowan, D., 1991. Declining soil loss with increasing age of plantation forests in the Uawa catchment, East Coast region, North Island, New Zealand., in: International Conference on Sustainable Land Management. Napier, pp. 358–361.

Marden, M., Phillips, C.J., 2013. Survival and growth of poplar and willow pole plantings on East Coast hill country.

Marden, M., Rowan, D., 1993. Protective value of vegetation on Tertiary terrain before and during Cyclone Bola, East Coast, North Island, New Zealand. New Zeal. J. For. Sci. 23, 255–263.

Martini, L., Cavalli, M., Picco, L., 2022. Predicting sediment connectivity in a mountain basin: A quantitative analysis of the index of connectivity. Earth Surf. Process. Landforms 1–14. https://doi.org/10.1002/esp.5331

Masi, E.B., Segoni, S., Tofani, V., 2021. Root Reinforcement in Slope Stability Models: A Review. Geosciences 11, 212. https://doi.org/10.3390/geosciences11050212

McDowell, R.W., 2014. Estimating the mitigation of anthropogenic loss of phosphorus in New Zealand grassland catchments. Sci. Total Environ. 468–469, 1178–1186. https://doi.org/10.1016/j.scitotenv.2013.03.056

McDowell, R.W., Monaghan, R.M., Smith, C., Manderson, A., Basher, L., Burger, D.F., Laurenson, S., Pletnyakov, P., Spiekermann, R., Depree, C., 2020. Quantifying contaminant losses to water from pastoral land uses in New Zealand III. What could be achieved by 2035? New Zeal. J. Agric. Res. 0, 1–21. https://doi.org/10.1080/00288233.2020.1844763

McDowell, R.W., Schallenberg, M., Larned, S., 2018. A strategy for optimizing catchment management actions to stressor-response relationships in freshwaters. Ecosphere 9, e02482. https://doi.org/10.1002/ecs2.2482

McGregor, E., Mackay, A., Dodd, M., Kemp, P., 1999. Silvopastoralism using tended poplars on New Zealand hill country: The opportunities. Proc. New Zeal. Grassl. Assoc. 89, 85–89. https://doi.org/10.33584/jnzg.1999.61.2360

McIvor, I., Clarke, K., Douglas, G.B., 2015. Effectiveness of conservation trees in reducing erosion following a storm event, in: LD, C., LL., B. (Eds.), Proceedings 28th Annual Fertiliser and Lime Research Centre Workshop 'Moving Farm Systems to Improved Attenuation'. Occasional Report 28. Palmerston North: Fertiliser and Lime Research Centre.

McIvor, I., Douglas, G., Dymond, J., Eyles, G., Marde, M., 2011. Pastoral Hill Slope Erosion in New Zealand and the Role of Poplar and Willow Trees in Its Reduction, in: Godone, D., Stanchi, S. (Eds.), Soil Erosion Issues in Agriculture. InTech, pp. 257–278. https://doi.org/10.5772/24365

McIvor, I.R., Douglas, G.B., Benavides, R., 2009. Coarse root growth of Veronese poplar trees varies with position on an erodible slope in New Zealand. Agrofor. Syst. 76, 251–264. https://doi.org/10.1007/s10457-009-9209-y

McIvor, I.R., Douglas, G.B., Hurst, S.E., Hussain, Z., Foote, A.G., 2008. Structural root growth of young Veronese poplars on erodible slopes in the southern North Island, New Zealand. Agrofor. Syst. 72, 75–86. https://doi.org/10.1007/s10457-007-9090-5

Millner, J.P., Kemp, P.D., 2012. Seasonal growth of Eucalyptus species in New Zealand hill country. New For. 43, 31–44. https://doi.org/10.1007/s11056-011-9264-x

Moir, J.L., Scotter, D.R., Hedley, M.J., Mackay, A.D., 2000. A climate-driven, soil fertility dependent, pasture production model. New Zeal. J. Agric. Res. 43, 491–500.

https://doi.org/10.1080/00288233.2000.9513445

Monaghan, R., Manderson, A., Basher, L., Spiekermann, R., Dymond, J., Smith, C., Muirhead, R., Burger, D., McDowell, R., 2021. Quantifying contaminant losses to water from pastoral landuses in New Zealand II. The effects of some farm mitigation actions over the past two decades. New Zeal. J. Agric. Res. 0, 1–25. https://doi.org/10.1080/00288233.2021.1876741

Mondini, A.C., Guzzetti, F., Reichenbach, P., Rossi, M., Cardinali, M., Ardizzone, F., 2011. Semi-automatic recognition and mapping of rainfall induced shallow landslides using optical satellite images. Remote Sens. Environ. 115, 1743–1757. https://doi.org/10.1016/J.RSE.2011.03.006

Montagnini, F., Nair, P.K.R., 2004. Carbon sequestration: An underexploited environmental benefit of agroforestry systems. Agrofor. Syst. 61–62, 281–295. https://doi.org/10.1023/B:AGFO.0000029005.92691.79

Moore, I.D., Burch, G.J., Mackenzie, D.H., 1988. Topographic Effects on the Distribution of Surface Soil Water and the Location of Ephemeral Gullies. Trans. ASAE 31, 1098–1107. https://doi.org/10.13031/2013.30829

Moore, I.D., Grayson, R.B., Ladson, A.R., 1991. Digital terrain modelling: A review of hydrological, geomorphological, and biological applications. Hydrol. Process. 5, 3–30. https://doi.org/https://doi.org/10.1002/hyp.3360050103

Moos, C., Bebi, P., Graf, F., Mattli, J., Rickli, C., Schwarz, M., 2016. How does forest structure affect root reinforcement and susceptibility to shallow landslides? Earth Surf. Process. Landforms 41, 951–960. https://doi.org/10.1002/esp.3887

Moreno, G., 2008. Response of understorey forage to multiple tree effects in Iberian dehesas. Agric. Ecosyst. Environ. 123, 239–244. https://doi.org/https://doi.org/10.1016/j.agee.2007.04.006

Moreno, G., Pulido, F.J., 2008. The Functioning, Management and Persistence of Dehesas, in: Rigueiro-Rodróguez, A., McAdam, J., Mosquera-Losada, M.R. (Eds.), Agroforestry in Europe: Current Status and Future Prospects. Springer Science, Dordrecht, pp. 127–160. https://doi.org/10.1007/978-1-4020-8272-6_7

Moreno Marcos, G., Obrador, J.J., García, E., Cubera, E., Montero, M.J., Pulido, F., Dupraz, C., 2007. Driving competitive and facilitative interactions in oak dehesas through management practices. Agrofor. Syst. 70, 25–40. https://doi.org/10.1007/s10457-007-9036-y

Mosquera-Losada, M.R., Rigueiro-Rodríguez, A., Fernández-Núñez, E., 2018. Deciduous plantations established on former agricultural land in northwest of Spain as silvopastoralism: Tree growth; pasture production and vascular plant biodiversity. Catena 169, 1–10. https://doi.org/10.1016/j.catena.2018.05.012

Muenchow, J., Schratz, P., Brenning, A., 2017. RQGIS: Integrating R with QGIS. R J. 9, 409–428.

Murgia, I., Giadrossich, F., Mao, Z., Cohen, D., Capra, G.F., Schwarz, M., 2022. Modeling shallow landslides and root reinforcement: A review. Ecol. Eng. 181, 106671. https://doi.org/10.1016/j.ecoleng.2022.106671

Nair, P.K.R., Kumar, B.M., Nair, V.D., 2021. An Introduction to Agroforestry, 2nd ed. Springer International Publishing, Cham. https://doi.org/10.1007/978-3-030-75358-0

Najafi, S., Dragovich, D., Heckmann, T., Sadeghi, S.H., 2021a. Sediment connectivity concepts and approaches. Catena 196, 104880. https://doi.org/10.1016/j.catena.2020.104880

Najafi, S., Sadeghi, S.H., Heckmann, T., 2021b. Analysis of sediment accessibility and availability concepts based on sediment connectivity throughout a watershed. L. Degrad. Dev. 32, 3023–3044. https://doi.org/10.1002/ldr.3964

Neverman, A., Djanibekov, U., Soliman, T., Walsh, P., Spiekermann, R., Basher, L., 2019. Impact testing of a proposed sediment attribute: Identifying erosion and sediment control mitigations to meet proposed sediment attribute bottom lines and the costs and benefits of those mitigations. Client report prepared by Manaaki Whenua – Landcare R.

New Zealand Government, 2020a. National Policy Statement for Freshwater Management 2020.

New Zealand Government, 2020b. Resource Management Amendment Act 2020.

Newsome, P.F.J., Wilde, R.H., Willoughby, E.J., 2008. Land Resource Information System Spatial: Data Layers. Landcare Research New Zealand.

Nilaweera, N.S., Nutalaya, P., 1999. Role of tree roots in slope stabilisation. Bull. Eng. Geol. Environ. 57, 337–342. https://doi.org/10.1007/s100640050056

Norton, D.A., Suryaningrum, F., Buckley, H.L., Case, B.S., Hamish Cochrane, C., Forbes, A.S., Harcombe, M., 2020. Achieving win-win outcomes for pastoral farming and biodiversity conservation in New Zealand. N. Z. J. Ecol. 44. https://doi.org/10.20417/nzjecol.44.15

Norton, J.D., 2021. The Material Theory of Induction Stated and Illustrated, The Material

Theory of Induction. University of Calgary Press.

O'Brien, R.M., 2007. A caution regarding rules of thumb for variance inflation factors. Qual. Quant. 41, 673–690. https://doi.org/10.1007/s11135-006-9018-6

Obrador, O.J.J., García, L.E., Moreno, G., 2004. Consequences of Dehesa Land Use on Nutritional Status of, in: Schnabel, S., Ferreira, A. (Eds.), Sustainability of Agrosilvopastoral Systems: Dehesas, Montados. Advances in Geo-Ecology, Volume 37. Catena, pp. 327–340.

Owens, P.N., 2009. Adaptive management frameworks for natural resource management at the landscape scale: Implications and applications for sediment resources. J. Soils Sediments 9, 578–593. https://doi.org/10.1007/s11368-009-0137-2

Ozier-Lafontaine, H., Lecompte, F., Sillon, J.F., 1999. Fractal analysis of the root architecture of Gliricidia sepium for the spatial prediction of root branching, size and mass: Model development and evaluation in agroforestry. Plant Soil 209, 167–179. https://doi.org/10.1023/A:1004461130561

Page, M. ~J., Trustrum, N. ~A., Dymond, J. ~R., 1994. Sediment budget to assess the geomorphic effect of a cyclonic storm, New Zealand. Geomorphology 9, 169–188. https://doi.org/10.1016/0169-555X(94)90061-2

Page, M.J., Reid, L.M., Lynn, I.H., 1999. Sediment production from Cyclone Bola landslides, Waipaoa catchment. J. Hydrol. (New Zealand) 38, 289–308.

Pan, S., Guan, H., Chen, Y., Yu, Y., Nunes Gonçalves, W., Marcato Junior, J., Li, J., 2020. Land-cover classification of multispectral LiDAR data using CNN with optimized hyper-parameters. ISPRS J. Photogramm. Remote Sens. 166, 241–254. https://doi.org/10.1016/j.isprsjprs.2020.05.022

Papathoma-Köhle, M., Glade, T., 2013. The role of vegetation cover change for landslide hazard and risk., in: The Role of Ecosystems in Disaster Risk Reduction. UNU-Press, Tokyo, Japan, pp. 293–320.

Parminter, I., Dodd, M.B., Mackay, A.D., 2001. Economic analysis of poplar planting on steep hill country. Proc. New Zeal. Grassl. Assoc. 63, 127–130.

Peri, P.L., Bahamonde, H.A., Lencinas, M. V., Gargaglione, V., Soler, R., Ormaechea, S., Pastur, G.M., 2016. A review of silvopastoral systems in native forests of Nothofagus antarctica in southern Patagonia, Argentina. Agrofor. Syst. 90, 933–960. https://doi.org/10.1007/s10457-016-9890-6

Peri, P.L., Caballé, G., Hansen, N.E., Bahamonde, H.A., Lencinas, M. V., Müller, A.R. von, Ormaechea, S., Gargaglione, V., Soler, R., Sarasola, M., Rusch, V., Borrelli, L., Fernández, M.E., Gyenge, J., Tejera, L.E., Lloyd, C.E., Martínez Pastur, G., 2018. Silvopastoral systems in Patagonia, Argentina. Temp. Agrofor. Syst. 252–273. https://doi.org/10.1079/9781780644851.0252

Persichillo, M.G., Bordoni, M., Meisina, C., 2017. The role of land use changes in the distribution of shallow landslides. Sci. Total Environ. 574, 924–937. https://doi.org/10.1016/j.scitotenv.2016.09.125

Petschko, H., Brenning, A., Bell, R., Goetz, J., Glade, T., 2014. Assessing the quality of landslide susceptibility maps - Case study Lower Austria. Nat. Hazards Earth Syst. Sci. 14, 95–118. https://doi.org/10.5194/nhess-14-95-2014

Phillips, C., Hales, T., Smith, H., Basher, L., 2021. Shallow landslides and vegetation at the catchment scale : A perspective. Ecol. Eng. 173, 106436. https://doi.org/10.1016/j.ecoleng.2021.106436

Phillips, C., Marden, M., 2005. Reforestation Schemes to Manage Regional Landslide Risk, in: Glade, T., Anderson, M.G., Crozier, M.J. (Eds.), Landslide Hazard and Risk. John Wiley & Sons, Ltd., pp. 517–547.

Phillips, C., Marden, M., Basher, L.R., 2018. Geomorphology and forest management in New Zealand's erodible steeplands: An overview. Geomorphology 307, 107–121. https://doi.org/10.1016/j.geomorph.2017.07.031

Phillips, C.J., Ekanayake, J.C., Marden, M., 2011a. Root site occupancy modelling of young New Zealand native plants: Implications for soil reinforcement. Plant Soil 346, 201–214. https://doi.org/10.1007/s11104-011-0810-2

Phillips, C.J., Ekanayake, J.C., Marden, M., 2011b. Root site occupancy modelling of young New Zealand native plants: Implications for soil reinforcement. Plant Soil 346, 201–214. https://doi.org/10.1007/s11104-011-0810-2

Phillips, C.J., Marden, M., 2000. Review of plant performance for erosion control in the East Coast region.

Phillips, C.J., Marden, M., McIvor, I.R., Ekanayake, J.C., 2008. Decision support for sustainable land management: effectiveness of wide-spaced trees.

Phillips, C.J., Marden, M., Suzanne, L.M., 2014. Observations of root growth of young poplar and willow planting types. New Zeal. J. For. Sci. 44, 15. https://doi.org/10.1186/s40490-

014-0015-6

Phillips, C.J., Watson, A.J., 1994. Structural tree root research in New Zealand : a review, Landcare Research science series; no. 7. Manaaki Whenua Press. https://doi.org/http://doi.org/10.7931/DL1-LRSS-7

Pierret, A., Doussan, C., Capowiez, Y., Bastardie, F., Pagès, L., 2007. Root functional architecture: A framework for modeling the interplay between roots and soil. Vadose Zo. J. 6, 269–281. https://doi.org/10.2136/vzj2006.0067

Pirotti, F., Kobal, M., Roussel, J.R., 2017. A comparison of tree segmentation methods using very high density airborne laser scanner data. Int. Arch. Photogramm. Remote Sens. Spat. Inf. Sci. - ISPRS Arch. 42, 285–290. https://doi.org/10.5194/isprs-archives-XLII-2-W7-285-2017

Pisano, L., Zumpano, V., Malek, Rosskopf, C.M., Parise, M., 2017. Variations in the susceptibility to landslides, as a consequence of land cover changes: A look to the past, and another towards the future. Sci. Total Environ. 601–602, 1147–1159. https://doi.org/10.1016/j.scitotenv.2017.05.231

Plieninger, T., Hartel, T., Martín-López, B., Beaufoy, G., Bergmeier, E., Kirby, K., Montero, M.J., Moreno, G., Oteros-Rozas, E., Van Uytvanck, J., 2015. Wood-pastures of Europe: Geographic coverage, social-ecological values, conservation management, and policy implications. Biol. Conserv. 190, 70–79. https://doi.org/10.1016/j.biocon.2015.05.014

Plieninger, T., Huntsinger, L., 2018. Complex Rangeland Systems: Integrated Social-Ecological Approaches to Silvopastoralism. Rangel. Ecol. Manag. 71, 519–525. https://doi.org/10.1016/j.rama.2018.05.002

Poeppl, R.E., Dilly, L.A., Haselberger, S., Renschler, C.S., Baartman, J.E.M., 2019. Combining soil erosion modeling with connectivity analyses to assess lateral fine sediment input into agricultural streams. Water (Switzerland) 11. https://doi.org/10.3390/w11091793

Poeppl, R.E., Fryirs, K.A., Tunnicliffe, J., Brierley, G.J., 2020. Managing sediment (dis)connectivity in fluvial systems. Sci. Total Environ. 736. https://doi.org/10.1016/j.scitotenv.2020.139627

Pollen, N., Simon, A., 2005. Estimating the mechanical effects of riparian vegetation on stream bank stability using a fiber bundle model. Water Resour. Res. 41, 1–11. https://doi.org/10.1029/2004WR003801

Pondard, N., Daly, M., 2011. Natural hazards risk modelling: an approach providing risk

management solutions for local government. GNS Sci. Misc. Ser. 38 12. https://doi.org/10.13140/RG.2.1.1316.3364

Power, I.L., Dodd, M.B., Thorrold, B.S., 2001. Deciduous or evergreen: Does it make a difference to understorey pasture yield and riparian zone management? Proc. New Zeal. Grassl. Assoc. 121–125. https://doi.org/10.33584/jnzg.2001.63.2443

Preston, N.J., 2008. Off-slope sediment delivery from landsliding during a storm, muriwai hills, North Island, New Zealand. IAHS-AISH Publ. 237–241.

Provenza, F.D., Balph, D.F., 1988. Development of dietary choice in livestock on rangelands and its implications for management. J. Anim. Sci. 66, 2356–2368. https://doi.org/10.2527/jas1988.6692356x

Qarinur, M., 2015. Landslide Runout Distance Prediction Based on Mechanism and Cause of Soil or Rock Mass Movement. J. Civ. Eng. Forum 1. https://doi.org/10.22146/jcef.22728

Qiao, C., Ou, G. qiang, Pan, H. li, Ouyang, C. jun, Jia, Y., 2018. Long runout mechanism of the Shenzhen 2015 landslide: insights from a two-phase flow viewpoint. J. Mt. Sci. 15, 2247–2265. https://doi.org/10.1007/s11629-017-4595-5

Quinn, J.M., Wilcock, R.J., Monaghan, R.M., McDowell, R.W., Journeaux, P.R., 2009. Grassland farming and water quality in New Zealand. Tearmann Irish J. Agri-Environmental Res. 7, 69–88.

Quinn, P., Beven, K., Chevallier, P., Planchon, O., 1991. The prediction of hillslope flow paths for distributed hydrological modelling using digital terrain models. Hydrol. Process. 5, 59–79. https://doi.org/10.1002/hyp.3360050106

Rahn, P.H., 2005. Geomorphology, in: Selley, R.C., Cocks, L.R.M., Plimer, I.R.B.T.-E. of G. (Eds.), Encylopedia of Geology. Elsevier, Oxford, pp. 90–95. https://doi.org/https://doi.org/10.1016/B0-12-369396-9/00209-4

Rattenbury, M.S., Isaac, M.J., 2012. The QMAP 1:250 000 Geological Map of New Zealand project. New Zeal. J. Geol. Geophys. 55, 393–405. https://doi.org/10.1080/00288306.2012.725417

Raz-Yaseef, N., Rotenberg, E., Yakir, D., 2010. Effects of spatial variations in soil evaporation caused by tree shading on water flux partitioning in a semi-arid pine forest. Agric. For. Meteorol. 150, 454–462. https://doi.org/10.1016/j.agrformet.2010.01.010

Reichenbach, P., Busca, C., Mondini, A.C., Rossi, M., 2014. The Influence of Land Use Change on Landslide Susceptibility Zonation: The Briga Catchment Test Site (Messina, Italy).

Environ. Manage. 54, 1372–1384. https://doi.org/10.1007/s00267-014-0357-0

Reichenbach, P., Rossi, M., Malamud, B.D., Mihir, M., Guzzetti, F., 2018. A review of statistically-based landslide susceptibility models. Earth-Science Rev. 180, 60–91. https://doi.org/10.1016/j.earscirev.2018.03.001

Reid, L.M., Page, M.J., 2002. Magnitude and frequency of landsliding in a large New Zealand catchment. Geomorphology 49, 71–88. https://doi.org/10.1016/S0169-555X(02)00164-2

Reid, R., Moore, R., 2018. Agroforestry systems in temperate Australia. Temp. Agrofor. Syst. 195–223. https://doi.org/10.1079/9781780644851.0195

Reubens, B., Poesen, J., Danjon, F., Geudens, G., Muys, B., 2007. The role of fine and coarse roots in shallow slope stability and soil erosion control with a focus on root system architecture: A review. Trees - Struct. Funct. 21, 385–402. https://doi.org/10.1007/s00468-007-0132-4

Rickenmann, D., 2005. Runout prediction methods, in: Jakob, M., Hungr, O. (Eds.), Debris-Flow Hazards and Related Phenomena. Springer Berlin Heidelberg, Berlin, Heidelberg, pp. 305–324. https://doi.org/10.1007/3-540-27129-5_13

Rickenmann, D., 1999. Empirical relationships for debris flows. Nat. Hazards 19, 47–77. https://doi.org/10.1023/A:1008064220727

Rigon, E., Comiti, F., Lenzi, M.A., 2012. Large wood storage in streams of the Eastern Italian Alps and the relevance of hillslope processes. Water Resour. Res. 48, 1–18. https://doi.org/10.1029/2010WR009854

Riley, S.J., DeGloria, S.D., Elliot, R., 1999. Terrain_Ruggedness_Index.pdf. Intermt. J. Sci.

Roering, J.J., Schmidt, K.M., Stock, J.D., Dietrich, W.E., Montgomery, D.R., 2003. Shallow landsliding, root reinforcement, and the spatial distribution of trees in the Oregon Coast Range. Can. Geotech. J. 40, 237–253. https://doi.org/10.1139/T02-113

Romeijn, J., 2009. Statistics as Inductive Inference Statistics as Inductive Inference An inductive logic is a system of inference that describes the relation be- 4–5.

Root-Bernstein, M., Vargas, B.H., Bondoux, A., Guerrero-Gatica, M., Zorondo-Rodríguez, F., Huerta, M., Valenzuela, R., Bello, Á.V., 2022. Silvopastoralism, local ecological knowledge and woodland trajectories in a category V- type management area. Biodivers. Conserv. https://doi.org/10.1007/s10531-021-02349-7

Rosser, B., Ross, C., 2011. Erosion soil loss and recovery on eastern North Island hillcountry–

Implications for nutrient management and pasture productivity. Adding to Knowl. Base Nutr. … 1–15.

Rosser, B.J., Ross, C.W., 2011. Recovery of pasture production and soil properties on soil slip scars in erodible siltstone hill country, Wairarapa, New Zealand. New Zeal. J. Agric. Res. 54, 23–44. https://doi.org/10.1080/00288233.2010.535489

Rossi, M., Guzzetti, F., Reichenbach, P., Mondini, A.C., Peruccacci, S., 2010. Optimal landslide susceptibility zonation based on multiple forecasts. Geomorphology 114, 129–142. https://doi.org/10.1016/j.geomorph.2009.06.020

Ruff, M., Czurda, K., 2008. Landslide susceptibility analysis with a heuristic approach in the Eastern Alps (Vorarlberg, Austria). Geomorphology 94, 314–324. https://doi.org/10.1016/j.geomorph.2006.10.032

Ruiz-Mirazo, J., Gonzalez-Rebollar, J.L., 2013. Growth and structure of a young Aleppo pine planted forest after thinning for diversification and wildfire prevention. For. Syst. 22, 47–57. https://doi.org/10.5424/fs/2013221-02500

Safari, S., Baratloo, A., Elfil, M., Negida, A., 2016. Evidence Based Emergency Medicine; Part 5 Receiver Operating Curve and Area under the Curve. Emerg. (Tehran, Iran) 4, 111–3. https://doi.org/10.22037/emergency.v4i2.11903

Sakals, M.E., Sidle, R.C., 2004. A spatial and temporal model of root cohesion in forest soils. Can. J. For. Res. 34, 950–958. https://doi.org/10.1139/x03-268

Salter, R.T., Frederick, C.T., Noble, K.E., 1983. Storm damage assessment of the Thames-Te Aroha area following the storm of April 1981, Publication / Soil Conservation Centre, Aokautere, 0111-7971 ; no. 1 TA - TT -. Soil Conservation Centre, Aokautere, Ministry of Works and Development for the National Water and Soil Conservation Organisation, Palmerston North, N.Z.

Salvatici, T., Tofani, V., Rossi, G., D'Ambrosio, M., Tacconi Stefanelli, C., Benedetta Masi, E., Rosi, A., Pazzi, V., Vannocci, P., Petrolo, M., Catani, F., Ratto, S., Stevenin, H., Casagli, N., 2018. Application of a physically based model to forecast shallow landslides at a regional scale. Nat. Hazards Earth Syst. Sci. 18, 1919–1935. https://doi.org/10.5194/nhess-18-1919-2018

Sappington, J.M., Longshore, K.M., Thompson, D.B., 2007. Quantifying Landscape Ruggedness for Animal Habitat Analysis: A Case Study Using Bighorn Sheep in the Mojave Desert. J. Wildl. Manage. 71, 1419–1426. https://doi.org/10.2193/2005-723

Scheip, C., Wegmann, K., 2022. Insights on the growth and mobility of debris flows from repeat high-resolution lidar. Landslides. https://doi.org/10.1007/s10346-022-01862-2

Schlögel, R., Marchesini, I., Alvioli, M., Reichenbach, P., Rossi, M., Malet, J.P., 2018. Optimizing landslide susceptibility zonation: Effects of DEM spatial resolution and slope unit delineation on logistic regression models. Geomorphology 301, 10–20. https://doi.org/10.1016/j.geomorph.2017.10.018

Schlüter, S., Blaser, S.R.G.A., Weber, M., Schmidt, V., Vetterlein, D., 2018. Quantification of root growth patterns from the soil perspective via root distance models. Front. Plant Sci. 9, 1–11. https://doi.org/10.3389/fpls.2018.01084

Schmaltz, E.M., Steger, S., Glade, T., 2017. The influence of forest cover on landslide occurrence explored with spatio-temporal information. Geomorphology 290, 250–264. https://doi.org/10.1016/j.geomorph.2017.04.024

Schmidt, K.M., Roering, J.J., Stock, J.D., Dietrich, W.E., Montgomery, D.R., Schaub, T., 2001. The variability of root cohesion as an influence on shallow landslide susceptibility in the Oregon Coast Range. Can. Geotech. J. 38, 995–1024. https://doi.org/10.1139/cgj-38-5-995

Schwarz, M., Cohen, D., Or, D., 2012. Spatial characterization of root reinforcement at stand scale: Theory and case study. Geomorphology 171–172, 190–200. https://doi.org/10.1016/j.geomorph.2012.05.020

Schwarz, M., Cohen, D., Or, D., 2010a. Root-soil mechanical interactions during pullout and failure of root bundles. J. Geophys. Res. 115, F04035. https://doi.org/10.1029/2009JF001603

Schwarz, M., Giadrossich, F., Cohen, D., 2013. Modeling root reinforcement using a root-failure Weibull survival function. Hydrol. Earth Syst. Sci. 17, 4367–4377. https://doi.org/10.5194/hess-17-4367-2013

Schwarz, M., Lehmann, P., Or, D., 2010b. Quantifying lateral root reinforcement in steep slopes - from a bundle of roots to tree stands. Earth Surf. Process. Landforms 35, 354–367. https://doi.org/10.1002/esp.1927

Schwarz, M., Phillips, C., Marden, M., McIvor, I.R., Douglas, G.B., Watson, A., 2016. Modelling of root reinforcement and erosion control by 'Veronese' poplar on pastoral hill country in New Zealand. New Zeal. J. For. Sci. 46, 4. https://doi.org/10.1186/s40490-016-0060-4

Schwarz, M., Preti, F., Giadrossich, F., Lehmann, P., Or, D., 2010c. Quantifying the role of vegetation in slope stability: A case study in Tuscany (Italy). Ecol. Eng. 36, 285–291. https://doi.org/10.1016/j.ecoleng.2009.06.014

Scorpio, V., Cavalli, M., Steger, S., Crema, S., Marra, F., Zaramella, M., Borga, M., Marchi, L., Comiti, F., 2022. Storm characteristics dictate sediment dynamics and geomorphic changes in mountain channels: A case study in the Italian Alps. Geomorphology 403, 108173. https://doi.org/10.1016/j.geomorph.2022.108173

Seidel, D., Fleck, S., Leuschner, C., Hammett, T., 2011. Review of ground-based methods to measure the distribution of biomass in forest canopies. Ann. For. Sci. 68, 225–244. https://doi.org/10.1007/s13595-011-0040-z

Sidle, R.C., Ochiai, H., 2006. Natural Factors Influencing Landslides, in: Sidle, R.C., Ochiai, H. (Eds.), Landslides: Processes, Prediction, and Land Use. American Geophysical Union, pp. 41–119. https://doi.org/10.1029/18WM04

Simoni, S., Vignoli, G., Mazzorana, B., 2017. Enhancing sediment flux control and natural hazard risk mitigation through a structured conceptual planning approach. Geomorphology 291, 159–173. https://doi.org/10.1016/j.geomorph.2017.01.026

Skole, D.L., Mbow, C., Mugabowindekwe, M., Brandt, M.S., Samek, J.H., 2021. Trees outside of forests as natural climate solutions. Nat. Clim. Chang. 11, 1013–1016. https://doi.org/10.1038/s41558-021-01230-3

Sloan, S., Kemp, P., Green, S., McIvor, I., 2014. Effect of space-planted ‘Veronese’ poplars on pasture production in hill country.

Smale, M.C., McLeod, M., Smale, P.N., 1997. Vegetation and soil recovery on shallow landslide scars in tertiary hill country, East Cape Region, New Zealand. N. Z. J. Ecol. 21, 31–41.

Smith, H.G., Spiekermann, R., Betts, H., Neverman, A.J., 2021. Comparing methods of landslide data acquisition and susceptibility modelling: Examples from New Zealand. Geomorphology 381, 107660. https://doi.org/https://doi.org/10.1016/j.geomorph.2021.107660

Somarriba, E., 1992. Revisiting the past: an essay on agroforestry definition. Agrofor. Syst. 19, 233–240. https://doi.org/10.1007/BF00118781

Song, R.H., Hiromu, D., Abe, K., Usio, K., Sumio, M., 2008. Modeling the potential distribution of shallow-seated landslides using the weights of evidence method and a

logistic regression model: a case study of the Sabae Area, Japan. Int. J. Sediment Res. 23, 106–118. https://doi.org/10.1016/S1001-6279(08)60010-4

Spiekermann, R., Brandt, M., Samimi, C., 2015a. Woody vegetation and land cover changes in the Sahel of Mali(1967-2011). Int. J. Appl. Earth Obs. Geoinf. 34, 113–121. https://doi.org/10.1016/j.jag.2014.08.007

Spiekermann, R., Kienberger, S., Norton, J., Briones, F., Weichselgartner, J., 2015b. The Disaster-Knowledge Matrix – Reframing and evaluating the knowledge challenges in disaster risk reduction. Int. J. Disaster Risk Reduct. 13, 96–108. https://doi.org/10.1016/j.ijdrr.2015.05.002

Spiekermann, R.I., McColl, S., Fuller, I., Dymond, J., Burkitt, L., Smith, H.G., 2021. Quantifying the influence of individual trees on slope stability at landscape scale. J. Environ. Manage. 286, 1–18. https://doi.org/10.1016/j.jenvman.2021.112194

Spiekermann, R.I., Smith, H.G., McColl, S., Burkitt, L., Fuller, I.C., 2022. Quantifying effectiveness of trees for landslide erosion control. Geomorphology 396, 1–16. https://doi.org/10.1016/j.geomorph.2021.107993

Stankey, G.H., 1985. The Limits of acceptable change (LAC) system for wilderness planning, The Limits of acceptable change (LAC) system for wilderness planning. USDA, Forest Service, Intermountain Forest and Range Experiment Station, Ogden, Utah : https://doi.org/10.5962/bhl.title.109310

Steger, S., Brenning, A., Bell, R., Glade, T., 2017. The influence of systematically incomplete shallow landslide inventories on statistical susceptibility models and suggestions for improvements. Landslides 14, 1767–1781. https://doi.org/10.1007/s10346-017-0820-0

Steger, S., Brenning, A., Bell, R., Glade, T., 2016a. The propagation of inventory-based positional errors into statistical landslide susceptibility models. Nat. Hazards Earth Syst. Sci. 16, 2729–2745. https://doi.org/10.5194/nhess-16-2729-2016

Steger, S., Brenning, A., Bell, R., Petschko, H., Glade, T., 2016b. Exploring discrepancies between quantitative validation results and the geomorphic plausibility of statistical landslide susceptibility maps. Geomorphology 262, 8–23. https://doi.org/10.1016/j.geomorph.2016.03.015

Steiner, F.R., Osterman, D.A., 1988. Landscape planning: a working method applied to a case study of soil conservation. Landsc. Ecol. 1, 213–226. https://doi.org/10.1007/BF00157694

Sterlacchini, S., Frigerio, S., Giacomelli, P., Brambilla, M., 2007. Landslide risk analysis : a multi-disciplinary methodological approach 657–675.

Stokes, A., Atger, C., Bengough, A.G., Fourcaud, T., Sidle, R.C., 2009. Desirable Plant root traits for protecting natural and engineered slopes against landslides. Plant Soil 324, 1–30. https://doi.org/10.1007/s11104-009-0159-y

Stokes, A., Douglas, G.B., Fourcaud, T., Giadrossich, F., Gillies, C., Hubble, T., Kim, J.H., Loades, K.W., Mao, Z., McIvor, I.R., Mickovski, S.B., Mitchell, S., Osman, N., Phillips, C., Poesen, J., Polster, D., Preti, F., Raymond, P., Rey, F., Schwarz, M., Walker, L.R., 2014. Ecological mitigation of hillslope instability: Ten key issues facing researchers and practitioners. Plant Soil 377, 1–23. https://doi.org/10.1007/s11104-014-2044-6

Stone, E.L., Kalisz, P.J., 1991. On the maximum extent of tree roots. For. Ecol. Manage. 46, 59–102. https://doi.org/10.1016/0378-1127(91)90245-Q

Storey, R., Wadhwa, S., 2009. An Assessment of the Lengths of Permanent, Intermittent and Ephemeral Streams in the Auckland Region. Auckl. Reg. Counc. Tech. Rep. 0504.

Styczen, M.E., Morgan, R.P.C., 1995. Engineering properties of vegetation, in: Morgan, R.P.C., Rickson, R.J. (Eds.), Slope Stabilization and Erosion Control: A Bioengineering Approach: A Bioengineering Approach. Chapman & Hall, London, pp. 4–60.

Süzen, M.L., Kaya, B.Ş., 2012. Evaluation of environmental parameters in logistic regression models for landslide susceptibility mapping. Int. J. Digit. Earth 5, 338–355. https://doi.org/10.1080/17538947.2011.586443

Team, R.C., 2021. R: A language and environment for statistical computing. R Foundation for Statistical Computing.

Temgoua, A.G.T., Kokutse, N.K., Kavazović, Z., 2016. Influence of forest stands and root morphologies on hillslope stability. Ecol. Eng. 95, 622–634. https://doi.org/10.1016/j.ecoleng.2016.06.073

Thevathasan, N.V., Coleman, B., Zabek, L., Ward, T., Gordon, A.M., 2018. Agroforestry in Canada and its Role in Farming Systems, in: Gordon, A.M., Newman, S.M., Coleman, B.R.W. (Eds.), Temperate Agroforestry Systems. CAB International, pp. 7–49.

Thompson, R.C., Luckman, P.G., 1993. Performance of biological erosion control in New Zealand soft rock hill terrain. Agrofor. Syst. 21, 191–211. https://doi.org/10.1007/BF00705230

Tibshirani, R., 1996. Regression Shrinkage and Selection via the Lasso. J. R. Stat. Soc. Ser. B

(Methodological), 58, 267–288.

Tölgyesi, C., Bátori, Z., Gallé, R., Urák, I., Hartel, T., 2018. Shrub Encroachment Under the Trees Diversifies the Herb Layer in a Romanian Silvopastoral System. Rangel. Ecol. Manag. 71, 571–577. https://doi.org/10.1016/j.rama.2017.09.004

Torabzadeh, H., Leiterer, R., Hueni, A., Schaepman, M.E., Morsdorf, F., 2019. Tree species classification in a temperate mixed forest using a combination of imaging spectroscopy and airborne laser scanning. Agric. For. Meteorol. 279, 107744. https://doi.org/10.1016/j.agrformet.2019.107744

Torizin, J., Wang, L. chao, Fuchs, M., Tong, B., Balzer, D., Wan, L. qin, Kuhn, D., Li, A., Chen, L., 2018. Statistical landslide susceptibility assessment in a dynamic environment: A case study for Lanzhou City, Gansu Province, NW China. J. Mt. Sci. 15, 1299–1318. https://doi.org/10.1007/s11629-017-4717-0

Trodahl, M.I., Jackson, B.M., Deslippe, J.R., Metherell, A.K., 2017. Investigating trade-offs between water quality and agricultural productivity using the Land Utilisation and Capability Indicator (LUCI)–A New Zealand application. Ecosyst. Serv. 26, 388–399. https://doi.org/10.1016/j.ecoser.2016.10.013

Trustrum, N.A., Thomas, V.J., Lambert, M.G., 1984. Soil slip erosion as a constraint to hill country pasture production. Proc. - New Zeal. Grassl. Assoc. 45, 66–76.

Turley, M., Hassan, M.A., Slaymaker, O., 2021. Quantifying sediment connectivity: Moving toward a holistic assessment through a mixed methods approach. Earth Surf. Process. Landforms 1–19. https://doi.org/10.1002/esp.5191

UNDRO, 1980. Natural Disasters and Vulnerability Analysis. Geneva.

Van Den Eeckhaut, M., Hervás, J., Jaedicke, C., Malet, J.-P., Montanarella, L., Nadim, F., 2012. Statistical modelling of Europe-wide landslide susceptibility using limited landslide inventory data. Landslides 9, 357–369. https://doi.org/10.1007/s10346-011-0299-z

Van Den Eeckhaut, M., Reichenbach, P., Guzzetti, F., Rossi, M., Poesen, J., 2009. Combined landslide inventory and susceptibility assessment based on different mapping units: An example from the Flemish Ardennes, Belgium. Nat. Hazards Earth Syst. Sci. 9, 507–521. https://doi.org/10.5194/nhess-9-507-2009

Van Den Eeckhaut, M., Vanwalleghem, T., Poesen, J., Govers, G., Verstraeten, G., Vandekerckhove, L., 2006. Prediction of landslide susceptibility using rare events logistic regression: A case-study in the Flemish Ardennes (Belgium). Geomorphology 76, 392–

410. https://doi.org/10.1016/j.geomorph.2005.12.003

van der Fels-Klerx, H.J., Edwards, S.G., Kennedy, M.C., O'Hagan, S., O'Mahony, C., Scholz, G., Steinberg, P., Chiodini, A., 2014. A framework to determine the effectiveness of dietary exposure mitigation to chemical contaminants. Food Chem. Toxicol. 74, 360–371. https://doi.org/10.1016/j.fct.2014.10.027

Van Dijk, A.I.J.M., Bruijnzeel, L.A., 2001. Modelling rainfall interception by vegetation of variable density using an adapted analytical model. Part 1. Model description. J. Hydrol. 247, 230–238. https://doi.org/10.1016/S0022-1694(01)00392-4

Van Kraayenoord, C.W.S., Hathaway, R.L., 1986. Plant Materials Handbook for Soil Conservation: Volume 2; Introduced Plants, Water and Soil miscellaneous publication no. 94. Ministry of Works and Development.

van Noordwijk, M, Hairiah, K., Tata, H., Lasco, L., 2019. How can agroforestry be part of disaster risk management?, in: van Noordwijk, Meine (Ed.), Sustainable Development through Trees on Farms: Agroforestry in Its Fifth Decade. World Agroforestry (ICRAF) Southeast Asia Regional Program, Bogor, Indonesia, pp. 251–267.

van Westen, C.J., Castellanos, E., Kuriakose, S.L., 2008. Spatial data for landslide susceptibility, hazard, and vulnerability assessment: An overview. Eng. Geol. 102, 112–131. https://doi.org/10.1016/j.enggeo.2008.03.010

van Zadelhoff, F.B., Albaba, A., Cohen, D., Phillips, C., Schaefli, B., Dorren, L.K.A., Schwarz, M., Karel, A., Schwarz, M., 2021. Introducing SlideforMap; a probabilistic finite slope approach for modelling shallow landslide probability in forested situations. Nat. Hazards Earth Syst. Sci. Discuss. 2021, 1–33. https://doi.org/10.5194/nhess-2021-140

Vergani, C., Schwarz, M., Soldati, M., Corda, A., Giadrossich, F., Chiaradia, E.A., Morando, P., Bassanelli, C., 2016. Root reinforcement dynamics in subalpine spruce forests following timber harvest: a case study in Canton Schwyz, Switzerland. CATENA 143, 275–288. https://doi.org/https://doi.org/10.1016/j.catena.2016.03.038

Wagenaar, D.J., Dahm, R.J., Diermanse, F.L.M., Dias, W.P.S., Dissanayake, D.M.S.S., Vajja, H.P., Gehrels, J.C., Bouwer, L.M., 2019. Evaluating adaptation measures for reducing flood risk: A case study in the city of Colombo, Sri Lanka. Int. J. Disaster Risk Reduct. 37, 101162. https://doi.org/10.1016/j.ijdrr.2019.101162

Wahren, A., Feger, K.H., Schwärzel, K., Münch, A., 2009. Land-use effects on flood generation - Considering soil hydraulic measurements in modelling. Adv. Geosci. 21, 99–107. https://doi.org/10.5194/adgeo-21-99-2009

Wainwright, J., Turnbull, L., Ibrahim, T.G., Lexartza-Artza, I., Thornton, S.F., Brazier, R.E., 2011. Linking environmental régimes, space and time: Interpretations of structural and functional connectivity. Geomorphology 126, 387–404. https://doi.org/10.1016/j.geomorph.2010.07.027

Waldron, L.J., 1977. The Shear Resistance of Root-Permeated Homogeneous and Stratified Soil. Soil Sci. Soc. Am. J. 41, 843–849. https://doi.org/10.2136/sssaj1977.03615995004100050005x

Walker, S.H., Duncan, D.B., 1967. Estimation of the Probability of an Event as a Function of Several Independent Variables. Biometrika 54, 167–179. https://doi.org/10.2307/2333860

Wall, A.J., Kemp, P.D., Mackay, A.D., 2006. Predicting pasture production under poplars using canopy closure images. Proc. New Zeal. Grassl. Assoc. 325–330. https://doi.org/10.33584/jnzg.2006.68.2625

Wall, A.J., Mackay, A.D., Kemp, P.D., Gillingham, A.G., Edwards, W.R.N., 1997. A review of the impacts of widely spaced soil conservation trees on hill pastoral systems. Benavides al., 2009. Silvopastoralism New Zeal. Rev. Eff. Evergr. deciduous trees pasture Dyn. Agroforestery Syst. n°76, p327-350. 177, 171–177.

Wang, L., Liu, H., 2006. An efficient method for identifying and filling surface depressions in digital elevation models for hydrologic analysis and modelling. Int. J. Geogr. Inf. Sci. 20, 193–213. https://doi.org/10.1080/13658810500433453

Wang, X., Huang, F., Fan, X., Shahabi, H., Shirzadi, A., Bian, H., Ma, X., Lei, X., Chen, W., 2022. Landslide susceptibility modeling based on remote sensing data and data mining techniques. Environ. Earth Sci. 81, 1–19. https://doi.org/10.1007/s12665-022-10195-1

Wang, Yunni, Cao, G., Wang, Yanhui, Webb, A.A., Yu, P., Wang, X., 2019. Response of the daily transpiration of a larch plantation to variation in potential evaporation, leaf area index and soil moisture. Sci. Rep. 9, 1–11. https://doi.org/10.1038/s41598-019-41186-1

Watson, A., Marden, M., Rowan, D., 1995. Tree species performance and slope stability, in: Vegetation and Slopes: Stabilisation, Protection and Ecology. Thomas Telford Publishing, pp. 161–171. https://doi.org/10.1680/vasspae.20313.0018

Watson, A., O'Loughlin, C., 1990. Structural root morphology and biomass of the three age-classes of Pinus Radiata. New Zeal. J. For. Sci. 20, 97–110.

Watson, A., Phillips, C., Marden, M., 1999. Root strength, growth, and rates of decay: Root

reinforcement changes of two tree species and their contribution to slope stability, in: Plant and Soil. pp. 39–47. https://doi.org/10.1023/a:1004682509514

Watson, A.J., Marden, M., 2004. Live root-wood tensile strengths of some common New Zealand indigenous and plantation tree species. New Zeal. J. For. Sci. 34, 344–353.

Wechsler, S.P., Kroll, C.N., 2013. Quantifying DEM Uncertainty and its Effect on Topographic Parameters. Photogramm. Eng. Remote Sens. 72, 1081–1090. https://doi.org/10.14358/pers.72.9.1081

Weinmann, M., Weidner, U., 2018. Land-Cover and Land-Use Classification Based on Multitemporal Sentinel-2 Data, in: IGARSS 2018 - 2018 IEEE International Geoscience and Remote Sensing Symposium. pp. 4946–4949. https://doi.org/10.1109/IGARSS.2018.8519301

Weinstein, B.G., Marconi, S., Bohlman, S., Zare, A., Singh, A., Graves, S.J., White, E., 2020a. NEON Crowns: a remote sensing derived dataset of 100 million individual tree crowns. bioRxiv 2020.09.08.287839. https://doi.org/https://doi.org/10.1101/2020.09.08.287839

Weinstein, B.G., Marconi, S., Bohlman, S., Zare, A., White, E., 2019. Individual tree-crown detection in rgb imagery using semi-supervised deep learning neural networks. Remote Sens. 11, 1–13. https://doi.org/10.3390/rs11111309

Weinstein, B.G., Marconi, S., Bohlman, S.A., Zare, A., Singh, A., Graves, S.J., White, E.P., 2021. A remote sensing derived data set of 100 million individual tree crowns for the National Ecological Observatory Network. Elife 10, 1–18. https://doi.org/10.7554/eLife.62922

Weinstein, B.G., Marconi, S., Bohlman, S.A., Zare, A., White, E.P., 2020b. Cross-site learning in deep learning RGB tree crown detection. Ecol. Inform. 56, 101061. https://doi.org/10.1016/j.ecoinf.2020.101061

Wever, L.A., Flanagan, L.B., Carlson, P.J., 2002. Seasonal and interannual variation in evapotranspiration, energy balance and surface conductance in a northern temperate grassland. Agric. For. Meteorol. 112, 31–49. https://doi.org/10.1016/S0168-1923(02)00041-2

Whitehead, D., Kelliher, F.M., 1991. A canopy water balance model for a Pinus radiata stand before and after thinning. Agric. For. Meteorol. 55, 109–126. https://doi.org/10.1016/0168-1923(91)90025-L

Wichmann, V., Heckmann, T., Haas, F., Becht, M., 2009. A new modelling approach to

delineate the spatial extent of alpine sediment cascades. Geomorphology 111, 70–78. https://doi.org/10.1016/j.geomorph.2008.04.028

Wilkinson, A.., 1999. Poplars and willows for soil erosion control in New Zealand. Biomass and Bioenergy 16, 263–274. https://doi.org/10.1016/S0961-9534(99)00007-0

Wohl, E., Brierley, G., Cadol, D., Coulthard, T.J., Covino, T., Fryirs, K.A., Grant, G., Hilton, R.G., Lane, S.N., Magilligan, F.J., Meitzen, K.M., Passalacqua, P., Poeppl, R.E., Rathburn, S.L., Sklar, L.S., 2019. Connectivity as an emergent property of geomorphic systems. Earth Surf. Process. Landforms 44, 4–26. https://doi.org/10.1002/esp.4434

Wolman, M.G., Miller, J.P., 1960. Magnitude and Frequency of Forces in Geomorphic Processes. J. Geol. 68, 54–74.

Wu, T.H., 1995. Slope Stabilization, in: R.P.C.Morgan, R.J. Rickson (Eds.), Slope Stabilization and Erosion Control: A Bioengineering Approach. E & FN Spon, London, pp. 233–281.

Wu, T.H., McKinnell, W.P., Swanston, D.N., 1979. Strength of Tree Roots and Landslides on Price of Wales Island, Alaska. Can Geotech J 16, 19–33. https://doi.org/10.1139/t79-003

Wu, T.H., Watson, A., 1998. In situ shear tests of soil blocks with roots. Can. Geotech. J. 35, 579–590. https://doi.org/10.1139/cgj-35-4-579

Wu, W., Sidle, R.C., 1995. A Distributed Slope Stability Model for Steep Forested Basins. Water Resour. Res. 31, 2097–2110. https://doi.org/10.1029/95WR01136

Xiao, T., Segoni, S., Chen, L., Yin, K., Casagli, N., 2020. A step beyond landslide susceptibility maps: a simple method to investigate and explain the different outcomes obtained by different approaches. Landslides 17, 627–640. https://doi.org/10.1007/s10346-019-01299-0

Xiong, J., Tang, C., Gong, L., Chen, M., Li, N., Shi, Q., Zhang, X., Chang, M., Li, M., 2022. How landslide sediments are transferred out of an alpine basin: Evidence from the epicentre of the Wenchuan earthquake. Catena 208, 105781. https://doi.org/10.1016/j.catena.2021.105781

Yang, L., Wei, Y., Wang, W., Zhu, S., 2019. Numerical runout modeling analysis of the loess landslide at Yining, Xinjiang, China. Water (Switzerland) 11. https://doi.org/10.3390/w11071324

Yang, R., Fan, B., Wei, R., Wang, Y., Zhou, Q., 2022. Land Cover Classification from Hyperspectral Images via Weighted Spatial-Spectral Kernel Collaborative Representation with Tikhonov Regularization. Land 11. https://doi.org/10.3390/land11020263

Zanandrea, F., Michel, G.P., Kobiyama, M., Cardozo, G.L., 2019. Evaluation of different DTMs in sediment connectivity determination in the Mascarada River Watershed, southern Brazil. Geomorphology 332, 80–87. https://doi.org/10.1016/j.geomorph.2019.02.005

Zevenbergen, L.W., Thorne, C.R., 1987. Quantitative analysis of land surface topography. Earth Surf. Process. Landforms 12, 47–56. https://doi.org/https://doi.org/10.1002/esp.3290120107

Zhao, G., Gao, P., Tian, P., Sun, W., Hu, J., Mu, X., 2020. Assessing sediment connectivity and soil erosion by water in a representative catchment on the Loess Plateau, China. Catena 185, 104284. https://doi.org/10.1016/j.catena.2019.104284

Zhen, Z., Quackenbush, L.J., Zhang, L., 2016. Trends in automatic individual tree crown detection and delineation-evolution of LiDAR data. Remote Sens. 8, 1–26. https://doi.org/10.3390/rs8040333

Ziemer, R.R., 1981. Roots and the stability of forested slopes, in: Davies, T.R.H., Pearce, A.J. (Eds.), Christchurch Symposium: Erosion and Sediment Transport in Pacific Rim Steeplands. pp. 343–361.

Ziemer, R.R., Lewis, J., Rice, R.M., Lisle, T.E., 1991. Modeling the Cumulative Watershed Effects of Forest Management Strategies. J. Environ. Qual. 20, 36–42. https://doi.org/10.2134/jeq1991.00472425002000010008x

Zillgens, B., Merz, B., Kimbauer, R., Tilch, N., 2007. Analysis of the runoff response of an alpine catchment at different scales. Hydrol. Earth Syst. Sci. 11, 1441–1454. https://doi.org/10.5194/hess-11-1441-2007

Zörner, J., Dymond, J., Shepherd, J., Wiser, S., Jolly, B., 2018. LiDAR-Based Regional Inventory of Tall Trees—Wellington, New Zealand. Forests 9, 1–16. https://doi.org/10.3390/f9110702

10 APPENDIX

MASSEY UNIVERSITY
TE KUNENGA KI PŪREHUROA
UNIVERSITY OF NEW ZEALAND

GRADUATE RESEARCH SCHOOL

STATEMENT OF CONTRIBUTION
DOCTORATE WITH PUBLICATIONS/MANUSCRIPTS

We, the student and the student's Main Supervisor, certify that all co-authors have consented to their work being included in the thesis and they have accepted the student's contribution as indicated below in the Statement of Originality.

Student name:	Raphael Spiekermann
Name/title of main supervisor:	Prof Ian Fuller
In which chapter is the manuscript/published work?	Chapter 3

Please select one of the following three options:

(●) The manuscript/published work is published or in press

- Please provide the full reference of the research output:

Spiekermann, R. I., S. McColl, I. Fuller, J. Dymond, L. Burkitt, and H. G. Smith. 2021. Quantifying the influence of individual trees on slope stability at landscape scale. Journal of Environmental Management 286(112194):1–18.

( ) The manuscript is currently under review for publication – please indicate:

- The name of the journal:
- The percentage of the manuscript/published work that was contributed by the student: 90 %
- Describe the contribution that the student has made to the manuscript/published work:

Raphael led the the conceptualization, developed the methodology, including code, validation, formal analysis, and investigation. He wrote the original draft manuscript and created all visualizations.

( ) It is intended that the manuscript will be published, but it has not yet been submitted to a journal

Student's signature:	Raphael Spiekermann — Digitally signed by Raphael Spiekermann Date: 2022.06.09 21:59:47 +12'00'
Main supervisor's signature:	Prof. Ian Fuller — Digitally signed by Prof. Ian Fuller Date: 2022.06.23 13:59:52 +12'00'

This form should appear at the end of each thesis chapter/section/appendix submitted as a manuscript/ publication or collected as an appendix at the end of the thesis.

MASSEY UNIVERSITY
TE KUNENGA KI PŪREHUROA
UNIVERSITY OF NEW ZEALAND

GRADUATE RESEARCH SCHOOL

STATEMENT OF CONTRIBUTION DOCTORATE WITH PUBLICATIONS/MANUSCRIPTS

We, the student and the student's Main Supervisor, certify that all co-authors have consented to their work being included in the thesis and they have accepted the student's contribution as indicated below in the Statement of Originality.

Student name:	Raphael Spiekermann
Name/title of main supervisor:	Prof Ian Fuller
In which chapter is the manuscript/published work?	Chapter 4

Please select one of the following three options:

(●) The manuscript/published work is published or in press

- Please provide the full reference of the research output:

Spiekermann, R. I., H. G. Smith, S. McColl, L. Burkitt, and I. C. Fuller. 2022. Quantifying effectiveness of trees for landslide erosion control. Geomorphology 396(107993):1–16.

( ) The manuscript is currently under review for publication – please indicate:

- The name of the journal:

- The percentage of the manuscript/published work that was contributed by the student: 90 %
- Describe the contribution that the student has made to the manuscript/published work:

Raphael led the the conceptualization, developed the methodology, including code, validation, formal analysis, and investigation. He wrote the original draft manuscript and created all visualizations.

( ) It is intended that the manuscript will be published, but it has not yet been submitted to a journal

Student's signature:	Raphael Spiekermann — Digitally signed by Raphael Spiekermann Date: 2022.06.09 21:59:47 +12'00'
Main supervisor's signature:	Prof. Ian Fuller — Digitally signed by Prof. Ian Fuller Date: 2022.06.23 13:59:29 +12'00'

This form should appear at the end of each thesis chapter/section/appendix submitted as a manuscript/ publication or collected as an appendix at the end of the thesis.

MASSEY UNIVERSITY
TE KUNENGA KI PŪREHUROA
UNIVERSITY OF NEW ZEALAND

GRADUATE RESEARCH SCHOOL

STATEMENT OF CONTRIBUTION DOCTORATE WITH PUBLICATIONS/MANUSCRIPTS

We, the student and the student's Main Supervisor, certify that all co-authors have consented to their work being included in the thesis and they have accepted the student's contribution as indicated below in the Statement of Originality.

Student name:	Raphael Spiekermann
Name/title of main supervisor:	Prof Ian Fuller
In which chapter is the manuscript/published work?	Chapter 5

Please select one of the following three options:

(●) The manuscript/published work is published or in press

- Please provide the full reference of the research output:

Spiekermann, R. I., H. G. Smith, S. McColl, L. Burkitt, and I. C. Fuller. 2022. Development of a morphometric connectivity model to mitigate sediment derived from storm-driven shallow landslides. Ecological Engineering 180(106676):106676.

( ) The manuscript is currently under review for publication – please indicate:

- The name of the journal:

- The percentage of the manuscript/published work that was contributed by the student: 95 %
- Describe the contribution that the student has made to the manuscript/published work:

Raphael led the the conceptualization, developed the methodology, including code, validation, formal analysis, and investigation. He wrote the original draft manuscript and created all visualizations.

( ) It is intended that the manuscript will be published, but it has not yet been submitted to a journal

Student's signature:	Raphael Spiekermann — Digitally signed by Raphael Spiekermann Date: 2022.06.09 21:59:47 +12'00'
Main supervisor's signature:	Prof. Ian Fuller — Digitally signed by Prof. Ian Fuller Date: 2022.06.23 13:58:58 +12'00'

This form should appear at the end of each thesis chapter/section/appendix submitted as a manuscript/ publication or collected as an appendix at the end of the thesis.